Non-Covalent Interactions in Organocatalysis

DISS. ETH NO. 22066

Non-Covalent Interactions in Organocatalysis

A thesis submitted to attain the degree of

DOCTOR OF SCIENCES of ETH ZURICH
(Dr. sc. ETH Zurich)

presented by

Mareike Claudia Holland

MSc ETH Chemistry, ETH Zürich

born on *10.10.1987*
Citizen of the Federal Republic of Germany

accepted on the recommendation of
Prof. Dr. Ryan Gilmour, co-examiner
Prof. Dr. Erick Carreira, examiner
Prof. Dr. Antonio Togni, co-examiner

Zürich 2014

What is a scientist after all?
It is a curious man looking through a keyhole,
the keyhole of nature, trying to know what's going on.
- Jacques-Yves Cousteau, 1971 -

Meiner Familie

Acknowledgments

This work would not have been possible without the scientific and moral support of numerous people.

First of all, I want to thank Prof. Ryan Gilmour for being a great mentor. I am very grateful for all the advise, trust and encouragement, and for always believing in me. I also want to thank him for the support concerning my future career.

I want to give my sincere thanks to Prof. Erick Carreira for very kindly agreeing to be my PhD supervisor from ETH Zurich, thus allowing me to continue my doctoral studies at this great university. My gratitude also goes to Prof. Antonio Togni for kindly accepting to be my co-supervisor.

I would like to thank Prof. François Diederich and Dr. Henrik Sundén for supporting me and for helping me to secure the great opportunity of a postdoctoral research stay with Prof. Ken Houk. I want to thank Prof. Ken Houk for accepting my application and I am very much looking forward to joining your lab.

My gratitude goes to my collaborators. I want to thank Dr. Christian Mück-Lichtenfeld from the WWU Münster (D) and Dr. Anthony Meijer from the University of Sheffield (UK) for performing the computations presented in this work and for the helpful discussions. I want to say thank you to Shyeni Paul and Prof. Mayr from the LMU Munich (D), and Dr. Lakhdar from the ENSICAEN (F) for the collaboratorive work on the kinetic studies. My thanks also go to Dr. Klaus Bergander from WWU Münster (D) for the collaboration on the NMR conformer population analyses. I would like to thank Priv.-Doz. Mathias Schäfer from the University of Cologne (D), Prof. Jos Oomens and Dr. Berden from the Radboud University Nijmegen (NL) and the rest of the FELIX team for the exciting beam time session and for staying all night to keep FELIX running for our studies! My gratitude also goes to Dr. Fabian Meemken and Prof. Alfons Baiker from ETH Zurich (CH) for the collaboration on the chiral modifiers for asymmetric heterogeneous catalysis work and for adopting me into the group during the course of the study.

I would like to thank the Master students I had the pleasure to work with: Sophie Haberland, Vivian Müller, Patrick Bentler, Katharina Martinewski, Maximilian von Gröning, and Jan Metternich, I wish you all the best for your future!

I want to thank the service departments and technical staff both at ETH Zurich and WWU Münster: Dr. Bernd Schweizer and Michael Solar (ETH) and Dr. Constantin Daniliuc and Birgit Wibbeling (WWU) for measuring my X-ray structures. The NMR service staff Prof. Bernhard Jaun, Dr. Marc-Olivier Ebert, Rainer Frankenstein, Philipp Zumbrunnen, and René Arnold (ETH) as well as Dr. Klaus Bergander, Karin Voß, and Ingo Gutowski (WWU) for their help in measuring numerous NMR spectra. My gratitude goes to the MS services, Dr. Xianyang Zhang, Louis Bertschi, Oswald Greter, and Rolf Häfliger (ETH) and Dr. Matthias Letzel, Jens Paweletz, Cornelia Linz, and Bärbel Wippich (WWU) for measuring my mass spectra. I also want to thank the staff from the Schalter (ETH) and the Chemikalienausgabe (WWU), the members of the mechanical workshop, and everyone else, who keeps the place running.

I want to thank all the former and present members of the Gilmour group for a terrific time in and outside the lab! We always made a great team, maintaining an inspiring, positive and productive working atmosphere while never forgetting when it was time to go for a beer and share a laugh. I want to thank Dr. Christoph Bucher, Estelle Durantie, Dr. Susann Paul, Yannick Rey, Dr. Christof Sparr, Dr. Eva-Maria Tanzer, and Dr. Lucie Zimmer for the wonderful time in Zürich! Thank you for always having time to discuss my chemistry and cheering me up when I felt stuck. Thank you also for the fun group activities, hiking and skiing trips and even horseback riding! A big thanks goes to Eva-Maria for being a good friend and listener. I especially want to thank Yannick Rey who was the only other group member moving to Münster. It was a tough time and without you the move and especially getting settled in Münster would have been a lot more difficult. It was great seeing the group grow at WWU and welcoming a lot of wonderful new members. I want to thank Dr. Nuria Aiguabella, Dr. Randy Benedict, Patrick Bentler, Andrea Kapries, Vanessa Lewe, Jan Metternich, István Gábor Molnár, Yannick Rey, Dr. Nico Santschi, and Christian Thiehoff for the great time in Münster and for supporting me especially during the last few intense weeks! I am grateful to Dr. Nuria Aiguabella, Dr. Randy Benedict, Patrick Bentler, Jan Metternich, and Yannick Rey for proof-reading parts of my thesis. I want to thank Patrick Bentler and Jan Metternich for continuing on some of my projects and for the productive discussions.

I am very fortunate to have many great friends that have supported me and there is no space to thank all of them, but there are some people from Zürich and Münster I would like to mention that have been especially important during my Ph.D. studies. I would like to thank

the Diederich group members for inviting me to many of their group activities; I always had a great time. I especially want to thank Dr. Michael Seet for a great friendship! I also want to thank him and Dr. Johannes Teichert, Judit Teichert, and Michael Harder for our regular Doppelkopf sessions and for staying in touch. I want to thank Anne Engmann, Ann-Kristina Fritz, Carina Klein, Karen Haenraets, and Lisa Henning for many good times and their wonderful friendship. I especially want to thank Lisa Henning for always being there for me. Here in Münster, I want to thank the Haufe and the Glorius groups for warmly welcoming us and including us in many group activites, making the start in Münster so much easier. I want to thank Renate Rohlmann for helping me to format my thesis and for her friendship. A big thank you goes to Hella Berlemann, Vysakh Prasad, and Daniel Ramb for their friendship and for recharging coffee and dinner breaks especially during the last few months.

I want to thank my parents and my sister for always believing in me, for your neverending support and for being there for me. You made everything so much easier for me and I am very grateful to have you. I want to thank my grandparents and my whole family for their motivational words and for being proud of me.

I want to thank my boyfriend Markus for loving me, for supporting me, and understanding me. I also want to thank you for taking up with so many years of far-distance relationship and making it work. Without your love and your ability to calm me down when I felt like drowning in work, the last years would have been a whole lot more difficult.

Thank You! Vielen Dank! Merci vielmal!

Publications

Parts of this thesis have been published in:

Published:

Infrared Multiphoton Dissociation (IRMPD) Spectroscopic Analysis of Non-Covalent Interactions in Organocatalysis.
M. C. Holland, G. Berden, J. Oomens, A. J. H. M. Meijer, M. Schäfer and R. Gilmour, *Eur. J. Org. Chem.*, **2014**, *26*, 5675.

Non-Covalent Interactions in Organocatalysis: Modulating Conformational Diversity and Reactivity in the MacMillan Catalyst.
M. C. Holland, S. Paul, W. B. Schweizer, K. Bergander, C. Mück-Lichtenfeld, S. Lakhdar, H. Mayr, and R. Gilmour, *Angew. Chem. Int. Ed.* **2013**, *52*, 7967.

Molecular Recognition at the Active Site of Factor Xa: Cation–π Interactions, Stacking on Planar Peptide Surfaces, and Replacement of Structural Water.
L. M. Salonen, M. C. Holland, P. Kaib, W. Haap, J. Benz, J.-L. Mary, O. Kuster, W. B. Schweizer, D. W. Banner, and F. Diederich, *Chem. Eur. J.* **2012**, *18*, 213.

Submitted:

Chiral Imidazolidinone and Proline-Derived Surface Modifiers for the Pt-Catalyzed Asymmetric Hydrogenation of Activated Ketones.
M. C. Holland, F. Meemken, A. Baiker, and R. Gilmour. Full paper, **2014**.

Deconstructing Organocatalytic Reactions.
M. C. Holland and R. Gilmour. Review, **2014**.

Adsorption and stability of chiral modifiers based on 1-(1-naphthyl)-ethylamine for Pt catalysed heterogeneous asymmetric hydrogenations.
F. Meemken, M. C. Holland, R. Gilmour, and A. Baiker. Full paper, **2014**.

In Preparation:

M. C. Holland, H. Sundén, A. Probst-Larsen, and R. Olsson, *Manuscript in preparation.*

M. C. Holland, J. B. Metternich, C. Mück-Lichtenfeld, and R. Gilmour, *Manuscript in preparation.*

Oral and Poster Presentations

Parts of this thesis have been presented in:

Oral Presentations:

Zerlegung des MacMillan Organokatalysators, presented at the annual workshop of the "Friends of the Chemistry-Olympiad", 04.01.2014, Münster.

Modulating Conformational Diversity and Reactivity in the MacMillan Catalyst, presented at the laboratory of organic chemistry intergroup seminar, 25.04.2013, Münster.

Poster Presentations:

Transferring Enzymatic Principles to Organocatalysis – Illuminating Non-Covalent Interactions in the MacMillan Catalyst, M. C. Holland, S. Paul, W. B. Schweizer, K. Bergander, C. Mück-Lichtenfeld, S. Lakhdar, H. Mayr, and R. Gilmour, presented at the Münster Symposium on Cooperative Effects in Chemistry 2013, awarded with the 1st place poster prize.

Transferring Enzymatic Principles to Organocatalysis – Illuminating Non-Covalent Interactions in the MacMillan Catalyst, M. C. Holland, S. Paul, W. B. Schweizer, K. Bergander, C. Mück-Lichtenfeld, S. Lakhdar, H. Mayr, and R. Gilmour, presented at the Münster Symposium Forschung der Chemischen Industrie 2013.

Non-Covalent Interactions in Organocatalysis: Modulating Conformational Diversity and Reactivity in the MacMillan Catalyst, M. C. Holland, S. Paul, W. B. Schweizer, K. Bergander, C. Mück-Lichtenfeld, S. Lakhdar, H. Mayr, and R. Gilmour, presented at the European Symposium on Organic Chemistry 2013 in Marseille, awarded with the Syngenta poster prize.

Non-Covalent Interactions in Organocatalysis: Modulating Conformational Diversity and Reactivity in the MacMillan Catalyst, M. C. Holland, S. Paul, W. B. Schweizer, K. Bergander, C. Mück-Lichtenfeld, S. Lakhdar, H. Mayr, and R. Gilmour, presented at the Syngenta Symposium 2013 in Stein.

Table of Contents

Abbreviations

6-311G*	Pople basis set
$[\alpha]_D$	specific rotation, sodium D line (589 nm)
$A^{1,3}$	1,3-allylic strain
Ac	acetyl
Alloc	allyloxycarbonyl
ATR	attenuated total reflection
Ar	aryl / aromatic
Arg	arginine
b	broad
B3LYP	Becke, 3-parameter, Lee-Yang-Parr
BMI	2-*tert*-butyl-3-methyl-4-imidazolidinone
Bn	benzyl
Boc	*tert*-butyloxycarbonyl
Bu	Butyl
c	concentration
CAM	cerium ammonium molybdate
cat	catalyst /catalytic
CH	cyclohexane
conc.	concentrated
COSY	correlation spectroscopy
δ	chemical shift
d	doublet
DAST	*N*,*N*-diethylaminosulfur trifluoride
dd	doublet of doublets
DEPT	distortionless enhancement by polarisation transfer
DFT	density functional theory
DIPEA	*N*,*N*-diisopropylethylamine
DMAP	4-(dimethyl)aminopyridine
DMF	*N*,*N*-dimethylformamide
DMPU	1,3-dimethyltetrahydro-pyrimidin-2(1*H*)-one
DMSO	dimethylsulfoxide
DNA	deoxyribonucleic acid
d.r.	diastereomeric ratio
E	electrophilicity parameter / energy
ee	enantiomeric excess
EI	electron ionisation
equiv./eq.	equivalents
e.r.	enantiomeric ratio
ESI	electrospray ionisation
ESP	electrostatic potential

Et	ethyl
EWG	electron withdrawing group
FELIX	free electron laser for infrared experiments
FID	flame ionisation detector
FT-ICR	Fourier transform ion cyclotron resonance
GABA	*gamma*-aminobutyric acid
GC	gas chromatography
His	Histidine
HMBC	heteronuclear multiple-bond correlation spectroscopy
HMDS	hexamethyldisilazane
HOESY	heteronuclear Overhauser effect spectroscopy
HOMO	highest occupied molecular orbital
HPLC	high performance liquid chromatography
HR	high resolution
HSQC	heteronuclear single-quantum correlation spectroscopy
IR	infrared spectroscopy
IR-MPD	infrared multiphoton dissociation
J	coupling constant
k_2	second-order rate constant
k_{obs}	observed rate constant
KPL	ketopantolactone
λ	wavelength
λ_i	group electronegativity
LDA	lithium diisopropylethylamine
LUMO	lowest unoccupied molecular orbital
Lys	Lysine
m	multiplet / medium
MBF	methylbenzoylformate
M.p.	melting point
Me	methyl
MM3	molecular mechanics force field
MS	molecular sieves / mass spectrometry
MTO	methyltrioxorhenium
N	nucleophilicity parameter
NHC	*N*-heterocyclic carbine
NMR	nuclear magnetic resonance
NOESY	nuclear Overhauser effect spectroscopy
o/n	overnight
Ph	phenyl
Phe	phenylalanine
ppm	parts per million
Pr	propyl
q	quartet

quant.	quantitative
Q_{zz}	traceless quadrupole moment tensor orthogonal to the aromatic ring
rac.	racemic
R_f	retardation factor
RT	room temperature
σ	bonding sigma orbital
σ*	*anti*-bonding sigma orbital
σ_m	Hammett constant, *meta*
σ_p	Hammett constant, *para*
s	singlet / strong
SM	starting material
s_N	nucleophile-specific sensitivity parameter
S_N1	nucleophilic substitution, unimolecular
SOMO	singly occupied molecular orbital
t	triplet
Tf	triflate
TFA	trifluoroacetic acid
TFAP	trifluoroacetophenone
THF	tetrahydrofuran
TLC	thin layer chromatography
TMS	trimethylsilyl
Trp	tryptophan
Trt	trityl
Ts	*p*-toluenesulfonyl
Tyr	tyrosine
UHP	urea hydrogen peroxide
UV/VIS	ultraviolet-visible spectroscopy
w	weak

Summary

Since its renaissance in 2000, organocatalysis has established itself as the third pillar of contemporary catalysis together with enzymatic and metal mediated approaches. The field has rapidly developed and numerous prestigious laboratories have contributed to the identification of various powerful small-molecule catalysts ranging from biomolecules to thiourea catalysts and *N*-heterocyclic carbenes (NHCs). The underlying principles of asymmetric induction and mechanism are often not well understood and are yet to be unraveled. Most organocatalysts consist of the same building blocks as biomolecules and intermediates are often stabilised by the same structural features found in enzymes. In this thesis, one of the most renowned organocatalysts, the MacMillan imidazolidinone, was studied. It was proposed that stereoinduction is governed by non-covalent interactions in the transition state.

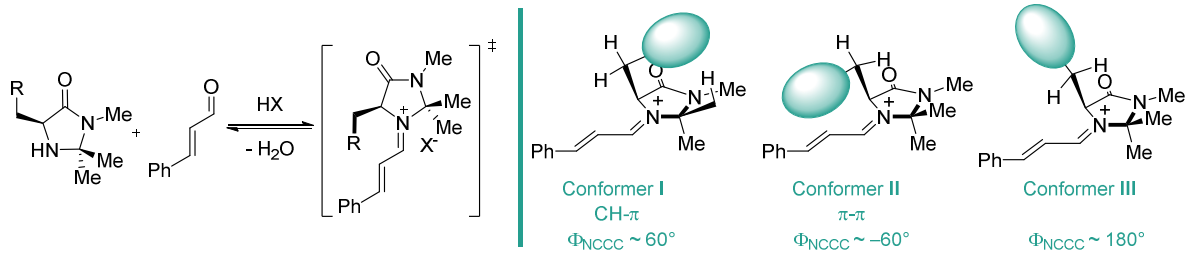

Scheme 1 *Left: MacMillan 1st generation catalyst and the iminium ion intermediate. Right: Three possible staggered conformers of the intermediate.*

MacMillan's imidazolidinone organocatalysts have proven themselves to be highly effective in mediating various organic reactions involving enamine and iminium ion intermediates. The transient iminium ion formed by condensation of the 1st generation catalyst with an α,β-unsaturated aldehyde (Scheme 1) is geometrically optimised to undergo stabilising CH-π and π-π interactions similar to those found in enzymes, providing an excellent playground to study these interactions in a small molecule. In this work, numerous catalyst sites were modified in a logical molecular editing study to identify the essential features and interactions for effective catalyst performance.

From structural biology studies of large peptides and proteins it is known that non-bonding CH-π and π-π interactions are sensitive to electronic modulation. The iminium ion

intermediate of the phenylalanine-derived MacMillan catalyst can undergo the same interactions depending on the conformation (Scheme 1, right). The effect of electronic modifications of the phenyl-ring on conformational behaviour, reactivity and selectivity was investigated. For this purpose a library of new catalysts was synthesized with the aromatic group ranging from very electron-deficient (e.g., R = C_6F_5) to very electron-rich [e.g., R = $C_6H_2(OMe)_3$]. The traceless quadrupole moment tensors perpendicular to the aromatic ring (Q_{zz}) was calculated to reflect the electronic property of a given aryl group and ESP maps were computed to illustrate the electronic distribution (Figure 1, upper). Using spectroscopic ground-state conformational analysis in combination with kinetic and catalysis studies, it was possible to show that the conformational preferences can be biased by adjusting the electronic properties of the shielding group. Whereas iminium ions with shielding groups that have electronic properties similar to phenyl, predominantly populate conformer **I**, an increased population of conformer **II** was attained with more electron-rich derivatives. Electron-deficient systems on the other hand result in high population of conformer **III.** It was achieved to obtain X-ray structures of each of these three staggered conformers (Figure 1, lower). The conformational study was complemented and verified by a computational analysis of the lowest energy conformers.

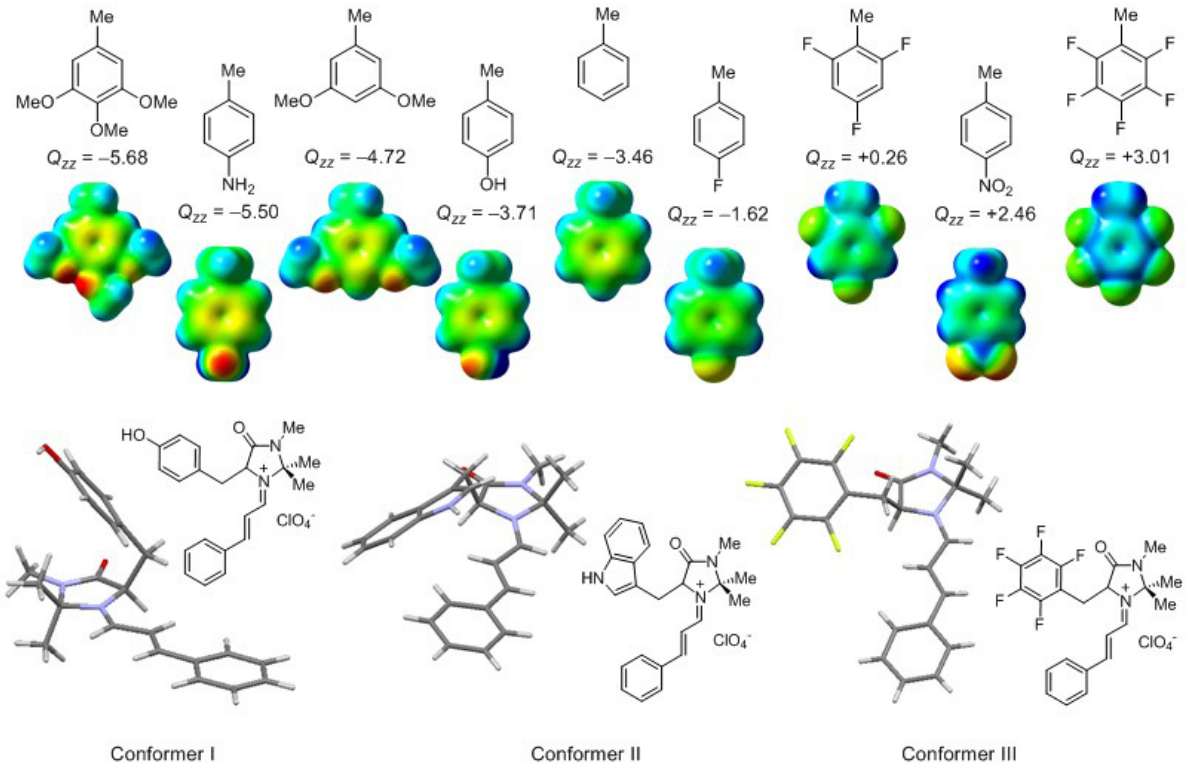

Figure 1 *Upper: ESP maps and Q_{zz} of the electronically modified shielding groups. Lower: X-ray structures of all three possible staggered conformers.*

The importance of the electronic nature of the shielding group was highlighted by the observed direct linear correlation between the obtained enantioselectivity in the Friedel-Crafts reaction of *N*-methyl pyrrole and (*E*)-cinnamaldehyde and the Q_{zz}. Furthermore, an improved catalyst was developed [R = $C_6H_2(OMe)_3$], enabling the reaction to be performed at RT within 3 h giving a selectivity of 94% *ee* [the MacMillan catalyst (R = Ph) gave 93% *ee* after 42 h at –30 °C].

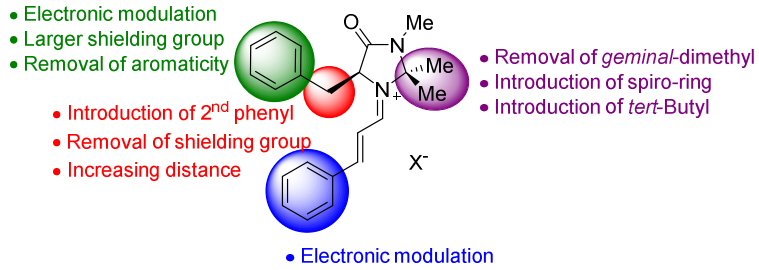

Figure 2 *Overview of MacMillan catalyst analogues.*

Further modifications of the catalyst were investigated as is summarised in Figure 2. It was found that the non-covalent interactions and consequently the observed enantioselectivities in the model reaction are not only sensitive to electronic modulations of the shielding group, but also to steric constraints of the shielding group (e.g., geometrical "fixation", enlargement, introduction of a 2nd phenyl group, and displacement) or the *geminal*-dimethyl group (e.g., deletion, replacement by spiro-rings). Electronic modifications of the substrate on the other hand only resulted in minor changes in conformational behaviour. Because determination of the Q_{zz} is not applicable to all compounds and the quantity requires computation, a spectroscopic quantity correlating with the observed *ee* was desired. The NMR shift-differences of the *syn*- and the *anti*-methyl groups of the *geminal*-dimethyl moiety ($\Delta\delta^1H_{syn/anti}$) were identified to be an adequate, easily accessible quantity that correlates beautifully with the conformational behaviour of the iminium salt and the enantioselectivity of the model reaction.

The accuracy of solid state and solution phase conformational analysis is bound to suffer from counterion, packing and/or solvent effects. Therefore, the conformational behaviour of a selection of isolated iminium ions was investigated by IR-MPD spectroscopy in the gas phase using the free electron laser FELIX at the Radboud University in Nijmegen. It should be noted that this is the first time this technique has been applied to the field of organocatalysis. It was demonstrated that the diagnostic conformations of these iminium

ions, which are a consequence of non-covalent interactions, give rise to characteristic fingerprint C=O stretching frequencies which can be directly observed by IR-MPD spectroscopy. Thus, by comparing the experimental spectra with the computed spectra for each computed minium structure, theory and experiment validate our working hypothesis and provide guidelines for catalyst design.

The organocatalytic Friedel-Crafts reaction of *N*-methyl indole and (*E*)-cinnamaldehyde was studied using the large imidazolidinone library. Trends observed for the reaction using *N*-methyl pyrrole were retained [correlation between obtained enantioselectivity and the Q_{zz} of the shielding group and the spectroscopically dertermined ($\Delta\delta^1H_{syn/anti}$)]. With catalysts proceeding *via* an iminium ion predominantly populating conformer **III**, reversal of selectivity was observed and a pincer-like model was proposed as explanation. This model also offers an explanation of the observed different behaviour of indoles as compared to pyrroles in the reaction.

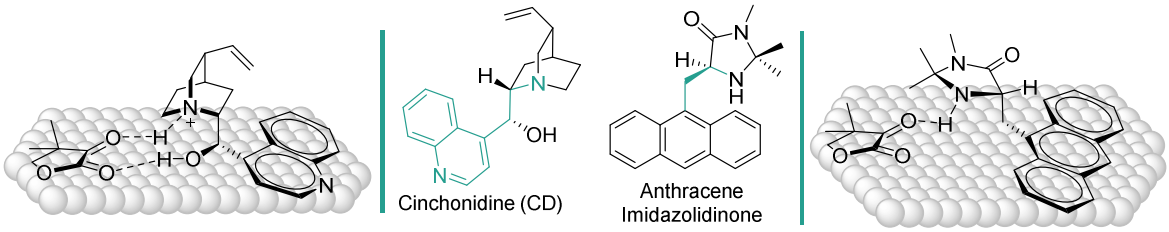

Figure 3 *Comparison of cinchonidine (CD) with MacMillan derivatives for heterogeneous catalysis and proposed surface binding.*

The structural resemblance of the MacMillan catalysts with cinchonidine (CD) led to the postulation that these species might be good chiral modifiers for heterogeneous hydrogenation reactions. The aromatic group of the molecule is expected to anchor to the metal surface, as is the case for CD, forming a chiral pocket in which the substrate is bound by the secondary amine moiety (Figure 3). It was anticipated that the catalysts equipped with a large, electron-rich aromatic groups (e.g., anthracene) would be especially promising. Even though in an initial screen these novel modifiers were not able to compete against the established CD, preliminary validation of the concept is presented. For example, application of the new modifiers in the reduction of ketopantolactone (KPL) on Pt/Al_2O_3 resulted in *ee*s between 16%-21% as compared to CD giving 40% *ee* under the same reaction conditions.

Zusammenfassung

Seit ihrer Neuentdeckung im Jahr 2000 hat sich die Organokatalyse, neben enzymatischen und metallorganischen Strategien, als dritte Säule der gegenwärtigen homogenen Katalyse etabliert. Das Forschungsgebiet hat sich rasant entwickelt und zahlreiche angesehene Forschungsgruppen haben zu der Entwicklung von vielfältigen, leistungsfähigen Organokatalysatoren beigetragen. Diese reichen von Biomolekülen über Thioharnstoffe bis hin zu *N*-heterocyclischen Carbenen (NHCs). Die zugrundeliegenden Prinzipien der asymmetrischen Induktion und die Mechanismen sind oft nicht gut verstanden und benötigen Aufklärung. Die meisten Organokatalysatoren bestehen aus den gleichen Bildungsblöcken, aus denen auch Biomoleküle aufgebaut sind und die reaktiven Intermediate werden oft durch die gleichen strukturellen Besonderheiten stabilisiert, die man von Enzymen kennt. In dieser Doktorarbeit wurde das MacMillan Imidazolidinon, einer der renommiertesten Organokatalysatoren, untersucht. Es wurde postuliert, dass die Stereoinduktion von nicht kovalenten Wechselwirkungen im Übergangszustand bestimmt wird.

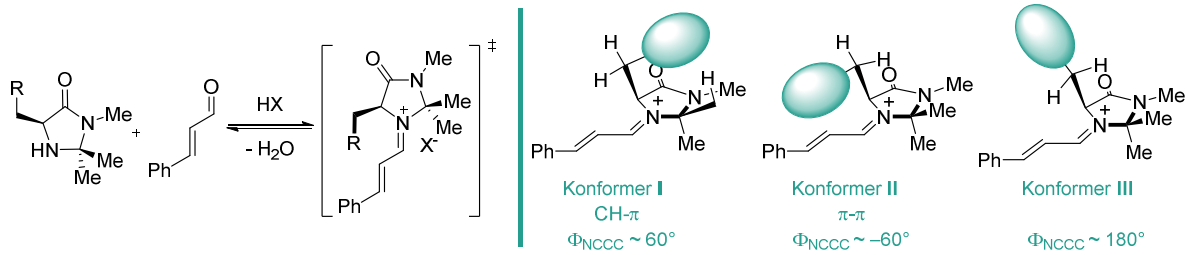

Schema 1 *Links: MacMillan's Katalysator der ersten Generation und das Iminiumionen Intermediat. Rechts: Drei mögliche gestaffelte Konformere des Intermediats.*

Die Imidazolidinon-Organokatalysatoren, die von MacMillan entwickelt wurden, haben sich als sehr effektiv in vielzahligen organischen Reaktionen, die über ein Enamin oder ein Iminiumion ablaufen, erwiesen. Das, durch Kondensation des Katalysators erster Generation mit einem α,β-ungesättigten Aldehyd entstehende, kurzlebige Iminiumion (Schema 1, links) ist geometrisch dazu optimiert, stabilisierende CH-π und π-π Wechselwirkungen ähnlich denen in Enzymen einzugehen und bietet somit ein ideales Model für Untersuchungen dieser Wechselwirkungen in einem kleinen Molekül. Um die essentiellen Bestandteile und Interaktionen für eine effektive Katalyseleistung zu identifizieren, wurden verschiedene Komponenten des Katalysators in einer molekularen Editierungstudie modifiziert.

Von strukturellen Studien von Biomolekülen weiß man, dass nichtbindende CH-π und π-π Wechselwirkungen empfindlich gegenüber elektronischen Modulationen sind. Das Iminiumionen Intermediat des von Phenylalanin abgeleiteten MacMillan Katalysators kann, abhängig von der Konformation, diese Wechselwirkungen eingehen (Schema 1, rechts). Es wurde untersucht, welche Auswirkungen elektronische Modifikationen der abschirmenden Phenylgruppe auf die Konformation, die Reaktivität und die Selektivität haben. Hierfür wurde eine Bibliothek neuer Katalysatoren synthetisiert, deren aromatische Gruppen von sehr elektronenreich [z.B. $R = C_6H_2(OMe)_3$] bis sehr elektronenarm (z.B., $R = C_6F_5$) spannen. Die spurlosen Quadrupolmomenttensoren senkrecht zum aromatischen Ring (Q_{zz}) wurden berechnet, um die elektronischen Eigenschaften der aromatischen Gruppen zu beschreiben und die ESP Abbildungen wurden berechnet, um die Elektronenverteilung widerzuspiegeln (Abbildung 1, oben). Mittels spektroskopischen Untersuchungen des Grundzustandes zusammen mit kinetischen und Katalysestudien, war es möglich zu zeigen, dass das konformelle Verhalten durch elektronische Modulation der Abschirmungsgruppe beeinflusst werden kann. Während Iminiumionen mit Abschirmungsgruppen die Phenyl elektronisch ähnlich sind bevorzugt Konformer **I** populieren, weisen elektronenreichere Derivate eine erhöhte Population von Konformer **II** auf. Dagegen resultieren elektronenarme Systeme in hoher Population von Konformer **III**. Erfreulicherweise wurde es errreicht von jedem der drei gestaffelten Konformere eine Kristallstruktur zu erhalten (Abbildung 1,

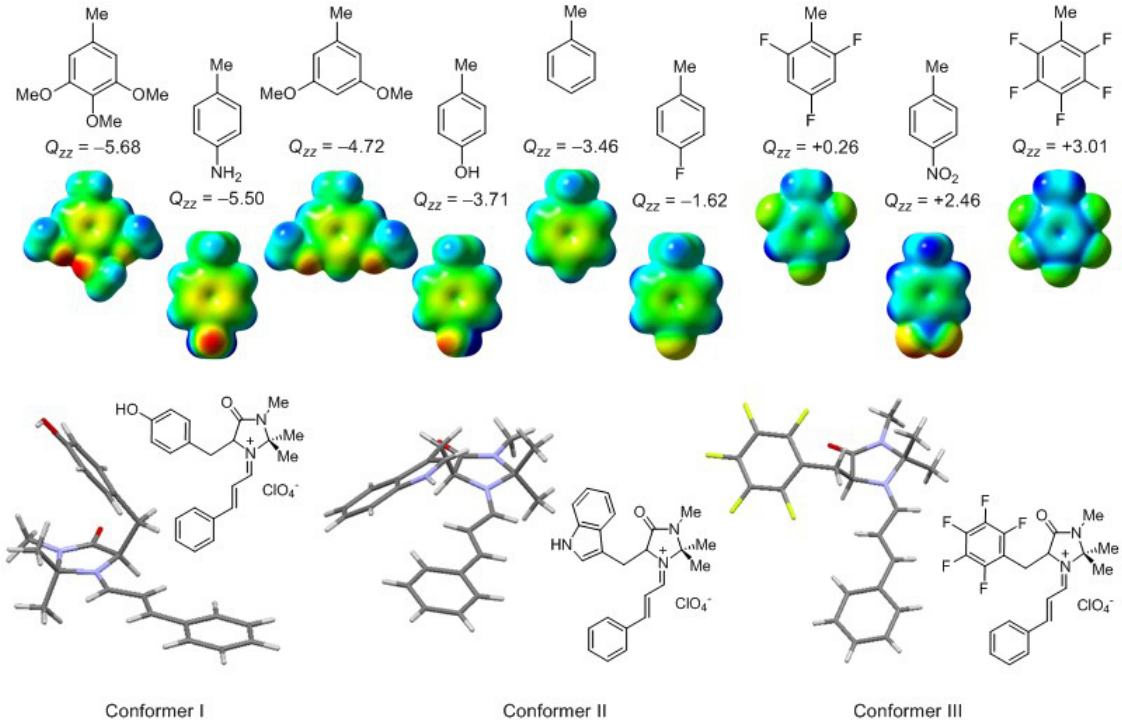

Abbildung 1 *Oben: ESP Abbildungen und Q_{zz} der elektronisch modifizierten Abschirmungsgruppen. Unten: Kristallstrukturen der drei gestaffelten Konformere.*

unten). Die Konformationsstudie wurde durch eine theoretische Analyse der energetisch niedrigsten Konformere ergänzt und verifiziert.

Eine beobachtete direkt-lineare Abhängigkeit zwischen den erhaltenen Enantioselektivitäten in der Friedel-Crafts Reaktion von *N*-Methyl Pyrrol und (*E*)-Zimtaldehyd und den Q_{zz} hebt die Bedeutung der elektronischen Eigenschaften der Abschirmungsgruppe hervor. Zudem wurde ein verbesserter Katalysator entwickelt [R = $C_6H_2(OMe)_3$], der es möglich macht, die Reaktion in 3 h bei RT mit einer Selektivität von 94% *ee* durchzuführen [der MacMillan Katalystor (R = Ph) führte zu 93% *ee* nach 42 h bei –30 °C].

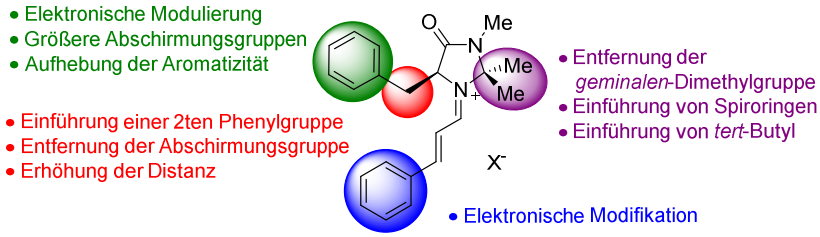

Abbildung 2 *Überblick über MacMillan Katalysatorderivate.*

Es wurden weitere Modifikationen des Katalysators untersucht (Abbildung 2). Dabei wurde entdeckt, dass die nichtbindenden Wechselwirkungen und somit die beobachteten Enantioselektivitäten nicht nur empfindlich gegenüber elektronischen Modifikationen der Abschirmungsgruppe sind, sondern auch gegenüber sterischen Einschränkungen der Abschirmungsgruppe (z.B. durch geometrische Fixierung, Vergrößerung, Einführung einer zweiten Phenylgruppe, Erhöung der Distanz) oder der *geminalen*-Dimethylgruppe (z.B. durch Entfernung oder Einführung von Spiroringen). Dagegen scheinen elektronische Modifikationen des Substrates nur geringen Einfluss auf das konformelle Verhalten zu haben. Da nicht für alle Verbinungen ein Q_{zz} bestimmt werden kann und diese Größe von theoretischen Berechnungen abhängig ist, wurde nach einer spektroskopischen Größe, die mit dem erhaltenen *ee* korreliert, gesucht. Die Unterschiede in der chemischen Verschiebung (NMR) der *syn*- und *anti*-Methylgruppen der *geminalen*-Dimethylgruppe ($\Delta\delta^1H_{syn/anti}$) wurde als hierfür geeignete, einfach zugängliche Größe identifiziert, die sehr gut mit dem konformellen Verhalten des Iminiumsalzes und der erhaltenen Enantioselektivität in der Testreaktion korreliert. Analysen von Festkörpern oder von Lösungen haben den Nachteil, dass Einflüsse von Gegenionen und/oder vom Lösungsmittel sowie Packungseffekte, nicht ausgeschloßen werden können. Deswegen wurde das Konformationsverhalten von einer Selektion von isolierten Iminiumionen in der Gasphase mit Hilfe von IR-MPD

Spektroskopie unter Verwendung des Freie-Elektronen-Lasers FELIX an der Radboud Universität in Nijmegen untersucht. Es sollte beachtet werden, dass dies die erste Verwendung dieser Analysemethode im Forschungsgebiet der Organokatalyse ist. Es wurde gezeigt, dass die spezifische Konformation eines Iminiumions, die eine Konsequenz der nichtbindenden Wechselwirkungen ist, charakteristische C=O Streckschwingungsfrequenzen im Fingerprintbereich bewirkt, die mit Hilfe von IR-MPD Spektroskopie beobachtet werden können. Durch Vergleich der experimentellen Spektren mit den theoretischen Spektren ein jeder Energieminimumsstruktur, war es möglich, Theorie und Experiment zu validieren und hilfreiche Richtlinien für zukünftiges Katalysatordesign zu liefern. Die organokatalytische Friedel-Crafts Reaktion von *N*-Methyl Indol und (*E*)-Zimtaldehyd wurde mittels der entwickelten Katalysatorbibliothek untersucht. Die Tendenzen, die in der Reaktion unter Verwendung von *N*-Methyl Pyrrol beobachtet wurden, konnten reproduziert werden [Korrelation zwischen der erhaltenen Enantioselektivität und dem Q_{zz} der Abschirmungsgruppe und der spektroskopisch bestimmten ($\Delta\delta^1H_{syn/anti}$)]. Mit Katalysatoren, die ein Iminiumion bilden, das bevorzugt Konformer **III** populiert, wurde eine Umkehr der Selektivität beobachtet und ein Pincer-artiges Model wurde zur Erklärung vorgeschlagen. Dieses Model liefert auch eine Erklärung für das beobachtete unterschiedliche Verhalten von Indolen und Pyrrolen in dieser Reaktion.

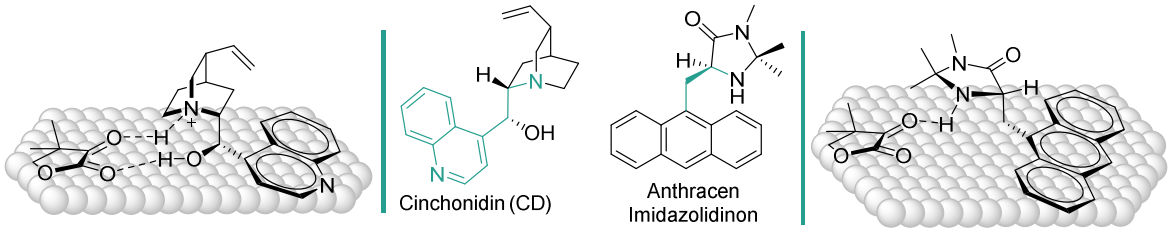

Abbildung 3 *Vergleich von Cinchonidine (CD) mit MacMillan Derivaten für heterogene Katalyse.*

Die strukturelle Ähnlichkeit der MacMillan Katalysatoren mit Cinchonidin (CD) führte zu dem Vorschlag, dass diese Strukturen gute chirale Modifikatoren für heterogene Hydrierungen sein könnten. Der Aromat des Moleküls könnte als Anker zur Metalloberfläche dienen, wie es für CD der Fall ist, und so eine chirale Tasche formen, in der das Substrat von dem sekundären Amin gebunden wird (Abbildung 3). Es wurde erwartet, dass Katalysatoren mit großen Aromaten (z.B. Anthracen) priviligiert sind. Obwohl die Imidazolidinone in einem ersten Screening nicht gegen CD konkurrieren konnten, wurde eine erste Validation der Idee präsentiert.

1 Introduction

1.1 Asymmetric Organocatalysis and Reaction Deconstruction

1.1.1 History and Overview

The field of asymmetric catalysis has traditionally been dominated by enzyme and organometallic catalysis. However, in 2000, two independent publications by List, Barbas, and Lerner and by Ahrendt, Borths, and MacMillan triggered enormous interest in the field of organocatalysis leading to the vast amount of methods available today.[8] It is surprising that organocatalysis did not emerge earlier when considering, that the first organocatalytic transformation (benzoin condensation catalysed by cyanide) was reported almost 170 years earlier by Wöhler and Liebig.[9] The term "*organische Katalysatoren*" however, has been proposed many years later by Langenbeck in 1928.[10] A selection of early, important contributions is summarised in Figure 4.[11]

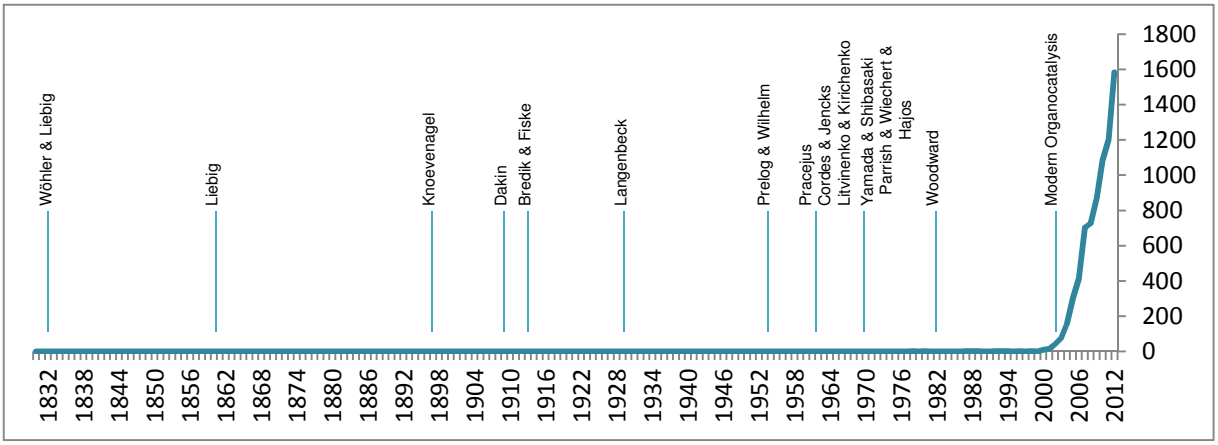

- **1832 Wöhler & Liebig:** Benzoin condensation.[9]
- **1860 Liebig:** Acetaldehyde as catalyst in synthesis of oxamide.[12]
- **1894/1896 Knoevenagel:** First iminium catalysed reaction.[13]
- **1886 Dennstedt/Zimmermann:** Isolation of acylated pyridine.[14]
- **1901 Verley/Bölsing:** Catalytic use of pyridine in acylation of alcohols.[15]
- **1909 Dakin:** Catalytic action of amino acids.[16]
- **1912 Bredik/Fiske:** First asymmetric reaction using cinchona base.[17]
- **1929/1937 Langenbeck:** Explanation of Liebig's 1860 observations / iminium ion catalysed conjugate addition.[1b;18]
- **1943/1958 Ukai/Breslow:** Structural and reactivity work on the mechanism of thiamine.[19]
- **1954 Prelog/Wilhelm:** Mechanism of asymmetric cyanohydrin synthesis.[20]
- **1960/1964 Pracejus:** First high levels of selectivity with cinchona alkaloids.[21]
- **1962 Cordes/Jencks:** Iminium catalysed transimination.[22]
- **1967/1969 Litvinenko/Kirichenko & Steglich/Höfle:** Discovery of DMAP as an acylation catalyst.[23]
- **1969 Yamada/Otani:** Proline-catalysed (stoichiometric) asymmetric Robinson annulations.[24]
- **1971 Eder/Sauer/Wiechert/Hajos/Parrish:** Catalytic, asymmetric aldol reaction using proline.[25]
- **1981 Woodward:** Total synthesis of erythromycin.[26]
- **1989 Jung:** Asymmetric Diels-Alder reactions of chiral alkoxy iminium salts.[27]

Figure 4 *Upper: Timeline highlighting the late emerge of organocatalysis, the y-axis refers to number of Sci-Finder hits for the term 'organocat'. Lower: Selected important, early contributions to the field of organocatalysis.*

A notable feature of organocatalysts is their bio-mimetic nature. The catalysts can activate the substrate covalently or by non-bonding interactions similar to the way in which enzymes bind substrates. Many organocatalysts are derived from the same building blocks as enzymes (i.e., amino acids), thus, it is hardly surprising that similar types of interactions are observed.[28] During intramolecularisation, a conformational change of the catalyst scaffold is often observed, leading to stabilisation of the reactive intermediate. An instructive comparison highlighting the parallels between enzyme and organocatalysis is the way in which proline binds carbonyl compounds reflecting the activation mode of type I aldolases, both forming reactive enamines (Figure 5).[29]

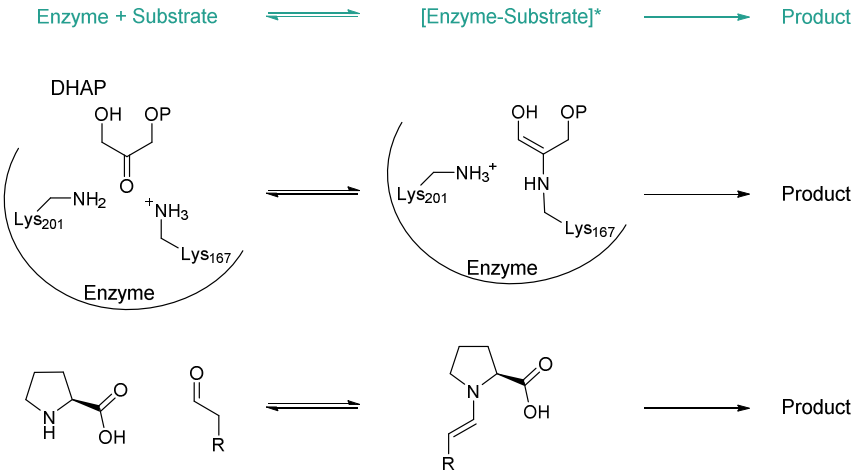

Figure 5 *Upper: General activation mode common to enzyme and organocatalysis. Middle: Activation mode of type I aldolase. Lower: Activation mode of L-proline.*

Highly enantioselective organocatalysts for various activation pathways have been developed and the major classes will be discussed herein. In Figure 6, catalysts engaging the substrate (generally a carbonyl compound) in a covalent manner are summarised. L-proline derived catalysts and MacMillan type catalysts are both secondary amines and have proven to be effective for the activation of carbonyl compounds for subsequent reaction with an electrophile, by forming an enamine (HOMO raising).[30] Alternatively, the secondary amines can condense with an α,β-unsaturated carbonyl system to give an iminium salt, activated for condensation with a nucleophile or a diene (LUMO lowering).[31] Furthermore, MacMillan type catalysts have recently been shown to successfully activate *meso*-cyclopropane carbaldehydes towards attack of a nucleophile.[32] Cinchona alkaloids carrying a primary amine are useful for stereoselective reactions proceeding *via* an enamine or an iminium salt.[33] Chiral dimethyl amino pyridine (DMAP)-analogues are especially valuable

for acyl-transfer and related reactions and function by activating the corresponding electrophile.[34] Finally, *N*-heterocyclic carbenes complement the library through an *Umpolung*-activation mode, activating formerly electrophilic carbonyl-moieties towards reactions with nucleophiles.[19b;35]

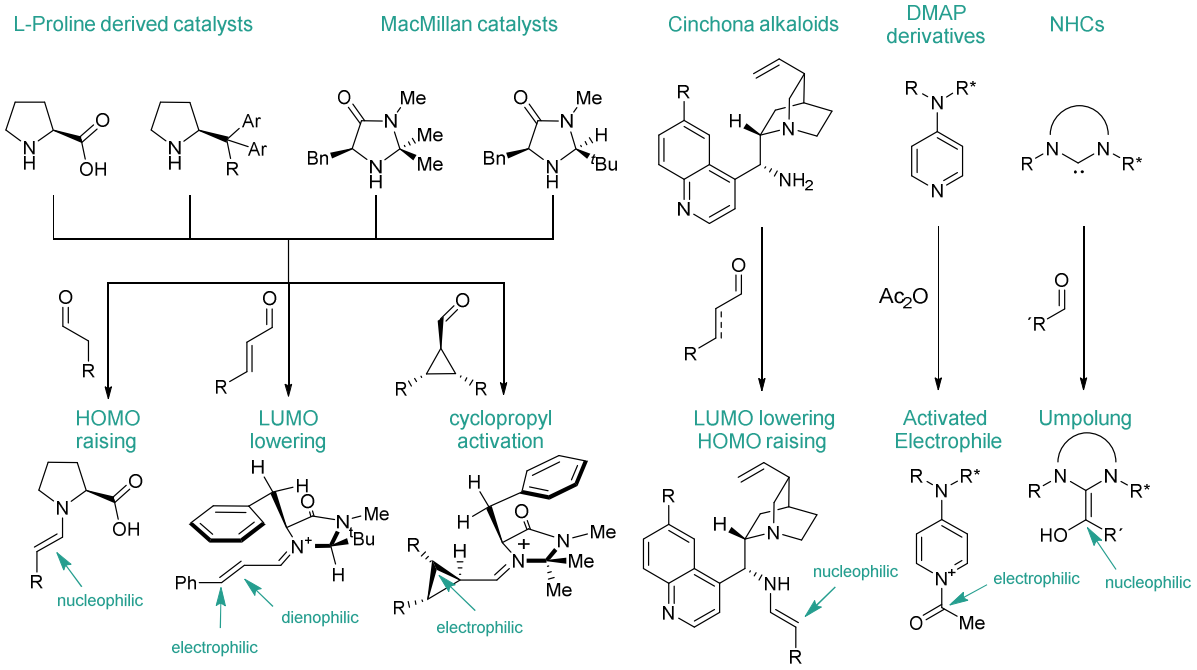

Figure 6 *Overview over the major classes of organocatalysts working via covalent activation modes and the corresponding reactive intermediates.*

Complementing covalent catalysis, a number of scaffolds for non-covalent catalysis have been developed (Figure 7). These include chiral thioureas introduced by Schreiner and co-workers and Jacobsen,[36] Brønsted acids pioneered by Akiyama and Terada[37] and chiral quaternary ammonium salts used as phase transfer catalysts.[38] Furthermore, carbohydrate derived organocatalysts such as the Shi epoxidation catalyst[39] and peptide derivatives[40] enrich this toolbox.

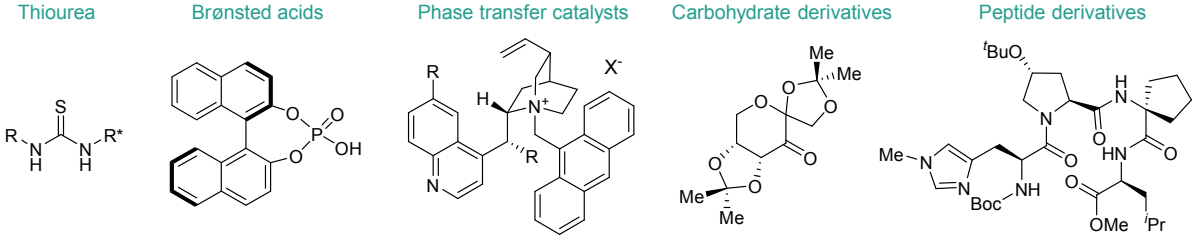

Figure 7 *Major classes of organocatalysts activating the substrate by non-covalent interactions.*

With the plethora of organocatalytic methods available today, research interests are now beginning to focus on mechanistic understanding of these processes. In contrast to the non-covalent processes, the organocatalytic reactions proceeding *via* a covalently bound catalyst-substrate complex form intermediates that are feasible to isolate. This allows for isolation and investigation of these structures by spectroscopic, crystallographic and kinetic techniques. By studying these important intermediates, organocatalytic reactions can be deconstructed and valuable insights into their conformational and reaction behaviour can be gained, ultimately leading to guidelines for rational reaction design. As the conformations of these intermediates are often governed by non-covalent interactions, an understanding of these interactions is crucial for reaction deconstruction. A short overview of the interactions important for the context of this thesis is therefore given in chapter 1.2. In the following section, mechanistic work on reactions proceeding *via* iminium salts derived from secondary amines and α,β-unsaturated aldehydes/ketones is discussed.

1.1.2 Deconstruction of Organocatalytic Reactions Proceeding *via* an Iminium Ion Derived from Secondary Amines and α,β-Unsaturated Aldehydes/Ketones

Intramolecularisation involving a secondary amine and an α,β-unsaturated aldehyde or ketone leads to the formation of an iminium salt, with concomitant lowering of the lowest unoccupied molecular orbital (LUMO, Figure 8, upper).[1c;41] This intermediate can readily interact with a number of different nucleophiles or dienophiles.[31] In the case of initial nucleophilic attack in the β-position, the transient enamine can be trapped, thus allowing for fast construction of molecular complexity by organo-cascade catalysis (Figure 8, lower).[42]

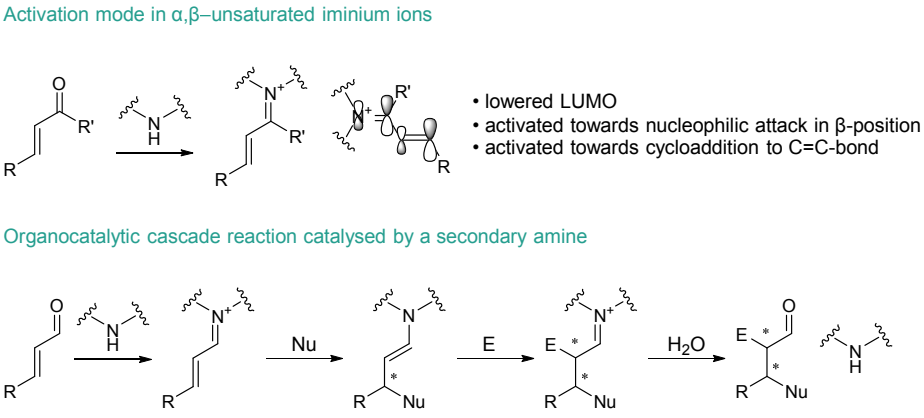

Figure 8 *Upper: Activation mode in α,β-unsaturated iminium ions.*
Lower: General sequence of an organocatalytic cascade reaction catalysed by a secondary amine

A number of secondary amine catalysts have been developed in the recent years. The most prominent examples are all related to L-proline or the L-phenylalanine derived MacMillan catalyst (Figure 9), rendering most of these catalysts readily available.

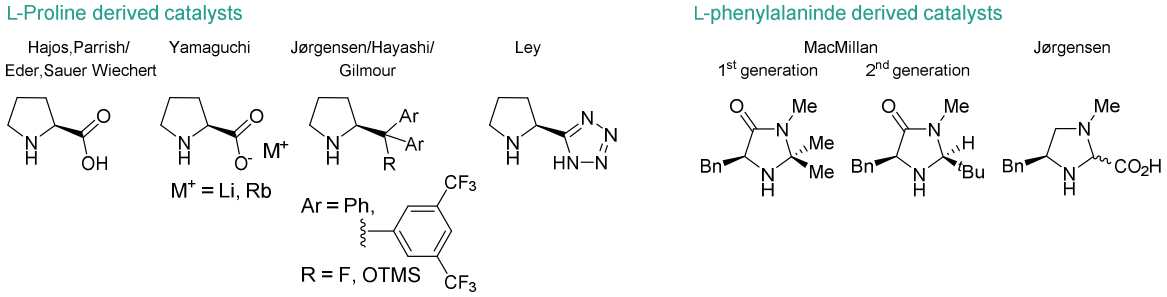

Figure 9 *Common secondary amine catalysts for iminium catalysis.*

Studies of iminium salts derived from L-diarylprolinol analogues:

L-diarylprolinol-derivatives have been introduced independently by Jørgensen and Hayashi in 2005 and since then found numerous applications in asymmetric organic synthesis.[43] Experimental structural insights into the corresponding iminium ion formed by condensation with (*E*)-cinnamaldehyde have been reported by Seebach and co-workers.[5;44] X-ray crystallographic analysis (Figure 10, left) and NMR studies suggested, that the conformation around the C=N^+-bond is predominantly (*E*) and that the facial shielding is provided by the silyl-group and one of the phenyl groups.[5] Recent mechanistic studies on the prominent diarylprolinol-catalysed (R = OTMS) Jørgensen epoxidation of α,β-unsaturated aldehydes by hydrogen peroxide have revealed that a secondary intermediate (peroxyhydrate) plays a crucial role in accelerating the reaction (Figure 10, centre).[6] Gilmour *et al.* developed diarylprolinol organocatalysts with a fluorine substituent instead of the silylether-moiety in the benzylic position.[7;45] In the corresponding β-fluoroiminium salt a stabilising fluorine-iminium ion *gauche* effect ($\sigma_{CH} \rightarrow \sigma_{CF}^*$ and $N^+ \cdots F^{\delta-}$) places the fluorine substituent in the *synclinal-endo* arrangement, thus directing one of the phenyl groups in the molecular space over the iminium chain. This working hypothesis was supported by crystallographic and spectroscopic analysis of several fluorine bearing iminium ions (Figure 10, right). Furthermore, the diphenylfluoroprolinol derivative was shown to be highly effective in enantioselective epoxidations and aziridinations.[45-46]

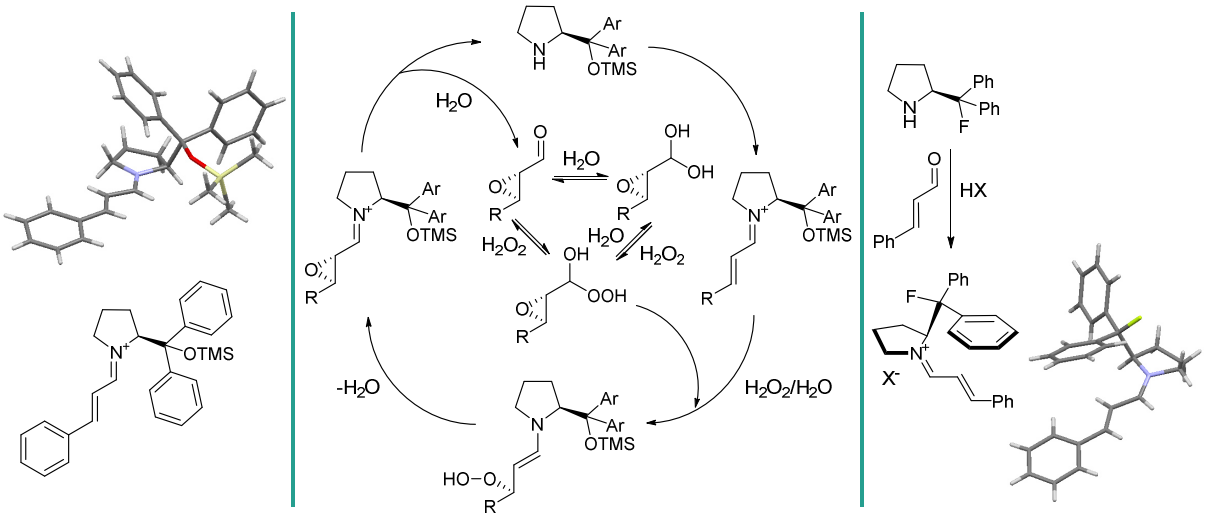

Figure 10 *Left: X-ray structure of the iminium salt of diphenylprolinol trimethylsilylether and (E)-cinnamaldehyde.*[5]
Centre: Proposed catalytic cycle for the Jørgensen-epoxidation.[6]
Right: Application of the fluorine-iminium ion gauche effect for molecular pre-organisation.[7]

Studies of iminium salts derived from MacMillan catalysts:

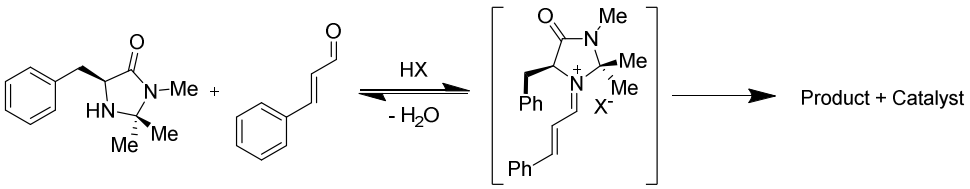

Figure 11 *1st generation MacMillan organocatalyst and the corresponding iminium ion generated by condensation with (E)-cinnamaldehyde.*

The 1st generation MacMillan catalyst (Figure 11) was originally reported in 2000 as catalyst for "*the first highly effective organocatalytic Diels-Alder reaction*".[8a] The seminal report by MacMillan *et al.* included a computational investigation of the corresponding α,β-unsaturated iminium ion using MM3-9 and proposed that the stereoinduction originated from selective formation of the (*E*)-conformation around the C=N$^+$-bond and selective positioning of the aryl shielding group over the iminium chain (conformer **II**, Figure 12, right). In general, the iminium ion formed from the imidazolidinone and, for example, (*E*)-cinnamaldehyde is a well-defined intermediate with a rigid geometry and only few degrees of freedom. The core five-membered ring is virtually flat as a consequence of the three sp^2-hybridised atoms, and the pendant iminium chain is fixed in the same plane. The *geminal*-dimethyl group is perpendicular to this plane, leaving the benzyl-moiety solely

responsible for discriminating the two faces. Of the three staggered conformers resulting by rotation around the benzylic bond, conformer **II** is presumably stabilised by a π-π interaction and conformer **I** was postulated to be stabilised by a CH-π interaction. In addition to the three possible staggered conformers, a fourth staggered conformer (**IV**) has been identified to be relevant (Figure 12, right).[47] The geometry around the N=C$^+$ was found to be (*E*)-selective (>95%, NMR studies), which was attributed to minimisation of A^{1,3}-type interactions.[1d;44a;48] These features are beautifully illustrated in the first reported X-ray structure of this iminium salt (Figure 12, left).[49] In the crystal structure, conformer **I** is adopted, in contrast to the conformation postulated by MacMillan, but consistent with higher level theoretical investigations and experimental studies.

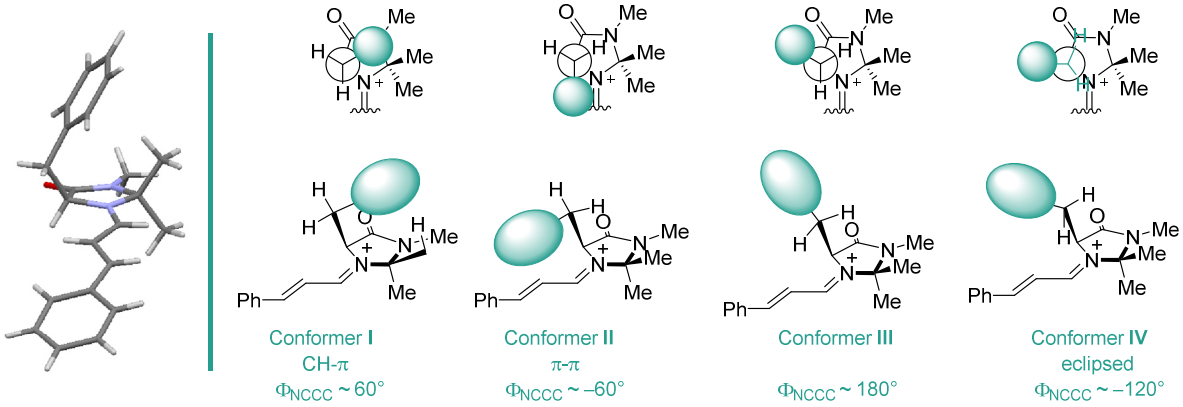

Figure 12 *Left: X-ray structure of the 1st generation MacMillan catalyst-derived iminium salt, counterion omitted for clarity. Right: Conformational diversity in the iminium salt.*

In a detailed theoretical conformational study by Houk, the global energy minimum of the MacMillan iminium ion derived from (*E*)-crotonaldehyde was found to be a structure stabilised by a CH-π interaction (conformer **I**), whilst conformer **II** was found to be 0.3 kcal/mol higher in energy. Conformers **IV** and **III** were found at +1.3 and +5.5 kcal/mol, respectively.[47] Tomkinson and co-workers also identified conformer **I** to be the global minimum of the (*E*)-cinnamaldehyde and reported an even larger energetic difference between conformer **I** and **II** (ΔE = 1.2 kcal/mol). Furthermore, they found that in the ^{1}H NMR spectrum the *syn*-methyl group of the *geminal*-dimethyl moiety is significantly shifted up field as compared to the *anti*-methyl group and attributed this to predominant population of conformer **I,** in which the phenyl group is shielding the *syn*-methyl group.[49] Further experimental and theoretical proof came from Seebach and a collaborative work by Seebach and Grimme, validating conformer **I** to be the global minimum structure.[50]

To probe the influence of the two low lying conformers **I** and **II**, this laboratory has developed geometrically fixed analogues by virtue of the fluorine-iminium ion *gauche* effect.[4] By introduction of a configurationally defined fluorine substituent in the benzylic position, two diastereoisomers were generated, functioning as so-called "*conformer equivalents*" (Figure 13). Addition of nucleophiles to these systems independently suggested that interplay of both conformers is important for high levels of selectivity. It was postulated, that conformation **II** is responsible for high levels of (*E*)/(*Z*) geometric control, while conformer **I** assures high levels of enantioinduction.

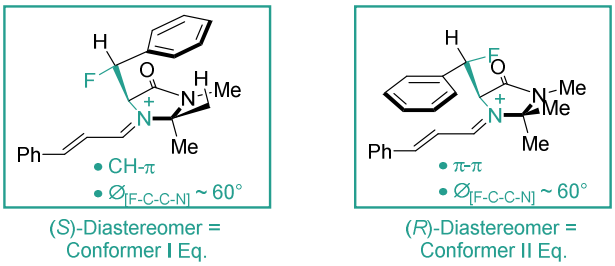

Figure 13 *Iminium ions of "conformer equivalents".*

This laboratory has also extended the concept of iminium catalysis to cyclopropyl iminium activation.[51] Key to this reaction design are the parallels that exist between cyclopropanes and olefins as a consequence of the Walsh orbitals and the reminiscence of the resulting cyclopropyl iminium ion to the cyclopropyl carbonyl cation. Enantioselective 1,3-dichlorination was achieved, thus extending the substrate scope of unsaturated carbonyl compounds through formal *Umpolung* of the γ-position (Figure 14).

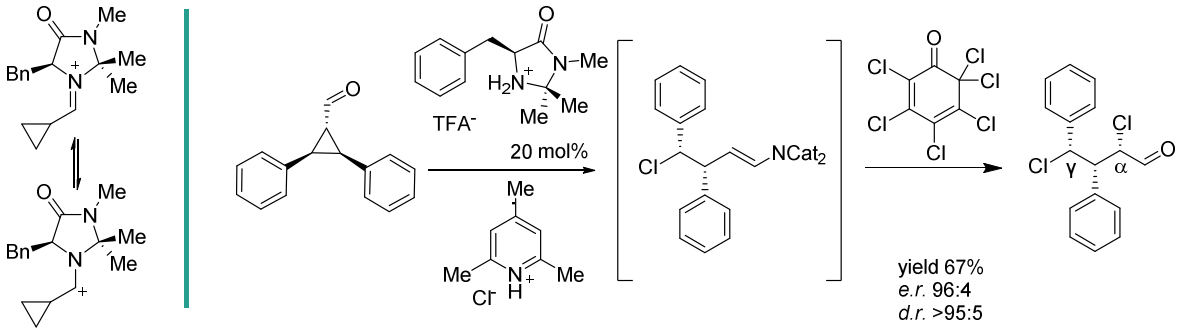

Figure 14 *Cyclopropyl iminium activation for the preparation α,γ-chlorinated aldehydes.*

In the 2nd generation MacMillan catalyst, the *geminal*-dimethyl group is replaced by a *syn*-*tert*-butyl group (Figure 15). While the 1st generation catalyst proved to be highly stereoselective in the Friedel-Crafts reaction of *N*-methyl pyrrole and α,β-unsaturated aldehydes, it only gave low levels of enantioinduction in addition reactions using less reactive *N*-methyl indole. For this transformation, the 2nd generation catalyst resulted in faster conversion and higher levels of enantioselectivity.[52] The increased reaction rates were attributed to the more exposed nitrogen lone pair, due to removal of the *anti*-methyl group. Furthermore, Mayr *et al.* reported in 2011, that the (*E*)-cinnamaldehyde derived iminium ion of the 2nd generation catalyst (Figure 15) is about 10^2 times more reactive than that of the 1st generation catalyst.[53]

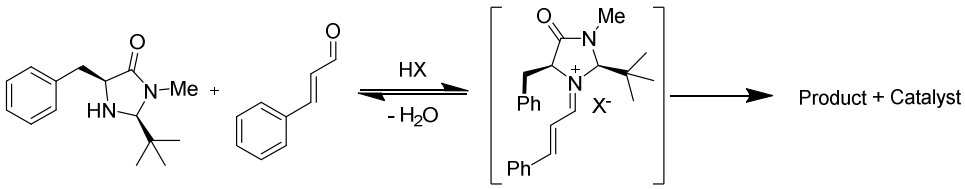

Figure 15 *2nd generation MacMillan organocatalyst and the corresponding iminium ion generated by condensation with (E)-cinnamaldehyde.*

Computational conformational analysis of the iminium ion by Houk[47] as well as by Seebach and Grimme[50b] indicated that conformer **II** is the global minimum, while conformer **I** is much higher in energy for this compound presumably due to steric repulsion between the aryl shielding group and the *tert*-butyl group. A second low lying conformer identified was conformer **IV**. Furthermore, Seebach and Grimme proposed conformers **II** and **IV** to be connected by an energetic plateau in their "*windshield-wiper*" model.

While the increased reaction rates when employing the 2nd generation MacMillan catalyst are well understood, the differences in stereoselectivity when changing from *N*-methyl pyrrole to *N*-methyl indole require clarification.

These small molecules present themselves as excellent platforms to study non-covalent interactions and these interactions have proven to play a significant role in catalysis.

1.2 Non-Covalent Aromatic Interactions

1.2.1 Overview of Chemical Bonding in Organic Chemistry

The existence of non-covalent interactions was first postulated by Van der Waals during his PhD studies in the 1870s.[54] He observed that attracting forces between gas molecules/atoms are responsible for the deviations in behaviour of real gases as compared to ideal gases. His studies revolutionised several fields of physics and chemistry and he was rewarded with the Nobel Prize in Physics 1910 "*for his work on the equation of state for gases and liquids*".[55] Non-covalent interactions, next to covalent bonds, are now accepted as the second most important form of chemical bonding in organic chemistry. These interactions are especially common and important in biology[56] and supramolecular chemistry,[57] as they are predominantly responsible for the secondary and tertiary structure of macromolecules and chemical recognition processes. The importance of stabilising non-covalent interactions to every other aspect of organic chemistry is also increasingly recognised. In organocatalysis for example, they have been exploited for hydrogen bonding catalysis.[28b;58] A common feature of non-covalent interactions is that they are less directional and have smaller bond energies than their covalent counterparts.[59] Even though individual contributions might be small, the cooperativity and additivity of several non-bonding interactions can accumulate, resulting in significant interactions. There are four categories of non-covalent interactions (Figure 16): Electrostatic interactions, Van der Waals forces, hydrophobic effects, and

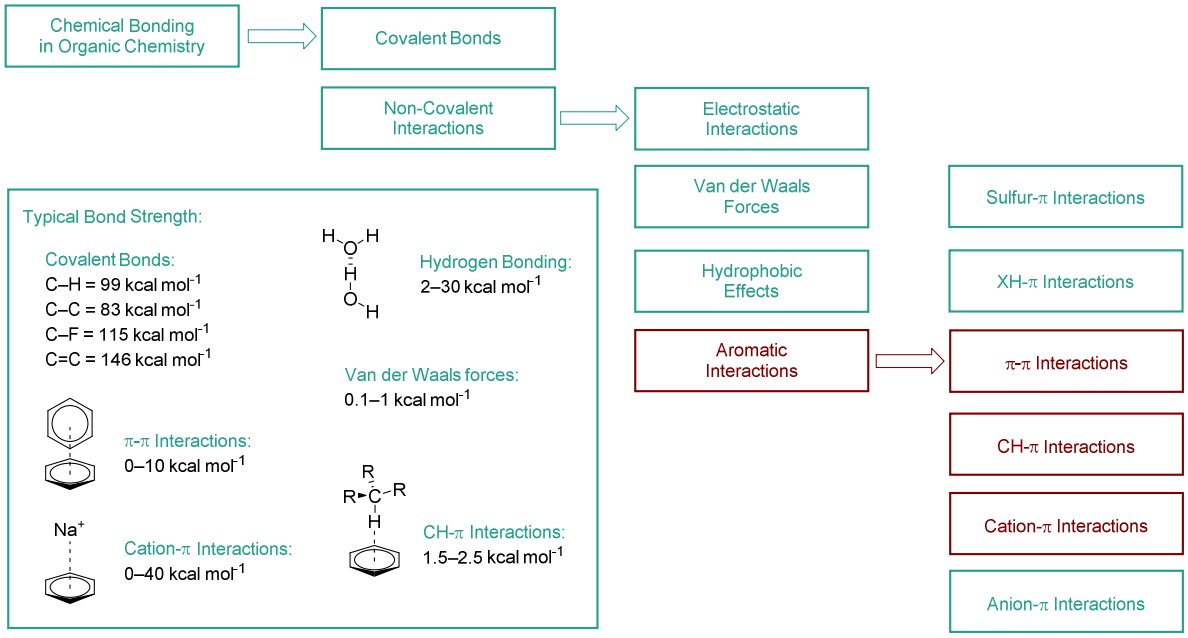

Figure 16 *Types of chemical bonding in organic chemistry. Left Box: Typical bond strength for a selection of interactions.*

aromatic interactions. Herein, only the aromatic interactions relevant for the content of this thesis will be discussed (Figure 16, red).

Aromatic interactions are attractive forces involving π-electron-rich systems and have been proposed to consist of all other three non-covalent interactions, i.e., electrostatic interactions, Van der Waals forces (dispersion and repulsion), and hydrophobic effects.[60] This complexity renders their investigation difficult, and the contribution of each force is still under debate.[61] Generally, the electrostatic component, which arises from the interaction of the quadrupolar moment, provides a good, simplified quantity for qualitative analyses of these interactions. The quadrupolar moment component perpendicular to the aromatic plane Q_{zz} describes the charge distribution resulting from the π-system above and below the plane (Figure 17). The Q_{zz} is discussed in greater detail in chapter 2.2.2. Benzene has an electron-rich π-cloud above the ring (negative Q_{zz}), which can undergo stabilising interactions with electron-deficient moieties (e.g., cations). By introducing electron-donating or electron-withdrawing substituents, the electron-density can be increased or decreased, respectively. Introduction of highly electron-withdrawing groups or several electron-withdrawing groups leads to inversion of the polarity, resulting in a positive Q_{zz}. Interestingly, the magnitude of the Q_{zz} of hexafluorobenzene is similar to that of benzene, but with opposite polarity.[60]

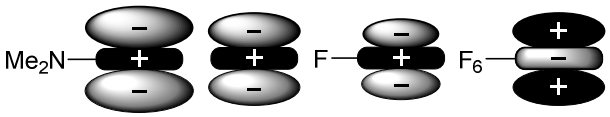

Figure 17 *Schematic representation of the charge distribution in benzene and benzene-derivatives*

The importance of non-covalent interactions has triggered research in this area, and numerous reports investigating individual aromatic interactions by rational design of small molecules have enriched the field.[62] Furthermore, many of these interactions have been studied computationally. Herein, exemplary highlights from both, experimental and theoretical, approaches will be described and examples of applications discussed.

1.2.2 Arene-Arene (π-π)-Interactions

Arene-arene interactions are of upmost importance in biology. The stacking interactions between the nucleotides in DNA are largely responsible for the formation of the double helix.[63] Furthermore, about 60% of the aromatic side chains in proteins have been reported to participate in arene-arene interactions.[64] The simplest and probably most studied π-π-interaction is the stacking between two benzene rings. It should be noted, that the term stacking is highly misleading since it has been demonstrated, that the face-to-face orientation is not the preferred situation for a benzene-dimer.[65] The three interaction geometries that have been computationally identified as energetic minima, are termed parallel-displaced, T-shaped edge-to-face, and eclipsed face-to-face (Figure 18): The first two are energetically more favourable. The face-to-face interaction was found to be 0.7–1.5 kcal/mol higher in energy, which is attributed to the repulsive interaction between the two negatively charged π-clouds. The interactions between benzene-dimers have been calculated to result in a stabilisation of –1.6 to –2.4 kcal/mol in the gas phase.[62a]

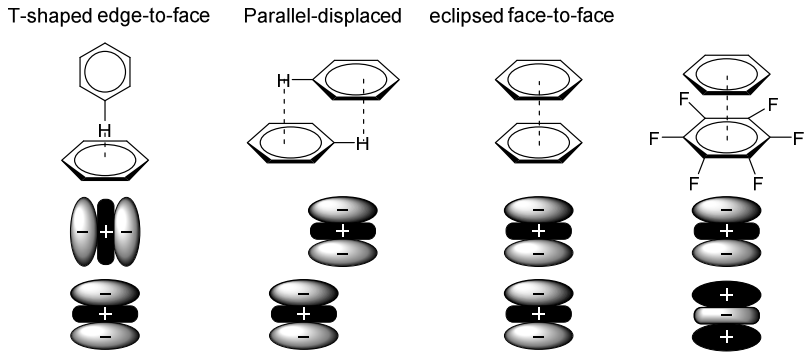

Figure 18 *Left: Interaction geometries of benzene dimers. Right: Interaction geometry of benzene with hexafluorobenzene.*

Similar observations were made for hexafluorobenzene dimers. However, the picture changes when looking at 1:1 mixtures of benzene and hexafluorobenzene. Instead of the parallel-displaced interaction observed for the two separate compounds, in the mixture an alternating eclipsed face-to-face orientation has been reported. The resulting crystalline mixture has a significantly higher melting point than either benzene or hexafluorobenzene (297 K as compared to 278 K for both).[66] This is a consequence of optimised interaction of the two opposing quadrupolar moments and C–H···F–C interactions.[67] The binding energy of one dimer has been calculated to be in the range of –3.7 to –5.6 kcal/mol.[68] Recently, the

heterodimer of indole and hexafluorobenzene has been calculated to also adopt the eclipsed face-to-face orientation.[69]

Several rationally designed synthetic receptors for the quantification of substituent effects and solvent dependencies have been reported in the literature. Examples include molecular balances[70], e.g., the molecular torsion balance developed by Diederich *et al.* for the investigation of edge-to-face interactions (Figure 19).[71] It was found that for the compound with R^1 = H the folding preference was essentially independent of R^2, while for the balance with R^1 = CF_3 a strong dependence on R^2 was observed and a clear correlation between the free enthalpy of folding (ΔG_{fold}) and the Hammett constant σ_m was observed. This observation was consistent in C_6D_6 and $CDCl_3$.

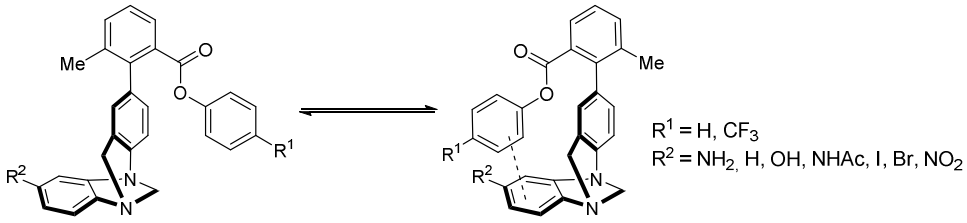

Figure 19 *Molecular balance reported by Diederich et al. for the quantification of arene-arene interactions.*

A clear correlation between the Hammett constant σ_m and barrier of rotation (ΔG_{rot}) has also been observed by Siegel and co-workers in their studies of parallel displaced interactions in substituted benzophenanthrenes (Figure 20).[72] They found that the rotation barrier increased with increasingly electron-withdrawing groups.

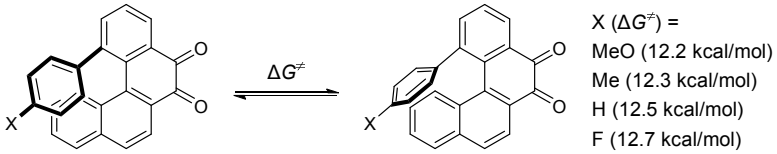

Figure 20 *Benzophenanthrene system developed by Siegel et al. for the investigation of parallel-displaced interactions.*

Another type of receptor developed for studying aromatic stacking interactions are molecular tweezers and clips for guest complexation.[73] The host-guest complexation only takes place, if stabilising non-covalent interactions occur. Among the most successful receptors are the tweezers developed by Kärner *et al.* (Figure 21)[74]. The electron-rich pre-organised structures were found to effectively bind electron-deficient aromatic systems and cations, while electron-rich arenes were not complexated.

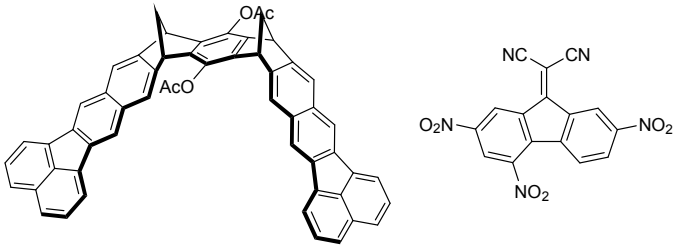

Figure 21 *Example of a host-guest system reported by Kärner et al.*

Hunter and co-workers have developed a multitude of thermodynamic, synthetic double mutant cycles for the quantification of free energy changes due to π-π-stacking and other non-covalent interactions.[75] Using the double mutant cycle shown in Figure 22, the group determined the magnitude of stabilisation resulting from one terminal edge-to-face π-π-interaction to be –0.3 kcal/mol. Free energies of π-π-interactions employing various substituted aryl moieties and heterocycles were quantified using this method.[75] A general trend observed is that the magnitude of interaction increases with increasing electron-density difference of the two interacting aromatics. This method has also been applied for the quantification of other non-covalent interactions including cation-π,[76] halogen-π,[77] and carbohydrate-π interactions.[78]

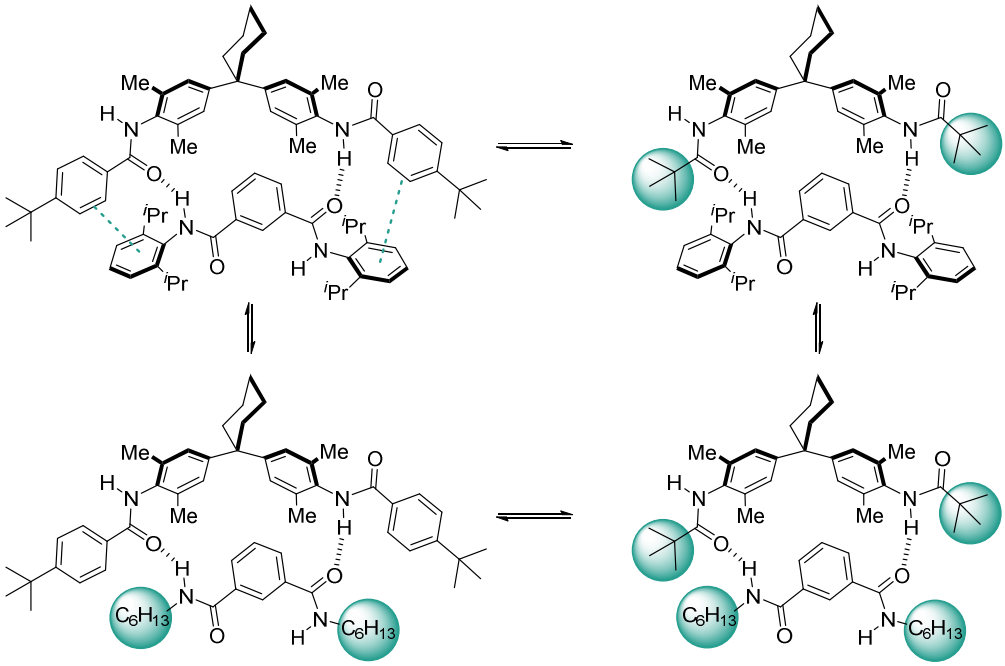

Figure 22 *Double mutant cycle for the quantificcation of two terminal edge-to-face π-π-interactions.*

Substituent effects have also been extensively studied by computational methods. For the face-to-face geometry monosubstituted dimers were found to be generally more stable than the parent benzene-benzene dimer independent of the electronic nature of the substituent.[79] In the face-to-edge orientation, *para*-substitution of the edge-component led to stabilisation only in the case of electron-withdrawing substituents, while electron-donating substituents resulted in the opposite effect.[80] Houk and co-workers have reported, that direct electrostatic interactions between the substituents on one arene with the other arene govern how the substituents influence the electron density and, thus, the π-π-stacking interaction. The strength of these direct interactions was also found to correlate with the Hammett constant σ_m.[81]

Understanding π-π-stacking interactions is not only important for unravelling biological processes, but also for protein design[82] and development of novel materials,[83] and highly selective organic synthesis protocols.[84] One of the best studied systems for stereoselective synthesis utilising a π-π-stacking interaction is the chiral auxiliary 8-phenylmenthol developed by Corey and co-workers.[85] The auxiliary has proven powerful among other transformation for the asymmetric Diels-Alder reaction of its acrylate esters as has beautifully been shown in the Coreys synthesis of prostaglandins. The asymmetric induction has been shown to be due to π-π-stacking interactions between the arene and the enoate by computational,[86] crystallographic[87] and spectroscopic analyses.[88]

1.2.3 CH-π Interactions

First postulated in 1952 by Tamres *et al.*[89], the CH-π interaction is ubiquitous in organic molecules. A crystallographic database study revealed that >29% of organic compounds[90] and >42% of the peptide structures[91] bearing at least one aryl ring exhibit at least one CH-π interaction and that this interaction is crucial for numerous supramolecular host-guest complexes.[92] Evidence for this interaction has also come from spectroscopic, thermodynamic, and bond critical point analysis.[93] Much debate is found in the literature on the classification of this weak interaction. Originally described as soft base-soft acid hydrogen bond,[94] it has been suggested that the CH-π interaction should not be classified as a hydrogen bond since electrostatic components are less important and dispersion components are more important than for XH-π interactions.[62b;95] However, the electrostatic component (dipole/quadrupole and charge-transfer interactions) is important for the directionality of the interaction and numerous reports support the hydrogen bond nature of the interaction.[94;96] Thus, herein the CH-π interaction will be treated as special form of hydrogen bond.

A special feature of the CH-π interaction is that it is operational in polar as well as in nonpolar solvents, which is a consequence of the large contribution of the dispersion energy.[94] As mentioned, the directionality of the interaction is crucial and is dominated by electrostatic interactions, thus differentiating the CH-π interaction from London dispersion forces. The simplest example, the methane-benzene dimer has been studied by Sakaki *et al.*[97] In the preferred conformation the methane is positioned on the axis perpendicular to the centre of the benzene ring with one C–H bond oriented towards the arene (Figure 23, **a**). The stabilisation for this conformation was calculated to be –0.57 kcal/mol. The second lowest conformation was found to be only slightly less stabilising (–0.49 kcal/mol, **b**).

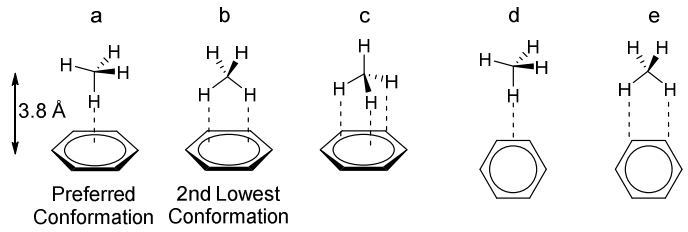

Figure 23 *Selection of possible conformers for methane-benzene dimers.*

In a recent publication by Tsuzuki using a different level of theory and a larger basis set, the same conformational preferences were found, but larger interaction energies were postulated (–1.45 and –1.23 kcal/mol for **a** and **b**, respectively).[98] The optimal distance between the hydrogen donor carbon and the hydrogen acceptor aryl was found to be 3.8 Å. Furthermore, the interaction energy with benzene was found to increase with increasing acidity of the hydrogen in the series of ethane, ethylene, and acetylene. Similar trends have been observed in other computational analyses[96a;96c;99] and as a rule of thumb it can be concluded that the stronger the proton donating ability of the CH group, the larger the stabilising effect of CH-π interactions.

As a consequence of the weak and poorly directional nature of the CH-π interactions, they have primarily been studied by computational analyses and in crystal structures. Recently, Carroll and co-workers have reported a series of molecular balances for quantification of CH-π interactions by solution phase NMR analyses (Figure 24).[100] This report highlights how delicate these interactions are and how difficult experimental quantification is.

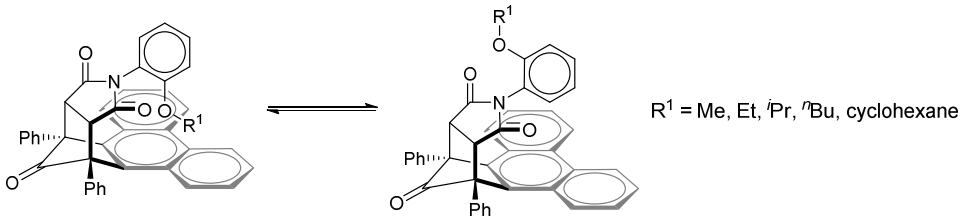

Figure 24 *Molecular balance developed by Carroll et al. for the quantification of CH-π interactions.*

A second molecular switch based on proline containing peptides has been reported by Zondlo (Figure 25).[101] The authors found that the population-ratio of *cis* and *trans*-configured amide bond is tunable by electronic-modification of the aryl moiety, and that systems containing more electron-rich aromatic groups show a higher population of the *cis*-conformer. When employing *para*-substituted phenylalanines, a correlation between the Hammett constant σ_m and the *cis*/*trans*-ratio was observed. This report supports the notion that CH-π interaction strength are not only dependent on the acidity of the CH-donor, but also on the electron-density of the aromatic hydrogen-acceptor.

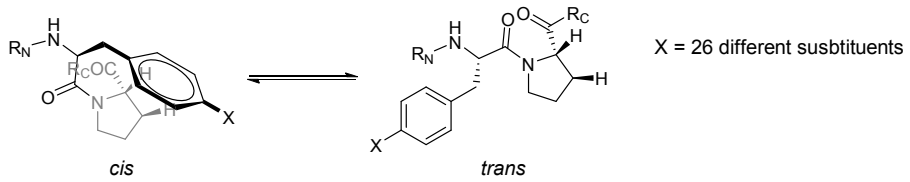

Figure 25 *Peptide structure developed by Zondlo exhibiting tunable CH-π interactions.*

Carbohydrate recognition is one of the most important applications of the CH-π interaction.[102] Another beautiful application has been reported by Martín and co-workers. The authors achieved chiral recognition of amino acid derivatives with a synthetic receptor. Analysis using a double mutant cycle proposed that 70% of the enantioselectivity is caused by a single CH-π interaction.[103] In the last decade, several reports have suggested the importance of a CH-π interaction for facial discrimination in reactions catalysed by the 1st generation MacMillan catalyst (see chapter 1.1.2).

1.2.4 Cation-π Interactions

Cation-π interactions are stabilising interactions between the face of an electron-rich π-system and an adjacent cation.[104] First experimental support for these interactions came from mass spectrometry and ion cyclotron resonance studies in 1981 and the following years.[105] These studies postulated strong interactions between cations like K^+ and NH_4^+ with simple aromatics. Furthermore, it was established that several of these interactions are of similar strength as the corresponding cation-water interactions (e.g., K^+–H_2O was found to have an interaction energy of 18 kcal/mol, while the one for K^+–benzene was found to be 19 kcal/mol). It is now widely established that cation-π interactions are ubiquitous in nature and play important roles in protein-DNA binding and protein-protein interactions.[106] Especially prevalent are interactions between the aromatic amino acids Phe, Tyr, and Trp and protonated amino acid side chains (i.e., Arg, His^+, Lys) and neurotransmitters (Acetylcholine, GABA, and serotonin).[106b] The geometry of the interaction has been studied computationally and it has been shown that the cation is placed over the centroid of the aromatic ring (Figure 26).[104a] It has been postulated, that the dominating force in cation-π interactions is the electrostatic component (cation-quadrupole interaction). One of the trends supporting this notion is that smaller ions exhibit stronger affinity (Figure 26).[106d] Thus, a good qualitative evaluation of these interactions can be achieved by studying the

electron surface potential maps (ESP) of the aromatic moiety. The cation affinity is strongest at the most electron-rich position of the π-system. Another important feature of these interactions is that they are generally much stronger than other non-covalent interactions. Recent work by Houk and co-workers postulated, that effects of substituents to the aromatic part of the interacting dimer arises due to through-space effects of the substituent and not due to polarisation of the π-system.[81;107]

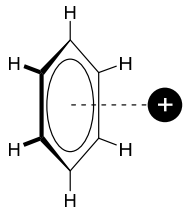

Cation	Binding Energy (-ΔH)
Li^+	38 kcal/mol
Na^+	28 kcal/mol
K^+	19 kcal/mol
Rb^+	16 kcal/mol
NH_4^+	19 kcal/mol
NMe_4^+	9 kcal/mol

Figure 26 *Orientation of the Cation-π interaction and selection of gas phase binding energies.*

Cation-π interactions have extensively been studied by Doughtery and co-workers.[104a] The group has developed a series of cyclophane hosts which were able to complex numerous cations in aqueous media, thus demonstrating the strength of the interaction. An example of such a cyclophane and complexed cations is shown in Figure 27.

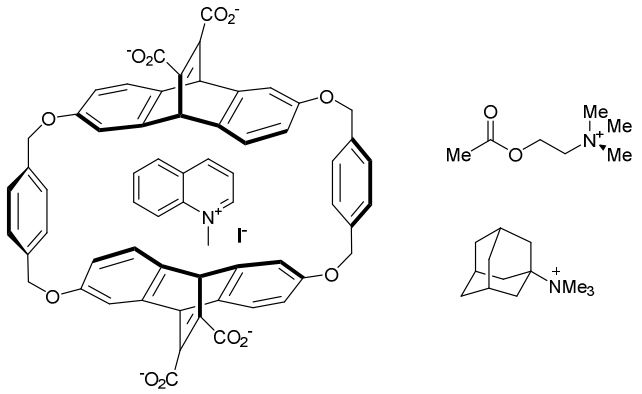

Figure 27 *Cyclophane hosts developed by Doughtery and examples of guests.*

Valuable contributions to the development of artificial receptors for cation complexation have also come from the groups of Schneider[108], Lehn[109], and others,[104a] but will not be discussed further.

Several examples of cation-π interactions in organocatalysis have been reported in the literature. Jacobsen and co-workers have developed several hydrogen-bond donor catalysis protocols, for which the enantioselectivity of the transition state is achieved by cation-π

interactions.[28b;110] Recently, *ab initio* calculations of the α,β-unsaturated iminium ion derived from the 2nd generation MacMillan catalyst by Yamada *et al.*[111] suggested, that a cation-π interaction stabilises the lowest energy conformer. Furthermore, this study reported that introducing an electron-donating *para*-substituent to the shielding aryl group leads to increase of the interaction strength, while electron-withdrawing substituents exhibit the opposite effect.

2 Molecular Editing of the MacMillan Catalyst Derived Iminium Ion Intermediate

2.1 Introduction

2.1.1 The MacMillan Catalyst

The L-phenylalanine-derived imidazolidinone catalyst **1** (Figure 28) developed by MacMillan *et al.* was introduced in 2000 as the first highly enantioselective organocatalyst for the enantioselective Diels-Alder reaction.[8a] More importantly, this publication formalised the notion of iminium ion catalysis, an activation mode that is used frequently in the rapidly evolving field of organocatalysis. Although the seminal example of what is now termed iminium ion catalysis was reported as early as 1894 by Knoevenagel[13] (see chapter 1.1.1), MacMillan was the first to describe iminium ion activation in more general terms as a LUMO-lowering phenomenon, thus making parallels to Lewis acid catalysis. The introduction of this seminal report has let to considerable increased interest in this field and a large number of related transformations have since been developed.[31] Consequently, not only various reactions proceeding *via* an iminium ion have been developed,[52;112] but also several transformations proceeding *via* the enamine,[113] and SOMO[114] activation have been described. The mode of activation, along with previous work on structural and mechanistic aspects of the MacMillan catalyst, is discussed in the introductory part of this thesis (see chapter 1.1.2).

2.1.2 Conformational Diversity in the MacMillan Catalyst Derived Iminium Salts

Organocatalysts operate by similar mechanisms as have been formalised for general enzyme catalysis (Figure 28).[115] The catalyst, in this case the imidazolidinone **1**, binds the substrate, in this case condensation with (*E*)-cinnamaldehyde **2**, causing a conformational change. In a second step, the bond forming process takes place, and then the product is released (by hydrolysis). The catalyst is hereon available for the next cycle. For reactions proceeding *via* a reactive intermediate, the transition-state can be assumed to closely resemble this intermediate (Hammond-Leffler postulate).[116] Consequently, the origin of selectivity can be explored by studying the isolatable iminium ion **1a**.

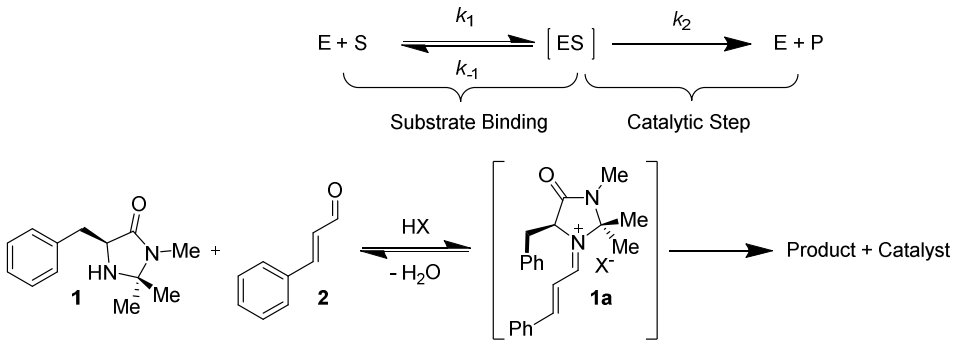

Figure 28 *Parallels in the mechanisms of enzyme and iminium ion catalysis.*

The iminium ion intermediate **1a** is rigid with only few degrees of conformational freedom.[4;8a] The core imidazolidinone ring is virtually planar due to three sp^2-hybridized atoms in the five-membered ring. The bound substrate also lies flat in this same plane with the *geminal*-dimethyl group being perpendicular. Only the aryl shielding group discriminates between the two faces of the planar electrophile. These features are beautifully illustrated by the crystal structure of the iminium ion **1a** derived from the 1st generation MacMillan catalyst **1** and *trans*-cinnamaldehyde **2** by Tomkinson *et al.* (Figure 29, left).[49] For effective catalyst performance, the (*E*)/(*Z*)-geometry of the C=N$^+$ iminium bond must be controlled. It was reported in a computational study by Houk, and in experimental studies by Mayr, Seebach, and Gilmour, that the (*E*)-isomer is selectively formed to avoid $A^{1,3}$-type allylic strain between the pendant iminium chain and the *geminal*-dimethyl group (Figure 29, right).[1a;1c;1d;117]

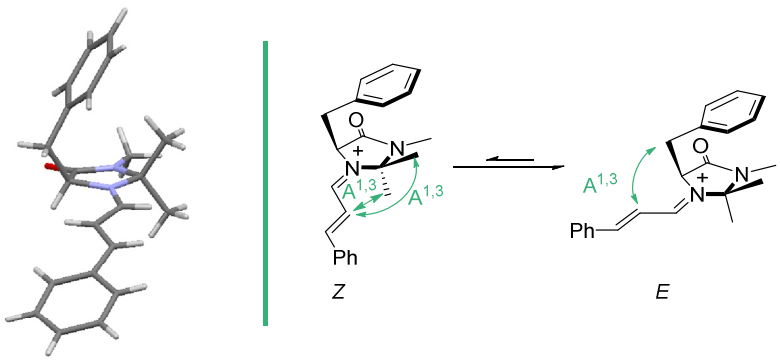

Figure 29 *Left: X-ray structure of* ***1a*** *as the PF_6^- salt. The counter ion has been omitted for clarity. Right: Selective formation of the (E)-isomer due to $A^{1,3}$-allylic strain.*[1]

The facial selectivity of the MacMillan-catalyst promoted reactions proceeding through an iminium ion intermediate must largely be induced by the aryl shielding group. Rotation around the benzylic C–C bond leads to three possible staggered conformers (Figure 30).

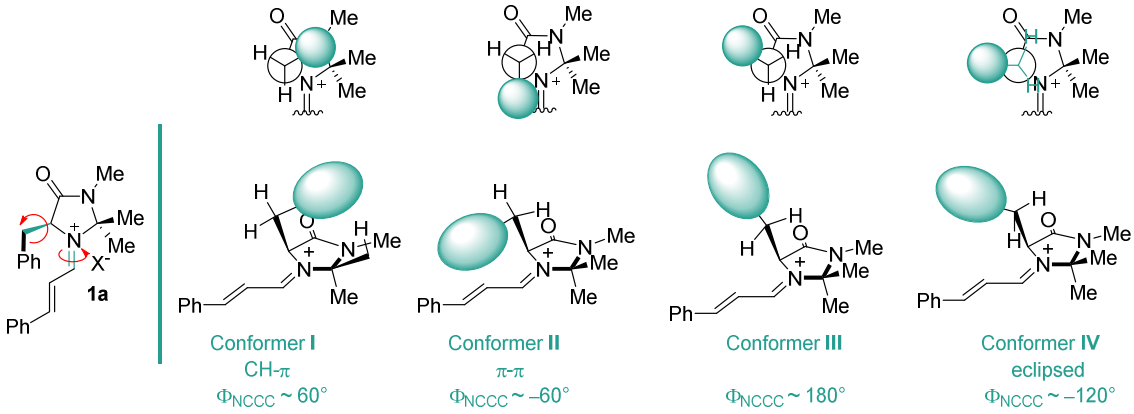

Figure 30 *Four possible low-energy conformers of the MacMillan catalyst derived α,β-unsaturated iminium ion* ***1a****.*

Conformer **I** is predisposed to undergo a stabilizing CH-π interaction with the *syn*-methyl group and has been reported to be the global energy minimum.[1a;47;50b] This is consistent with the solid state structure identified by X-ray crystallographic analysis (see Figure 29). Conformer **II**, which was originally reported by MacMillan to be the predominantly populated conformation,[8a] is presumably stabilised by a π-π interaction between the aryl shielding group and the iminium chain. The third staggered conformation with the aryl group pointing away from the reaction centre (conformer **III**), was found to not be an energetic minimum by Houk[47] as well as Seebach and Grimme.[50b] A third conformer that has been proposed by computational analysis is conformer **IV**, in which the shielding group eclipses with the adjacent hydrogen. A more detailed discussion on previous studies can be found in chapter 1.1.2.

2.1.3 Project Overview

Whilst the MacMillan catalyst **1** is now widely established as a highly efficient and broadly applicable catalyst for iminium activation, the mode of enantioinduction remains to be clarified. Iminium salts are attractive candidates for reaction deconstruction as their covalent nature allows for isolation and analysis. It was envisaged that a detailed, logical molecular

editing study of the intermediate iminium ion **1a** would assist in identifying which features and interactions are essential for effective catalyst performance, and ultimately lead to a better understanding of the catalytic behaviour. Moreover, the postulated stabilising non-bonding CH-π and π-π interactions associated with the MacMillan catalyst derived iminium ions (Figure 30)[1a;3;44a;47;49-50;111;118] mirror those found in many biomolecules,[28b;106b;106e;119] providing an excellent platform to study these important interactions in a small molecule. Conversely, one can exploit advances in structural biology and supramolecular chemistry regarding intra- and intermolecular interactions and employ them in the design of highly selective organocatalysts. It was of particular interest in this work to investigate how the modifications would influence conformational and kinetic behaviour and to find general guidelines for catalyst design derived from our findings. The sites of the catalyst, which were investigated are summarised in Figure 31. Experimental designs and results are discussed separately for each site in the following chapters. In chapter 2.2 the consequence of electronically modulating the shielding aryl group by substituent variation is discussed in detail. It is known that CH-π and π-π interactions are sensitive to electron-density, thus it was expected that the polarity of the aryl group is determinant for conformational behaviour.

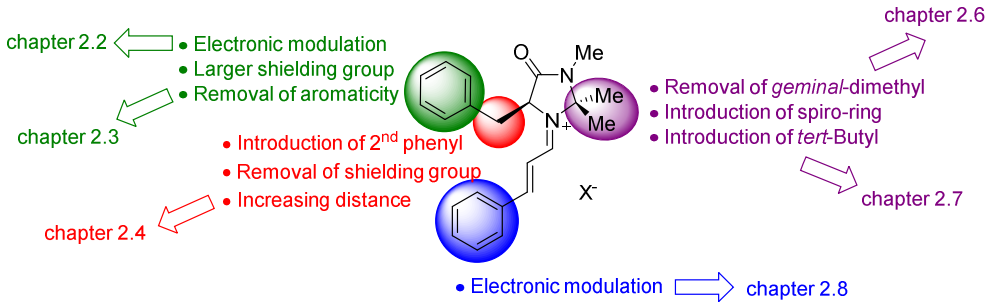

Figure 31 *An overview of the molecular editing study of the MacMillan catalyst derived iminium salt* ***1a****.*

In the following chapter 2.3, additional modifications of the aryl group are discussed. The necessity of an aromatic shielding group was envisaged to be proven by studying the saturated cyclohexyl analogue. Furthermore, it was investigated how extension of the aromatic system and employment of heterocycles would influence catalyst behaviour. Next, the benzylic position was investigated (chapter 2.4). To explore the influence of steric bulk, the number of aryl shielding groups was varied. The flexibility of the system was enhanced by increasing the distance between the shielding group and the imidazolidine moiety. Also the results of introducing fluorine in the benzylic position to generate "*conformer equivalents*" are addressed.[4] In chapter 2.6, differently sized spiro rings were introduced in

place of the *geminal*-dimethyl group to study the influence of geometric control on the ability of the system to undergo CH-π interactions. Additionally, the dimethyl group was removed, which was expected to be destructive on the control of iminium ion bond geometry. Subsequently, a series of second generation catalysts with a *tert*-butyl group instead of the *geminal*-dimethyl group is looked at (chapter 2.7). In chapter 2.8, the electronic modification of the substrate´s aryl ring by substituent variation is studied. It was expected that the kinetic behaviour of the iminium ions will be especially sensitive to electronic modulation of the bound substrate. This has also been verified by Mayr *et al.* during the course of the herein reported study.[120]

2.2 Electronic Modulation of the Shielding Group

In recent years, evidence implicating that CH-π and π-π interactions stabilise conformers **I** and **II**, respectively, (Figure 32, upper) of the transient iminium ion formed by condensation of the MacMillan catalyst with an α,β-unsaturated aldehyde, has been reported.[1a;3;44a;47;49-50;111;118] From structural biology studies it is established that these interactions are sensitive to electronic alterations of the π-system or in its vicinity.[82;106a;106c;121] For a detailed discussion of non-covalent aromatic interactions see chapter 1.2. It was envisaged, that by introducing electron-donating or electron-withdrawing groups to the shielding aryl group, the conformational preferences and consequently catalytic performance could be modulated. For this purpose, a library of electronically modified MacMillan-type imidazolidinones was synthesised, ranging from highly electron-rich (**3**) to highly electron-deficient (**10**) aromatic systems (Figure 32, lower).

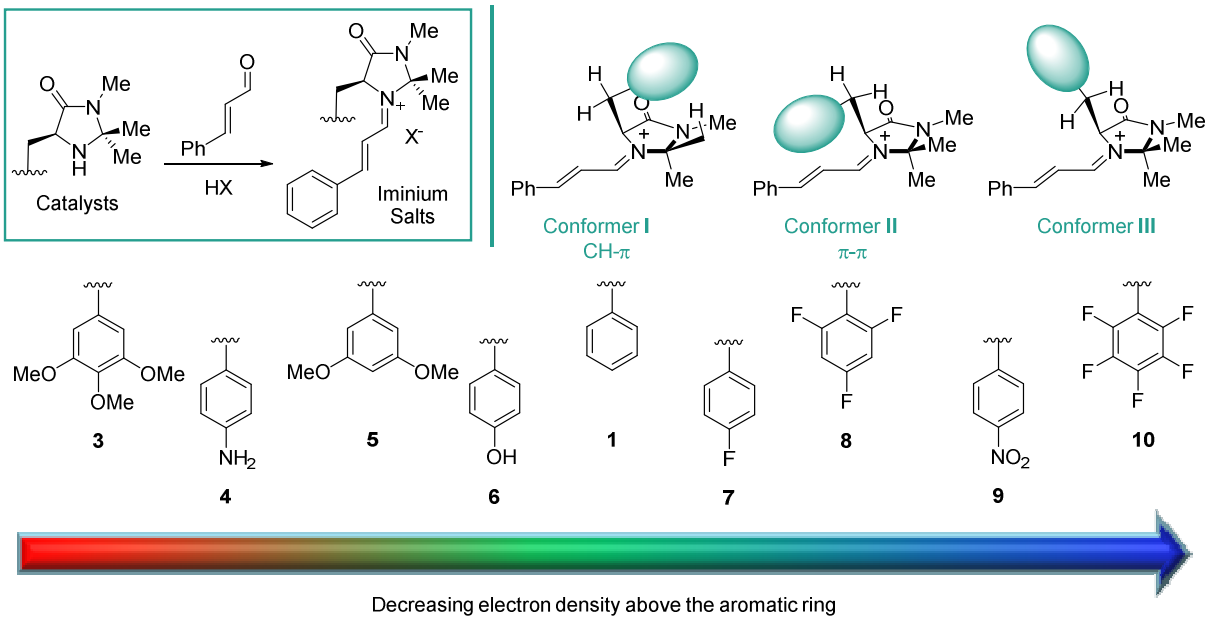

Figure 32 *Upper: Possible staggered conformers. Lower: Catalyst library with electronically modified aromatic groups.*

As measurement of the charge distribution of the aryl shielding group, the quadrupole moment tensor orthogonal to the aryl group (Q_{zz}) was calculated in collaboration with Dr. Mück-Lichtenfeld (Westfälische Wilhelms-Universität Münster). Moreover, the electronic surface potential (ESP) maps were computed to assist in visualising electronic properties. Subsequently, the effect of these structural changes on solid state and solution phase

conformational behaviour of the corresponding iminium salts, as well as on reactivity and efficiency in catalysis were studied.

2.2.1 Syntheses of Imidazolidinones with Electronically Modified Shielding Groups

The preparation of the catalysts with electronically modified shielding aryl substituents can be divided into two groups: Catalysts derived from natural amino acids (**1** and **6**) or commercially available unnatural amino acids (**4** and **9**), and catalysts derived from unavailable unnatural amino acids (**3**, **5**, **7**, **8**, and **10**).

Catalysts derived from natural amino acids or available unnatural amino acids:

The synthesis of imidazolidinones **1**, **4**, **6**, and **9** followed the same procedure reported by MacMillan for the preparation of **1** in a three step sequence.[8a] The commercially available amino acids (**11**-**14**) were converted into the corresponding methyl esters by treatment with thionyl chloride in MeOH. Next, the methyl amides (**15**-**18**) were prepared from the crude methyl esters by addition of an excess of methylamine in EtOH. In the final step, cyclisation with acetone in MeOH gave the desired imidazolidinones in good to excellent yields. Depending on the substrate, the yields of the cyclisation could be improved by addition of catalytic amounts of base (Et_3N) or acid (TsOH).

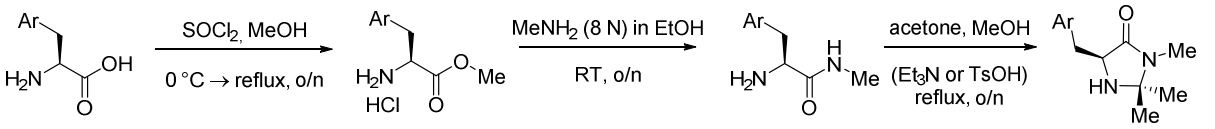

Ar = C_6H_5 (**11**)
$C_6H_4NH_2$ (**12**)
C_6H_4OH (**13**)
$C_6H_4NO_2$ (**14**)

Ar = C_6H_5 (**15**): 86%
$C_6H_4NH_2$ (**16**): quant.
C_6H_4OH (**17**): quant.
$C_6H_4NO_2$ (**18**): 91%

Ar = C_6H_5 (**1**): quant.
$C_6H_4NH_2$ (**4**): 85%
C_6H_4OH (**6**): 97%
$C_6H_4NO_2$ (**9**): quant.

Scheme 2 *General procedure for the syntheses of catalysts derived from natural amino acids or available unnatural amino acids (**1**, **4**, **6**, and **9**).*

Catalysts derived from unavailable unnatural amino acids:

The imidazolidinones derived from non-commercial amino acid derivatives (**3**, **5**, **7**, **8**, and **10**) were prepared following Seebach´s procedure for the selective α-functionalisation of amino acids.[122] This methodology was optimised for the unbranched glycine derivative BMI **19** as a general route to chiral α-amino acids. Herein, the method has been exploited using L-α-amino acids. The key intermediate BMI **19** can be prepared by cyclisation of

glycine methyl amide **20** with pivaldehyde **21** followed by chiral resolution of the resulting enantiomers using (*S*)-mandelic acid **22** (Scheme 3).[122b]

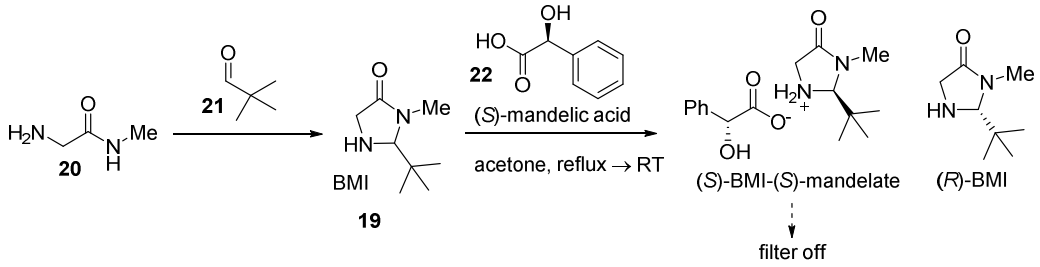

Scheme 3 *Synthesis and chiral resolution of BMI **19** as described by Seebach.*

Boc-protection gives the key intermediate (*S*)-*tert*-butyl-2-(*tert*-butyl)-3-methyl-4-oxo-1-imidazolidinonecarboxylate [(*S*)-Boc-BMI, **23**)] which is also commercially available (CAS: 119838-38-9). Deprotonation of (*S*)-Boc-BMI generates a chiral enolate which can then be selectively alkylated to form the *trans*-product. Finally, hydrolysis of the imidazolidinone gives the L-α-amino acid or methyl amide, depending on conditions. In this work, the BMI·TFA salt **19·TFA** was used as an economical starting point which was neutralised and Boc-protected in a two step procedure (81% yield; Scheme 4).

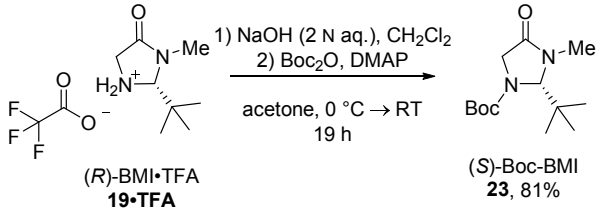

Scheme 4 *Synthesis of (S)-Boc-BMI **23** from (R)-BMI·TFA.*

For optimisation studies of the alkylation reaction, racemic Boc-BMI was prepared on large scale (Scheme 5) in a simple three step procedure. Amidation of glycine methyl ester hydrochloride **24** followed by cyclisation with pivaldehyde **21** gave BMI in good yield (74%). Subsequent Boc-protection using catalytic DMAP furnished the product **23** in 64% overall yield.

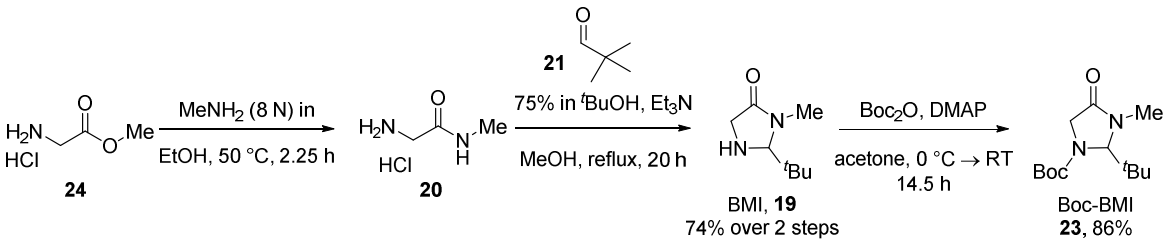

Scheme 5 *Synthesis of racemic Boc-BMI **23** for optimisation studies.*

With Boc-BMI **23** in hand, optimisation studies for the alkylation step were performed. In all cases, the substituted arylbromides were used as the electrophile; these were either commercially available or prepared from the corresponding alcohol using PBr_3. It was observed that the fluorinated arylbromides gave good yields using LDA as base (**27**-**29**) as originally reported by Seebach.[122b] In the case of the less reactive methoxy-substituted arylbromides the use of LiHMDS and addition of 1,3-dimethyltetrahydropyrimidin-2(1*H*)-one (DMPU) seemed to be beneficial due to increased solubility of the alkylating agent (**25**, **26**). The optimised conditions were then applied with (*S*)-Boc-BMI followed by cleavage of the Boc-group and hydrolysis to obtain optically pure L-phenylalanine *N*-methyl amide derivatives (**30**-**34**). Ring closure with acetone under basic conditions gave the target imidazolidinones in good overall yields (Scheme 6, 65%–77%).

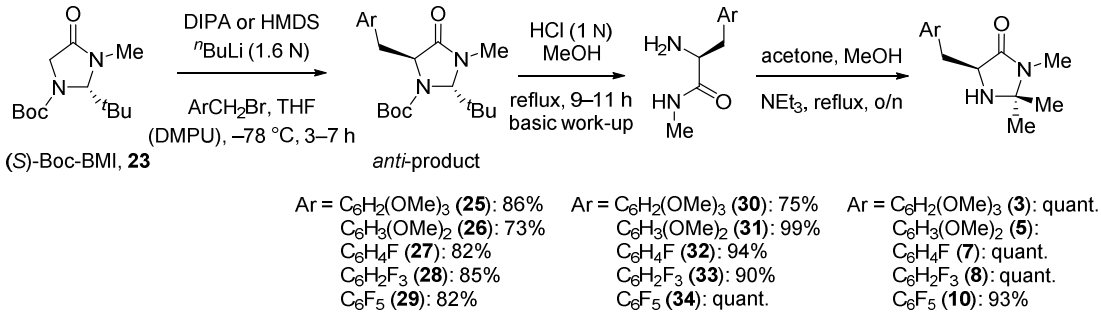

Scheme 6 *Syntheses of catalysts derived from unavailable unnatural amino acids **3**, **5**, **7**, **8**, and **10**.*

Syntheses of the iminium salts:

Having completed the preparation of catalysts **1** and **3**-**10**, the corresponding iminium salts (**1a** and **4a**-**10a**) were synthesised for structural analysis. These materials were successfully prepared as the perchlorate salts by condensation with (*E*)-cinnamaldehyde **2** (Scheme 7). Despite repeated attempts, the iminium salt of catalyst **3** (Ar = $C_6H_4NH_2$) and **7** (Ar = C_6H_4F) could not be isolated.

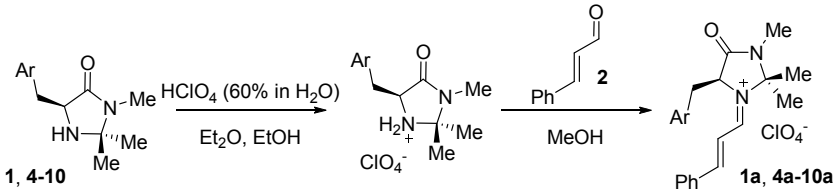

Scheme 7 *Synthesis of the iminium perchlorate salts **1a** and **4a-10a**.*

2.2.2 The Quadrupole Moment Q_{zz}

The charge distribution in a molecule can be conveniently expressed by multipoles. Topologically, monopoles look like s-orbitals, whilst dipoles look like p-orbitals and quadrupoles look like d-orbitals (Figure 33).[123] Chemists are familiar with describing point charges as monopoles. Furthermore, the term bond dipole is frequently used to express the charge distribution in polarised covalent bonds, and small molecules like CH_3CN or H_2O are known to exhibit molecular dipoles.[123] These concepts are helpful in understanding and predicting chemical reactivity and non-covalent interactions. Just as the dipole is a combination of two monopoles of equal and opposite charge, the quadrupole moment consists of two or more identical dipoles aligned *anti*-parallel such that there is no net dipole. Whereas higher multipoles become increasingly complicated for illustrative descriptions of molecular properties, the quadrupole moment is important in describing charge distribution in aryl rings. Aromatic interactions are of outmost importance for non-covalent interactions in molecular recognition and pre-organisation.[104a;121a;124] Although it must be kept in mind that other inherent properties like the electrostatic potential surface contribute to these phenomena, quadrupolar interactions are central to these phenomena and provide a good, simplified picture for qualitative investigations.[104a;125]

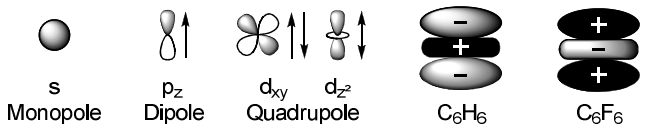

Figure 33 *Schematics of multipoles and the d_{z2} quadrupole moment of benzene and perfluorobenzene.*

Of particular interest for describing the properties of a benzene ring is the large permanent d_{z^2} quadrupole moment which is the sum of six sp^2–CH dipoles.[126] The permanent perfluorobenzene quadrupole moment is similar in magnitude but has the opposite polarity. The magnitude of d_{z^2} is represented by the traceless quadrupole moment tensor component perpendicular to the aromatic ring (Q_{zz}).[127]

In collaboration with Dr. Mück-Lichtenfeld (Westfälische Wilhelms-Universität Münster), the Q_{zz} for the toluene analogues of the electronically modified aryl rings and, for visual illustration, the electronic surface potential maps were computed (Figure 34). The DFT calculations were performed using TURBOMOLE.[128]

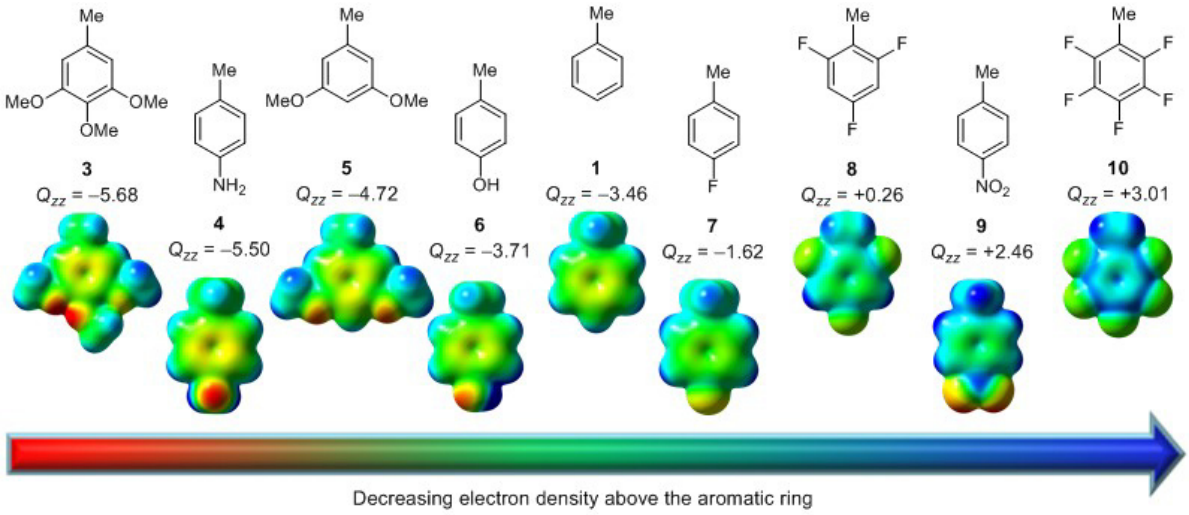

Figure 34 *Electron surface potential (ESP) maps and quadrupole moment tensor components perpendicular to the aromatic ring (Q_{zz}) of the toluene derivatives of the modified benzyl group given in Debeye·Ångstrom. Colour range of the electrostatic potential: −0.06 (red) to + 0.06 (blue).*

2.2.3 X-Ray Crystallographic Analysis of Imidazolidinone Hydrochloride Salts and Iminium Salts

*X-ray structures of the hydrochloride salts of the imidazolidinones **1**, **3**, and **8**-**10**:*

For most of the catalysts it was possible to obtain crystals suitable for X-ray crystallographic analysis as the hydrochloride salts (Figure 35). The crystal structure of **1** is taken from Burley and Gilmour,[3] in which the first solid state and computational study of this imidazolidinone is reported. For catalysts **3** and **10** the racemic analogues were used. The nitrogen of the amine function of all the imidazolidinones was found to be pyramidalised such that the resulting envelope allows for the benzylic substituent to be in *quasi*-equatorial position. Except for the trimethoxyphenyl-derived catalyst **3**, all other structures were found to adopt the staggered conformation with the aryl group rotated in proximity of the protonated amine (Φ_{NCCC} = –72.0° (**1**), –82.6° (**8**), –74.5° (**9**), and –83.0° (**10**)). The trimethoxy catalyst **3** on the other hand adopts the staggered conformer in which the aryl ring is rotated into proximity of the carbonyl moiety (Φ_{NCCC} = –170.0°).

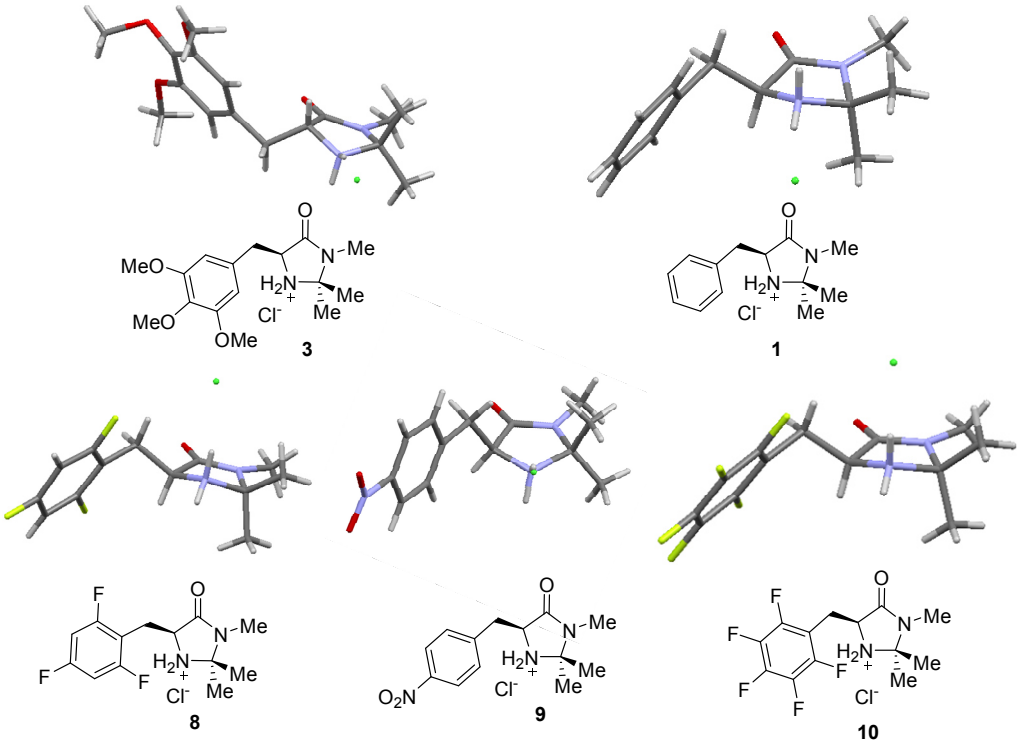

***Figure 35** X-ray structures of the hydrochloride salts of catalysts **1**[3], **3**, and **8**-**10**.*

X-ray structures of the catalysts derived iminium ions:

For most of the iminium salts derived from the imidazolidinones, it proved very difficult to obtain crystals suitable for X-ray analysis, due to poor stability in solution and tendencies to form an oil. Gratifyingly, crystallisation of one electron-rich (**6a**) and one electron-deficient (**10a**) example was achieved by vapour diffusion with Et_2O from a solution in CH_3CN or MeOH/CH_3CN (2:1), respectively. For both, the racemic analogues were used. The severe effect of electronic modulation on conformation is beautifully represented in the crystal structures. As expected, due to their similar Q_{zz}, the tyrosine-derived catalyst iminium salt **6a** adopts the same conformation (conformer **I**, Figure 30) as the parent phenylalanine-derived structure (Figure 29)[49] allowing for a stabilising CH-π contact. In contrast, the pentafluoro-analogue **10a** (Q_{zz} = +3.01) adopts a conformation with the aromatic group rotated away from the core five-membered ring (Φ_{NCCC} = –176.7°; conformer **III**, Figure 30). To the best of our knowledge, this is the first structural report of this conformation. Moreover, Houk and co-workers have calculated that conformer **III** is electronically disfavoured for the parent iminium salt **1a**, derived from crotonaldehyde (Me instead of Ph on substrate).[47] Similarly, Seebach and Grimme reported that this conformation is not an energetic minimum of **1a** in their "*windshield-wiper*" model.[50b] Also clearly visible from the crystal structures is the ideal planarity of the core ring-iminium chain moiety with the aromatic group solely discriminating the two faces.

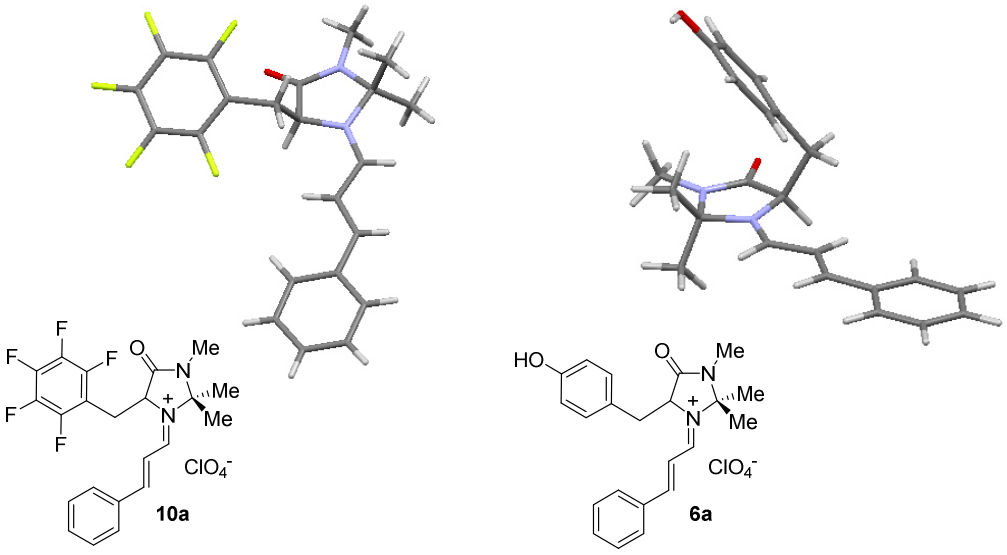

Figure 36 *X-ray structures of iminium perchlorate salts of **6a** and **10a**. The ClO_4^- counterions are omitted for clarity.*

2.2.4 NMR Analysis of the Electronically Modified Iminium Salts

Chemical shifts of the geminal-dimethyl group:

As reported by Tomkinson *et al.*[49] the CH-π interaction in conformer **I** of the iminium salts between the shielding group and the *syn*-methyl group of the *geminal*-dimethyl functionality is clearly visible by solution phase NMR (Figure 37). The interaction leads to a significant upfield shift of the *syn*-methyl as compared to the *anti*-methyl (benzyl: $\Delta\delta^{1}H_{syn/anti} = -0.89$ ppm; $\Delta\delta^{13}C_{syn/anti} = -2.77$ ppm). It was therefore envisaged, that the conformational preferences of the modified iminium salts would be qualitatively represented by the $\Delta\delta_{syn/anti}$ of the chemical shifts, because the magnitude of the differences should directly be connected to the population in conformer **I**. Therefore the chemical shifts (^{1}H and ^{13}C NMR) of the *geminal*-dimethyl group for all iminium salts were deduced from their NMR spectra (Table 1 and Figure 37). The large difference of the shifts of the two methyl groups [Δδ(*syn*/*anti*)] observed for electron-rich systems **1a**, **3a**, **5a**, and **6a** is a result of shielding of the *syn*-methyl group in conformer **I** due to the CH-π interaction. Smaller Δδ(*syn*/*anti*) in the spectra of **8a** and **10a** suggest lower population of this conformer. Notably, the nitro derivative **9a** exhibits a much larger shift-difference than the other electron-poor compounds, suggesting different conformational behaviour.

Table 1 *Differences of the chemical shifts of the geminal-dimethyl group observed by ^{1}H and ^{13}C NMR spectroscopy.*

Iminium Salt (Ar)	Q_{zz} **[D·Å]**	**Δδ(*syn/anti*)^{1}H [ppm]**	**Δδ(*syn/anti*)^{13}C [ppm]**
3a ($C_6H_2(OMe)_3$)	–5.68	–0.62	–1.87
5a ($C_6H_3(OMe)_2$)	–4.72	–0.62	
6a (C_6H_4OH)	–3.71	–0.78	–2.48
1a (C_6H_5)	–3.46	–0.89	–2.77
8a ($C_6H_2F_3$)	+0.26	–0.18	+0.06
9a ($C_6H_4NO_2$)	+2.46	–0.74	–1.79
10a (C_6F_5)	+3.01	–0.13	+0.36

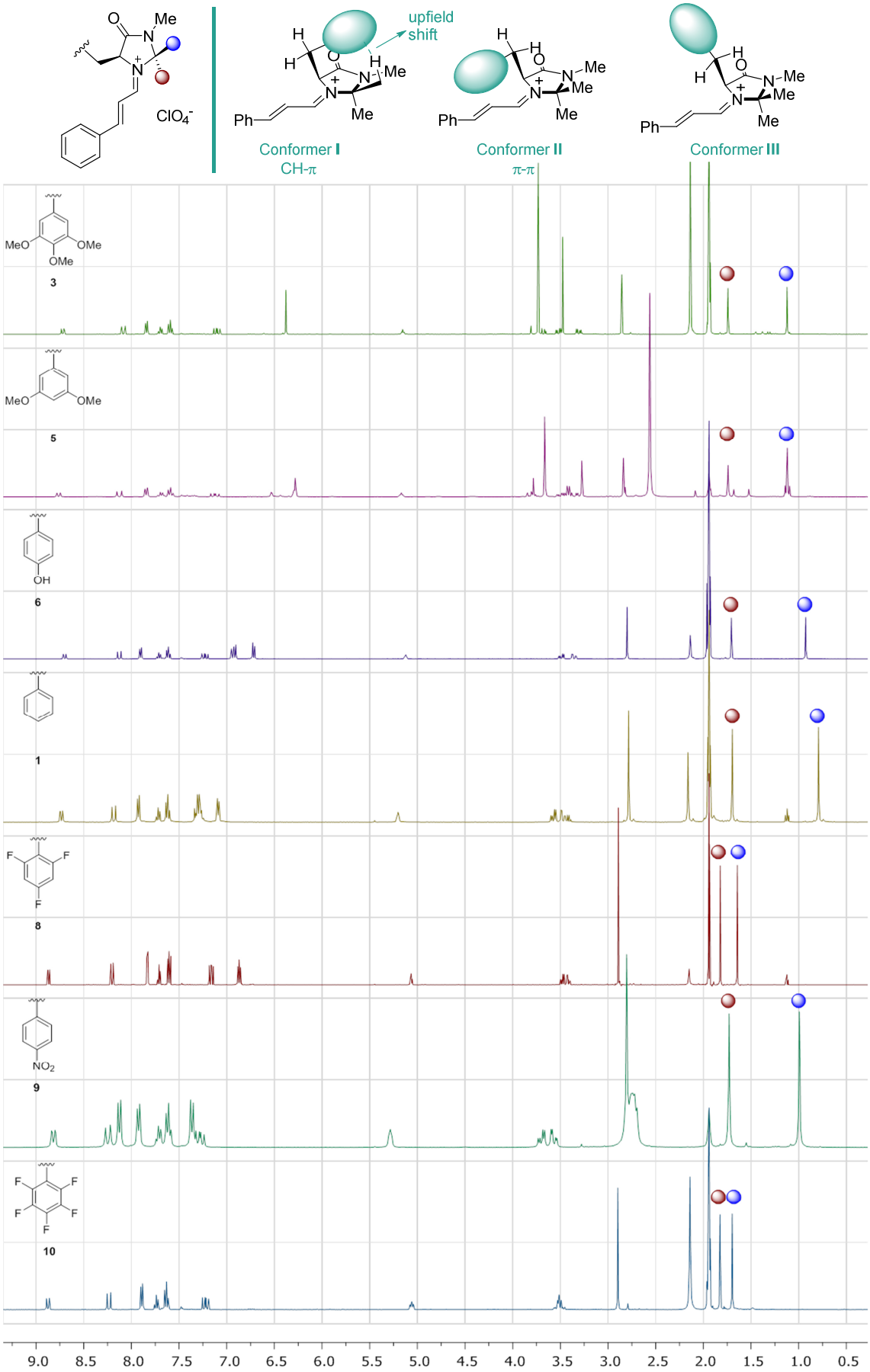

Figure 37 *Upper: The three staggered conformers of the imidazolidinone derived iminium salts. The CH-π interaction in conformer* ***I*** *results in an upfield shift of the syn-methyl group in the* ^{1}H *and* ^{13}C *NMR spectra. Lower:* ^{1}H*-NMR spectra.*

*Conformer population analysis of iminium salts **1a**, **3a**, **6a**, **8a**, **10a**, and **35a**:*

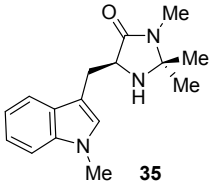

35

***Figure 38** Me-indole imidazolidione **35**.*

Together with Dr. K. Bergander from the NMR department at the Westfälische Wilhelms-Universität Münster, a detailed solution phase conformer population analysis was performed for a selection of catalysts (**1a**, **3a**, **6a**, **8a**, **10a**, and additionally the Me-indole derivative **35a**, Figure 38, discussed in greater detail in chapter 2.2.8). It was assumed that only the three staggered conformers **I**-**III** (Figure 37) should be significantly populated and therefore contribute to ^3J couplings. The mole fractions X_I, X_{II}, and X_{III} corresponding to the three conformers can be determined by solving a system of three linear equations:

$$X_I\ {}^3J(60°) + X_{II}\ {}^3J(300°) + X_{III}\ {}^3J(180°) = J_1(obs)$$
$$X_I\ {}^3J(60°) + X_{II}\ {}^3J(180°) + X_{III}\ {}^3J(300°) = J_2(obs)$$
$$X_I + X_{II} + X_{III} = 1$$

A solution to the system is given by:

$$X_{III} = \left[\frac{J_1 - {}^3J(60°)}{{}^3J(300°) - {}^3J(60°)} - \frac{J_2 - {}^3J(60°)}{{}^3J(180°) - {}^3J(60°)}\right] \Big/ \left[\frac{{}^3J(180°) - {}^3J(60°)}{{}^3J(300°) - {}^3J(60°)} - \frac{{}^3J(300°) - {}^3J(60°)}{{}^3J(180°) - {}^3J(60°)}\right]$$
$$X_{II} = \left[\frac{(J_1 - {}^3J(60°) - X_{III}({}^3J(180°) - {}^3J(60°)}{{}^3J(300°) - {}^3J(60°)}\right]$$
$$X_I = 1 - X_{II} - X_{III}$$

The expected ^3J values for the distinct rotamers [^3J(60°), ^3J(180°), and ^3J(300°)] were determined for each iminium salt using the Diez-Altona Donders equation with the aid of MestReJ (v1.1).[129] For this, the two diastereotopic benzylic protons were assigned *via* 1D-NOESY and HF-HOESY experiments and the experimental ^3J coupling constants ($ArCH_2$ to 5-H) were determined. The substituent parameters (group electronegativities) λ_i of all substituents attached to benzylic C-C bond were taken from Altona *et al.* or deduced from the corresponding ethane derivatives.[130] With the ^3J values for the distinct rotamers in hand, the mole fractions were calculated. The results for the iminium salts **1a**, **3a**, **6a**, **8a**, **10a**, and **35a** are summarised in Table 2.

Table 2 *Mole fractions X_I, X_{II} and X_{III} determined by NMR conformer population analysis at RT in CD_3CN.*

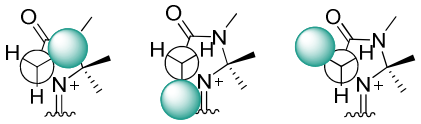

Iminium Salt	Q_{zz} [D·Å]	X_I	X_{II}	X_{III}
8a ($C_6H_2F_3$)	+0.26	0.39	0.21	**0.40**
10a (C_6F_5)	+3.01	0.37	0.16	**0.47**
1a (C_6H_5)	–3.46	**0.75**	0.03	0.23
6a (C_6H_4OH)	–3.71	**0.76**	0.04	0.20
3a ($C_6H_2(OMe)_3$)	–5.68	0.57	**0.28**	0.15
35a (Me-Indole)	–5.40	0.65	**0.17**	0.18

For the electron-rich species **1a**, **3a**, **6a**, and **35a**, conformer **I**, stabilized by a CH-π interaction, is predominantly populated. In contrast to the phenylalanine **1a** and tyrosine **6a** derived catalysts, the more electron-rich systems **3a** and **35a** significantly populate conformer **II**, stabilised by π-π-type interactions. The electron-deficient systems **8a** and **10a** showed very different mole fraction distributions. Unlike the other iminium salts, these systems do not predominantly populate conformer **I** (<40%), but exhibit a more diverse distribution. These observations are consistent with the trends deduced from the chemical shift-differences ($\Delta\delta$(*syn*/*anti*) ^{1}H and ^{13}C NMR) of the *geminal*-dimethyl group (Table 1).

2.2.5 Kinetic Analysis of two Iminium Salts by Photometric Monitoring

The rate constants of the reactions of the iminium salts from the most electron-rich **3a** (R = $C_6H_2(OMe)_3$) and most electron-deficient **10a** (R = C_6F_5) catalysts with silyl ketene acetals **36** and **37** were studied to quantify the influence of electronic modulation on electrophilic reactivity and to determine the electrophilicity parameter for these iminium salts (Scheme 8). The kinetic analysis described in this chapter was performed in collaboration with S. Paul, Dr. S. Lakhdar, and Prof. H. Mayr at the Ludwig-Maximilians-Universität München.

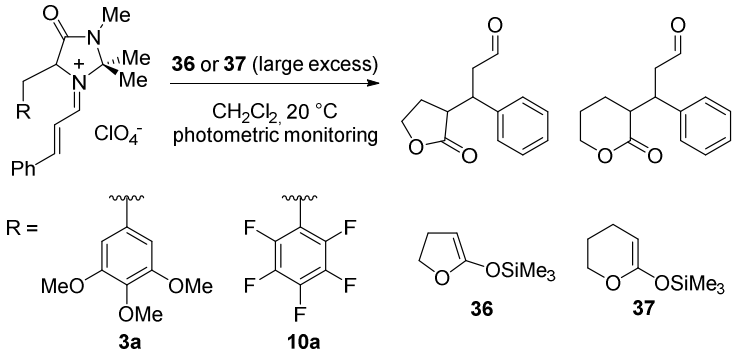

Scheme 8 *Determination of the electrophilicity of iminium salts **3** and **10**.*

Mayr and co-workers have elegantly demonstrated that reactions of various Michael acceptors with σ, n, and π nucleophiles can be described by Equation 1 (s_N = nucleophile-specific sensitivity parameter, E = electrophilicity parameter, N = nucleophilicity parameter).[131] Recently, it has been shown that electrophilicities of the 1st and the 2nd generation MacMillan catalyst-derived iminium salts fit this equation well.[53;117;132]

$$\log k_2\ (20\,°C) = s_N\ (E + N)$$

Equation 1 *Correlation between the rate constant of a reaction and the electrophilicity/nucleophilicity of the reaction partners.*

The reaction kinetics were followed photometrically by measuring the decay of absorbance of the iminium salts using UV/VIS spectroscopy (374/376 nm, CH_2Cl_2, 20 °C). Large excesses of the silyl ketene acetals were employed to ensure *pseudo*-first-order kinetics [k_{obs} (s^{-1})]. Furthermore, to obtain the second-order rate constants k_2 ($M^{-1}s^{-1}$), k_{obs} was determined for different concentrations of the nucleophile ([Nuc]). Plotting k_{obs} *versus* [Nuc] gave a linear relationship with k_2 as the slope. The second-order rate constants k_2 and electrophilicity parameter E obtained are shown in Table 3, and were compared to the results of iminium salt **1a** from previous studies.[117] Whereas **2a** exhibited comparable reactivity to **1a**, the pentafluoro-system **10a** proved to be about 9 times more reactive, thereby approaching the reactivity of MacMillan's 2nd generation catalyst (Figure 39).[53]

Table 3 *Second-order rate constants k_2 for the reactions of iminium salts **1a**, **3a** and **10a** with ketene acetals **36** and **37** (20 °C, CH_2Cl_2, counterion: **3a**, **10a** = ClO_4^-, **1a** = OTf^-).*

	k_2 (**36**) [M^{-1} s^{-1}]	k_2 (**37**) [M^{-1} s^{-1}]	***E***
1a	9.06×10^3	5.23×10^2	-7.2[a]
3a	8.13×10^4	3.43×10^3	-6.0
10a	1.49×10^4	5.78×10^2	-7.0

*The E parameter for **3a** and **10a** were determined from a least-squares minimisation of $\Delta^2 = \Sigma(\log k_2 - s_N(E + N))^2$ which uses k_2 (this table) and the nucleophile parameter N and s_N (for **36**: N = 12.56, s_N = 0.70; for **37**: N = 10.61, s_N = 0.86). [a] taken from [117].*

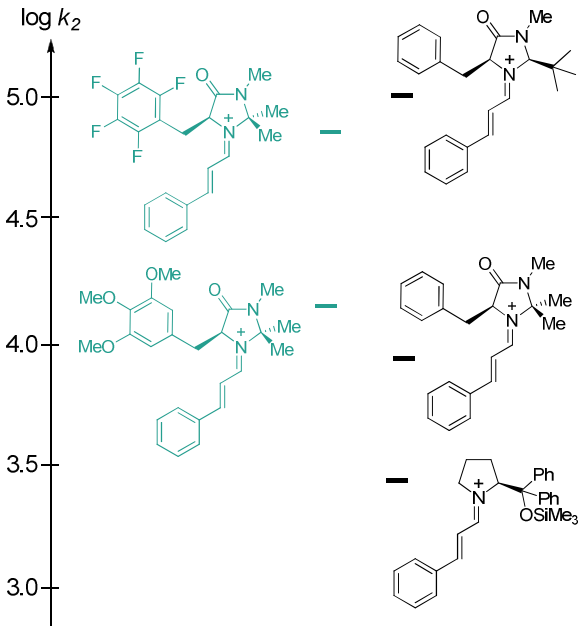

Figure 39 *Comparison of k_2 for the reactions of the iminium ions **1a**, **3a**, and **10a** with ketene acetal **36**.*

2.2.6 Catalysis Screening: Organocatalytic Friedel-Crafts Reaction of *N*-Me-Pyrrole

Finally, to test the performance of the electronically modified imidazolidinones in catalysis, the Friedel-Crafts reaction of *N*-methyl pyrrole (**38**) with (*E*)-cinnamaldehyde (**2**) was investigated. This reaction was selected due to the high effectiveness reported for the parent catalyst **1** by MacMillan *et al.* with enantioselectivities up to 93% *ee*.[112b] However, reaction temperatures of –30 °C led to long reaction times of 42 h. The aldehyde **2** was added in excess (3 eq.) and catalysts were used as TFA salts with catalyst loadings being 20 mol%. Enantioselectivities of the corresponding alcohols after *in situ* reduction with $NaBH_4$ were measured using chiral HPLC. The results of the first catalyst screen at RT are given in Table 4, left (blue) columns. When employing catalyst **4** (R = $C_6H_4NH_2$) no reaction occurred. This is consistent with the previous failure to isolate the iminium salt of this catalyst, likely due to the aniline function. All other catalysts proved to be competent with reactions reaching full conversion within 3 h. Interestingly, a clear relation between the electron-density of the aryl shielding group, expressed as the Q_{zz}, and the level of enantioinduction was observed. The more electron-rich the aromatic group, the higher the observed selectivity. An exception to this observation was found in the nitro derivative **9**, which may be explained by the different conformational behaviour observed in the NMR studies (2.2.4). Also catalyst **7** performed slightly better than expected.

Table 4 *Screening of the electronically modified catalysts in the Friedel-Crafts reaction of N-Me-pyrrole* ***38*** *to (E)-cinnamaldehyde* ***2****.*

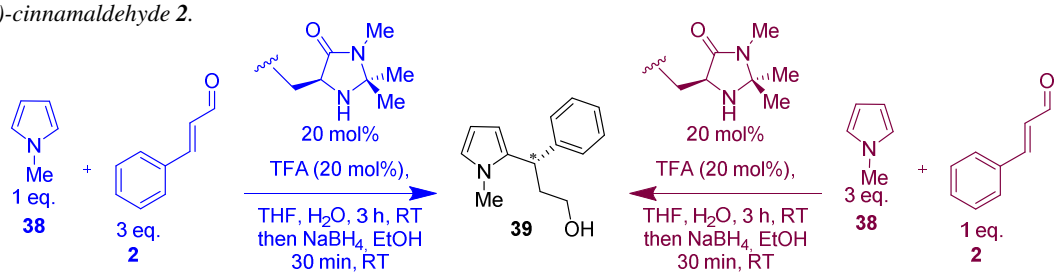

ee [%]	*e.r.*	*Qzz* [D·Å]	Catalyst	$\Delta\delta^1H_{syn/anti}$ [ppm]	*ee* [%]	*e.r.*
94	97:3	–5.68	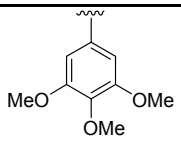 **3**	–0.62	76	88:12
–	–	–5.50	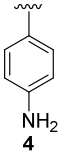 **4**	–	–	–
88	94:6	–4.72	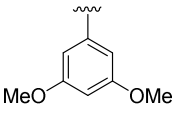 **5**	–0.62		
90	95:5	–3.71	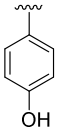 **6**	–0.78	67	83.5:16.5
85	92.5:7.5	–3.46	 **1**	–0.89	70	85:15
87	93.5:6.5	–1.62	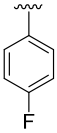 **7**	–		
70	85:15	+0.26	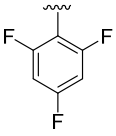 **8**	–0.18	43	71.5:28.5
91	95.5:4.5	+2.46	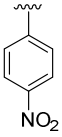 **9**	–0.74		
66	83:17	+3.01	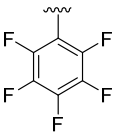 **10**	–0.13	39	69.5:30.5

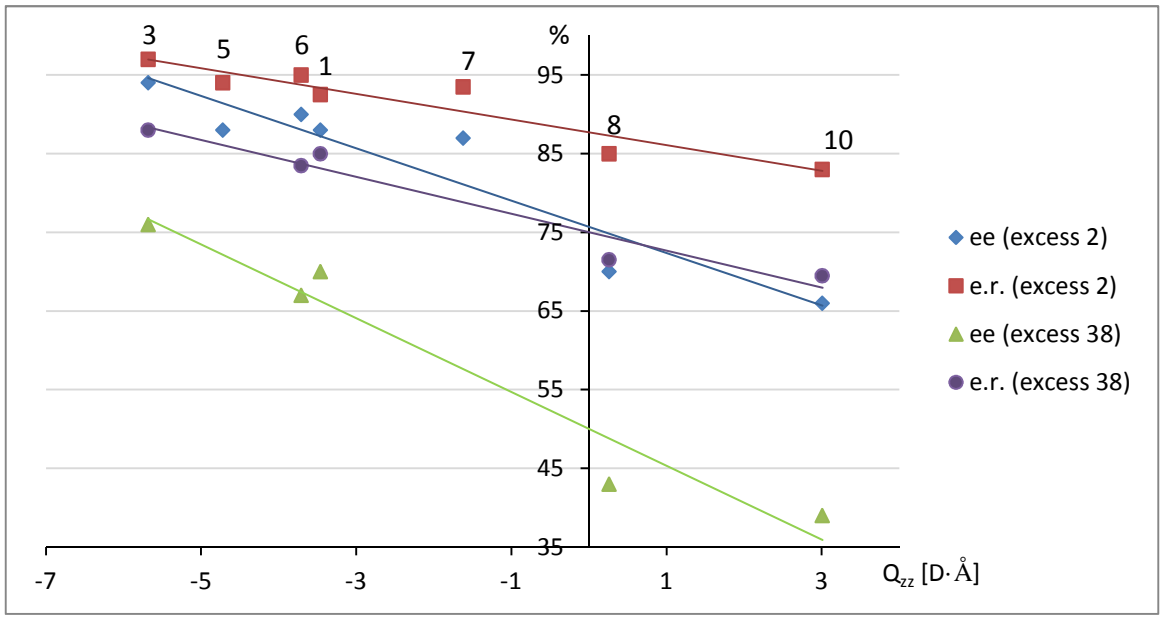

Figure 40 *Plot of the component of the traceless quadrupole moment tensor orthogonal to the aromatic ring of the Ar-CH_3 derivatives (Q_{zz}) with enantiomeric excess (ee), and enantiomeric ratio (e.r.).*

When plotting the observed *ee* values (or *e.r.* values) against the quadrupolar moment tensor perpendicular to the aromatic system (Q_{zz}) of catalysts **1**, **3**, **5**-**8**, and **10**, a direct linear relationship between the level of enantioinduction and the electron-density of the aryl group as function of the quadrupole moment tensor Q_{zz} was observed. While the electron-deficient catalysts **8** and **10** gave moderate selectivities (65% and 70% *ee*, respectively), the phenylalanine and tyrosine derived catalysts **1** and **6** gave improved selectivities of 84% and 90% *ee*, respectively. With the electron-rich trimethoxy imidazolidinone **3**, it was possible to achieve remarkable selectivity (94% *ee*), reaching similar levels of enantioselectivity as reported for the parent catalyst **1** (93% *ee*), while being able to perform the reaction at room temperature instead of –30 °C thus reducing reaction times from 42 h to 3 h. To further enhance the selectivities, the reaction was repeated at –55 °C using the two electronic extremes **3** and **10**, and the parent catalyst **1**. The selectivity of **10** was improved to 83% *ee*, while both **1** and **3** gave >99% *ee*.

Purification of the product **39** proved difficult because it exhibits the same retention time on TLC as cinnamyl alcohol (reduced **2** which was used in excess). To ease purification, a selection of reactions were repeated using an excess of *N*-methyl pyrrole (**38**, 3 eq.). Even though the plot of *ee* against Q_{zz} gives the same trend (Figure 40), reactions were marginally less selective (Table 4, right (red) columns).

2.2.7 Computational Analysis of Lowest Energy Conformers of Iminium Ions

To complement the experimental structural analysis of the imidazolidinone iminium salts used in this study, calculation of the lowest energy conformers were performed at the DFT level in a collaborative work with Dr. Anthony Meijer from the University of Sheffield (UK). For this computational analysis, the parent catalyst (**1a**), the two electronic extremes (**3a**, and **10a**) and two additional catalysts (**5a** and **8a**) were chosen. In Figure 41, the three staggered conformers and an eclipsed conformer (**IV**), which has previously been reported by Houk,[47] are illustrated.

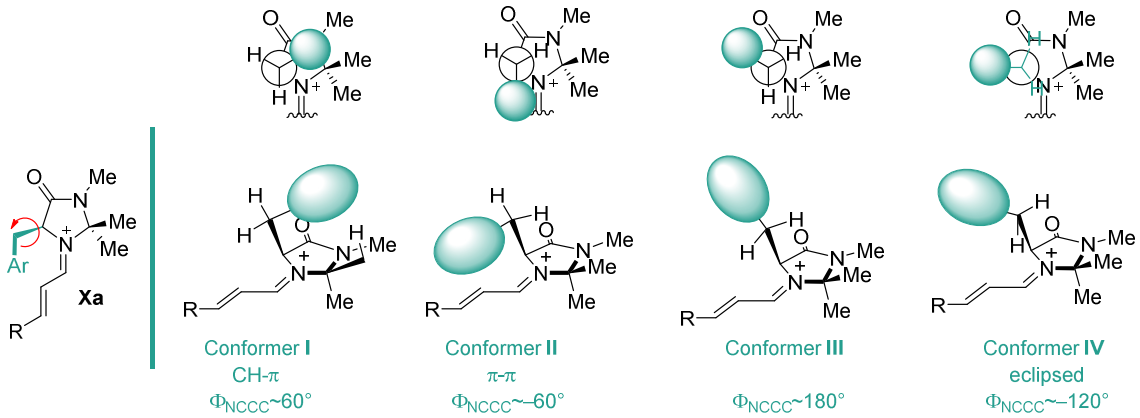

Figure 41 *Possible low-energy conformers of imidazolidinone derived α,β-unsaturated iminium salts* ***Xa****.*

First generation MacMillan catalyst derived iminium ion ***1a****:*

The iminium ion derived from condensation of the 1st generation MacMillan catalyst with crotonaldehyde (R = Me) has previously been studied using DFT computations by Houk[47] and with (*E*)-cinnamaldehyde (R = Ph) by Tomkinson[49] and Seebach.[50b] Houk reported three energy minima after optimisation for the rotation of the shielding group around the C–C-bond. The global minimum was found to be conformer **I** followed by conformer **II** (1.3 kJ/mol). A third minimum was found with the C–C bond to the phenyl ring almost eclipsing the adjacent C–H bond (conformer **IV**, 5.4 kJ/mol). Conformer **III** was not located as a minimum structure which was rationalised by a repulsive electrostatic interaction between the carbonyl group and the phenyl ring. In the calculations by Seebach as well as by Tomkinson the staggered conformer **IV** was unfortunately not considered. However, both groups reported very similar energetic differences between conformers **I** and **II** (5.5 kJ/mol and 5.0 kJ/mol, respectively) for the (*E*)-cinnamaldehyde derived iminium ions, which are considerably larger than those reported by Houk for crotonaldehyde. Interestingly, for the 2nd

generation MacMillan catalyst, Seebach *et al.* reported the potential-energy profile for the rotation around the $PhCH_2$–CH bond. It was shown, that there is an energetic plateau between conformation **II** and the staggered conformer **IV** whereas conformer **III** was again not identified as an energetic minimum. Moreover, the group reported relatively low rotational barriers, suggesting that at ambient temperature, the benzyl group rotates almost freely. This phenomenon was termed the "*windshield-wiper*" effect.[50b]

In this work, the iminium ion derived from the condensation with (*E*)-cinnamaldehyde was investigated by DFT studies (Figure 42, left). Consistent with the other reports, the CH-π conformer was found to be the global energy minimum ($\Phi_{NCCC} = 52.2°$). A second energy minimum is one in which the previously discussed staggered conformation **IV** is adopted (+4.7 kJ/mol, $\Phi_{NCCC} = -134.0°$). The reason that conformer **II** was not found to be a global minimum might be explained by a situation like the one described by Seebach *et al.* with an energetic plateau in which the shielding group oscillates.[50b]

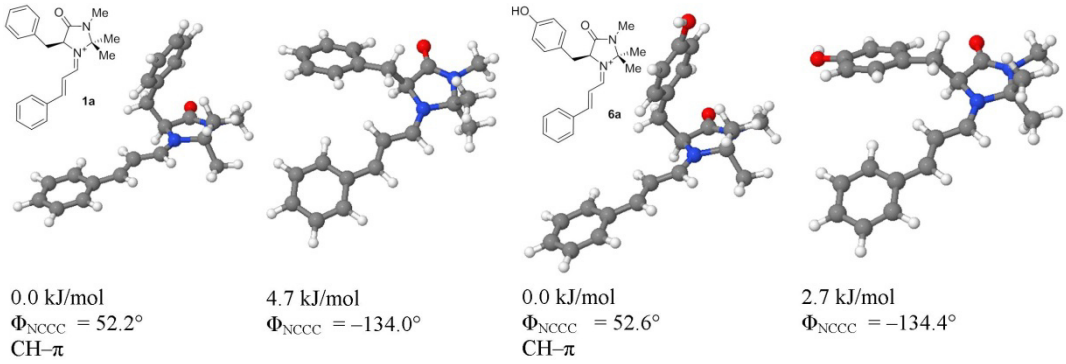

Figure 42 *Optimised geometries and relative energies for iminium ions* ***1a*** *(left) and* ***6a*** *(right).*

Tyrosine-derived imidazolidinone iminium ion ***6a****:*

Next, the electronically similar tyrosine-derived imidazolidinone iminium ion **6a** was investigated (Figure 42, right). As expected, similar energy minima as for **1a** were identified, but the energetic difference was found to be smaller ($\Delta E = 2.7$ kJ/mol). The higher population of the staggered conformer **IV**, which is believed to be connected by an energetic plateau with conformer **II**, could explain the slightly improved enantioselectivity of the tyrosine derived catalyst as compared to the phenylalanine derived catalyst (see 2.2.6).

*Electron-rich extreme: The trimethoxy-derivative **3a**:*

The most electron-rich system of the series gave the highest levels of enantiocontrol in the Friedel-Crafts alkylation (94% *ee*). From the solution phase studies, it was suggested, that conformer **II** is significantly populated at RT (see 2.2.4). Moreover, DFT studies point towards a different global energy minimum as for **1a** and **6a**. Whereas for the previously discussed iminium ions **1a** and **6a** this is conformer **I**, for **3a** there are two low lying structures, the global minima corresponds to conformer **II** and the staggered conformer **IV** was found at +0.08 kJ/mol ($\Phi_{NCCC} = -78.2°$ and $-132.2°$, respectively), presumably connected by an energetic plateau. Conformer **I** was found to be slightly higher in energy (+0.5 kJ/mol). Another low-lying conformer resembling conformer **II**, was identified (+3.3 kJ/mol). From this computational analysis, it seems likely that the molecular space over substrate from $\Phi_{NCCC} = -132.2°$ to +51.7° is shielded by the oscillating aryl group, consistent with the high levels of enantioinduction observed. This constitutes an extension of the "*windshield-wiper*' effect.

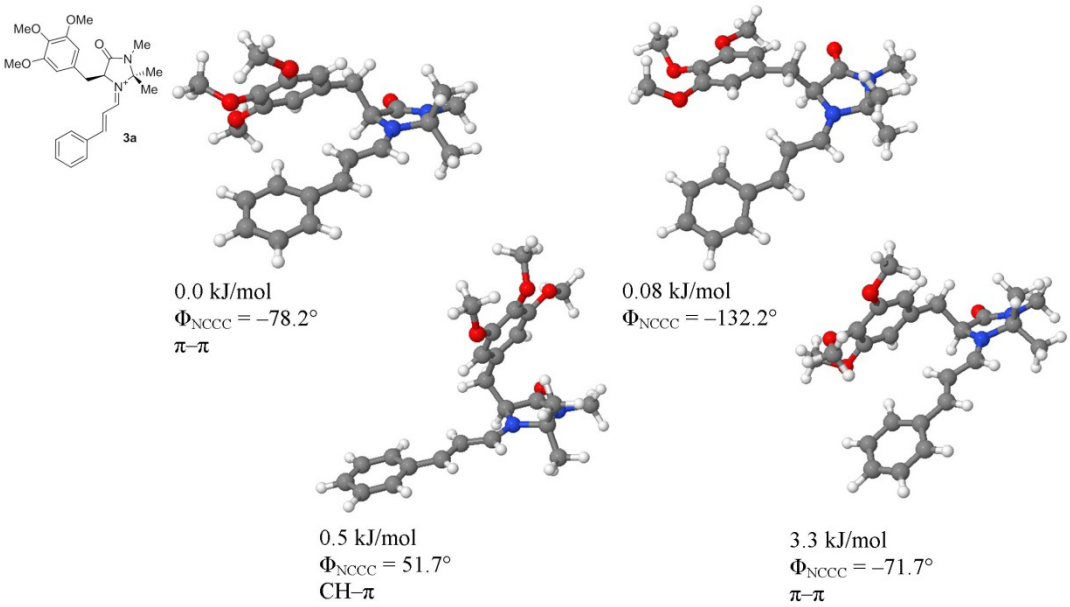

***Figure 43** Optimised geometries and relative energies for iminium ion **3a**.*

*Electron-deficient extreme: The pentafluoro-derivative **10a**:*

For the electron-deficient extreme of the series **10a** ($Q_{zz} = 3.01$, Figure 44), the global energetic minimum was found to be conformer **III** ($\Phi_{NCCC} = -168.8°$) which is in perfect agreement with the crystal structure and the other experimental findings. This constitutes, to

the best of our knowledge, the first theoretical description of this conformer. Moreover, the global minimum is the only conformer that is significantly populated. The other two identified minima corresponding to the π-π conformer **II** and a distorted conformer **I** in which a stabilising interaction between one hydrogen of the *syn*-methyl group with a carbon of the aromatic ring seems to occurs, lie much higher in energy (+7.1 kJ/mol and +11.8 kJ/mol, respectively). The predominant population of conformer **III** provides an explanation for the poor selectivity of the pentafluorophenyl-catalyst (65% *ee*).

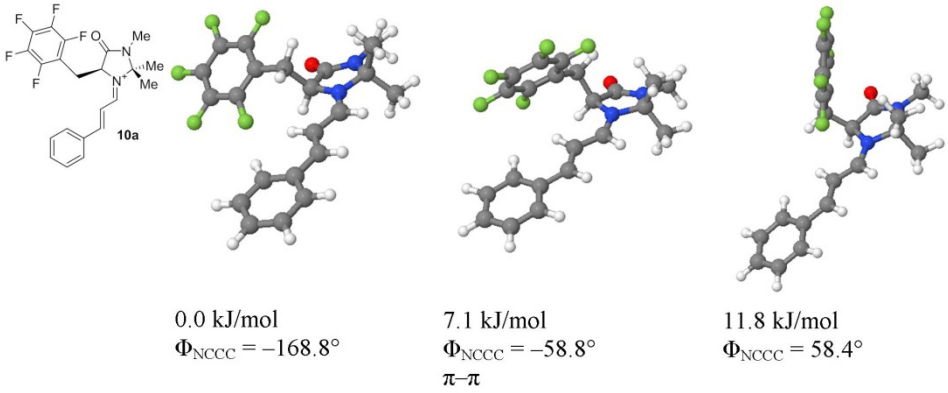

Figure 44 *Optimised geometries and relative energies for iminium ion* ***10a****.*

Trifluorophenyl-derived imidazolidinone iminium ion ***8a****:*

As expected, the electron-poor iminium ion **8a** was computed to preferentially adopt the same conformation as compound **10a** (conformer **III**, $\Phi_{NCCC} = -168.3°$). Also, a similar distorted conformer **I** was found to be an energy minimum (+10.7 kJ/mol). Surprisingly, conformer **II**, which was the second lowest energy minimum for iminium ion **10a**, was not identified.

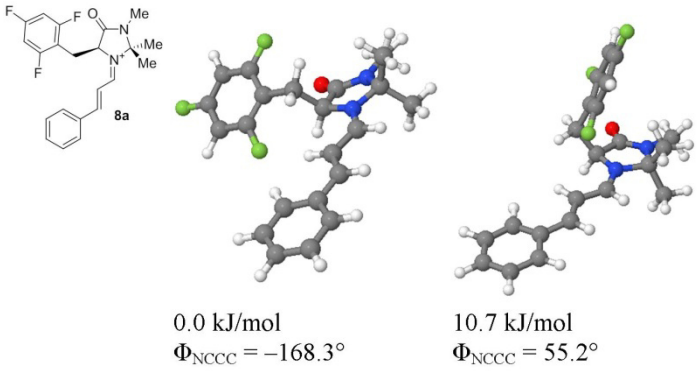

Figure 45 *Optimised geometries and relative energies for iminium ion* ***8a****.*

2.2.8 Conformational Analysis of the Transition State for the Friedel-Crafts Alkylation of N-Methyl Pyrrole to Iminium Ion 1a

It was assumed, that the transition-state of the Friedel-Crafts reaction proceeding *via* the discussed intermediate iminium ion, closely resembles this reactive intermediate according to the Hammond-Leffler postulate.[116] To verify this hypothesis, a conformational analysis of the transition state for the Friedel-Crafts reaction of *N*-methyl indole **38** and iminium salt **1a** was performed in collaboration with Dr. Mück-Lichtenfeld (Figure 46). The CH-π conformer **I** was identified as the global minimum in agreement with the conformational analysis of iminium salt **1a** (see page 42). Two other energy minima corresponding to conformers **II** and **IV** were both found to be +2.4 kcal/mol higher in energy. Thus, it is proposed, that the assumption that the transition state resembles the reactive intermediate is a good working model for the studied Friedel-Crafts reaction.

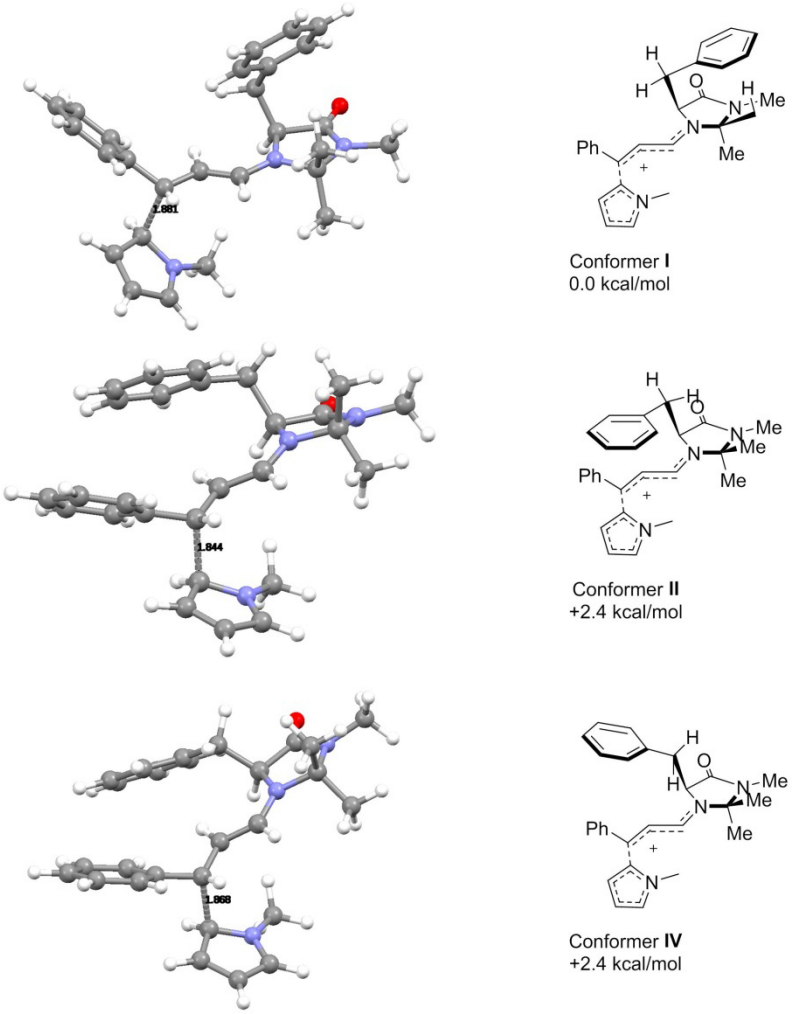

Figure 46 *Conformational analysis of the transition state for the addition of N-Me pyrrole to iminium ion* ***1a****.*

2.3 Additional Modifications of the Shielding Group

In the previous chapter 2.2, electronic modifications of the shielding group of MacMillan type catalysts have been described. It was established that decreasing the electron-density of the aromatic ring by introducing electron-withdrawing groups errodes the stereocontrol whilst substituting with electron-donating moieties improves the stereoselectivity. The next questions to be addressed in this study were: Can the enantioselectivity be improved further by extending the aryl group? Are the postulated CH–π and π–π interactions really crucial for governing stereoselectivity? How will other natural amino acid-derived catalysts bearing heterocyclic, aromatic rings perform in the reaction? To answer the first question, two extended aromatic systems were envisaged (Figure 47, left). The electron-rich *para*-pyrrolo-phenyl derivative **40** was postulated to show enhanced selectivity due to better shielding of the distant electrophilic reaction center. The highly electron-rich anthracene derivative **41** on the other hand, might be more effective in shielding based on simple steric arguments. To explore whether or not the non-covalent interactions between the aryl shielding group and the iminium π-system and *syn*-Me group are really necessary for effective catalytic performance, the reduced cyclohexyl-derivative **42** was also prepared (Figure 47, middle). To explore the performance of heteroaromatic amino acid derivatives, compounds **35**, **43**, and **44** were synthesised (Figure 47, right). Catalyst **43** has previously been reported to give good selectivity in the Diels-Alder reaction of *trans*-cinnamaldehyde **2** and cyclopentadiene[133] and in the addition of organoboronic acids to *ortho*-hydroxycinnamaldehyde.[134] Catalyst **44** has also already been identified as a competent catalyst for the enantioselective Diels-Alder reaction and conjugate addition of nitroalkanes to *trans*-cinnamaldehyde.[135]

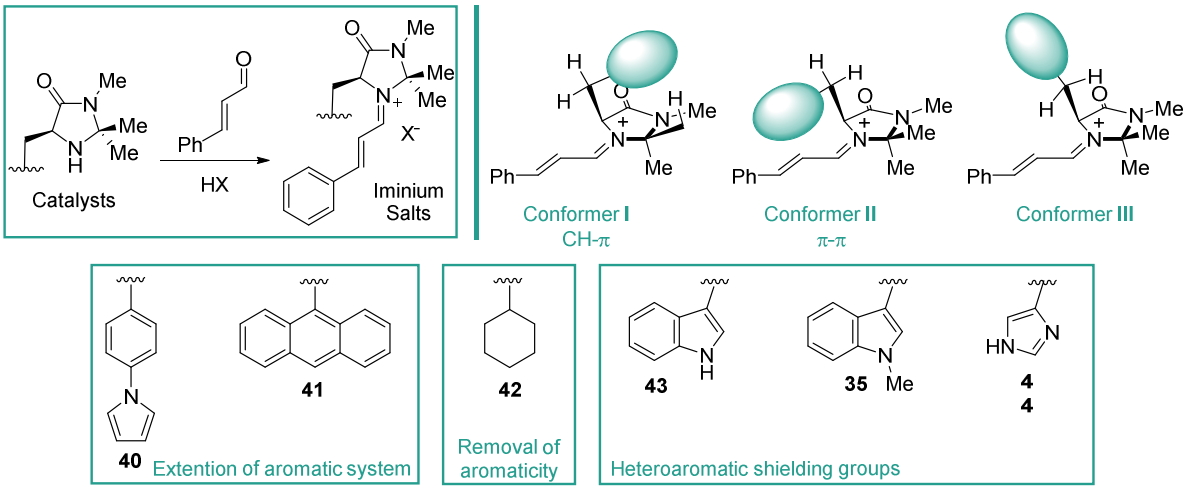

Figure 47 *Additional modifications of the shielding group.*

2.3.1 Syntheses of Catalysts 40-43

Imidazolidinones **40** and **41** were synthesised from (*S*)-Boc-BMI **23** following the procedure described in chapter 2.2.1. As for the other electron-rich benzyl bromide derivatives, a set of optimised conditions using LiHMDS and DMPU were employed (Scheme 9).

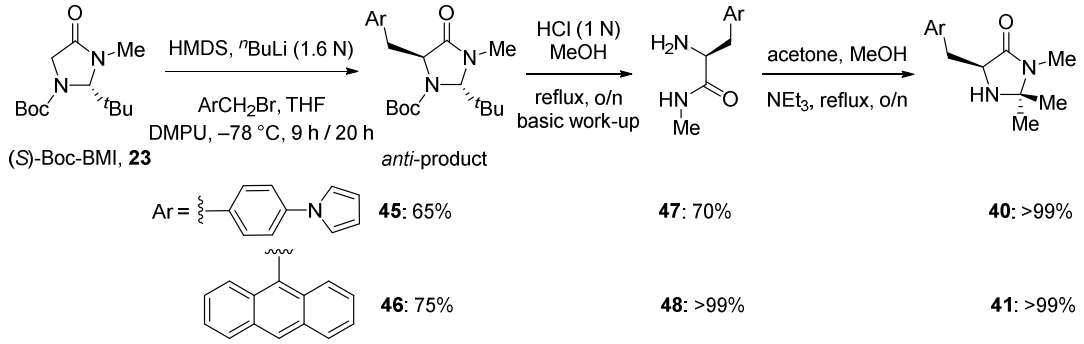

Scheme 9 *Syntheses of imidazolidinones with extended shielding groups **40** and **41**.*

The four other derivatives (**35** and **42**-**44**) were prepared from the corresponding amino acids (**49**-**51**) or histidine methyl ester dihydrochloride (**52**) in a 2-3 step procedure previously described in chapter 2.2.1.

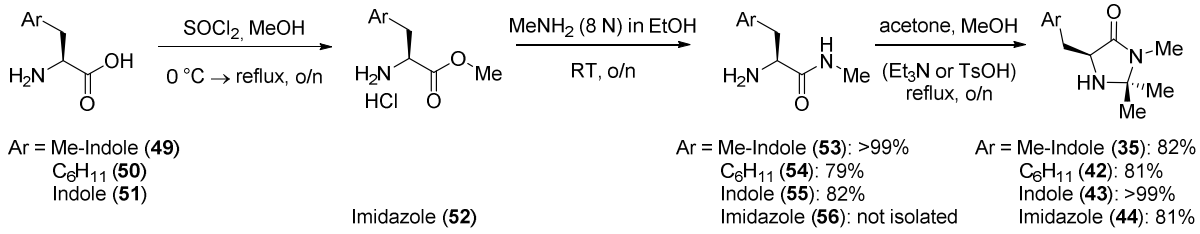

Scheme 10: *Syntheses of imidazolidinones derived from tryptophan (**35** and **43**), 3-cyclohexyl-L-alanine (**42**), and histidine methyl ester dihydrochloride (**44**).*

After successful preparation of the desired catalyst structures, the syntheses of the corresponding iminium salts were attempted by condensation with (*E*)-cinnamaldehyde **2**. Whilst it was not possible to isolate the iminium salts derived from catalyst **44** and **40**, the other targets were successfully isolated as the perchlorate salts (**35a**, **41a-43a**, Scheme 11).

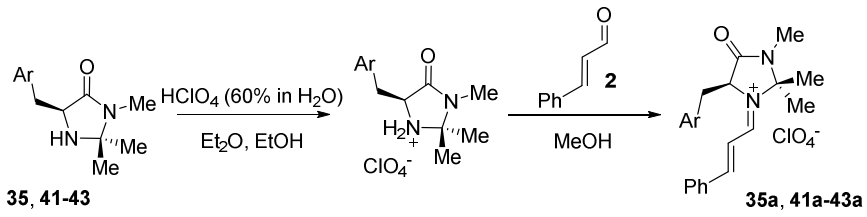

Scheme 11 *Syntheses of iminium salts* ***35a*** *and* ***41a-43a.***

2.3.2 The Quadrupolar Moment (Q_{zz}) of the Toluene Analogues of the Shielding Groups

The quadrupolar moment is described in detail in chapter 2.2.2. As for the electronically modified catalysts, the quadrupolar moments and ESP maps for the toluene analogues of the extended aromatic systems, the heteroaromatic groups and methyl-CH were computed.

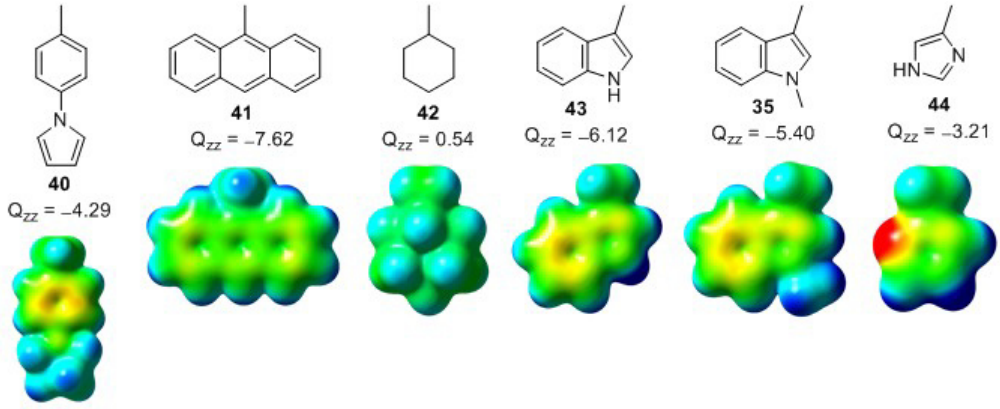

Figure 48 *Quadrupolar moment tensor components perpendicular to the aromatic plane in D·Å (Q_{zz}) and electron surface potential (ESP) of the toluene derivatives of imidazolidinones* ***35****, and* ***40-44****. Colour range of the electrostatic potential: –0.06 (red) to + 0.06 (blue).*

Whereas the anthracene derivative **41** has an even lower Q_{zz} than the most electron-rich example of the study thus far (trimethoxy analogue **3**, $Q_{zz} = –5.68$), the Q_{zz} of the two indole derivatives are of similar magnitude (**35** and **43**, $Q_{zz} = –5.40$ and –6.12, respectively). The quadrupolar moment tensors perpendicular to the aromatic plane of the toluene analogues of **40** and **44** ($Q_{zz} = –3.21$ and –4.29, respectively) are in the same range as the ones for derivative **6** and **1** ($Q_{zz} = –3.71$ and –3.46, respectively). The Q_{zz} of the cyclohexyl derivative was also calculated, even though it is not directly comparable to the other compounds, and was found to be slightly positive ($Q_{zz} = 0.54$).

2.3.3 X-Ray Crystallographic Analysis of Imidazolidinone Salts 42-44 and Iminium Salt 43a

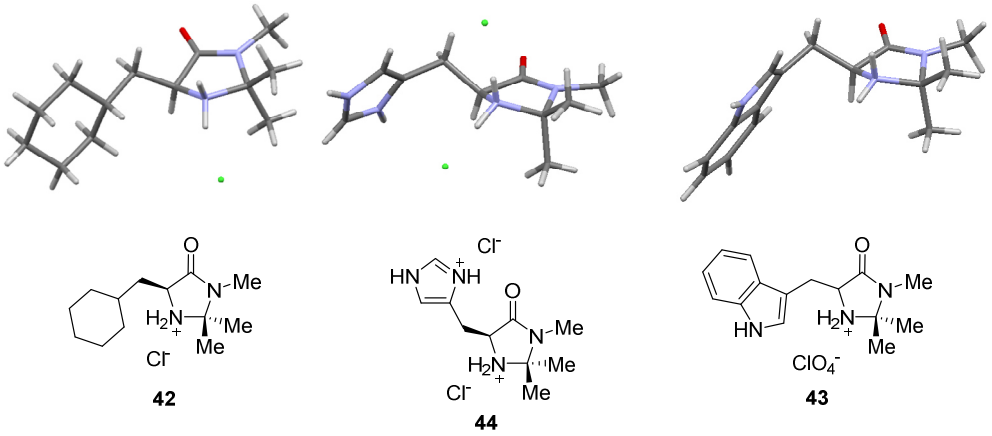

Figure 49 *X-ray structures of the hydrochloride salts of catalysts* ***42*** *and* ***44****, and of the perchlorate salt of* ***43****. The ClO_4^- counterion has been omitted for clarity.*

Gratifyingly, single crystals suitable for X-ray crystallographic analysis of the cyclohexyl and the histidine derived catalyst were obtained as the hydrochloride salts (Figure 49). Catalyst **44** crystallised as the dihydrochloride salt. For catalyst **43** it was possible to obtain crystals of the perchlorate salts. Analogous to previous observations in the crystal structures of the electronically modified catalyst series (chapter 2.2.3), the shielding groups reside in a *quasi*-equatorial orientation. Moreover, the shielding group is in proximity of the protonated amine [$\Phi_{NCCC} = -69.7°$ (**42**), –67.7° (**44**), and –67.2 (**43**)]; this torsional preference was also found in structures **1**, **8**, **9**, and **10**.

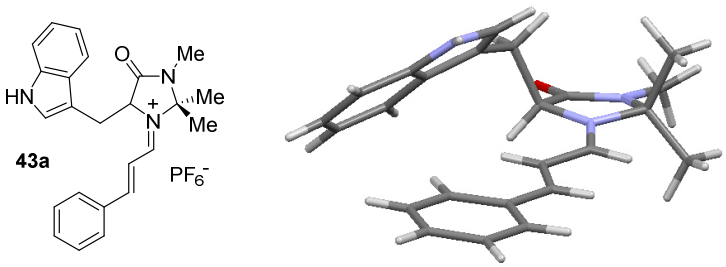

Figure 50 *X-ray structure of iminium hexafluorophosphate salt* ***43****. The PF_6^- counterion has been omitted for clarity.*

A racemic sample of the indole-derived iminium salt **43a** was successfully crystallised as the hexafluorophosphate salt. Interestingly, the compound adopts a tilted form of conformer **II**, which is postulated to be stabilised by a π-π interaction (Figure 50, $\Phi_{NCCC} = -74.1°$). In chapter 2.2.3, iminium salts adopting conformer **I** (**6a**, R = C_6H_4OH) and, for the first time,

conformer **III** (**10a**, R = C_6F_5) have already been discussed. Thus, a crystal structure for each three staggered conformers partitioned by 120° is presented in this work.

2.3.4 NMR Analysis of the Iminium Salts 35a, 41a, 42a, and 43a

The solution phase NMR spectroscopic analysis of the library of electronically modified phenyl analogues indicates that the shift-difference of the two methyl groups of the *geminal*-dimethyl moiety (chapter 2.2.4, $\Delta\delta^1H_{syn/anti}$ and $\Delta\delta^{13}C_{syn/anti}$) already gives good insights into the preferred conformational behaviour of the iminium salts. Furthermore, in the cases for which a significant $\Delta\delta^1H_{syn/anti}$ was observed, the enantioselectivity of the corresponding catalyst in the studied Friedel-Crafts reaction was generally good. To probe whether or not this observation could be generalised as an easy method for predicting the level of stereoinduction for a given catalyst, the $\Delta\delta^1H_{syn/anti}$ and $\Delta\delta^{13}C_{syn/anti}$ values for the iminium salts **35a** and **41a**-**43a** were determined (Table 5 and Figure 51). The indole derivatives **35a** and **43a** exhibit a similar magnitude of shift-differences as the trimethoxy catalyst **3a** ($\Delta\delta^1H_{syn/anti}$ = –0.58, –0.64, and –0.62 ppm, respectively). This is in agreement with the quadrupolar moment tensors, which were found to be in the same range (Q_{zz} = –5.40, –6.12, and –5.68, respectively). The iminium salt of **35** was also included in the conformer population analysis described in chapter 2.2.4 and was found to show similar conformational behaviour as the iminium salt derived from **3**. Therefore analogues **35** and **43** were predicted to give similar enantioselectivities as compound **3**. This hypothesis will be tested in chapter 2.3.5. The anthracene iminium salt **41a**, which was computed to have the highest electron-density over the aromatic ring (Q_{zz} = –7.62) of all studied structures, revealed a surprisingly small shift-difference of the dimethyl group ($\Delta\delta^1H_{syn/anti}$ = –0.26 ppm). This suggests that the anthracene moiety is likely positioned away from the *geminal*-dimethyl group probably due to unfavourable non-bonding interactions. This could possibly indicate a critical size effect of the shielding group on the selectivity of the reaction. Again, this will be investigated in the next chapter. The cyclohexyl bearing compound **42a** also exhibits a small shift-difference, which is consistent with the positive Q_{zz}. Consequently, the cyclohexyl analogue is expected to give low levels of enantioinduction.

Table 5 *Chemical shift-differences of the geminal-dimethyl group observed by ^{1}H and ^{13}C NMR spectroscopy.*

Iminium Salt (Ar)	Q_{zz} **[D·Å]**	**Δδ(*syn/anti*)^{1}H [ppm]**	**Δδ(*syn/anti*)^{13}C [ppm]**
41a (anthracene)	–7.62	–0.26	+0.10
42a (C_6H_{11})	+0.54	–0.03	+0.85
35a (Me-Indole)	–5.40	–0.58	–1.68
43a (Indole)	–6.12	–0.64	–1.83

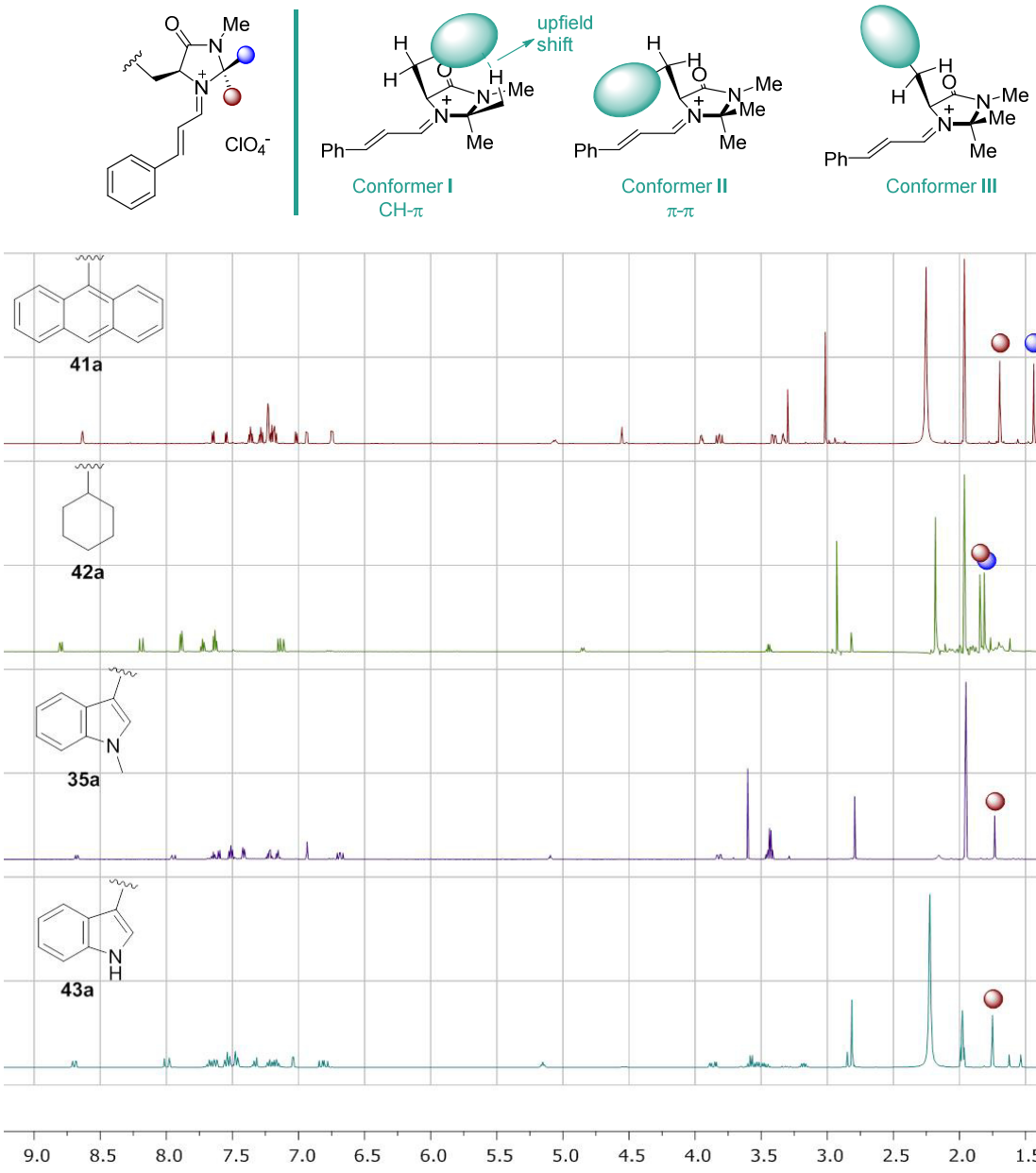

Figure 51 *Upper: The three staggered conformers of the imidazolidinone derived iminium salts. The CH-π interaction in conformer* ***I*** *results in an upfield shift of the syn-methyl group in the ^{1}H and ^{13}C NMR spectra. Lower: ^{1}H-NMR spectra.*

2.3.5 Catalysis Screening: Organocatalytic Friedel-Crafts Reaction of *N*-Me-Pyrrole

The performance of MacMillan catalyst analogues **35** and **40**-**44** were tested in the Friedel-Crafts reaction of *N*-methyl pyrrole **38** to (*E*)-cinnamaldehyde **2** (excess, 3 eq.). The enantioselectivities observed (determined using chiral HPLC after *in situ* reduction to the corresponding alcohols) were generally in very good agreement with the predictions made from the NMR analysis. The two catalysts **41** and **42** for which the corresponding iminium salts showed very small chemical shift-differences for the *geminal*-dimethyl group ($\Delta\delta^1H_{syn/anti}$ = –0.26 and –0.03 ppm, respectively) resulted in lower enantioselectivities in the studied reaction (*ee* = 55% and 38%, respectively) as expected. Steric congestion in the iminium salt is believed to account for the low enantioselectivity using the anthracene system. Conversely, in the *para* position extended phenyl-pyrrolo system **40** gave an acceptable enantiomeric excess of 87%. This is consistent with what would be expected from the Q_{zz} (–4.29), suggesting that extension of the aryl group into this direction is tolerated, but not beneficial in this reaction. The two indole derivatives **35** and **43** which displayed Q_{zz} values and chemical shift-differences in the same range as the trimethoxy-derivative **3**, showed enantioselectivities that are lower than expected (80% and 83%, respectively). Again, this might be a consequence of increased steric congestion. It is also important to note that for these derivatives the position of the quadrupolar moment tensor perpendicular to the aromatic ring is positioned differently due to the larger aromatic system and, thus direct comparison is not always valid. The histidine derived catalyst **44** showed the lowest level of enantioselectivity of all the catalysts tested so far (*ee* = 36%). This might at first be surprising considering the Q_{zz} of –3.21. But it must be kept in mind, that the imidazole moiety will be protonated under the reaction conditions which will inverse the polarity of the heterocycle.[136] Thus, the imidazole group will likely rotate away from the iminium chain, resembling conformer **III**.

Table 6 *Screening of the catalysts with modified shielding groups in the Friedel-Crafts reaction of N-Me-pyrrole* ***38*** *and (E)-cinnamaldehyde* ***2****.*

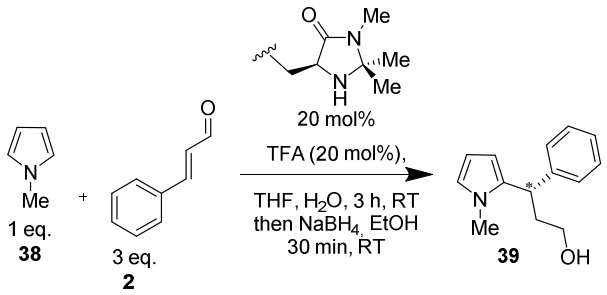

Catalyst	Q_{zz} [D·Å]	$\Delta\delta^1H_{syn/anti}$ [ppm]	*ee* [%]	*e.r.*
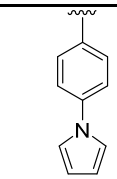 **40**	–4.29	–	87	93.5:6.5
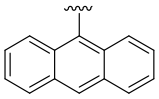 **41**	–7.62	–0.26	55	77.5:22.5
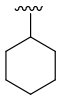 **42**	0.54	–0.03	38	69:31
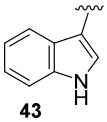 **43**	–6.12	–0.58	83	91.5:8.5
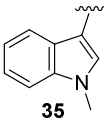 **35**	–5.40	–0.64	80	90:10
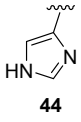 **44**	–3.21	–	36	68:32

2.3.6 Computational Analysis of Lowest Energy Conformers of Iminium Ions 35a, 41a, and 42a

To support the working hypothesis that the conformational preferences of the anthracene and indole derivatives are governed by steric repulsion, the ground-state energy minimum conformations of the iminium salts of **41a** and **35a** were computationally predicted. Additionally, the conformational behaviour of the CH analogue derived iminium ion **42a** was investigated. The calculations at the DFT level of theory were performed by Dr. Anthony Meijer at Sheffield University (UK).

*Anthracene-derived imidazolidinone iminium ion **41a**:*

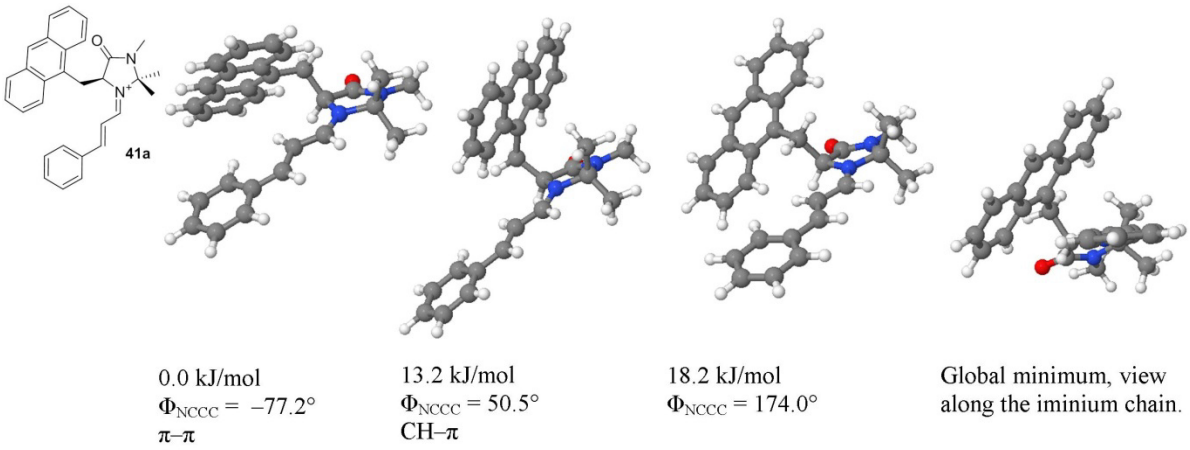

***Figure 52** Optimised geometries and relative energies for iminium ion **41a**.*

For the iminium ion derived from the anthracene catalyst **41a**, only one conformer was found to be significantly populated at RT (Figure 52). This conformer corresponds to conformer **II** stabilized by a π–π interaction ($\Phi_{NCCC} = -77.2°$). The anthracene moiety is significantly twisted out of plane presumably allowing for an edge-on interaction to the positively charged conjugated iminium chain (Figure 52, right). Consequently, shielding of the top face is insufficient. The other two identified minima corresponding to conformer **I** and **III** lie much higher in energy (+13.2 and +18.2 kJ/mol, respectively).

*Tryptophan-derived imidazolidinone iminium ion **35a**:*

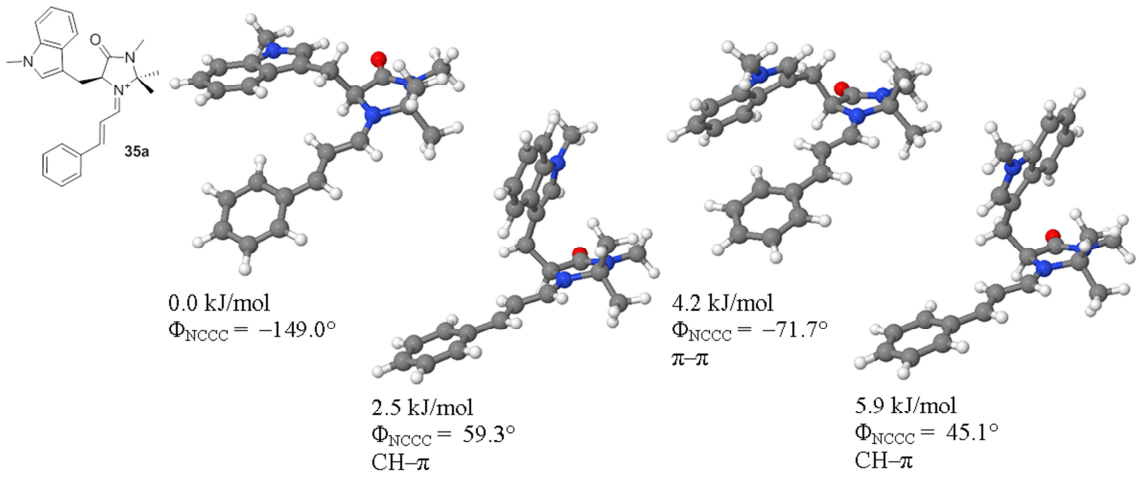

***Figure 53** Optimised geometries and relative energies for iminium ion **35a**.*

Computational analysis of the Me-indole iminium ion **35a** resulted in the identification of four energy minimum conformations. In the global minimum conformer the aromatic substituent was found to be positioned away from the reactive centre ($\Phi_{NCCC} = -149.0°$, between conformers **III** and **IV**). Two conformations resembling conformer **I** were identified at +2.5 kJ/mol and +5.9 kJ/mol. In both cases the stabilising CH-π interaction with the *syn*-methyl group was found to be directed to the centre of the five-membered ring of the indole moiety, but the heteroaromatic system was found to be flipped by 180° in the energetically higher lying conformer **I** as compared to the other one at +2.5 kJ/mol. A fourth low lying conformer resembling conformer **II** was found at +4.2 kJ/mol ($\Phi_{NCCC} = -71.7°$). The smaller energetic differences between the conformers explains the higher selectivity ($\Delta ee = 25\%$) of **35a** as compared to **41a**. Surprisingly, the obtained X-ray structure of the other indole iminium salt **43a** corresponds to the π-π conformer at +4.2 kJ/mol, suggesting that either **43a** exhibits a different conformational behaviour than the methylated-analogue **35a** or that packing effects govern the solid state conformation.

*Cyclohexyl-derived imidazolidinone iminium ion **42a**:*

For the saturated-cyclohexyl derivative **42a**, four energy minima were identified (Figure 54). By far the lowest lying conformation corresponds to conformer **III** ($\Phi_{NCCC} = -168.0°$), where the substituent is rotated away from the core ring, thus providing insufficient shielding. This is in agreement with the low enantioselectivity obtained with this catalyst (*ee* = 38%). In two additional energy minima identified, the group is also rotated away resembling conformer **III** (+7.1 kJ/mol and +10.5 kJ/mol). A structure resembling conformer **I** was found at 12.0 kJ/mol.

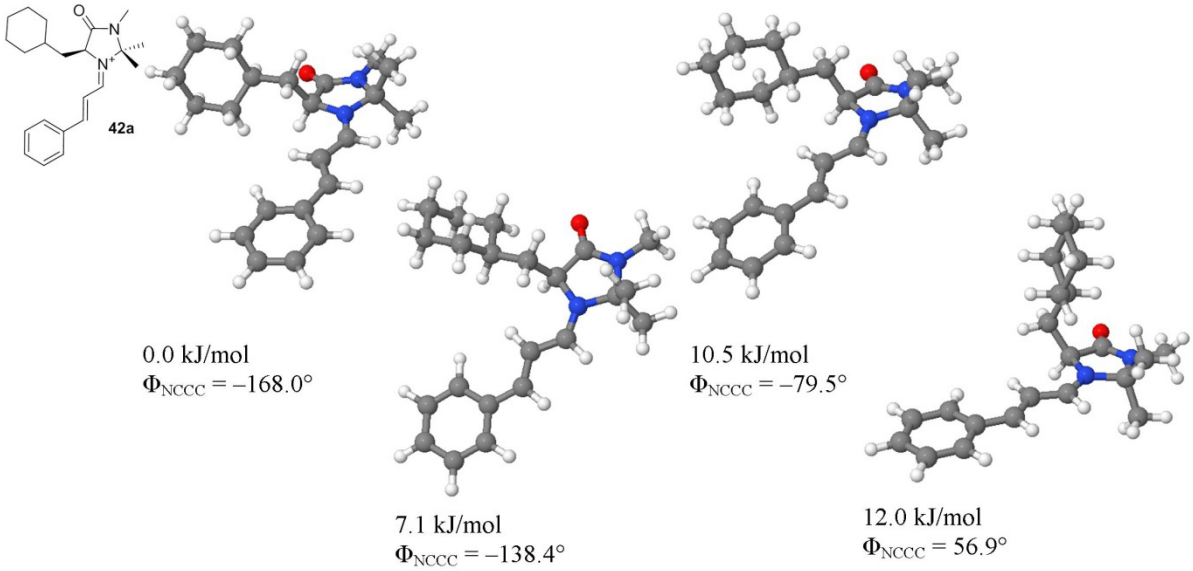

***Figure 54** Optimised geometries and relative energies for iminium ion **42a**.*

2.4 Modifications of the Benzylic Position

In the last two chapters 2.2 and 2.2.8, it was discussed how modifications of the aromatic shielding group influence the behaviour of the MacMillan catalyst and by extension the corresponding α,β-unsaturated iminium salt. In this chapter, a molecular editing study is described to investigate the benzylic site in α-position to the shielding group. The development of so-called "*conformer equivalents*" by the stereoselective introduction of fluorine in the benzylic position has been previously reported by this laboratory.[4] The iminium salts of the two diastereomers are postulated to be fixed in conformation **I** (**57a**, *S*) or in conformation **II** (**58a**, *R*), due to an interplay of a stabilising fluorine-iminium ion *gauche* effect and a CH–π or π–π interaction, respectively (Figure 55). Herein, the two diastereomers **57** and **58** are studied further, and a computational conformation analysis is enclosed.

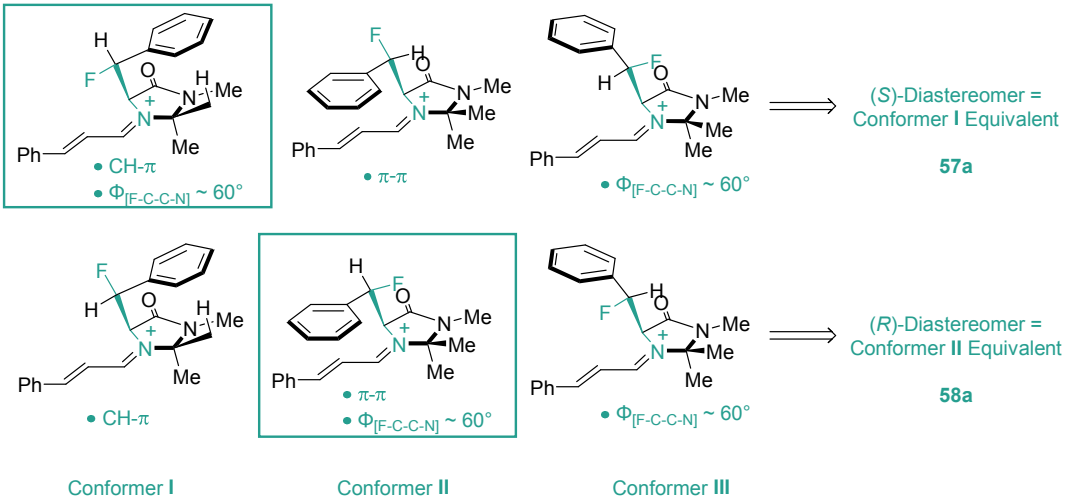

Figure 55 *Conformer equivalents* ***57a*** *and* ***58a*** *and mode of conformational control.*[4]

Furthermore, the ramifications of increasing the distance between the central imidazolidinone core and the aryl shielding group by introducing a CH_2-moiety (**59**) were studied. It was expected, that the phenyl group would no longer be able to undergo a CH–π interaction with the *syn*-methyl group. Likewise, it was predicted, that the increased flexibility would disfavour the population of conformer **II** due to increased rotational freedom. Additionally, it was planned to gradually increase the steric bulk by varying the number of shielding phenyl groups from zero (**60**) *via* monophenyl **1** and diphenyl **61** all the way to the trityl group (**62**). The modulations of the benzylic position discussed in this chapter are summarised in Figure 56.

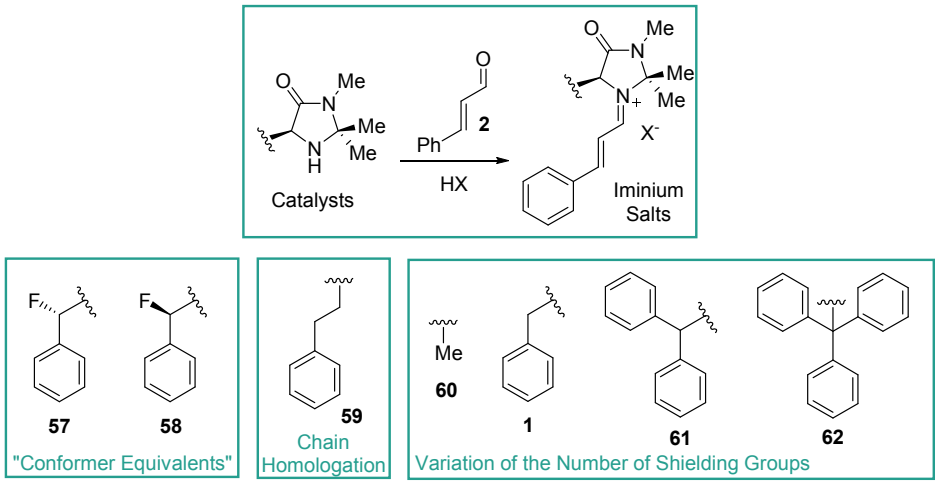

Figure 56 *Modulations of the MacMillan catalyst in the benzylic position.*

2.4.1 Syntheses of the MacMillan Analogues Modified in the Benzylic Position

"Conformer Equivalents" ***57*** *and* ***58****:*

The syntheses of the two diastereomers **57** and **58** bearing a configurationally defined fluorine in the benzylic position were carried out by Patrick Bentler in course of his Master thesis following the procedures developed by this laboratory.[4] Therefore, the synthesis will not be discussed in detail, but the key features are summarised below. Both catalysts can be constructed from a common precursor, L-*threo*-phenylserine **63** (Scheme 12).

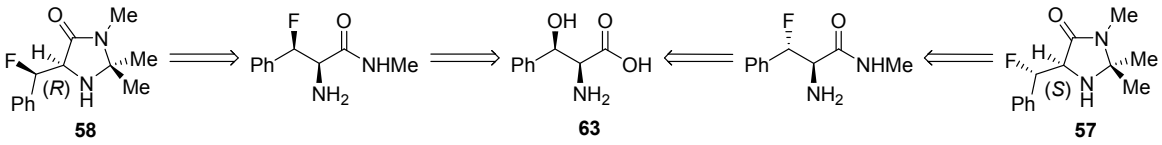

Scheme 12 *Retrosynthetic analysis of* ***57*** *and* ***58****.*

The key challenge in these protocols is the stereoselective deoxyfluorination of the benzylic position. To achieve this transformation a method described by Bach was modified and utilised.[137] The Bach model describes that facial selectivity of nucleophilic attack to chiral benzylic cations can be achieved by exploiting $A^{1,3}$-strain (Figure 57). The hydrogen substituent is positioned in plane with the aromatic ring to minimize $A^{1,3}$-strain. The nucleophile then attacks from the less hindered face in which the smaller substituent is placed. It should be noted, that because deoxyfluorinations in benzylic positions using DAST likely proceed *via* a S_N1 mechanism, this method is believed to be valid for the

described fluorination. The facial selectivity of the reaction can be controlled by adjusting the size of the amino and the carboxy function. The optimised structures were found to be L-phenylserine methyl amide **64** and compound **65** for the preparation of the (*R*,*R*)-diastereomer **66** and the (*S*,*R*)-diastereomer **67**, respectively. A possible rationalisation of the selectivity for these two structures is illustrated in Figure 57.

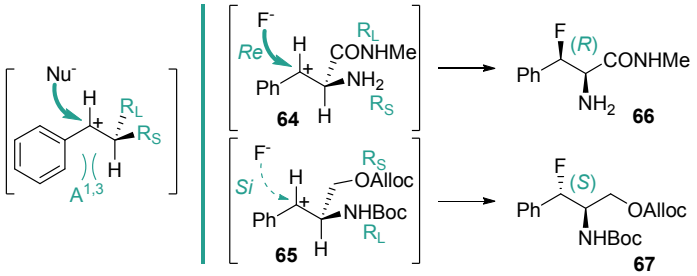

Figure 57 *The Bach model and application for the fluorination of L-threo-phenylserine derivatives* ***66*** *and* ***67****.*

Analogue with increased distance of the shielding group ***59****:*

Compound **59** was obtained from (*S*)-Boc-BMI **23** and (2-bromoethyl)benzene in a three step procedure in 26% overall yield (Scheme 13) following the procedure described in 2.2.1.

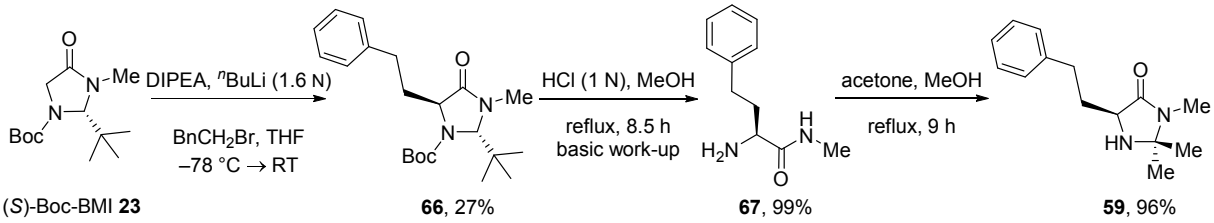

Scheme 13 *Synthesis of the MacMillan imidazolidinone analogue* ***59****.*

Synthesis of catalyst series with varied numbers of shielding groups:

The synthesis of the 1st generation MacMillan catalyst **1** is described in 2.2.1. The methyl-analogue **60** without an aryl shielding group was obtained from L-alanine ethyl ester hydrochloride **68** in a two step procedure in very good yield (Scheme 14).

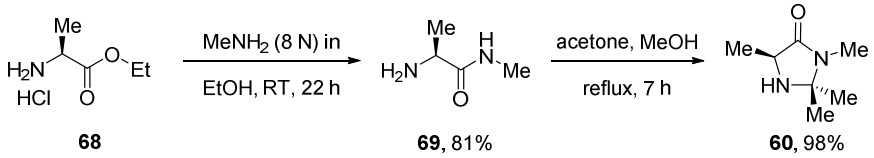

Scheme 14 *Synthesis of the alanine derived catalyst* ***60****.*

Similarly, the diphenyl catalyst **61** was synthesised from the corresponding commercially available amino acid (Scheme 15). Formation of the methyl amide **71** proceeded in good yield (87% over 2 steps). The product imidazolidinone **61** was isolated in only moderate yield (52%).

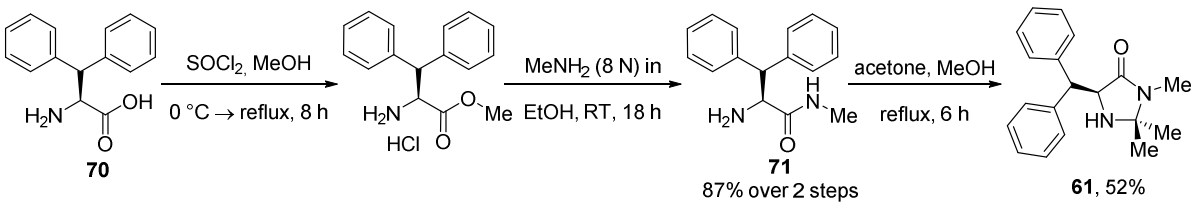

Scheme 15 *Synthesis of the diphenyl-derivative* ***61****.*

The synthesis of the trityl-derivative **62** was initially attempted *via* alkylation of Boc-BMI **23** using the Seebach procedure (see chapter 2.2.1). However, despite trying numerous reaction conditions, formation of the product was never observed (Scheme 16).

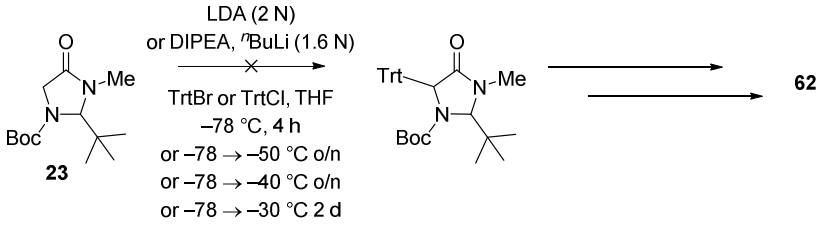

Scheme 16 *Attempted synthesis of* ***62****.*

Subsequently, a strategy was envisaged that has been reported for the synthesis of 2-tritylpyrrolidine (**72**, Scheme 17). The key step of this transformation is the nucleophilic attack of lithium triarylmethide (prepared *in situ*) to nitrone **73**.

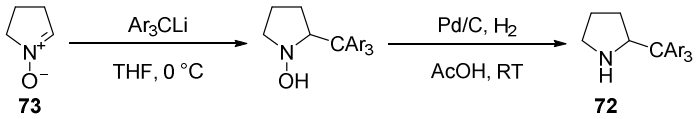

Scheme 17 *Synthesis of triarylpyrrolidine* ***72****.*

By employing the nitrone of BMI (**74**) it was envisaged that the *trans* product might be formed selectively. This proposal was supported by a report by Long *et al.* who used the chiral **74** in highly stereoselective cycloaddition reactions.[138] However, unfortunately this strategy proved unsuccessful for the synthesis of compound **62** (Scheme 18).

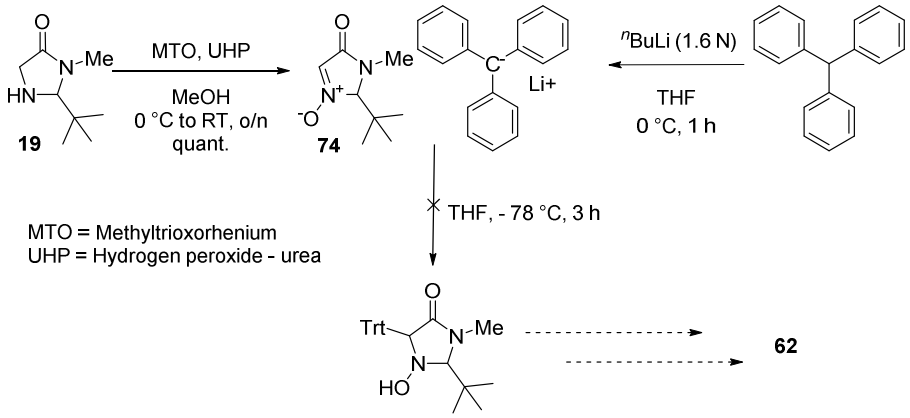

Scheme 18 *Attempted synthesis of* ***62*** *via nitrone* ***74****.*

A third attempt following a procedure by Klumpp *et al.* was investigated, using aminoalcohol **75**, benzene and CF_3SO_3H (Scheme 19). Compound **75** was prepared from commercially available methyl-(*S*)-3-Boc-2,2-dimethyl-4-oxazolidinecarboxylate (**76**) by Grignard addition of PhMgBr in 88% yield. The product was then treated with CF_3SO_3H in benzene at RT. The desired compound could not be isolated, but instead a mixture of products was formed. Finally, deprotection of the amine prior to the build-up of the trityl moiety was explored, but the protocols tested led to formation of the open-chain compound **77**. The preparation of **62** was not further investigated.

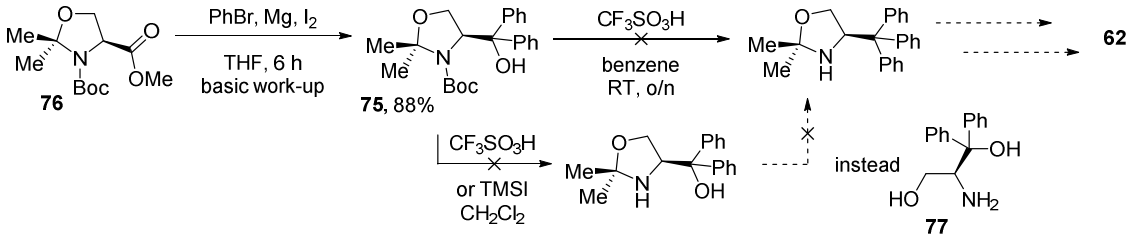

Scheme 19 *Attempted synthesis of* ***62*** *by reaction of aminoalcohol* ***75*** *with benzene and* CF_3SO_3H*.*

Syntheses of the iminium salts:

With the catalyst structures **57-61** in hand, the corresponding iminium salts **57a-61a** were prepared by formation of the perchlorate salts and subsequent condensation with *trans*-cinnamaldehyde **2** (Scheme 20). Despite repeated attempts, the iminium salt of **59** could not be isolated.

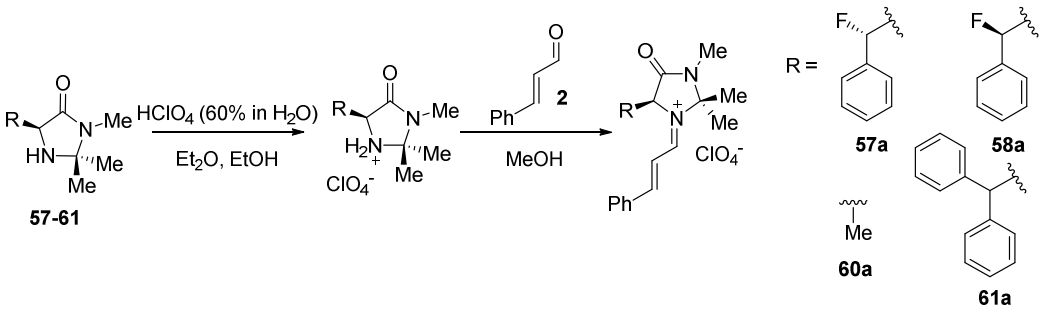

Scheme 20 *Syntheses of iminium perchlorate salts* ***57a***, ***58a***, ***60a***, *and* ***61a***.

2.4.2 X-Ray Crystallographic Analysis of Imidazolidinone and Iminium Salts

The crystal structures of the hydrochloride salt of **58** and of the hexafluorophosphate salt of **57** (Figure 58) have been reported previously.[4] Both compounds were crystallised from the racemic mixture. For **57** the other enantiomer is shown (*R*,*S*). As expected, in both imidazolidinone salts, the fluorine is positioned *gauche* to the protonated amine. For **58** the fluorine is in *synclinal-exo* arrangement ($\Phi_{NCCF} = 53.4°$), whilst for **57** the fluorine is *synclinal-endo* ($\Phi_{NCCF} = -73.0°$). Thus, in both structures the benzyl is rotated away from the core ring. In **58** the amine is pyramidalised to a similar extend as was observed for the previously discussed imidazolidinone salts placing the benzyl in quasi-equatorial position (chapter 2.2.3 and 2.3.3). However, in **57** the nitrogen is almost flat in plane.

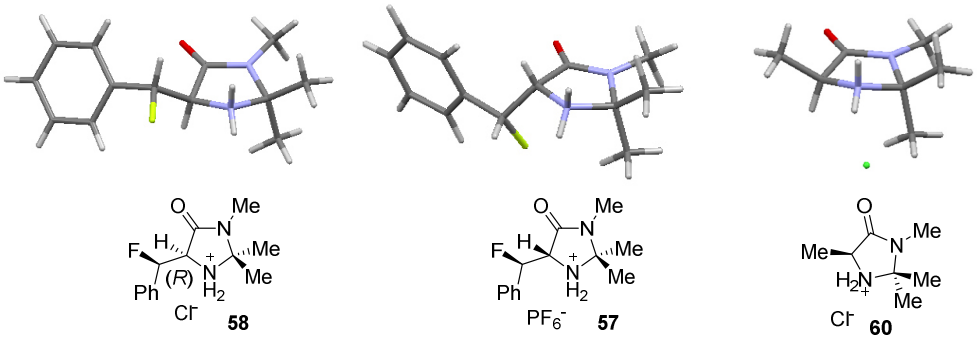

Figure 58 *X-ray structures of* ***58***·*HCl,* ***57***·*HPF*$_6$ *and* ***60***·*HCl. For* ***57*** *and* ***58*** *the counterions have been omitted for clarity.*

Additionally, single crystals suitable for X-ray crystallographic analysis of the methyl analogue **60** were isolated (Figure 58). The nitrogen is pyramidalised such that the methyl is in a *quasi*-equatorial position.

Gilmour and Sparr also reported the crystal structure of the iminium salt derived from imidazolidinone **58** and (*E*)-cinnamaldehyde **2**. The crystal structure beautifully demonstrates that the stereoselective introduction of fluorine in the benzylic position to give the *R*,*R* diastereomer forces the shielding group into conformer **II** (as opposed to conformer **I** for the parent structure described in 2.2.3). The fluorine substituent is positioned *synclinal-endo* to the nitrogen of the iminium moiety ($\Phi_{NCCF} = 64.6°$).

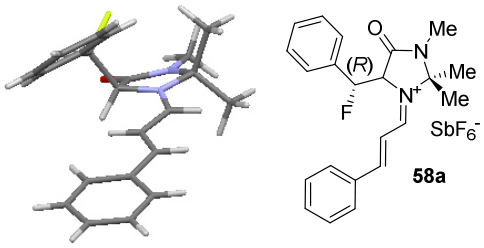

Figure 59 *X-ray structure of the hexafluoroantimonat salt of* ***58a****. The SbF_6^- counterion is omitted for clarity.*

2.4.3 NMR Analysis of the Iminium Salts 57a-61a

In chapter 2.3.4 it was shown that the NMR shift-differences observed for the two *geminal*-methyl groups in the imidazolidinone derived iminium salts already give a qualitative evaluation of the efficiency of the corresponding catalyst in the organocatalytic addition of *N*-methyl pyrrole to (*E*)-cinnamaldehyde. The upfield-shift of the *syn*-methyl group was attributed to a CH-π interaction with the aryl shielding group that occurs in conformer **I**. To test whether this prediction only holds true for the series of catalysts with modified aryl shielding groups, the $\Delta\delta^1H_{syn/anti}$ and $\Delta\delta^{13}C_{syn/anti}$ of iminium salts **20a-24a** were determined (Table 7). As expected, the conformer equivalent fixed in the CH-π position (**57a**) shows the largest differences in shifts of all the studied iminium salts. This is not surprising, because this compound is believed to almost solely populate conformer **I**. Similarly, the other conformer equivalent, which is believed to predominantly populate conformer **II**, shows very small shift-differences of the two methyl groups. ($\Delta\delta^1H_{syn/anti} = -0.06$ ppm). Also anticipated was the small $\Delta\delta^1H_{syn/anti}$ observed for the methyl derived iminium salt **60a**. The negligible shift-difference of the methyl analogue also serves as a proof for the shift occurring due to an interaction with the shielding group. The diphenyl analogue **61a** gave surprisingly low shift-differences ($\Delta\delta^1H_{syn/anti} = -0.57$ ppm) suggesting that the shielding of this moiety might not be as good as for a single phenyl group. This seemed surprising, but might be explained by the fact that the phenyl groups are probably forced to rotate out of

plane and are therefore unable to undergo nonbonding CH-π or π-π interactions. Thus, it is proposed from the NMR analysis, that the diphenyl catalyst **61** gives decreased levels of enantioselectivity as compared to the parent catalyst **1**. This is tested in the following chapter.

Table 7 *Differences of the chemical shifts of the geminal-dimethyl group observed by ^{1}H and ^{13}C NMR spectroscopy. [a] SbF_6^- salt.*[4]

Iminium Salt (R)	$\Delta\delta(syn/anti)^{1}H$ [ppm]	$\Delta\delta(syn/anti)^{13}C$ [ppm]
1a ($CH_2C_6H_5$)	–0.89	–2.77
57a (*S*-$CHFC_6H_5$)[a]	–1.08	–3.60
58a (*R*-$CHFC_6H_5$)[a]	–0.06	+0.60
60a (CH_3)	+0.03	+1.40
61a ($CH(C_6H_5)_2$)	–0.57	

2.4.4 Catalysis Screening: Organocatalytic Friedel-Crafts Reaction of *N*-Me-Pyrrole

To test the organocatalytic performance of the imidazolidinones modified in the benzylic position in a model reaction, and compare the results to predictions made from the NMR analysis, **57-61** were employed in the Friedel-Crafts reaction of *N*-methyl pyrrole **38** and (*E*)-cinnamaldehyde **2** (Table 8). All catalysts proved to be competent and completion of the reaction was observed within three hours at RT. The CH-π conformer equivalent **57** resulted in slightly improved enantioselectivity compared to the parent catalyst **1** (90% and 85% *ee*, respectively). The π-π conformer equivalent **57** on the other hand showed significantly decreased levels of enantioinduction (63% *ee*). This is consistent with the small $\Delta\delta^{1}H_{syn/anti}$ observed for **57**. Despite this agreement, the low stereoselectivity is surprising given that this iminium salt is predicted to predominantly populate conformer **II**, and in this conformer shielding should be effective. This finding requires clarification. Employment of the imidazolidinone with increased distance between the shielding group and the reaction centre **59** resulted in very low levels of enantioinduction (38% *ee*). This may suggest as predicted, that the aryl shielding group of this catalyst is not ideally positioned to undergo non-covalent interactions with the *syn*-methyl group and the iminium chain. As expected, the Me-analogue **60** gave the lowest levels of enantioinduction of all the structures studied so far (27% *ee*). The enantioselectivity obtained for the diphenyl-catalyst **61** was also low (51% *ee*) consistent with the small $\Delta\delta^{1}H_{syn/anti}$ observed.

Table 8 *Screening of the modified catalysts in the Friedel-Crafts reaction of N-Me-pyrrole* ***38*** *to (E)-cinnamaldehyde* ***2****. [a] SbF_6^- salts.*[4]

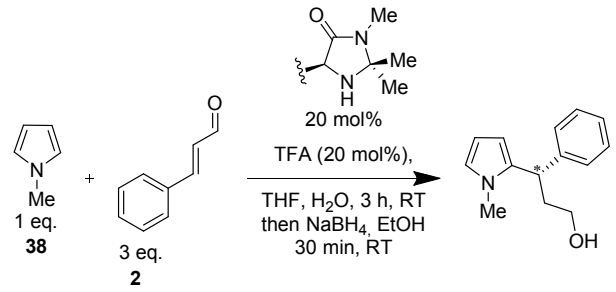

Catalyst	Δδ(*syn*/*anti*)^{1}H [ppm]	*ee* [%]	*e.r.*
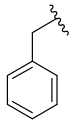 **1**	–0.89	85	92.5:7.5
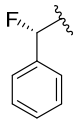 **57**	–1.08[a]	90	95:5
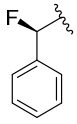 **58**	–0.06[a]	63	81.5:18.5
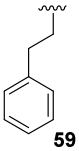 **59**	–	38	69:31
 **60**	+0.03	27	63.5:36.5
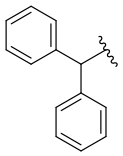 **61**	–0.57	51	75.5:24.5

2.4.5 Computational Analysis of Lowest Energy Conformers of Iminium Ions 57a, 58a, 61a, and 60a

To gain a more detailed insight into the conformational behaviour of the two conformer equivalents **57a** and **58a**, and of the iminium ion derived from the diphenyl-imidazolidinone **61**, a computational analysis of the lowest energy conformers was performed in collaboration with Dr. Anthony Meijer from the University of Sheffield (UK). Additionally, the methyl-analogue **60a** was investigated for completeness.

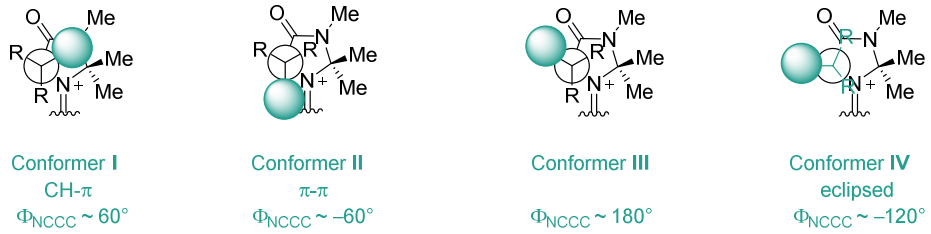

Figure 60 *Possible low-energy conformers of imidazolidinone derived iminium salts* ***Xa****.*

CH-π conformer equivalent ***57a****:*

For the iminium ion **57a** predicted to be "fixed" in conformer **I**, three energy minima were identified (Figure 61). As expected, the global minimum structure was found to be the CH-π conformer with the fluorine positioned *synclinal exo* to the nitrogen, thus satisfying the fluorine-iminium ion *gauche* preference ($\Phi_{NCCF} = -79°$). The second minimum identified is 8.8 kJ/mol higher in energy. In this conformer, the positions of the aryl shielding group and the fluorine are practically preserved, but the geometry of the N^+=C iminium bond is changed to the (*Z*)-isomer. Even higher in energy (+13.3 kJ/mol) is a third conformer in which the other *gauche*-conformation is engaged. Consequently, it can be concluded, that almost solely the anticipated conformer **I** is populated at RT.

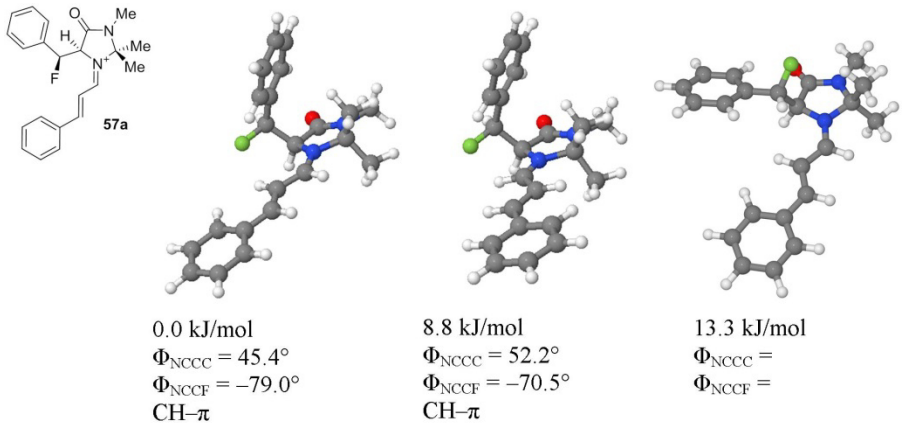

Figure 61 *Optimised geometries and relative energies for iminium ion* ***57a****.*

*π-π conformer equivalent **58a**:*

The compound that was designed as the conformer **II** equivalent was also identified to have three energy minima (Figure 62). Again, the global energetic minimum verifies the predicted conformation. The fluorine nitrogen relationship is *synclinal endo*. This is consistent with the crystal structure described in chapter 2.4.2, though the calculated conformation is slightly distorted as compared to the X-ray structure (Φ_{NCCF} = 48.8° and 64.6°, respectively). A second energy minimum was found to be conformer **IV** in which the bond to the shielding aryl group eclipses with the neighbouring C–H bond and the C–F bond eclipses with C–N^+ bond. In this conformation, which is only 1.3 kJ/mol higher in energy than the global minimum, the reaction centre is not very well shielded. These findings partially rationalise the reduced selectivity observed (63% *ee*). Much higher in energy at +18.8 kJ/mol is a conformation in which the fluorine is positioned *anti* to the iminium nitrogen, highlighting the power of the fluorine-iminium ion *gauche* effect.

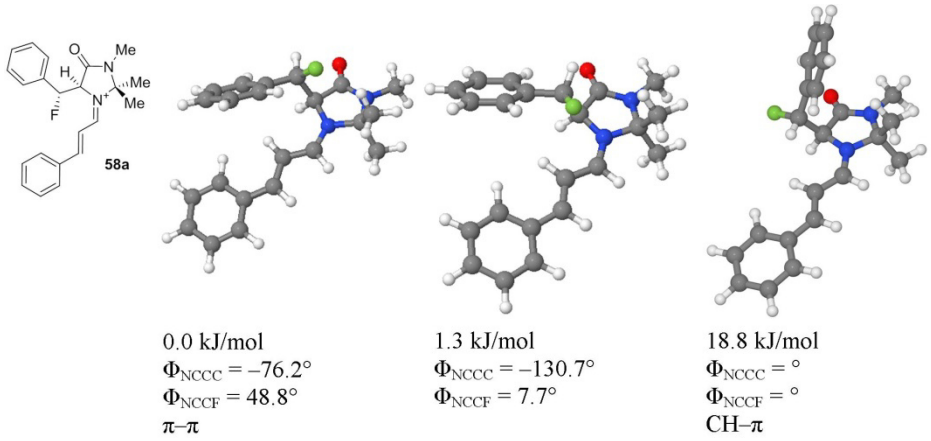

***Figure 62** Optimised geometries and relative energies for iminium ion **58a**.*

*Iminium ion derived from the diphenyl imidazolidinone **(61a)**:*

For the diphenyl analogue **61a**, three energy minimum conformations were identified (Figure 63). However, only one conformer was found to be significantly populated at RT. In this conformer, both phenyl groups are positioned far away from the reaction centre approximately populating conformer **III** (Figure 56), thus almost eclipsing the neighbouring C–H and C–C bonds (Φ_{NCCC} = 82.3° and –145.9°). The conformer is shown with the view along the CC–CN benzylic bond in Figure 63 for clarification. The other two energy minima identified, in which the shielding groups are placed in the space corresponding to conformer

II/III and conformer **I/II** lie much higher in energy (+16.2 and +22.3 kJ/mol, respectively). These findings correspond well to the small shift-differences ($\Delta\delta^1H_{syn/anti}$ = –0.57 ppm) observed for the two *geminal*-methyl groups by NMR analysis and the low levels of stereocontrol (51% *ee*) in the Friedel-Crafts addition of *N*-methyl pyrrole **38** to (*E*)-cinnamaldehyde **2**.

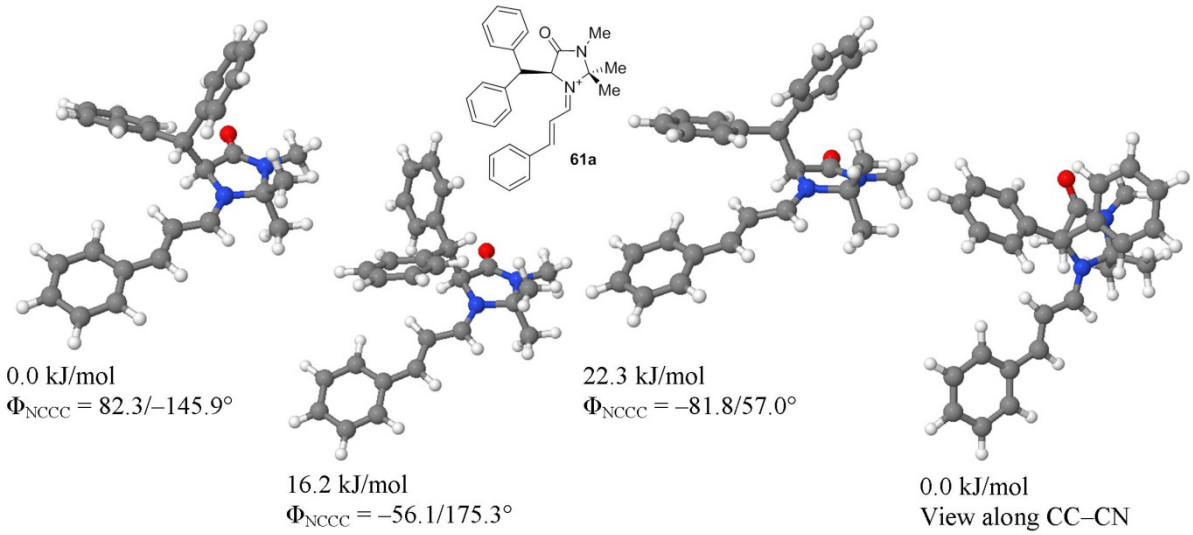

Figure 63 *Optimised geometries and relative energies for iminium ion* ***61a****.*

Iminium ion derived from the alanine-derived imidazolidinone ***(60a)****:*

For the α,β-unsaturated iminium ion **60a** of the alanine derived imidazolidinone, only one energy minimum was identified with the iminium chain in the (*E*)-conformation (Figure 64).

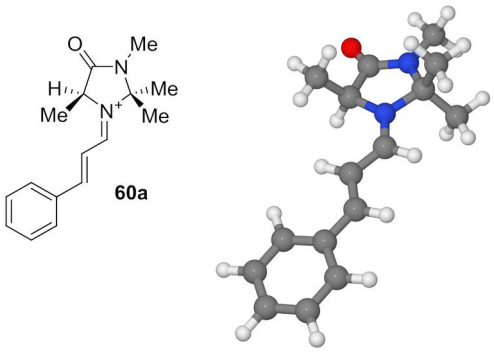

Figure 64 *Optimised geometry of the global energy minimum for iminium ion* ***60a****.*

2.5 Correlation between Conformational Preferences, Enantioselectivity and ^{1}H NMR-Shift of the *syn*-Methyl-Group

In chapters 2.2–1.1, a clear correlation between the shift-differences of the *syn*- and the *anti*-methyl groups of the *geminal*-dimethyl moiety ($\Delta\delta^1H_{syn/anti}$) in the iminium salts and the observed enantioselectivity in the addition of *N*-methyl pyrrole **38** and (*E*)-cinnamaldehyde **2**, was observed. The coherence was so general, that in several cases the enantioselectivity achieved with a given catalyst was well predicted based on the $\Delta\delta^1H_{syn/anti}$ of the corresponding iminium salt. This observation was not overly surprising, as both the $\Delta\delta^1H_{syn/anti}$ and the level of enantioinduction are direct consequences of the conformational behaviour of the iminium ion (Figure 65). To test the generality of this correlation, the $\Delta\delta^1H_{syn/anti}$ deduced from the NMR spectra of the α,β-unsaturated iminium ions were plotted against the enantioselectivity of the corresponding organocatalysts in the Friedel-Crafts reactions of *N*-methyl pyrrole **38** and (*E*)-cinnamaldehyde **2** (Figure 66). The diphenyl-derivative **61** was omitted from this analysis, since the influence of the diphenyl-moiety on the *syn*-methyl NMR-shift is not comparable to the other compounds.

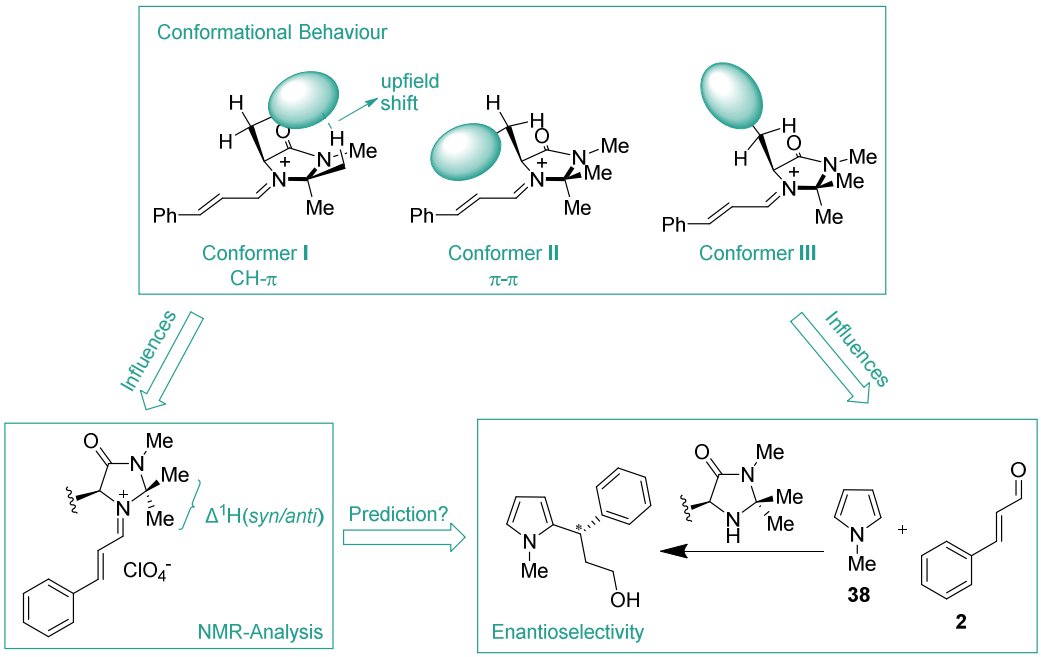

Figure 65 *Correlation between conformational behaviour of the iminium ion, the observed $\Delta\delta^1H_{syn/anti}$ and the enantioselectivity of the corresponding catalyst in the addition of N-methyl pyrrole* ***38*** *to (E)-cinnamaldehyde* ***2****.*

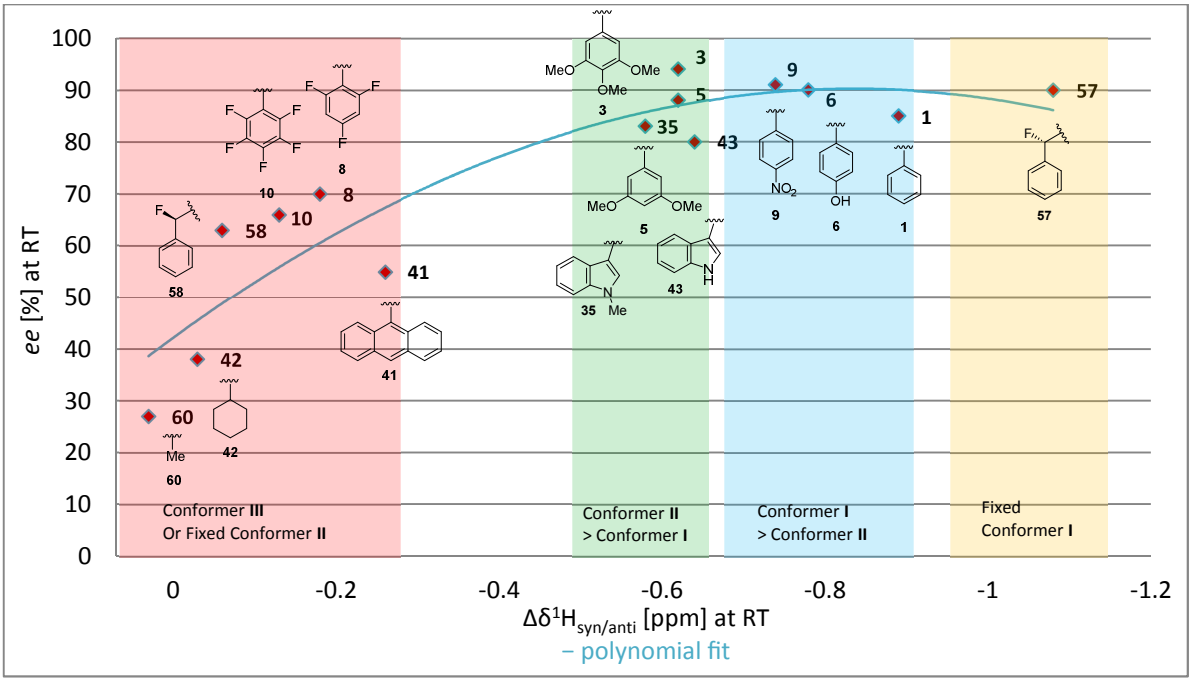

Figure 66 *Plot of the observed* $\Delta\delta^1H_{syn/anti}$ *of the MacMillan catalyst-derived iminium salts against the observed enantioselectivity of the corresponding catalyst in the Friedel-Crafts addition of N-methyl pyrrole* ***38*** *to (E)-cinnamaldehyde* ***2****. The coloured regions group iminium salts according to their conformational behaviour.*

The plot shows a clear correlation between $\Delta\delta^1H_{syn/anti}$ and the obtained selectivities, which is conveniently represented by a polynomial fit. Furthermore, the different regions of the graph can be attributed to distinct conformational preferences: The red region includes the catalysts giving poor enantioselectivities, with iminium salts displaying small differences in the chemical shifts of the *geminal*-dimethyl groups, and corresponds to the iminium salts predominantly populating conformer **III** and/or a distorted conformer **II**. The green region represents the iminium salts that are postulated to populate conformer **I** and conformer **II** with a slight preference for conformer **II**. The blue region includes the iminium ions with a similar conformational behaviour, but with a slight preference for conformer **I**. The 'conformer equivalent' fixed in conformer **I** resulted in the largest $\Delta\delta^1H_{syn/anti}$ (–1.08 ppm) and lies in the yellow region of the plot. This clearly illustrates, that the ^{1}H NMR spectra of these imidazolidinone-derived iminium ions give reliably predictions for the catalytic performance of the corresponding imidazolidinone-catalysts. Furthermore, it is believed, that this holds true for structural analogues and, thus, may prove useful for future catalyst design.

2.6 Modification of the *geminal*-Dimethyl group

Having investigated the consequences of altering the shielding group and the benzylic position in chapters 2.2–2.5, it was envisaged that a study of the effects of changing the *geminal*-dimethyl group of the MacMillan catalyst would be insightful. Therefore, as a first stage, the analogue with the dimethyl group removed (**78**) and a series with differently sized spiro rings **79-81** were planned (Figure 67).

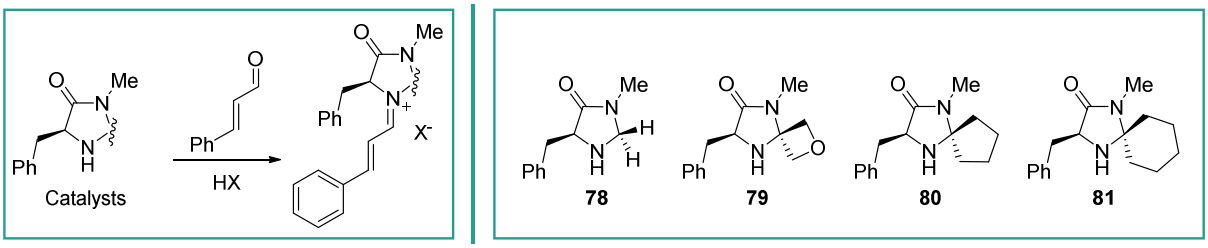

Figure 67 *Modification of the geminal-dimethyl group.*

It was expected that in the iminium salt of imidazolidinone **78** not only the conformational behaviour of the phenyl ring will be altered, but also that the (*E*)/(*Z*)–selectivity (for the conformational diversity of the iminium ions see Figure 68). Since conformer **I** is presumably no longer stabilised by a CH-π interaction, the phenyl group will likely be positioned in conformers **II** and **IV** in iminium salt **78a**. Additionally, the (*E*)/(*Z*)-ratio, which is believed to be controlled by $A^{1,3}$-allylic strain, could be profoundly influenced. For the geometrically controlled spiro-compounds, decreased abilities to undergo stabilising CH-π interactions with the aryl shielding group were expected, and it was predicted that this effect will be the more pronounced, the smaller the spiro ring. Oxetane was chosen as smallest spiro system. The properties and synthesis of this moiety has been extensively studied by Carreira and co-workers[139] and found valuable applications, especially in drug design. Carreira *et al.* reported, that the oxetanyl group occupies essentially the same van der Waals volume as a *geminal*-dimethyl group,[139a] thus, it is proposed, that substitution of the *geminal*-dimethyl group by oxetane should have negligible effects on the (*E*)/(*Z*)-ratio. But the geometry of the CH_2 group will be drastically changed as compared to the CH_3-groups. The *geminal*-dimethyl moiety was found to be in perfect tetrahedral arrangement with the angle between the two methyl groups being 111.5° and 112.3° for the iminium salt **1a** and the hydrochloride salt of imidazolidinone **1**, respectively. However, the C–C–C bond angle for 3,3-disubstituted oxetanes was reported to be 84.1±0.7°.[139d] Furthermore, the oxetane

was found to be essentially planar, unlike the structurally similar cyclobutane. The planarity renders the oxetanyl group particularly interesting for this study, because the hydrogen substituents that could undergo a stabilising CH-π interaction with the aryl shielding group are virtually fixed in the molecular space. The neighbouring oxygen further activates the hydrogen substituents towards a CH-π interaction, thus, inability to undergo this interaction can likely be solely attributed to geometric control. In extension to this study, the cyclopentane **80** and CH **81** spiro compounds were studied. These compounds have previously been tested on their efficiency as organocatalysts in the enantioselective Michael addition of aldehydes to enones by Gellman *et al.*[140] While the cyclopentane catalyst **80** gave good levels of enantioselectivity (up to 92% *ee*), the employment of catalyst **81** lead to racemic products. It was envisaged to study how these compounds would behave in a reaction proceeding *via* an iminium ion instead of an enamine.

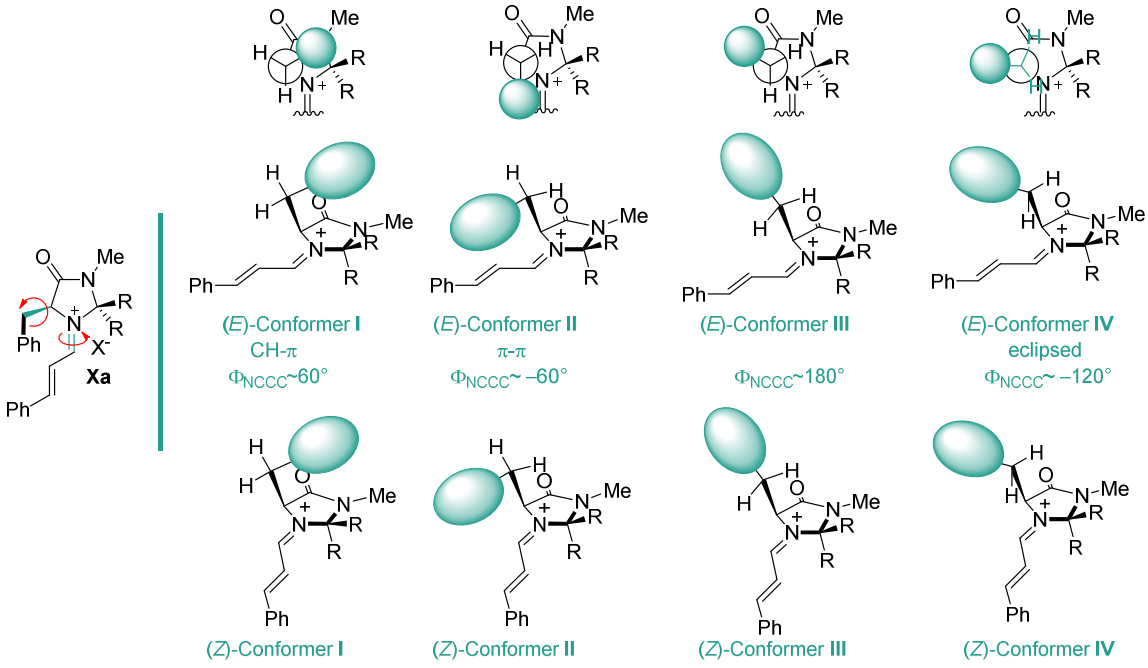

Figure 68 *Conformational diversity of the iminium salts derived from the imidazolidinones with substitution of the geminal-dimethyl group.*

2.6.1 Syntheses of the MacMillan Catalyst Analogues 78 to 81

The four compounds **78-81** were synthesised in one step by ring closure of L-phenylalanine methyl amide **15** with the corresponding ketone (Scheme 21). Oxetan-3-on for the synthesis of **79** was generously provided by Prof. Carreira (ETH Zurich). Compounds **79-81** were prepared using the same procedure used for the preparation of the *geminal*-dimethyl compound (chapter 2.2.1, Scheme 21 right). For the preparation of **78**, a procedure reported by Poloński was applied (Scheme 21 left).[141]

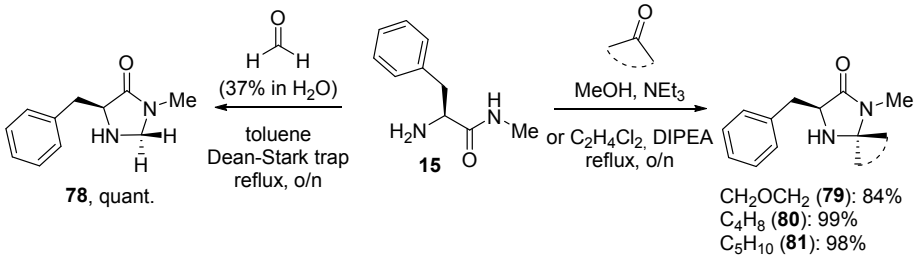

Scheme 21 *Syntheses of imidazolidinones **78-81**.*

The syntheses of the corresponding iminium salts proved to be difficult. It was not possible to form the iminium salts of **78** and **79**, while the iminium salt of **81** could not be isolated from a mixture of **81a·PF_6^-**, **81**, and (*E*)-cinnamaldehyde **2** (1:1.4:0.06). Only iminium salt **80a** was isolated cleanly as the hexafluorophosphate salt (Scheme 22).

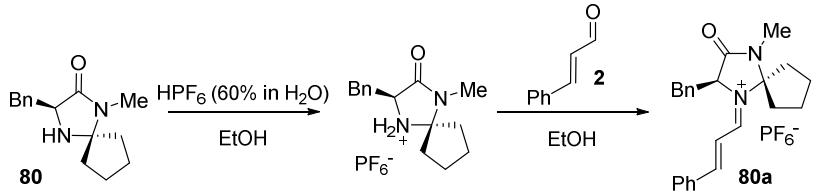

Scheme 22 *Synthesis of α,β-unsaturated iminium salt **80a**.*

2.6.2 X-Ray Crystallographic Analysis of Imidazolidinone Hydrochloride Salts 80 and 81 and Iminium Salt 80a

It was possible to obtain single crystals suitable for X-ray crystallographic analysis of the hydrochloride salts of **80** and **81** (Figure 69). In both salts the nitrogen is pyramidalised such that the benzyl group is placed in *quasi*-equatorial position consistent with the previously identified crystal structures (see chapters 2.2.3, 2.3.3, and 2.4.2). In both structures the phenyl ring is positioned *anti* to the amine function [Φ_{NCCC} = –165.6°(**80**) and –170.2°(**81**)],

a conformation that was so far only found in the crystal structure of the trimethoxy imidazolidinone salt **3** (chapter 2.2.3). The C–C–C bond angles around the spirocentre are perfectly tetrahedral [(106.8°(**80**) and 112.2° (**81**)]. For the CH-derivative **81**, one hydrogen substituent in the α-position to the spirocentre is oriented such that it could undergo a stabilising CH-π interaction with the aryl shielding group in the iminium salt. This interaction might be geometrically difficult in **80a**.

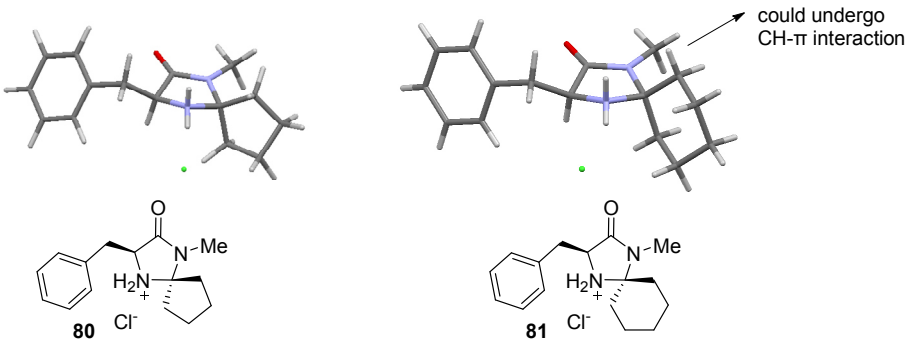

Figure 69 *X-ray structures of the hydrochloride salts of catalyst **80** and **81**.*

Nevertheless, in the crystal structure (Figure 70) of the hexafluorophosphate salt of **80a** reported by Mayr *et al.*,[53] it can be clearly seen that in the solid state the compound does adopt conformer **I** (Φ_{NCCC} = +51.9°), presumably stabilised by the aforementioned CH-π interaction. The C–C–C bond angle of 106.0° corresponds to a tetrahedral arrangement. The distance (3.54 Å) of the *syn*-α-carbon to the centroid of the shielding group also supports the existence of a CH-π interaction.

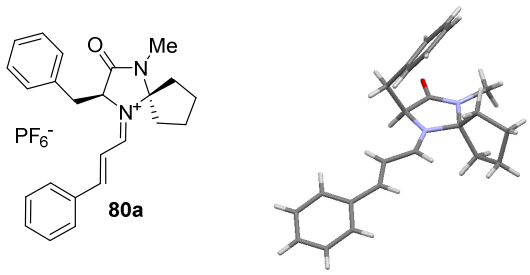

Figure 70 *X-ray structure of the hexafluorophosphate salt of **80a**. The PF_6^- counterion has been omitted for clarity.*

2.6.3 NMR Analysis of Iminium Salt 80a

For the imidazolidinone-derived iminium salts studied so far, an upfield-shift of the *syn*-methyl, as compared to the *anti*-methyl of the *geminal*-dimethyl group, could be observed. The magnitude of this difference was found to directly correlate with the predicted preference of CH-π conformer **I**. Furthermore, catalysts with significant differences were found to give higher enantioselectivities when employed in the Friedel-Crafts reactions of *N*-methyl-pyrrole and (*E*)-cinnamaldehyde. A similar observation was made for the iminium salt derived from the cyclopentane spirocompound **80**. The two CH_2 groups in α-position to the spiroatom showed hugely different NMR shifts in the ^1H (Figure 71) and ^{13}C NMR spectra of **80a** ($\Delta\delta^1H_{syn/anti} = -1.11$ ppm; $\Delta\delta^{13}C_{syn/anti} = -1.56$ ppm). This is consistent with the crystal structure discussed in chapter 2.6.2. Shift-differences of similar magnitude were found for the cyclohexyl-derivative **81a** ($\Delta\delta^1H_{syn/anti} = -1.10$ ppm; $\Delta\delta^{13}C_{syn/anti} = -1.77$ ppm).

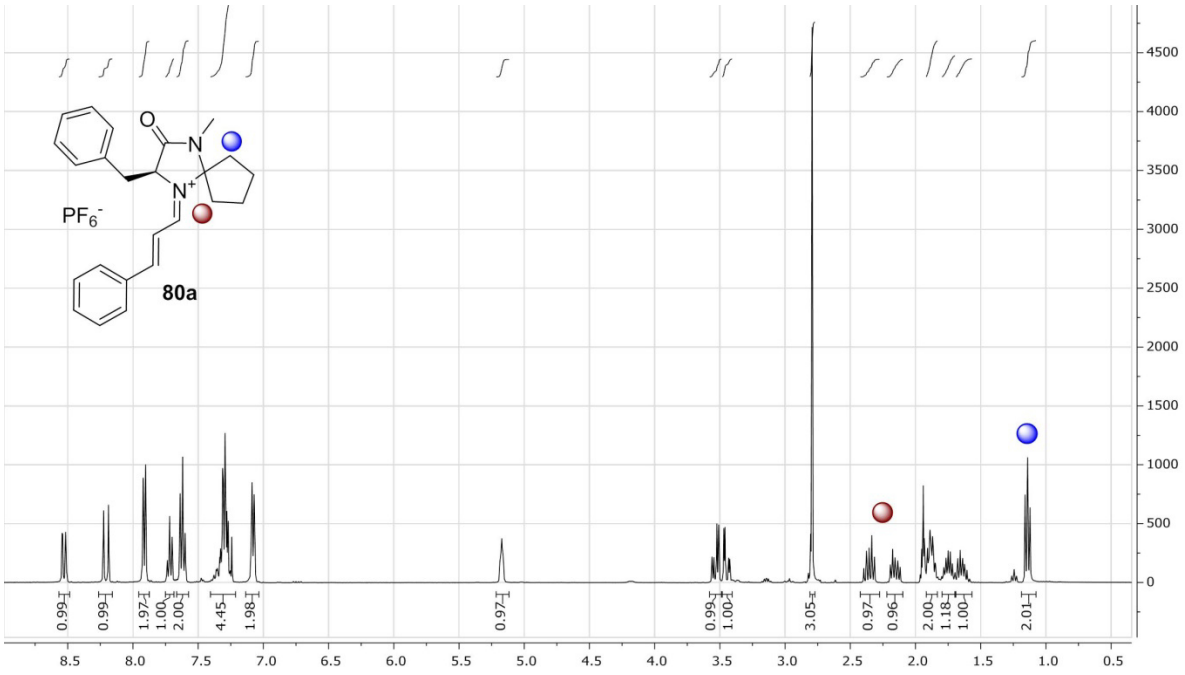

Figure 71 *^1H NMR spectrum of iminium salt **80a** displaying the large shift-differences of the two indicated CH_2-groups.*

2.6.4 Catalysis Screening: Organocatalytic Friedel-Crafts Reaction of *N*-Me-Pyrrole

Finally, the MacMillan catalysts modified in the position of the *geminal*-dimethyl group **78-81** were tested on in the Friedel-Crafts reaction of *N*-methyl-pyrrole **38** with (*E*)-cinnamaldehyde **2**. The catalyst **78** in which the *geminal*-dimethyl group was removed, and the oxetanyl-derivative **79** gave very low levels of enantioselectivity (20% and 22% *ee*, respectively). The low levels of enantioinduction of the second are a further verification for the importance of the CH-π interaction. Because the same enantiomer is obtained in excess, it is believed that even in **78a** the (*E*)-conformer is predominantly populated. The cyclopentane spiro-compound **80** also gave low levels of stereoselectivity, even though considerably higher than **78** and **79**. This finding is currently not well understood, since X-ray and solution phase NMR analyses of **80a** suggested significant population of conformer **I** and high levels of (*E*)/(*Z*)-control. Also the CH spirocompound **81** resulted in lower levels of enantioselectivity (72% *ee*) than expected.

Table 9 *Screening of the modified catalysts in the Friedel-Crafts reaction of N-Me-pyrrole **38** to (E)-cinnamaldehyde **2**.*

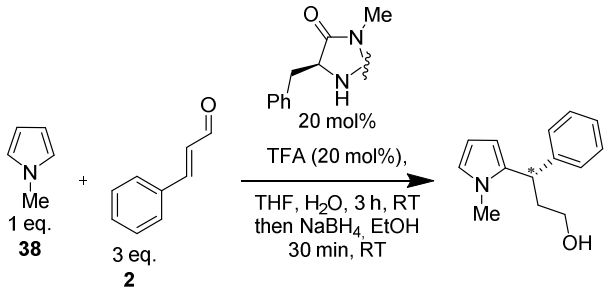

Catalyst	*ee* [%]	*e.r.*
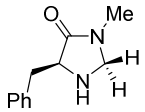 **78**	20	60:40
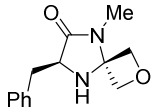 **79**	22	61:39
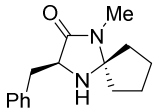 **80**	35	67.5:32.5
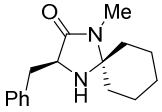 **81**	72	86:14

2.7 2nd Generation MacMillan Catalyst Derivatives

Whilst the 1st generation MacMillan catalyst was successfully applied in enantioselective Diels-Alder reactions,[8a] 1,3-dipolar cycloadditions with nitrones,[112a] the Friedel-Crafts alkylation using pyrroles[112b] and other reactions, diminished reactivity and enantioinduction were observed when using indoles or furans as π-nucleophiles. To overcome these constraints, MacMillan and co-workers introduced a 2nd generation catalyst (**82**, Figure 72, left) carrying a *tert*-butyl group instead of the *geminal*-dimethyl group in 2002.[52] The increased reaction rates and higher levels of enantiocontrol of this catalyst in the Friedel Crafts reaction of indoles was rationalised by the more exposed nitrogen and the decreased steric hinderance of the attack (see chapter 1.1.2). It was demonstrated in chapter 2.2 that increase of the electron-density of the aryl shielding group of the 1st generation MacMillan catalyst leads to enhanced enantioselectivities in the Friedel-Crafts reaction. Decreasing the electron-density on the other hand, lead to diminished selectivities. To probe whether a similar trend can be observed for the 2nd generation catalyst, the trimethoxy (**84**)- and the pentafluoro-derivative (**86**) were prepared (Figure 72). Additionally, for the parent catalyst and for these two analogues, the corresponding *anti*-diastereomers were prepared (**83**, **85**, and **87**). The so-called 3rd generation MacMillan catalyst (**19**)[112d] was also included in this study to test the enantiocontrol induced by solely the *tert*-butyl group in the Friedel-Crafts addition using *N*-methyl pyrrole (**38**).

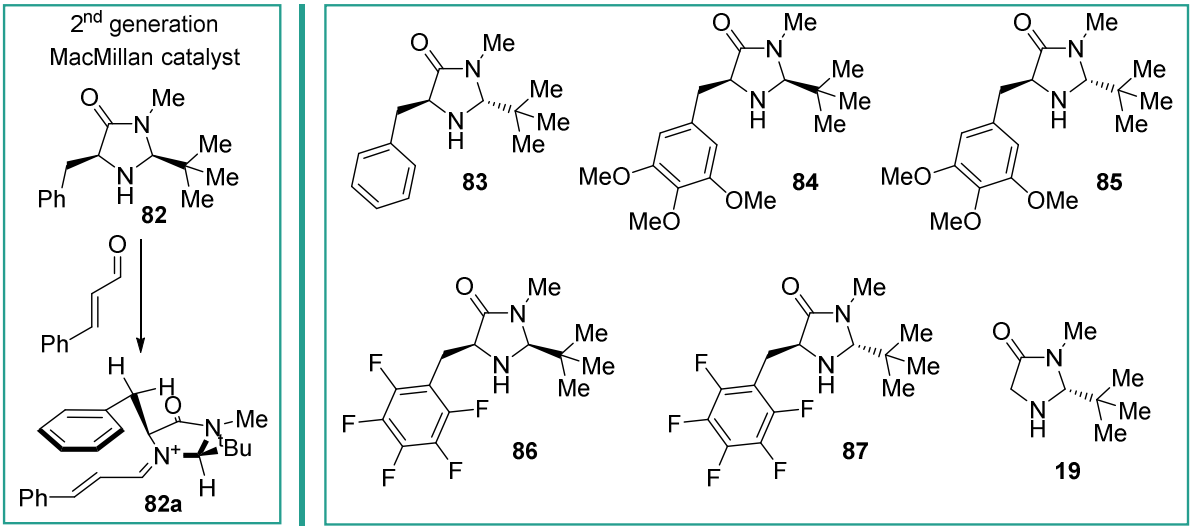

Figure 72 *Left: Mode of stereocontrol in the transition state proposed for the 2nd generation MacMillan catalyst* ***82****. Right: Libary of 2nd generation MacMillan catalyst derivatives and the 3rd generation MacMillan catalyst* ***19****.*

2.7.1 Syntheses of *syn* and *anti* 2nd Generation MacMillan Cataylst Derivatives

The 2nd generation imidazolidinones were prepared following a procedure reported by Tomkinson *et al.* from the corresponding aldehydes and pivaldehyde using catalytic amounts of $Yb(OTf)_3$.[142] A mixture of both diastereomers was obtained in all cases which could be separated by column chromatography (Figure 73).

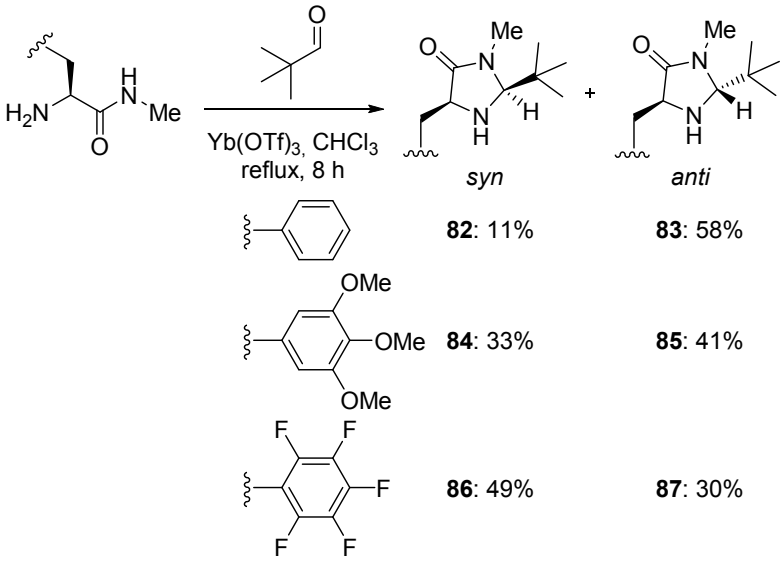

Figure 73 *Syntheses of 2nd generation MacMillan catalyst derivatives (syn and anti).*

It was possible to obtain crystals suitable for X-ray crystallographic analysis of the *syn*-pentafluoro-derivative as the hydrochloride salt (**86·HCl**, Figure 74). It was found that the compound adopts a very similar conformation as it was found for the 1st generation analogue (**10·HCl**, chapter 2.2.3), placing the aromatic group away from the core imidazolidinone ring (Φ_{NCCC} = –159.8°) and with the nitrogen pyramidalised such that the benzylic substituent and the *tert*-butyl group are in *quasi*-equatorial position.

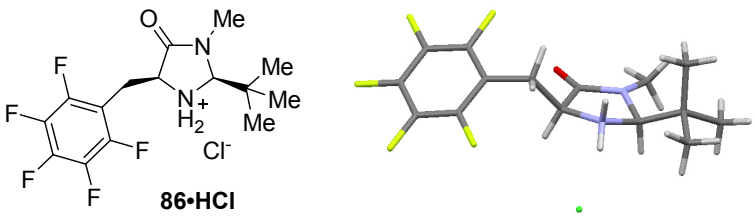

Figure 74 *X-ray crystallographic analysis of 86•HCl.*

2.7.2 Catalysis Screening: Organocatalytic Friedel-Crafts Reaction of *N*-Me-Pyrrole

Table 10 *Screening of the 2nd generation catalysts in the Friedel-Crafts reaction of N-Me-pyrrole* ***38*** *and (E)-cinnamaldehyde* ***2****.*

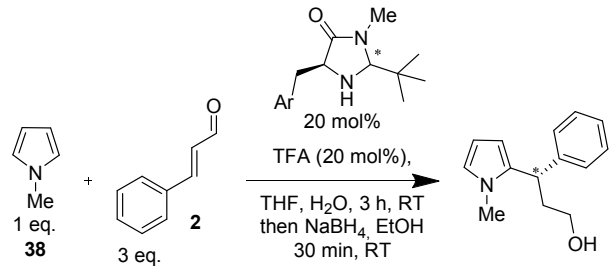

Catalyst	*ee* [%]	*e.r.*
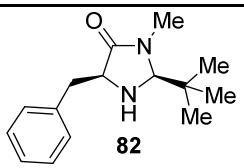 **82**	85	92.5:7.5
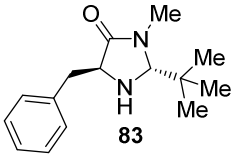 **83**	8	54:46
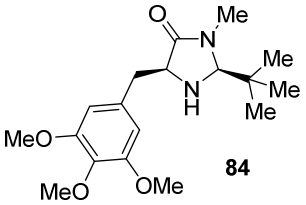 **84**	84	92:8
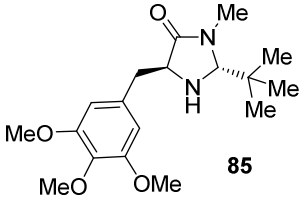 **85**	36	68:32
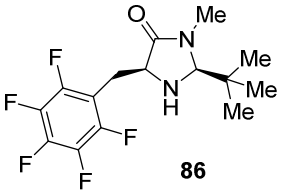 **86**	52	76:24
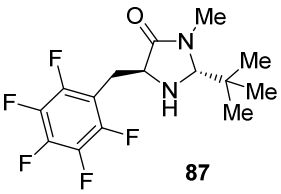 **87**	34	67:33
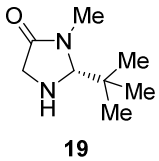 **19**	–34	33:67

The imidazolidinone catalysts were tested on their catalytic performance in the Friedel-Crafts addition of *N*-methyl pyrrole **2** and (*E*)-cinnamaldehyde **38** (Table 10). All reactions went to completion within 3 h. When using the parent catalyst **82** the same enantioselectivity as for the 1st generation benzyl catalyst **1** were obtained (both 85% *ee*, see chapter 2.2.6). But in contrast to what was achieved for the 1st generation system, the level of enantioinduction could not be increased by introduction of electron-donating substituents to the aryl shielding group (84% for the trimethoxy-system **84** as compared to 94% for the trimethoxy 1st generation catalyst **3**). Implementation of electron-withdrawing groups however, resulted in loss of enantioselectivity (R = C_6F_5, **86**, 52% *ee*) and in fact the selectivity was lower then the one obtained with the 1st generation analogue (R = C_6F_5, **10**, 66% *ee*). Unsurprisingly, employing the *anti*-imidazolidinones generally resulted in diminished enantioselectivities. Whilst the *anti*-benzyl derivative **83** led to almost complete loss of facial selectivity (8% *ee*), the *anti*-trimethoxy derivative **85** and the *anti*-pentafluoro system **87** both resulted in moderate selectivities of 36% and 34% *ee*, respectively. The level of stereocontrol obtained with the *tert*-butyl catalyst without a shielding group (**19**) was in the same range at 34% *ee*.

2.8 Electronic Modification of the Substrate (*E*)-Cinnamaldehyde

In chapter 2.2, it was established that the conformational behaviour of the reaction intermediates generated from condensation of MacMillan catalyst derivatives and (*E*)-cinnamaldehyde can be affected by introduction of electron-rich or electron-deficient substituents on the aryl shielding group. Furthemore, it was shown, that the level of stereocontrol is directly linked to the conformational behaviour. This immediately raises the question, what consequences would arise from electronic modifications of the π-system of the (*E*)-cinnamaldehyde substrate. Therefore a series of *para*-substituted (*E*)-cinnamaldehydes **88-91** were condensed with the parent MacMillan catalyst **1** (Figure 75) and the resulting iminium salts **92-95** studied *via* NMR spectroscopic analysis.

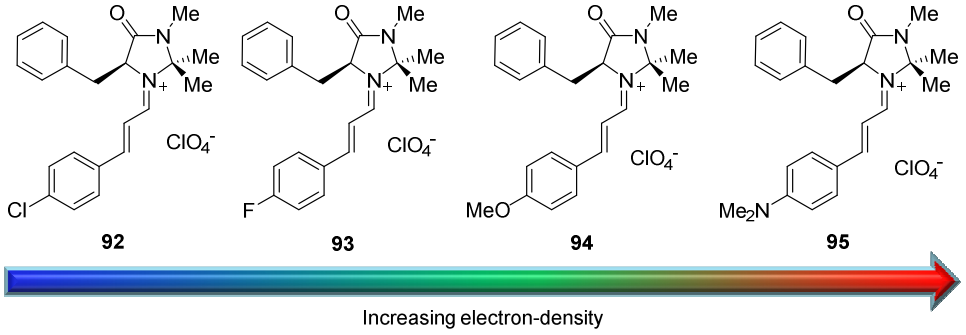

Figure 75 *Electronic modification of the π-system of the substrate.*

It was observed, that *para*-substitution of the condensed iminium leads to subtle changes in the shift-differences of the *syn*- and the *anti*-methyl groups of the *geminal*-dimethyl moiety ($\Delta\delta^{1}H_{syn/anti}$ and $\Delta\delta^{13}C_{syn/anti}$, Table 11 and Figure 76). The changes are delicate but follow a clear trend: The more electron-donating the substituent is the larger are $\Delta\delta^{1}H_{syn/anti}$ and $\Delta\delta^{13}C_{syn/anti}$.

Table 11 *Differences of the chemical shifts of the geminal-dimethyl group observed by ^{1}H and ^{13}C NMR spectroscopy.*

Iminium Salt (Ar)	**Hammett Constant σ_{para} [143]**	**$\Delta\delta(syn/anti)^{1}H$ [ppm]**	**$\Delta\delta(syn/anti)^{13}C$ [ppm]**
92 (*para*-Cl)	+0.23	–0.89	–2.72
93 (*para*-F)	+0.06	–0.90	–2.75
1a (*para*-H)	+0.00	–0.89	–2.77
94 (*para*-OMe)	–0.27	–0.92	–2.82
95 (*para*-NMe_2)	–0.83	–0.94	–2.84

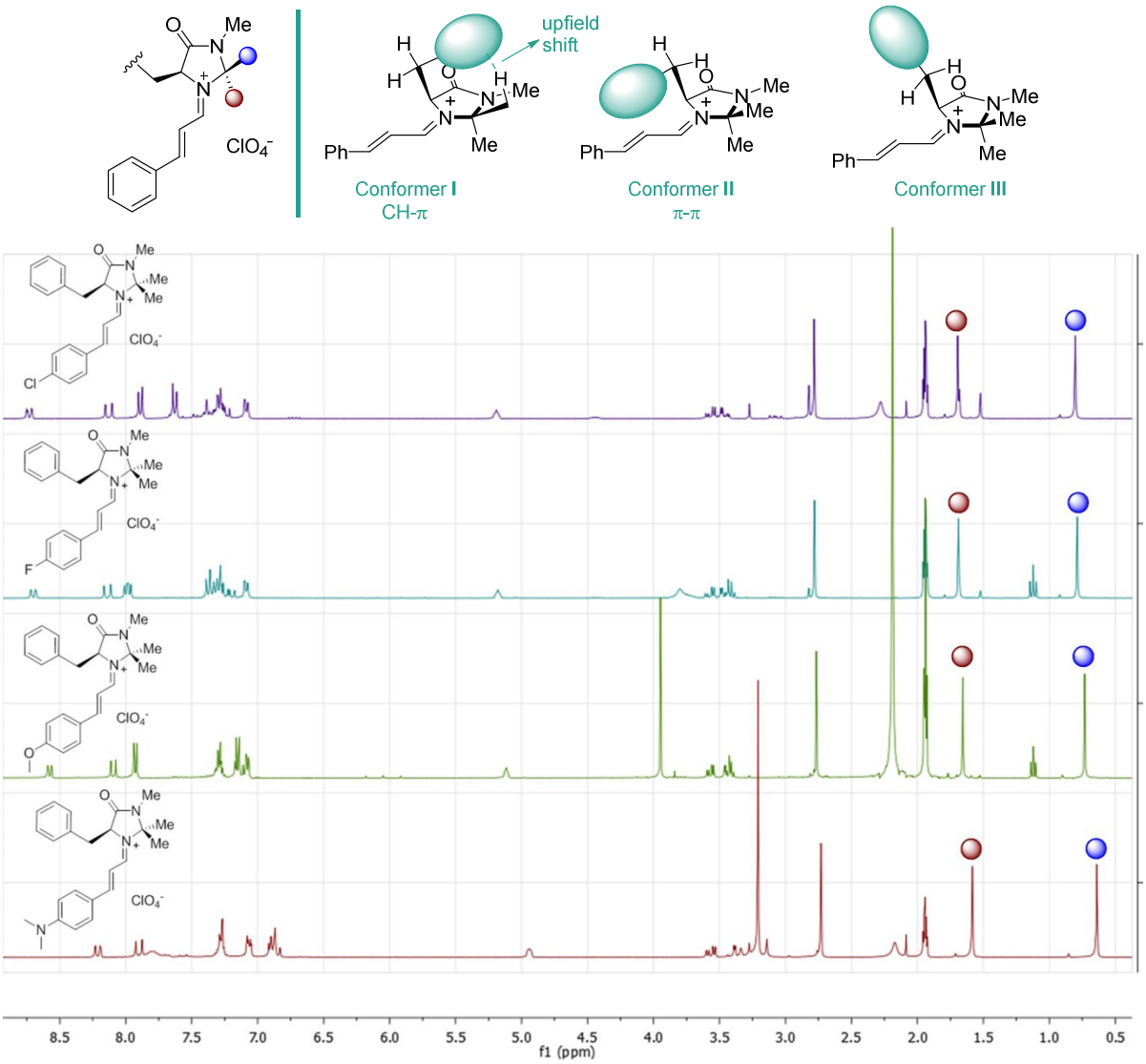

Figure 76 *Upper: The three staggered conformers of the imidazolidinone derived iminium salts. The CH-π interaction in conformer* ***I*** *results in an upfield shift of the syn-methyl group in the* ^{1}H *and* ^{13}C *NMR spectra. Lower:* ^{1}H*-NMR spectra.*

This suggests, that introduction of a *para*-substituent to the substrate (*E*)-cinnamaldehyde does not significantly influence the CH-π interaction between the *syn*-methyl group of the imidazolidinone moiety and the aryl-shielding group. It was possible to obtain single crystals suitable for X-ray crystalographic analysis of the *para*-chloro derivative **92** (Figure 77). The compound adopts conformer **I** stabilised by the discussed CH-π interaction (Φ_{NCCC} = +50.4°), thus, supporting this notion. Further spectroscopic and crystallographic evidence supporting this hypothesis can be found in a recent publication by Lakhdar and Mayr.[120]

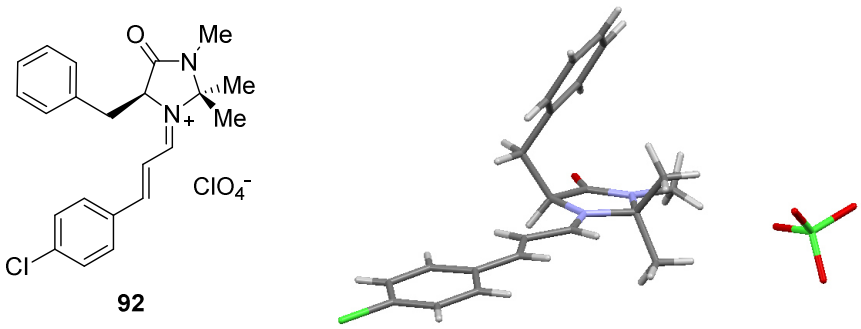

92

Figure 77 *X-ray structure of* ***92·HClO$_4$***, *conformer* ***I*** *is adopted.*

2.9 Conclusions and Outlook

A thorough molecular editing study of the MacMillan catalyst-derived iminium salt has been performed. By logical investigation of the different catalyst sites, the contributions of the different moieties and the importance of intramolecular interactions have been enlightened. A large number of α,β-unsaturated imidazolidinone iminium salts was prepared and conformational behaviour was experimentally investigated by solution phase NMR analyses and X-ray crystallographic studies. These results were complemented by computational analyses of lowest energy conformers. Consequently, performance of this MacMillan organocatalysts in the Friedel-Crafts reaction of *N*-methyl pyrrole to (*E*)-cinnamaldehyde was tested. Observed enantioselectivities were correlated to the postulated conformational behaviour. Besides identification of an improved catalyst structure leading to higher enantioselectivities, a clear correlation between preferred conformational behaviour has been unravelled. It was demonstrated, that high enantioselectivities in the Friedel-Crafts addition of *N*-methyl pyrrole to (*E*)-cinnamaldehyde can only be achieved when in the intermediate iminium only the aryl shielding group is predominantly placed in conformers **I** (CH-π) and **II** (π-π) and that a low energetic barrier between these two conformations is benefical.

3 Conformational Analysis of Organocatalytic Intermediates using IR-MPD Spectroscopy

The iminium ions generated by condensation of MacMillan catalyst-derived imidazolidinones with (*E*)-cinnamaldehyde were studied in the gas phase using Infrared Multiple Photon Dissociation (IR-MPD) spectroscopic analysis. It was envisaged that conformational behaviour would be directly reflected by characteristic shifts of the absorption bands of the typical fingerprint IR-chromophore C=O. By performing this analysis in the gas phase, influences from counterions or solvent molecules can be excluded. The combination of a free electron laser (FEL) with an ion trapping mass spectrometer makes it possible to record IR spectra in the gas phase over a wide wavelength range (500–2000 cm^{-1}). Currently, only a handful of free electron lasers for IR-measurements are available for external users, making beam time extremely valuable and competitive. Fortunately, it was possible to secure three days of beam time for the proposed project at the FELIX (Free-Electron Lasers for Infrared eXperiments) facility at Radboud University (Nijmegen) and experiments were performed in late December 2013.

3.1 Introduction: IR-MPD Experiments using FELIX

The experiments at the FELIX facility were performed in collaboration with Mathias Schäfer from the University of Cologne and the FELIX team in Nijmegen. I am particularly grateful to Prof. Jos Oomens and Dr. Giel Berden for their contribution to this work.

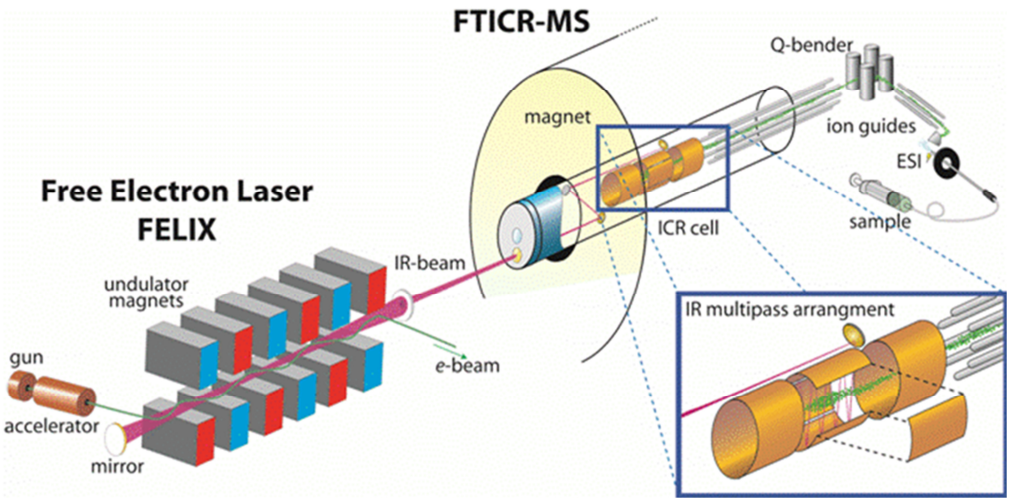

Figure 78 *Schematic representation of the instrumentation used to obtain gas phase IRMPD spectra over a wide wavelength-range. Figure taken from N. Polfer and J. Oomens, Phys. Chem. Chem. Phys.* ***2007****, 9, 3804.*

The iminium salts of interest were transferred into the gas phase from a solution in CH_3CN by electrospray ionization delivering very abundant, intact molecular ions. These ions were subsequently trapped in a Fourier transform ion cyclotron resonance (FT-ICR) mass spectrometer.[144] Due to the low abundance of ions in the mass spectrometer, direct IR absorption measurements are not possible.[145] Instead an "*action spectroscopy*" method was used, infrared multiple photon dissociation (IR-MPD).[146] The trapped ion was irradiated with a laser and, if the frequency of the laser is resonant to a vibrational mode in the molecule, photons were absorbed.[147] Tens to hundreds of photons must be absorbed to cause dissociation of the molecule, which can then be detected as loss of the parent ion mass and occurrence of fragment ions.[148] By using a widely tunable and powerful free electron laser, the molecular ion was irradiated at each wavelength over a wide range (3-250 μm) with relatively consistent irradiation times, while monitoring the extent of dissociation. The spectrum was then normalized with the relative laser power for each frequency. One of the biggest challenges is to create a stable, tunable free electron laser.[149] The experimental spectra were then compared to the theoretical spectra computed by Dr. A. Meijer from the University of Sheffield (UK) for each identified low-energy conformer.

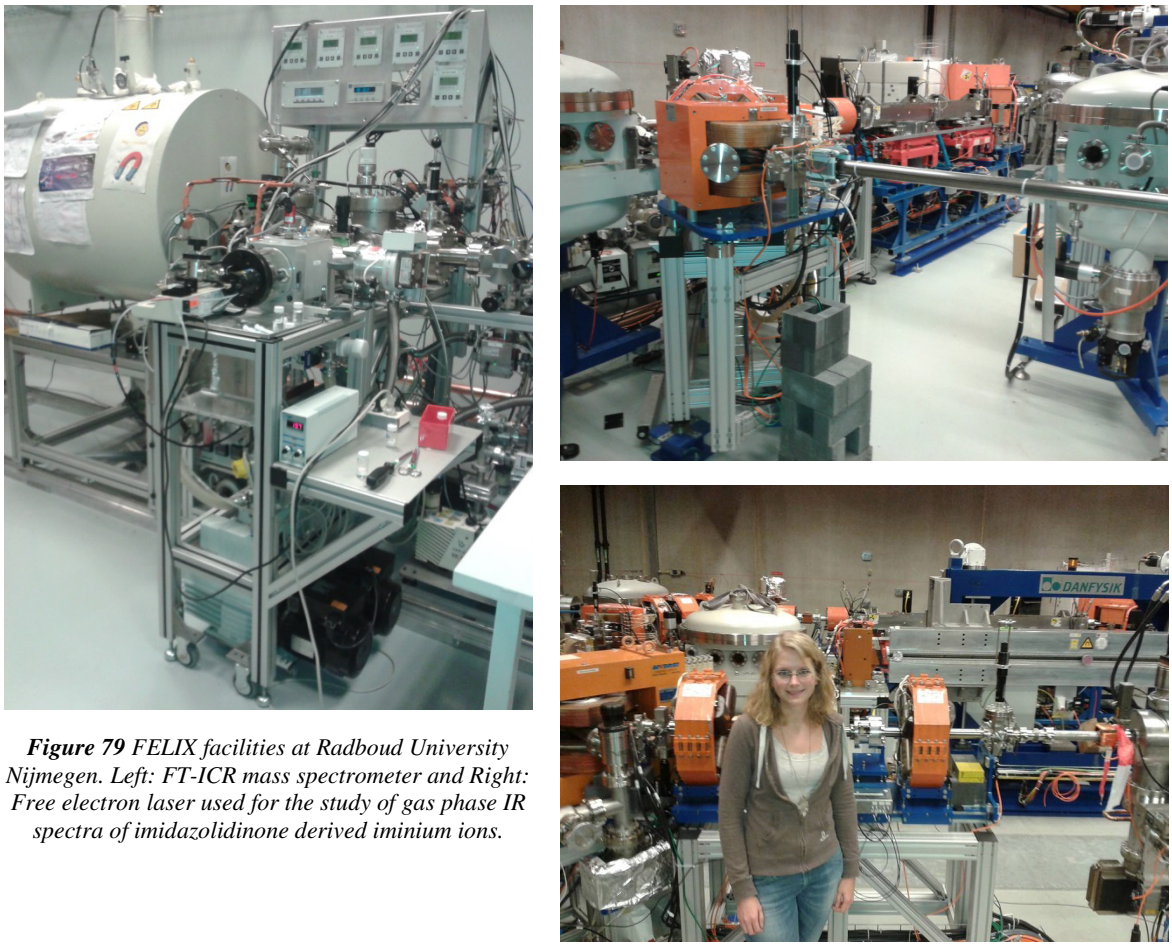

Figure 79 *FELIX facilities at Radboud University Nijmegen. Left: FT-ICR mass spectrometer and Right: Free electron laser used for the study of gas phase IR spectra of imidazolidinone derived iminium ions.*

3.2 Project Outline

Experimental analysis of the conformational behaviour of MacMillan catalyst-derived iminium ions has so far heavily relied on solution phase NMR analyses and X-ray crystallographic analyses. Whilst these are valuable methods, potential limitations have to be considered. Crystallography suffers from the drawback that packing effects might influence conformation. Similarly, solution phase analyses comes with the caveat that counterions may be influential, and in the context of organocatalysis using MacMillan catalysts, have been shown to be far from innocent.[150] To reconcile the clear requirement for methods to study iminium salt intermediates in the absence of counterions and solvents, infrared multiple photon dissociation (IR-MPD) spectroscopy has been explored as unique method for probing gas phase conformations of iminium ions derived from MacMillan's 1st generation catalyst (**1**). It was envisaged that the characteristic fingerprint C=O chromophore of the imidazolidinone ring moiety would be an excellent diagnostic signal. It was envisaged that the stretching frequency of the carbonyl group would be delicately influenced by the various conformations resulting from rotation around the C–C(Ph) bond (Figure 80, right). By comparing the recorded spectra to the computed spectra for each low-energy conformer identified that was significantly populated, it would be possible to verify previously postulated conformational behaviour. It should be noted, that this work constitutes the first application of IR-MPD spectroscopy to organocatalysis. So far, IR-MPD spectroscopy of organic molecules has predominantly been used to study small biologically relevant structures, e.g., amino acids and small peptides.[148a;151] Only recently, this method has been applied to study intermediates in the Diels-Alder reaction catalysed by cobalt-complexes.[152] Furthermore, a theoretical study by Sigman and co-workers has recently appeared in the literature demonstrating that selectivity in catalysis can be correlated to shifts in the theoretical IR spectrum.[153] To validate the utility of IR-MPD spectroscopy, eleven iminium ions were studied. For each of these compounds, the lowest energy conformers have been calculated using the B3LYP[154] functional of DFT with 6-311G**[155] basis set used on all atoms (see chapters 2.2.7, 2.3.6, and 2.4.5). For this study, the theoretical gas phase IR-spectra for each conformer significantly populated at RT were computationally predicted in collaboration with Dr. Anthony Meijer from the University of Sheffield .

To achieve pronounced electronic changes, five iminium ions with significantly differing quadrupole moments of the aryl shielding group (**1a**, **3a**, **6a**, **8a**, and **10a**, Q_{zz} = –5.68 D·Å to

+3.01 D·Å) were studied (Figure 80, top). Furthermore, two systems with extended shielding groups (**35a** and **41a**) and the saturated CH-derivative **42a** were also investigated (Figure 80, middle). Additionally, the conformational equivalents (**57a** and **58a**) frozen by virtue of the fluorine-iminium ion *gauche* effect were studied and, as a control compound, the methyl-derivative **60a** was investigated (Figure 80, lower). For all compounds, an IR-MPD spectrum was successfully recorded at FELIX. To ensure reliable detection of the minimal shift-differences in the range of 3–5 cm^{-1}, some analytes were measured as pairs, in doing so, they function as internal standard for each other. The prerequisite for this method is that the analytes and products differ in ion mass.

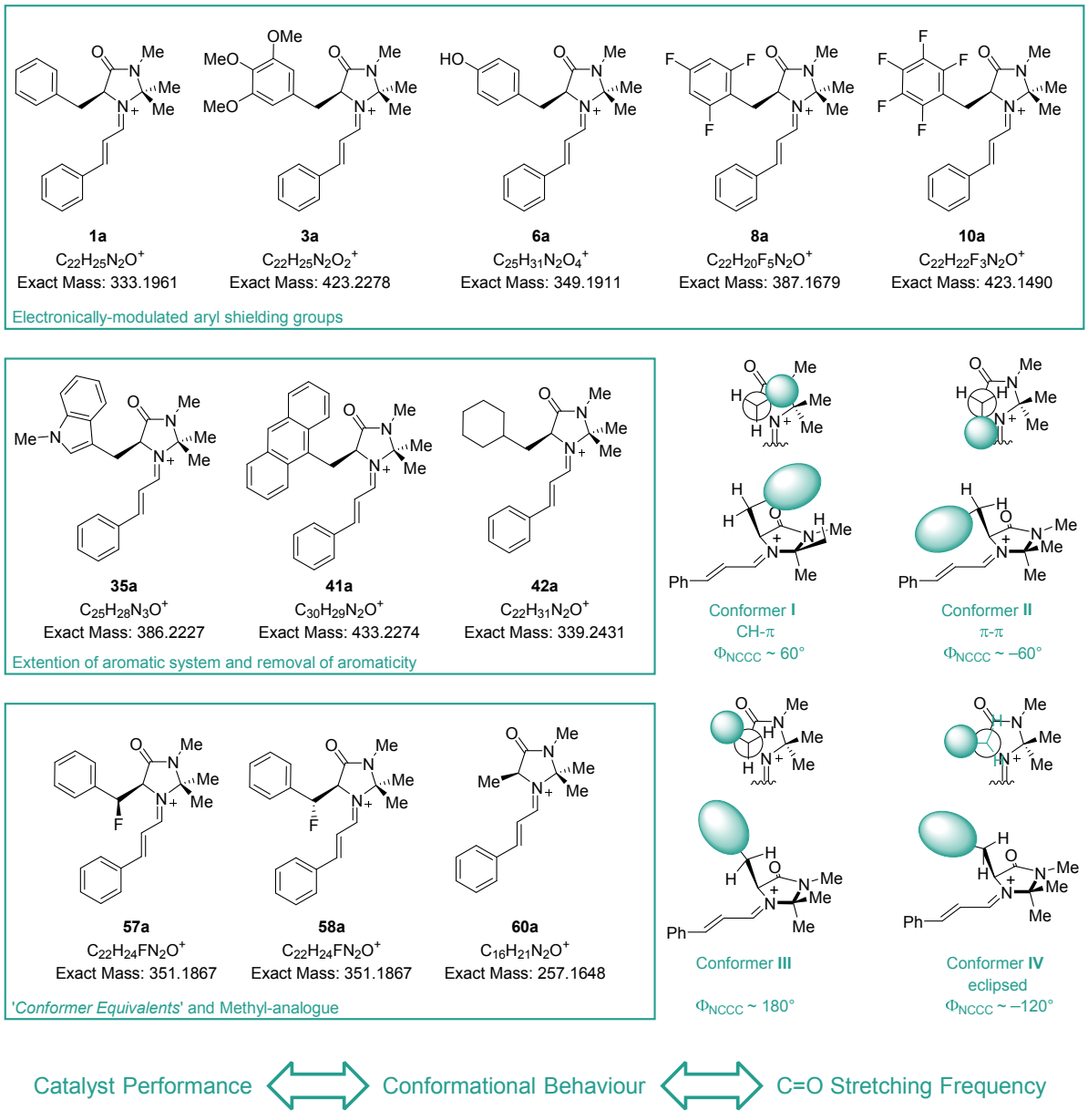

Figure 80 *Overview of the iminium ions studied by IR-MPD spectroscopy at the FELIX facilities (Radboud University Nijmegen) and of possible low-energy conformers. Bottom: Working hypothesis.*

3.3 Results of the IR-MPD Analysis

3.3.1 IR-MPD Analyses of Iminium Ions with Electronically Modulated Shielding Groups

The iminium ion derived from the parent 1st generation MacMillan catalyst:

As described in chapter 2.2, experimental analysis of the L-phenylalanine derived imidazolidinone iminium ion **1a** indicates that conformer **I** is predominantly populated. Computational conformer analysis supported this notion by identifying conformer **I** as the global minimum. A second significantly populated conformer was found to be conformer **IV** (+4.7 kJ/mol). The theoretical gas phase IR spectra of these two conformers were computed and compared to the experimentally obtained IR-MPD spectrum of **1a**. Unfortunately, for this compound the C=O stretching modes for the two energy minima proved to be almost identical (**I**:1753 cm^{-1} and **IV**:1752 cm^{-1}), thus, it was not possible to differentiate the two conformers based on this (Figure 81). However, by inspection of the region between 1200-1400 cm^{-1} and the intense band at 1500-1700 cm^{-1}, the experimental spectrum was found to show better agreement with the theoretical spectrum of conformer **I**, suggesting predominant population of this conformer, which is in agreement with theory.

*The iminium ion derived from the trimethoxy analogue **3a**:*

The most electron-rich example of the catalysts with electronically modified aryl shielding groups (**3**) gave the best enantioselectivities in the Friedel-Crafts reaction of *N*-methyl-pyrrole to (*E*)-cinnamaldehyde (94%, chapter 2.3.5). The conformational behaviour of the corresponding iminium ion was studied by experimental and computational analysis and the existence of two global minimum structures was discovered, i.e., conformers **II** and **IV**. However, conformer **I** was found to be only slightly higher in energy (+0.5 kJ/mol), and thus, is expected to be populated to a similar extend as **II** and **IV** at RT. A fourth conformer resembling conformer **II** was found at +3.3 kJ/mol. The theoretical IR-MPD spectra of those four conformers were computed and compared to the measured spectrum. The C=O stretching bands of the four conformers were found to be: 1747 cm^{-1} (0.0 kJ/mol, **II**), 1758 cm^{-1} (0.0 kJ/mol, **IV**), 1749 cm^{-1} (0.5 kJ/mol, **I**), and 1761 cm^{-1} (3.3 kJ/mol, **II**). The

measured C=O IR-band was found in between the theoretically predicted bands, thus, illustrating the distributed conformer population of **3a** (Figure 81).

*The iminium ion derived from the tyrosine-derived analogue **6a**:*

Because of their similar electronic properties, it was unsurprising that the iminium salt **6a** derived from tyrosine resembled the iminium salt of the parent catalyst (**1a**). Conformer **I** was found to be the global minimum of this system. However, the energy difference between conformer **I** and the energetically second lowest conformer **IV** was found to be smaller for **6a** than for **1a** (ΔE = 2.7 kJ/mol *versus* +4.7 kJ/mol). Accordingly, also the measured and calculated IR-MPD spectra closely resemble those for **1a**. While the C=O stretching frequencies are too close together to allow for conformer-assignment (1751 cm^{-1} and 1753 cm^{-1}), the region between 1200-1400 cm^{-1} again more closely resembles the calculated spectrum of the global minimum structure (Figure 81).

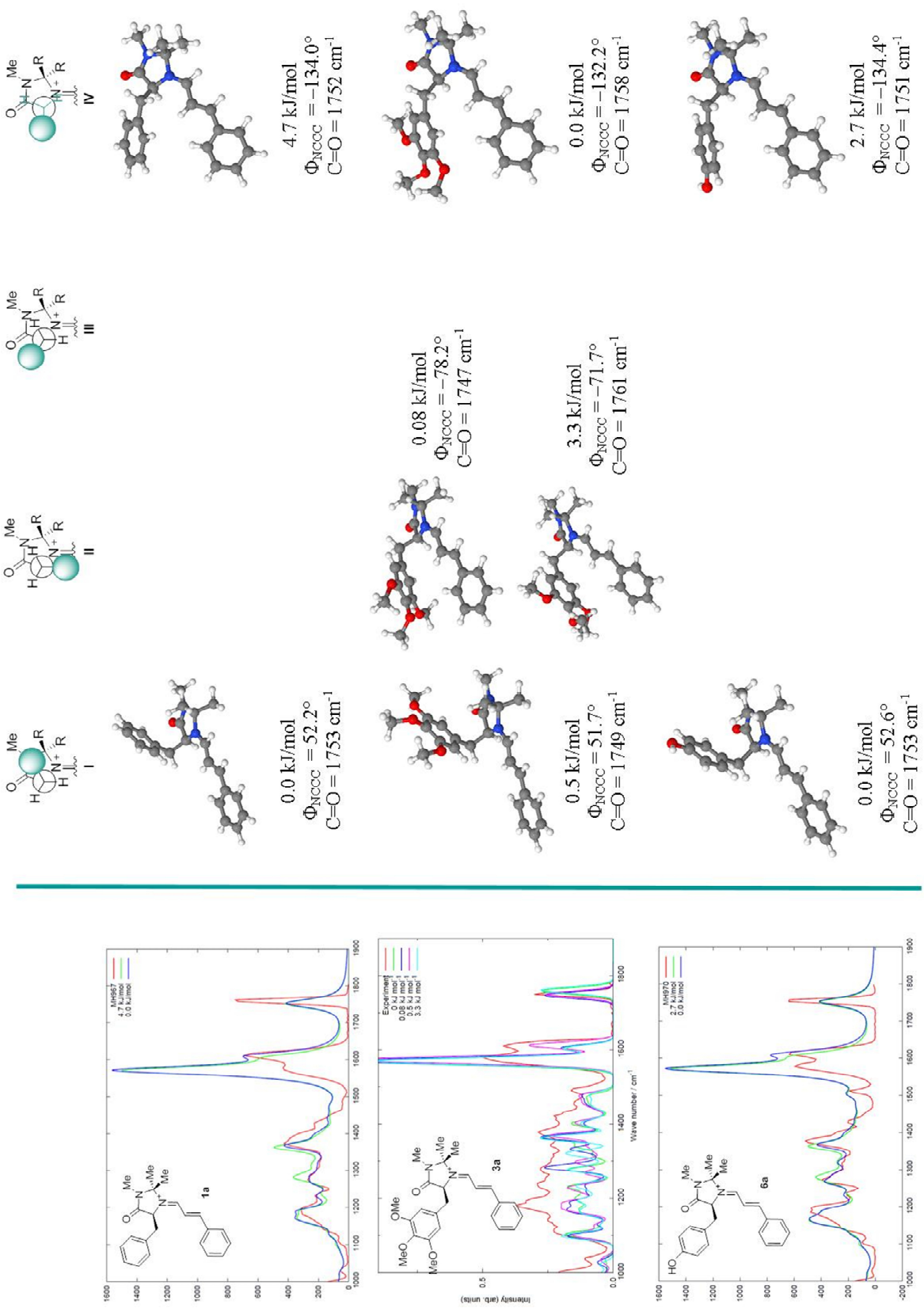

Figure 81 *IR-MPD-spectra of* ***1a*** *(left, upper),* ***3a*** *(left, middle), and* ***6a*** *(left, lower) overlaid with the theoretical spectra of the computationally identified energy minimum conformations (right). The torsion angles around the benzylic bonds (Φ_{NCCC}) and the wavelength of the C=O stretching modes are also indicated.*

*The iminium ion derived from the trifluorophenyl-derivative **8a**:*

For the α,β-unsaturated iminium ion **8a** only one significantly populated conformer corresponding to conformer **III** was identified. The measured C=O frequency at 1761 cm^{-1} fits perfectly to the theoretical value, whilst the second calculated energy minimum was much higher in energy (+10.7 kJ/mol, distorted conformer **I**) and is slightly blue-shifted (1764 cm^{-1}, Figure 82).

*The iminium ion derived from the pentafluorophenyl-analogue **10a**:*

Last of this series, the pentafluorophenyl-analogue **10a** was studied as the electron-deficient extreme (Figure 82). From the X-ray structure and other structural data it was concluded that this iminium ion preferentially adopts conformer **III** with the aromatic shielding group rotated away from the imidazolidinone core.[156] This conformer was also computationally identified as the global minimum structure. Two additional conformers were found: A structure resembling conformer **II** at +7.1 kJ/mol and a distorted conformer **I** at +11.8 kJ/mol were identified. Whilst the C=O stretching frequency computed for the global minimum structure (1760 cm^{-1}) and the measured frequency are in good agreement, the C=O stretching frequencies of the other two identified minima are slightly blue-shifted (1763 cm^{-1} and 1764 cm^{-1}, respectively).

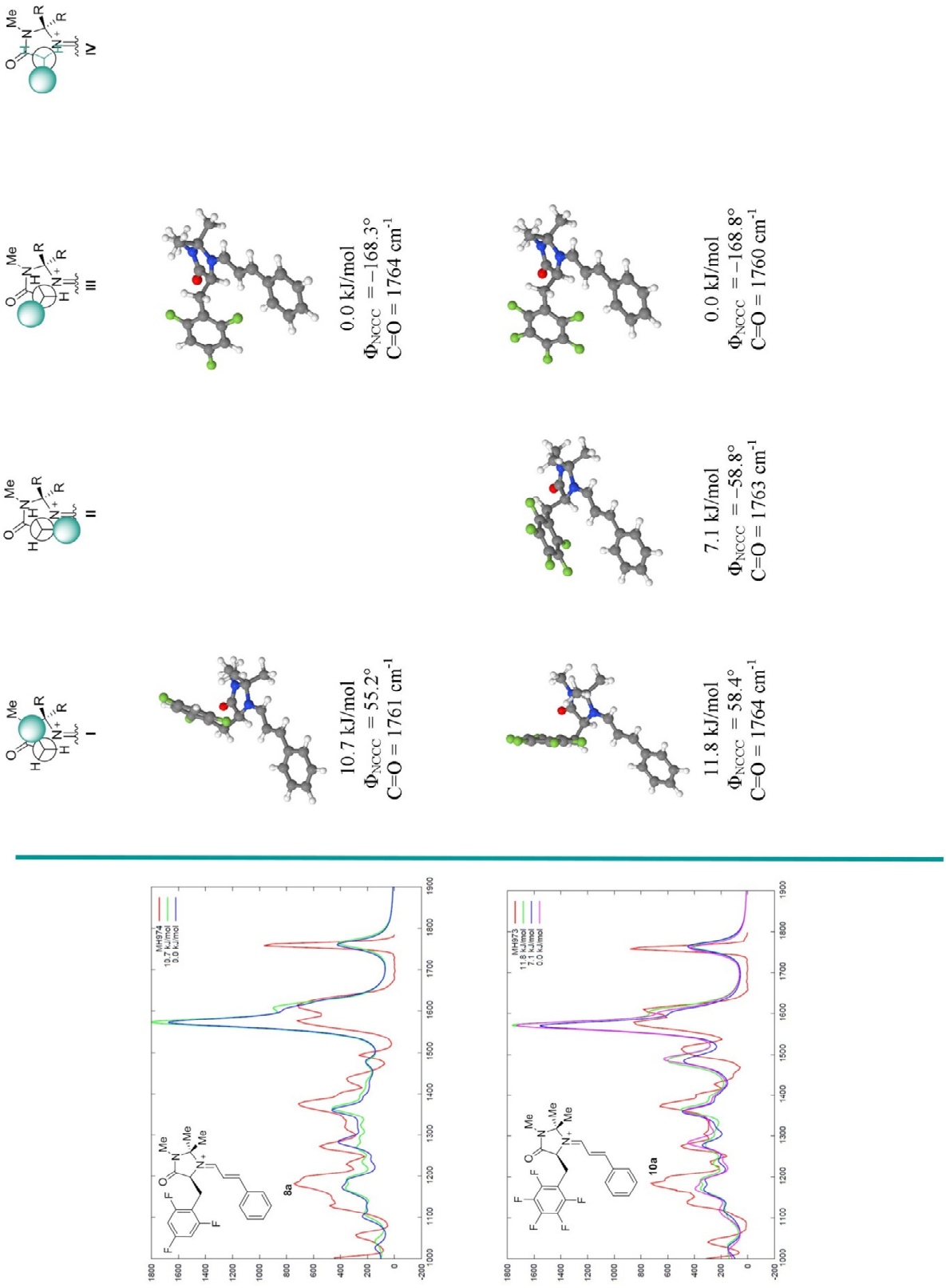

Figure 82 *IR-MPD-spectra of* ***8a*** *(left, upper) and* ***10a*** *(left, lower) overlaid with the theoretical spectra of the computationally identified energy minimum conformations (right). The torsion angles around the benzylic bonds (Φ_{NCCC}) and the wavelength of the C=O stretching modes are also indicated.*

3.3.2 IR-MPD Analyses of Iminium Ions with Extended Shielding Groups and of an Iminium Ion with a Saturated Shielding Group

*The iminium ion derived from the Me-indole-analogue **35a**:*

For the tryptophan-derived iminium ion **35a**, four low-lying conformers where identified. The global energy minimum was found correspond to conformer **II**. Furthermore, two minima adopting conformer **I** were found at +2.5 kJ/mol and +5.9 kJ/mol, and a further conformer reminiscent of conformer **IV** at +4.2 kJ/mol. Compared to the C=O stretching modes of the other conformers, the signature for the global minimum was computed to be considerably blue-shifted [1760 cm^{-1} as compared to 1751 cm^{-1} (+2.5 kJ/mol), 1748 cm^{-1} (+4.2 kJ/mol) and 1750 cm^{-1} (+5.9 kJ/mol)]. The C=O bond measured was found to fit best to the global minimum (Figure 83), but is considerably red-shifted likely due to significant population of the other conformers.

*The iminium ion derived from the anthracene-analogue **41a**:*

The iminium ion with the anthracene-moiety **41a** most beautifully illustrates the potential of IR-MPD spectroscopy in studying conformational behaviour. For each of the three possible conformers **I**, **II**, and **III** an energy minimum was computationally identified (13.2 kJ/mol, 0.0 kJ/mol, and 18.2 kJ/mol, respectively), but only conformer **II** is predicted to be significantly populated. Moreover, the corresponding C=O frequency shifts were found to clearly differ from each other (1751 cm^{-1}, 1755 cm^{-1}, and 1764 cm^{-1}, respectively). The IR-MPD carbonyl stretching frequency perfectly fits to the computed spectrum for conformer **II**, thus, validating the predominant population of this conformer (Figure 83).

*The iminium ion derived from the cyclohexyl-analogue **42a**:*

For the cyclohexyl-derivative **42a**, only one significantly populated conformation was computed (conformer **III**), with a carbonyl stretching frequency of 1753 cm^{-1}. Additionally, three higher lying conformations were identified, all with corresponding theoretical carbonyl stretching modes blue-shifted compared to the one for the global minimum (**III**, 7.1 kJ/mol, 1756 cm^{-1} and **IV**, 10.5 kJ/mol, 1761 cm^{-1} and **I**, 12.0 kJ/mol, 1759 cm^{-1}). The measured spectrum fits well to the predicted spectrum of the global minimum (Figure 83).

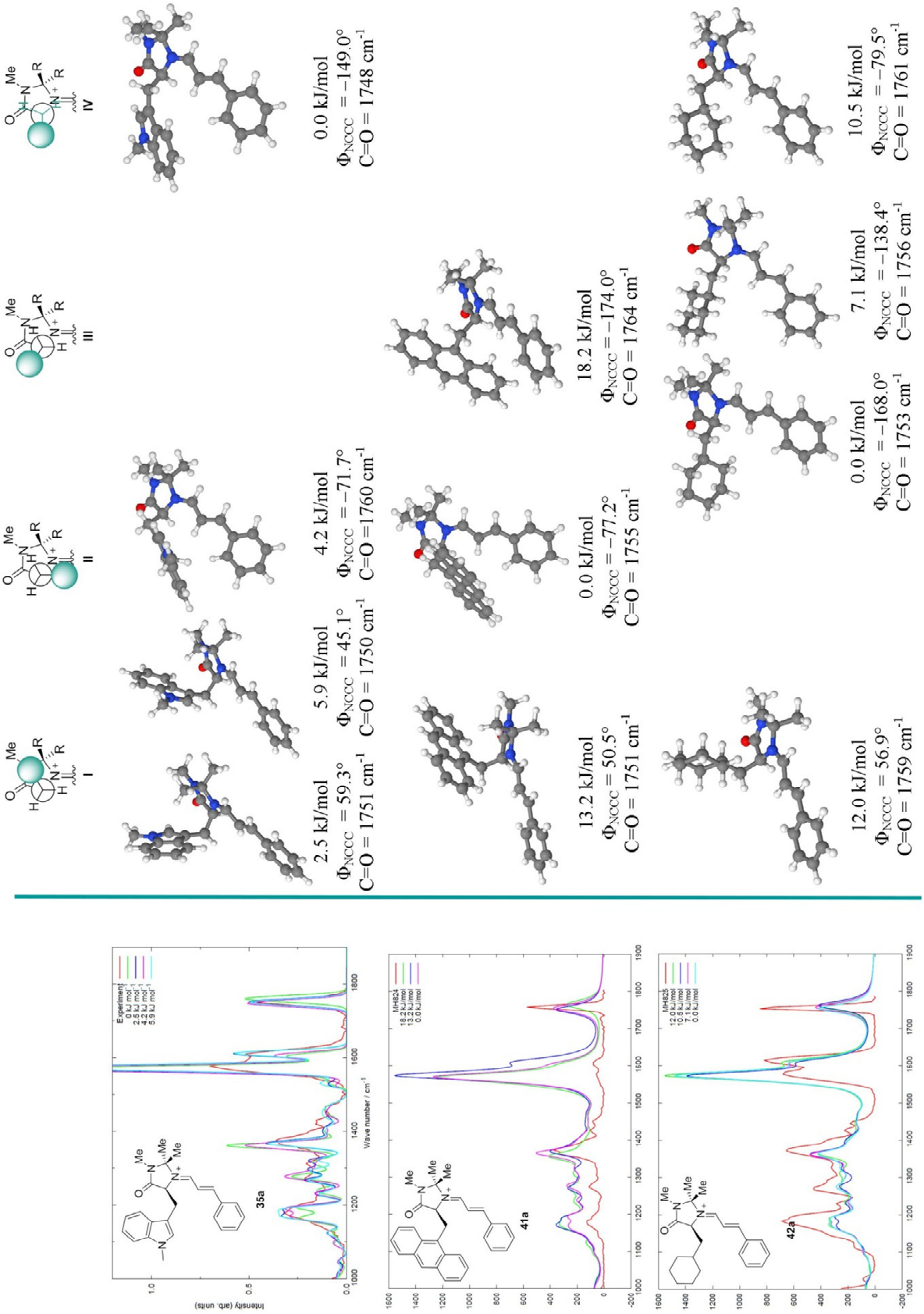

Figure 83 *IR-MPD-spectra of* ***35a*** *(left, upper),* ***41a*** *(left, middle) and* ***42a*** *(left, lower) overlaid with the theoretical spectra of the computationally identified energy minimum conformations (right). The torsion angles around the benzylic bonds (Φ_{NCCC}) and the wavelength of the C=O stretching modes are also indicated.*

3.3.3 IR-MPD Analyses of Iminium Ions with Modifications in the Benzylic Position

The CH-π "conformer equivalent" ***57a****:*

Unsurprisingly, the only significantly populated conformer for this iminium ion was found to be one corresponding to conformer **I**. Another energetically low lying conformation was identified to be a conformer also stabilised by an interaction with the *syn*-methyl group, but with the (*Z*)-conformation around the $C=N^+$ iminium bond (+8.8 kJ/mol). Higher in energy (+13.3 kJ/mol) is the other *gauche*-conformation directing the phenyl-ring away from the core ring. The computed IR spectra of the two CH-π conformations are very similar and the C=O stretching frequencies are too close together to make differentiation possible (Figure 84). However, for the (*Z*)-conformer, a band at around 1410 cm^{-1} was predicted, that could not found in the measured spectrum nor the theoretical spectrum of the global minimum conformation. The computed C=O stretching frequency of the other *gauche*-conformer is considerably blue-shifted compared to the other conformers and the measured frequency.

The π-π "conformer equivalent" ***58a****:*

For the π-π 'conformer equivalent, not only the predicted conformer **II** but a second significantly populated conformation corresponding to conformer **IV** was identified (+1.3 kJ/mol). The computed spectra of these two conformers show significantly different C=O stretching frequencies (1762 cm^{-1} and 1751 cm^{-1}, respectively). The experimental C=O band was found to have a stretching frequency in between those found computed for conformers **II** and **IV**, thus, supporting the notion that both conformers are significantly populated.

The iminium ion derived from the methyl-analogue ***60a****:*

Finally, the iminium ion derived from the methyl-derivative was investigated. Unsurprisingly, computational analysis predicted only one energetic minimum conformation. The predicted IR spectrum and the measured IR-MPD spectrum correspond well.

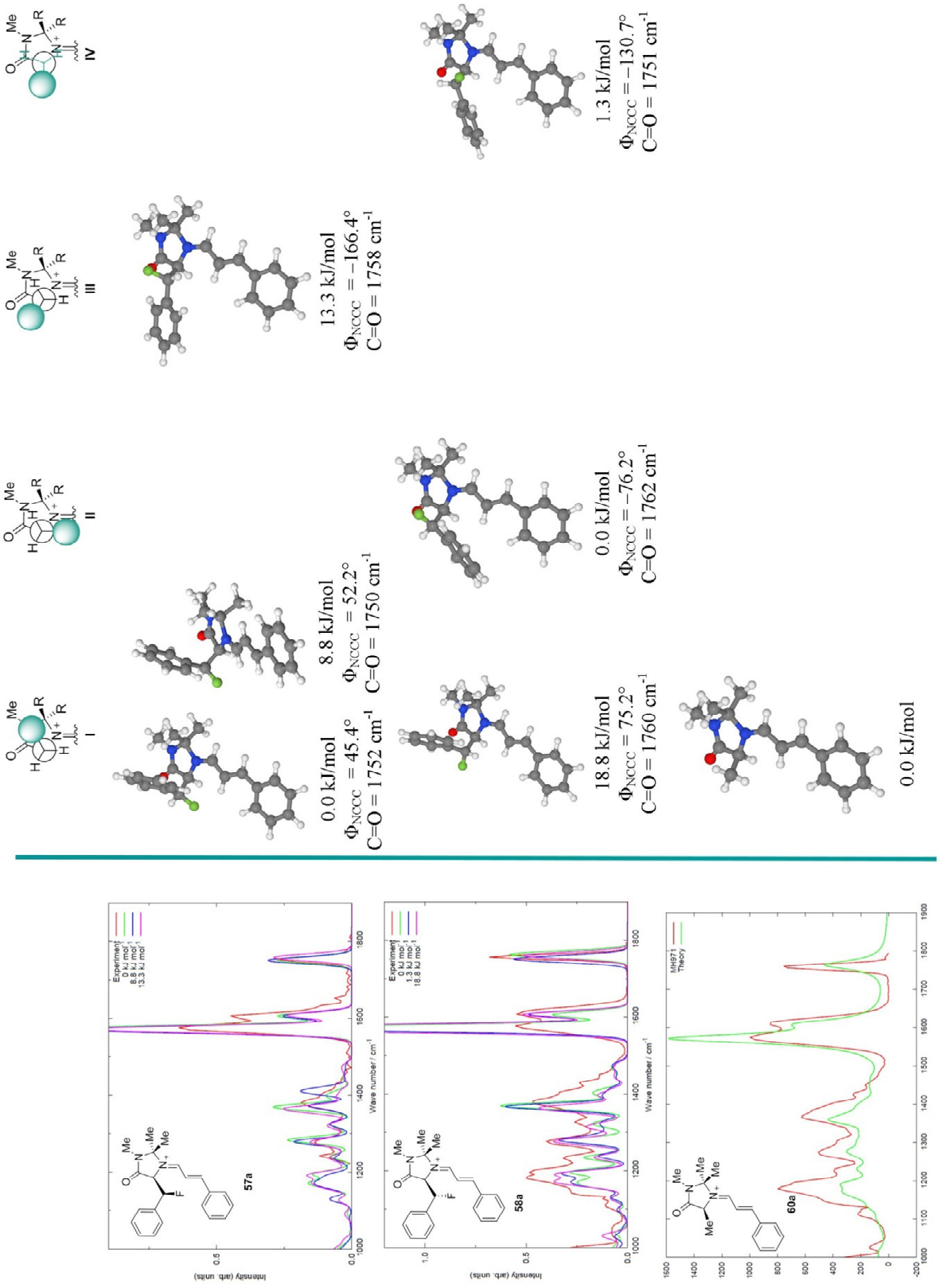

Figure 84 *IR-MPD-spectra of* ***57a*** *(left, upper),* ***58a*** *(left, middle) and* ***60a*** *(left, lower) overlaid with the theoretical spectra of the computationally identified energy minimum conformations (right). The torsion angles around the benzylic bonds (Φ_{NCCC}) and the wavelength of the C=O stretching modes are also indicated.*

3.4 Conclusions and Outlook

Herein, a preliminary validation of gas phase IR-MPD-spectroscopy for probing the conformational behaviour of low molecular weight organocatalytic intermediates is presented. The carbonyl stretching frequency was shown to depend on the position of the shielding substituent as a consequence of rotation around the central C–C bond. By comparison of the computed spectra for each energetic minimum conformation with the experimental gas phase IR-spectrum of a given compound, the conformational preferences could successfully be assigned in many cases, thus providing valuable structural insights. Unfortunately, in other cases, the frequency-differences were at the boundaries of reliable assignment. Thus, the current limitations of this method were illustrated. In future, with improved theoretical methods and more stable laser radiation, these limitations may be overcome. The current development of low-temperature gas phase IR spectroscopy will likely bring additional advances to the field. In conclusions, a preliminary validation of the potential of IR-MPD spectroscopy for investigating reaction intermediates and enlightening mechanistic subtleties is presented.

4 The Organocatalytic Friedel-Crafts Reaction of *N*-Me-Indole: An Unusual Selectivity Reversal

In the previous chapters of this thesis, the conformational behaviour of the α,β-unsaturated iminium salts of various MacMillan catalyst-derivatives was studied and correlated to trends observed in the Friedel-Crafts addition of *N*-methyl pyrrole **38** to (*E*)-cinnamaldehyde **2**. To investigate whether or not these trends are also found in the addition of other charge neutral nucleophiles to (*E*)-cinnamaldehyde, the Friedel-Crafts reaction of *N*-methyl indole **96** was studied using the catalysts discussed in chapter 2. MacMillan and co-workers reported that selectivities and reactions rates of this reaction are significantly improved when using the 2nd generation MacMillan catalyst **82** (88% *ee*, 98% yield at –40 °C, 4 h for crotonaldehyde) instead of the 1st generation catalyst **1** (56% *ee*, 85% yield at –40 °C, 48 h for crotonaldehyde).[52] These observations were attributed to the lower reactivity of indole-derivatives as compared to pyrrole-derivatives (see also chapter 1.1.2). While this explanation likely accounts for the increased reaction rate, it was proposed that additional effects must be responsible for the significant differences in selectivity. Particularly curious was the observation, that for *N*-methyl pyrrole both the 1st and the 2nd generation MacMillan catalysts gave virtually the same enantioselectivity of 85% *ee* (chapters 2.2.6 and 2.7.2). Furthermore, a recent publication by Seebach *et al.* reported on the reversal of the stereochemical outcome of the reaction when a fluorine substituent was introduced to the *syn*-methyl group, but not when it was introduced to the *trans*-methyl group (Scheme 23).[157]

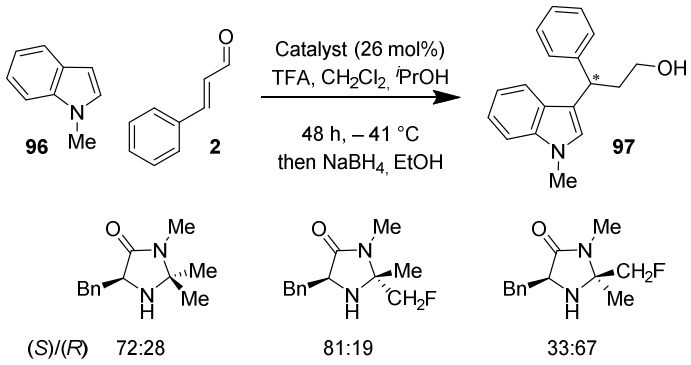

Scheme 23 *Reversal of selectivity in the Friedel-Crafts addition of N-methyl indole **96** and (E)-cinnamaldehyde **2** observed by Seebach et al.*

4.1 Catalysis Screening

4.1.1 Catalysts with Electronically Modulated Shielding Groups

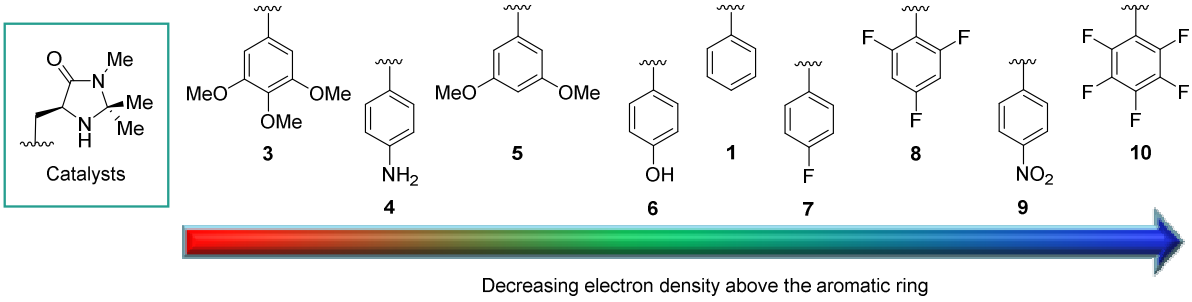

Figure 85 *Catalyst library with electronically modified shielding aryl groups.*

Initially, the 2nd generation MacMillan catalyst **82** was employed in the addition reaction of *N*-methyl indole **96** under the same conditions used throughout this study resulting in 76% *ee* at RT and 89% *ee* at –55 °C. Subsequently, the series of electronically modulated MacMillan-derivatives was tested (Figure 85). For these compounds, a clear correlation between the electron densities represented by the component of the quadrupolar moment tensors Q_{zz} perpendicular to the aryl shielding groups, and the obtained stereoselectivities was observed in the addition reaction of *N*-methyl pyrrole. Furthermore, the electron-rich extreme [**3**, R = $C_6H_2(OMe)_3$] resulted in the best stereoselectivities (94% *ee*) of the series. Both observations were repeated in the addition reaction using *N*-methyl indole. Even though selectivities were generally lower, a clear correlation between the *Qzz* and the *ee* (or *e.r.*) obtained was observed (Figure 86, Table 12). The best selectivity was reached using catalyst **3** (44% *ee*).

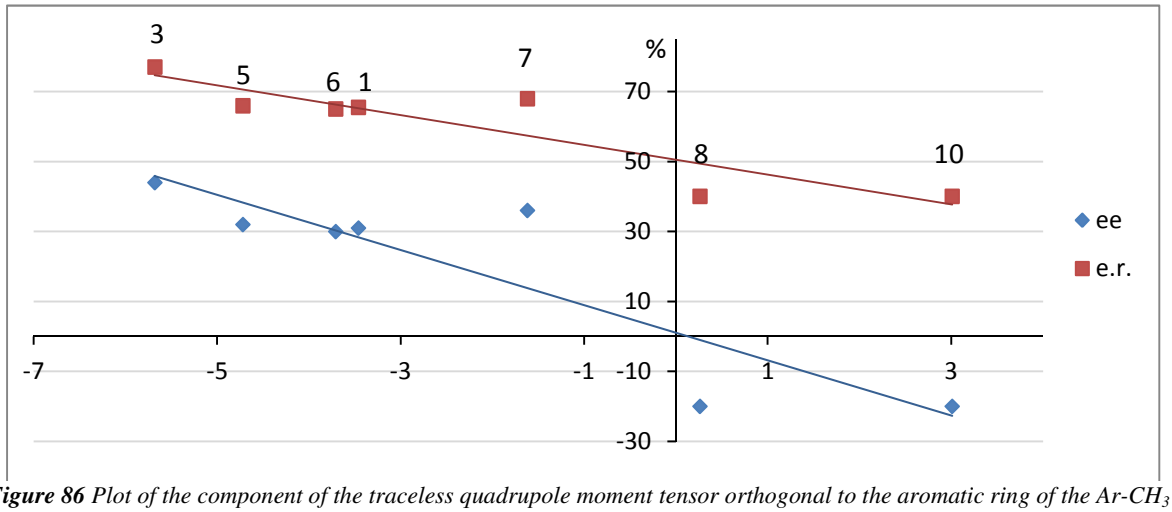

Figure 86 *Plot of the component of the traceless quadrupole moment tensor orthogonal to the aromatic ring of the Ar-CH_3 derivatives (Q_{zz}) with enantiomeric excess (ee), and enantiomeric ratio (e.r.). Nitro-analogue **9** was left out from this study due to different conformational behaviour that requires clarification.*

Table 12 *Screening of the electronically modified catalysts in the Friedel-Crafts reaction of N-methyl indole* ***96*** *to (E)-cinnamaldehyde* ***2****.*

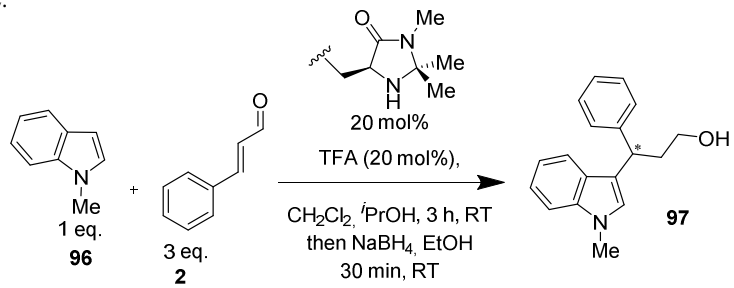

Catalyst	*Qzz* [D·Å]	$\Delta\delta^1H_{syn/anti}$ [ppm]	Postulated Conformer	*ee* [%]	*e.r.*
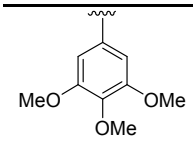 **3**	–5.68	–0.62	**II/I**	44	72:28
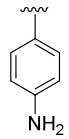 **4**	–5.50	–		–	–
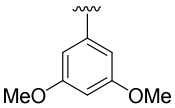 **5**	–4.72	–0.62	**II/I**	32	66:34
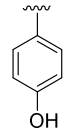 **6**	–3.71	–0.78	**I**	30	65:35
 **1**	–3.46	–0.89	**I**	31	65.5:34.5
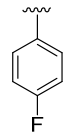 **7**	–1.62	–		36	68:32
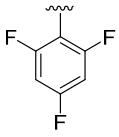 **8**	+0.26	–0.18	**III**	–20	40:60
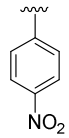 **9**	+2.46	–0.74	**I**	31	65.5:34.5
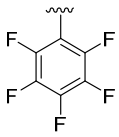 **10**	+3.01	–0.13	**III**	–20	40:60

Consistent with previous findings, no reaction was observed when employing catalyst **4** (R = $C_6H_4NH_2$), potentially due to imine formation with the substrate. Furthermore, also in this reaction, the nitro-substituted analogue **9** gave much higher selectivities than would be expected from the Q_{zz}, but consistant with the large $\Delta\delta^1H_{syn/anti}$ (–0.74 ppm). This is consistent with the findings described for the addition of *N*-methyl pyrrole (Chapter 2.2.6). Surprisingly, changing the nucleophile from *N*-methyl pyrrole **38** to *N*-methyl indole **96**, led to reversal of selectivity when using the perfluorinated-catalyst **10** or the trifluorophenyl-derivative **8** (–20% *ee* for both). This indicates that the difference in behaviour, already observed by MacMillan and Seebach, most likely cannot solely be attributed to reactivity differences. Interestingly, for the two corresponding α,β-unsaturated iminium ions **8a** and **10a**, it was postulated that no CH-π interactions between the aryl-shielding group and the *syn*-methyl group occur, and, thus, conformer **I** is essentially unpopulated. This might also be the key for the reversed stereoselectivity observed by Seebach *et al.* upon introduction of a fluorine-substituent on the *syn*-methyl group. The fluorine probably averts the CH-π interaction which stabilises conformer **I**.[157] To test whether selectivities could be improved by decreasing the reaction temperature, the reactions were repeated at 0 °C and –55 °C with the parent catalyst **1** and the two electronic extremes **3** [R = $C_6H_2(OMe)_3$] and **10** (R = C_6F_5) (Table 13). While no significant improvements were achieved for the electron-rich catalyst **3**, the stereoselectivity of the 1st generation MacMillan catalyst **1** increased to the same levels at –55 °C (44% *ee* as compared to 45% *ee* for **3**). Remarkably, the electron-deficient catalyst **10** gave almost the same enantiomeric excess, i.e. –40% *ee*, of the other enantiomer at –55 °C. Thus, solely by modifying the electron-density of the aryl shielding group by introducing electron-withdrawing or electron-donating groups, differences in enantioselectivity of 85% *ee* were obtained, highlighting the importance of non-covalent interactions in these low molecular weight organocatalysts. The reversal of selectivity is believed to be due to intermolecular interactions between the nucleophile and the iminium ion intermediate, which direct the nucleophile to attack from the top-face. This attack is supposedly only possible, when the shielding group is rotated away from the reaction centre as a consequence of prevention of the CH-π (and π-π) interaction. Since the only moiety discriminating the two faces of the iminium ion is the substituent in the 5-position (i.e. in the parent catalyst the benzyl group), the directing interaction must occur between this moiety and the nucleophile. In the case of the fluorinated-derivatives, one could invoke a π,π-stacking interaction between the electron-deficient aryl ring and the electron-rich π-system of the nucleophile, or of a CH-π interaction of the latter with the benzylic protons. The

indole-containing amino acid tryptophan is known to undergo various non-bonding interactions important for controlling protein-structures[106b;106e;158] and indole itself has recently been reported to undergo a π,π-stacking interaction with hexafluorobenzene,[69] thus, both directing effects seem reasonable. Naturally, the question arises, why this phenomenon was not observed for the nucleophile *N*-methyl pyrrole. Reasons for this might be the more electron-rich nature of indole as compared to pyrrole and the larger aromatic system. To gain a better understanding of the underlying mechanisms more imidazolidinone catalysts were studied.

Table 13 *Screening of catalysts **1**, **3**, and **10** in the Friedel-Crafts reaction of N-methyl indole **96** to (E)-cinnamaldehyde **2** at 0 °C and -55 °C.*

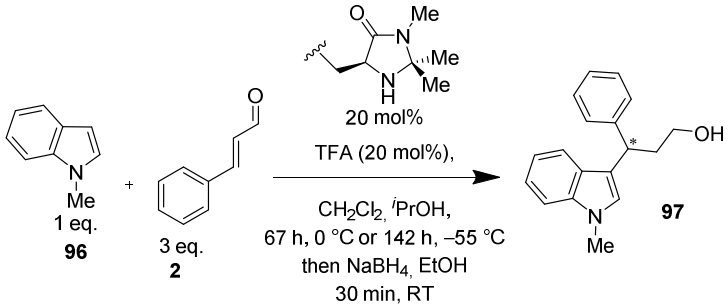

Catalyst	*Qzz* [D·Å]	$\Delta\delta^1H_{syn/anti}$ [ppm]	Postulated Conformer	T [°C]	*ee* [%]	*e.r.*
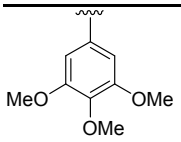 **3**	–5.68	–0.62	**II/I**	0	44	72:28
 **1**	–3.46	–0.89	**I**	0	36	68:32
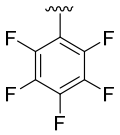 **10**	+3.01	–0.13	**III**	0	–28	36:64
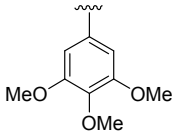 **3**	–5.68	–0.62	**II/I**	–55	45	72.5:27.5
 **1**	–3.46	–0.89	**I**	–55	44	72:28
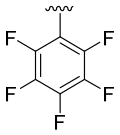 **10**	+3.01	–0.13	**III**	–55	–40	30:70

4.1.2 Catalysts with Additionally Modified Shielding Groups

Next, the remaining imidazolidinones with modified shielding groups (**35** and **40-44**, chapter 2.2.8) were tested on their catalytic behaviour in the discussed reaction (Table 14).

Table 14 *Screening of the imidazolidinone catalysts* ***35*** *and* ***40-44*** *in the Friedel-Crafts reaction of N-methyl indole* ***96*** *to (E)-cinnamaldehyde* ***2****.*

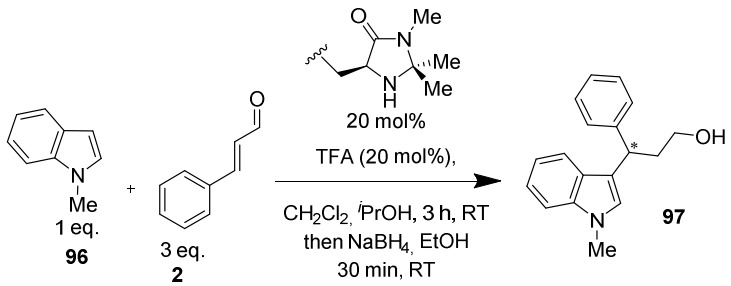

Catalyst	Q_{zz} [D Å]	$\Delta\delta^1H_{syn/anti}$ [ppm]	Postulated Conformer	*ee* [%]	*e.r.*
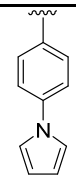 **40**	–4.29	–	**I**	33	66.5:33.5
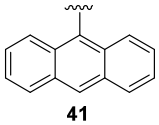 **41**	–7.62	–0.26	**II**	5	52.5:47.5
 **42**	0.54	–0.03	**III**	–22	39:61
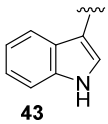 **43**	–6.12	–0.58	**II**	36	68:32
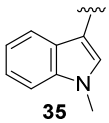 **35**	–5.40	–0.64	**II**	41	70.5:29.5
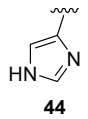 **44**	–3.21	–		–4	48:52

The selectivities obtained were generally in good agreement with the predictions made based on the proposed conformational behaviour, and the previous results from the addition of *N*-methyl pyrrole **38** to (*E*)-cinnamaldehyde **2**. The extended electron-rich system **40** gave similar levels of enantioinduction as the parent compound (33% *ee*). Both, the anthracene and the imidazole-derivatives **41** and **44** gave very low levels of selectivity (5% and –4% *ee*, respectively) as it was also observed for the addition of *N*-methyl pyrrole. The indole derivatives **35** and **43** gave moderate stereoselectivities only slightly lower than obtained with the trimethoxy-analogue **3** (36% and 41%, respectively, as compared to 44%,). With the cyclohexyl-catalyst **42**, which was postulated to predominantly populate conformer **III**, the reversed selectivity was again observed (–22% *ee*). Lowering the reaction temperature to –55 °C, while increasing the reaction time to 142 h led to –52% *ee* for **42**. This might implicate that a CH-π interaction between the indole substrate and the iminium ion as being responsible for the reversal of selectivity observed with catalysts which populate conformer **III**.

4.1.3 Catalysts with Modulations in the Benzylic Position

The next catalysts tested in the Friedel-Crafts reaction of *N*-methyl indole **96** to (*E*)-cinnamaldehyde **2** were the MacMillan-derivatives with modifications in the benzylic position (Table 15). The selectivities obtained with the two "*conformer equivalents*" **57** and **58** were surprising: While the diastereomer **58** with the corresponding iminium ion predominantly populating conformer **II** gave 20% *ee* of the expected enantiomer, **57** with the iminium ion fixed in conformer **I** exhibited reversal of selectivity. This was unexpected as it was previously believed that catalysts in which the corresponding iminium ions predominantly populate conformer **I** and/or **II** do not result in this inversed selectivity. The results obtained for **57** suggest, that this only holds true for conformer **I** when a certain degree of flexibility is ensured. For the other structures mainly populating conformer **I**, a non-diminishable population of conformer **II** was identified whereas for **57a** conformer **I** was found to be the only minimum structure (chapter 2.4.5). The diphenyl-catalyst **61** resulted in relatively low selectivities (21% *ee*), which is consistent with the previous observations. Reversal of selectivity was observed for both catalysts **59** and **60** (–27% and –32% *ee*). The iminium ion of catalyst **59**, in which the distance between the aryl shielding group and the reaction centre is extended by an additional CH_2-group, was proposed to

predominantly populate conformer **III**. Consequently, the reversal of selectivity for this catalyst was expected. The methyl-derivative **60** gave the highest levels of enantiomeric excess of the imidazolidinones resulting in reversed selectivity (–32% *ee*). Moreover, lowering the reaction temperature to –55 °C resulted in the highest selectivity observed for all 1st generation-derived catalysts so far, i.e. –58% *ee*. Therefore, it was assumed that a CH–π interaction between the methyl-group (or CH_2R-group in the other catalysts) and the *N*-methyl indole nucleophile functions as a directing effect.

Table 15 *Screening of MacMillan catalyst-derivatives modified in the benzylic position in the Friedel-Crafts reaction of N-methyl indole* ***96*** *to (E)-cinnamaldehyde* ***2****.*

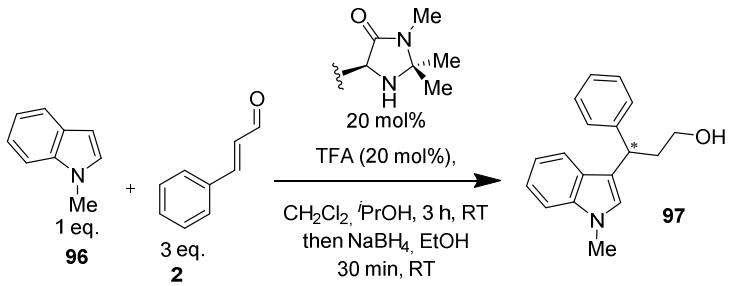

Catalyst	Δδ(*syn*/*anti*)^{1}H [ppm]	Postulated Conformer	*ee* [%]	*e.r.*
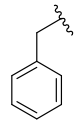 **1**	–0.89	**I**	31	65.5:34.5
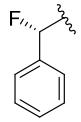 **57**	–1.08[a]	**I**	–13	43.5:56.5
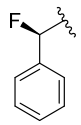 **58**	–0.06[a]	**II**	20	60:40
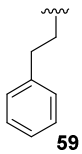 **59**		**III**	–27	36.5:63.5
 **60**	+0.03		–32	34:66
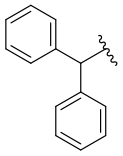 **61**	–0.57		21	60.5:39.5

4.2 Correlation between Conformational Preferences, Enantioselectivity and ^{1}H NMR-Shift of the *syn*-Methyl-Group Revisited

In chapter 2.5, it was shown that the conformational preferences of the isolable, intermediate iminium salts derived from the imidazolidinone catalysts, are reflected in the observed NMR-shift differences of the two signals obtained for the *geminal*-dimethyl group ($\Delta\delta^1H_{syn/anti}$). Since the conformational behaviour of the intermediate is also believed to govern the stereoselective outcome of the addition of a charge-neutral nucleophile, the utility of the experimental $\Delta\delta^1H_{syn/anti}$ value as a predictive tool was investigated. In chapter 2.5 the value of this approach was illustrated by plotting the $\Delta\delta^1H_{syn/anti}$ against the obtained enantiomeric excess and ascribing the different regions of the plot to distinct conformational behaviour. To test the generality of this correlation, a similar plot was created from the results of the catalyst screen in the addition of *N*-methyl indole **96** to (*E*)-cinnamaldehyde **2** Figure 87 and Figure 88).

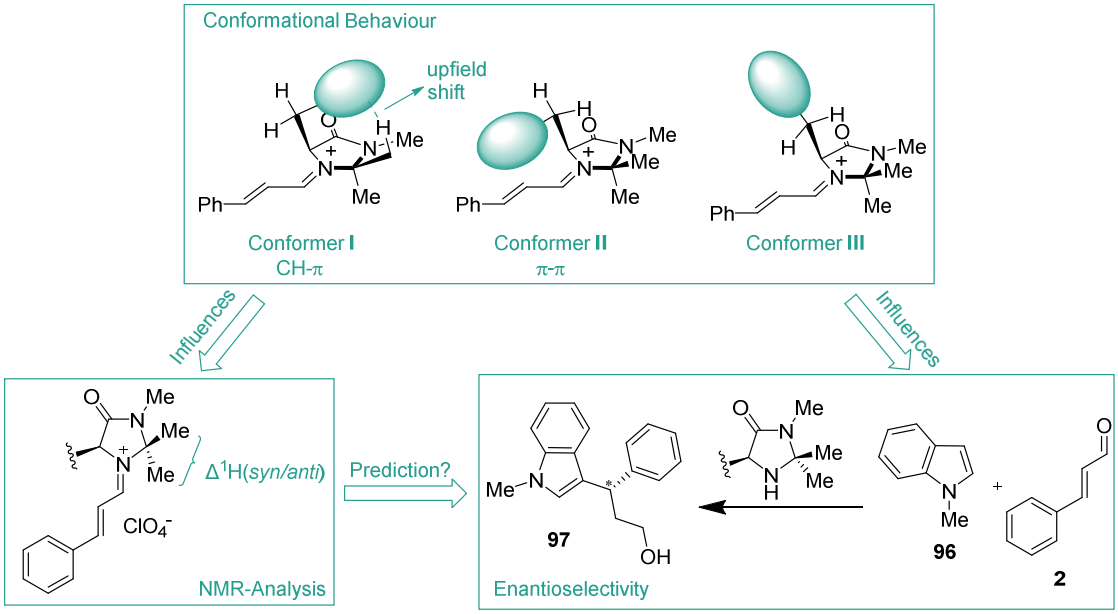

Figure 87 *Working hypothesis for the use of experimental $\Delta\delta^1H_{syn/anti}$ as tools for predicting the stereochemical outcome of Friedel-Crafts additions of N-methyl indole* ***96*** *to (E)-cinnamaldehyde* ***2*** *catalysed by MacMillan catalyst-analogues*

Gratifyingly, the correlation was even more pronounced for this particular reaction, probably due to a greater selectivity range from –32% *ee* to +44% *ee*. The trend is again well represented by a polynomial fit. The catalysts, for which the corresponding iminium salts exhibited only small $\Delta\delta^1H_{syn/anti}$, gave either very low selectivities (**41**, distorted conformer **II**) or resulted in reversal of selectivity (**8**, **10**, **42**, and **60**, conformer **III**). The only exception to these observations was found in "*conformer equivalent*" **58**. A probable explanation is that the spacial arrangement of the phenyl group in conformer **II** prevents the proposed directing effect. The catalysts with iminium ions populating conformer **III** or a rigid conformer **II** are combined in the red-coded region of the plot. The best selectivities were observed for the catalysts in the green region of the plot, which all contain a very electron-rich aromatic shielding group. The corresponding iminium salts were found to have a higher population in conformer **II** than in conformer **I**. The opposite behaviour was found for the catalysts highlighted in the blue region, which were proposed to have a (slight) preference of conformer **I** over conformer **II**. While these catalysts show a larger $\Delta\delta^1H_{syn/anti}$, the enantioselectivity is slightly diminished. In the yellow region the "*conformer equivalent*" fixed in conformer **I** is shown. As a consequence of the fixation in the CH-π stabilised conformation, the deduced $\Delta\delta^1H_{syn/anti}$ of this iminium salt is the largest of all compounds. Employing the corresponding catalyst in the studied reaction led to reversal of selectivity. Thus, it was shown that qualitative predictions of the enantioinduction of a MacMillan-type catalyst can be made from the experimental $\Delta\delta^1H_{syn/anti}$ of the corresponding iminium salt.

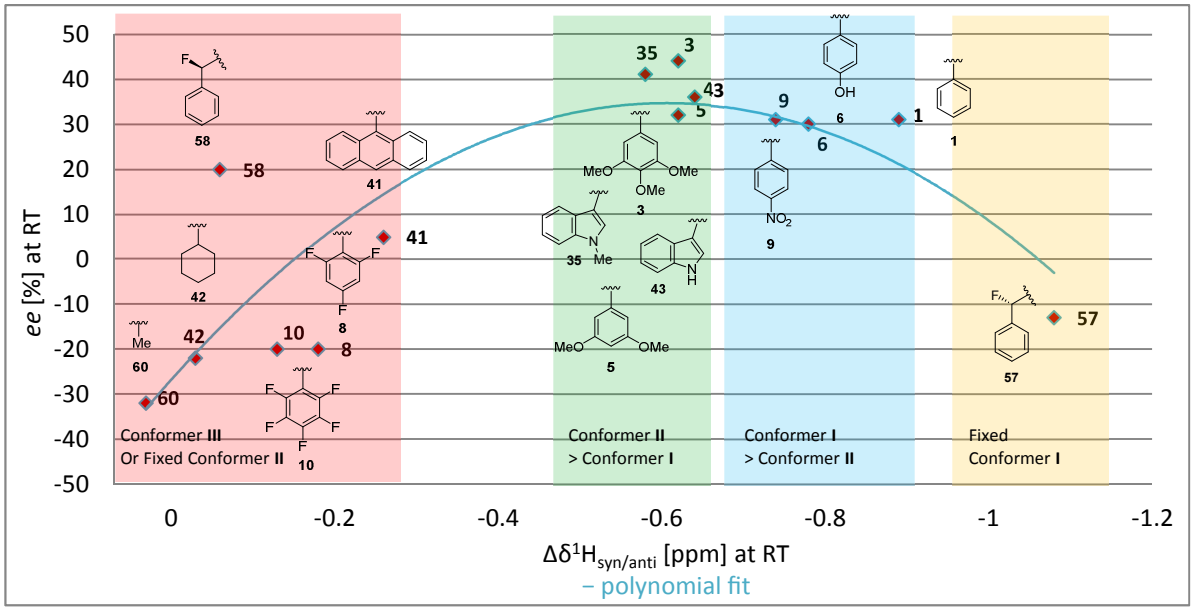

Figure 88 *Plot of the observed $\Delta\delta^1H_{syn/anti}$ of the MacMillan catalyst-derived iminium ions against the observed enantioselectivity of the corresponding catalyst in the Friedel-Crafts addition of N-methyl indole* ***96*** *to (E)-cinnamaldehyde* ***2****. The coloured regions group iminium ions according to their conformational behaviour.*

4.3 Catalysis Screening with Catalysts Modified at the *geminal*-Dimethyl Moiety

In the Friedel-Crafts addition of *N*-methyl pyrrole **2** to (*E*)-cinnamaldehyde **38** it was observed that removal of the *geminal*-dimethyl group leads to a drastic drop of enantioinduction. Furthermore, the *spiro*-compounds **79-81** gave lower levels of enantiocontrol than the parent catalyst and it was found that the enantioselectivity increases with increasing *spiro*-ring size (chapter 2.6.4). Similarly, employing catalyst **78** in the reaction using *N*-methyl indole **96** as the π-nucleophile resulted in very low selectivity of 8% *ee*. In contrast to the previous findings, for this reaction the cyclopentane-derivative **80** gave the best selectivity (better than the cyclohexyl-compound **81**) which was found to be in the same range as for the parent catalyst (34% as compared to 36% for **1**).

Table 16 *Screening of the modified catalysts in the Friedel-Crafts reaction of N-Me-indole **96** to (E)-cinnamaldehyde **2**.*

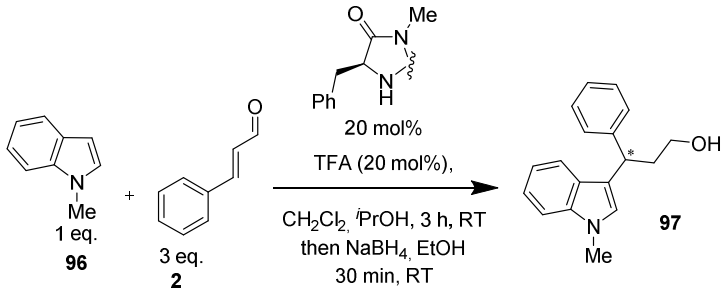

Catalyst	*ee* [%]	*e.r.*
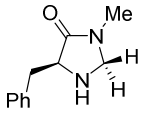 **78**	8	54:46
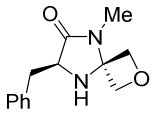 **79**	13	56.5:43.5
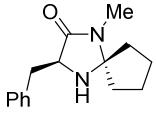 **80**	34	67:33
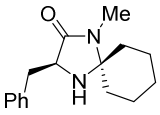 **81**	24	62:38

4.4 Catalysis Screening with 2nd Generation Catalysts

Table 17 *Screening of the 2nd generation catalysts in the Friedel-Crafts reaction of N-Me-indole* ***96*** *and (E)-cinnamaldehyde* ***2****.*

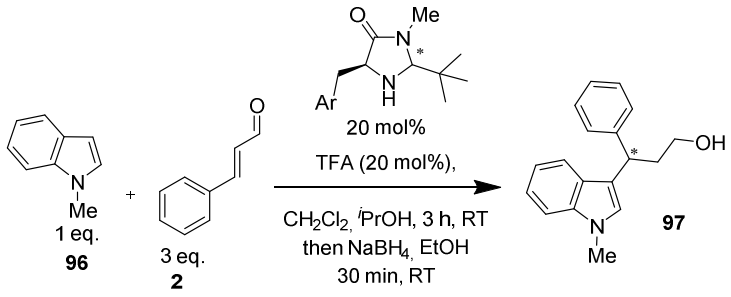

Catalyst	*ee* [%]	*e.r.*
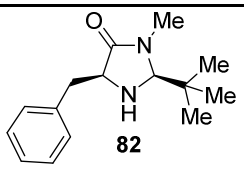 **82**	76	88:12
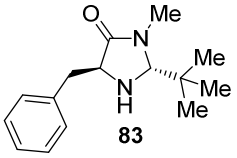 **83**	0	50:50
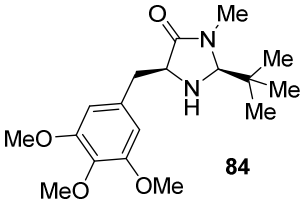 **84**	49	74.5:25.5
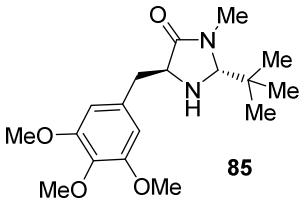 **85**	18	59:41
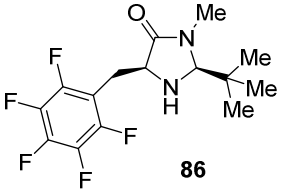 **86**	70	85:15
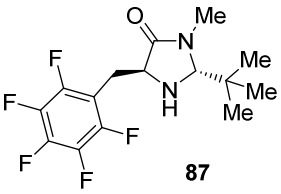 **87**	35	67.5:32.5
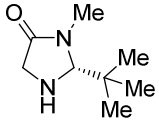 **19**	–53	23.5:76.5

The 2nd generation catalysts were tested on their performance in the organocatalytic Friedel-Crafts reaction of *N*-methyl indole **96** and (*E*)-cinnamaldehyde **2**. The highest selectivities were obtained with the parent 2nd generation MacMillan catalyst **82** (76% *ee*). The electron-deficient imidazolidinone **86** resulted in only slightly diminished *enantiomeric excess* of 70%, whilst surprisingly, the electron-rich catalyst **84** only gave 49% *ee*. The *anti*-analogues generally led to considerably decreased selectivities. The *anti*-benzyl catalyst **83** even resulted in racemic product, **85** [R = $C_6H_2(OMe)_3$] and **87** (R = C_6F_5) gave 18% and 35% *ee*, respectively. Interestingly, in the reaction using the 3rd generation catalyst **19** without an aryl shielding group the attack appears from the face opposite the *tert*-butyl group (53% *ee*).

4.5 Proposed Rationalisation for the Reversal of Selectivity

In Figure 89, the imidazolidinones for which the attack of the indole in the Friedel-Crafts addition of *N*-methyl indole **96** and (*E*)-cinnamaldehyde **2** was observed to occur from the same face of the intermediate, in which the substituent is positioned, are summarised. Common to all of these structures is that in the corresponding iminium salt conformer **II** is postulated to be virtually unpopulated. Moreover, with exception of "*conformer equivalent*" **57**, conformer **I** was also postulated not to be populated to a significant extent. **57** was the catalyst of this series giving the lowest level of facial discrimination.

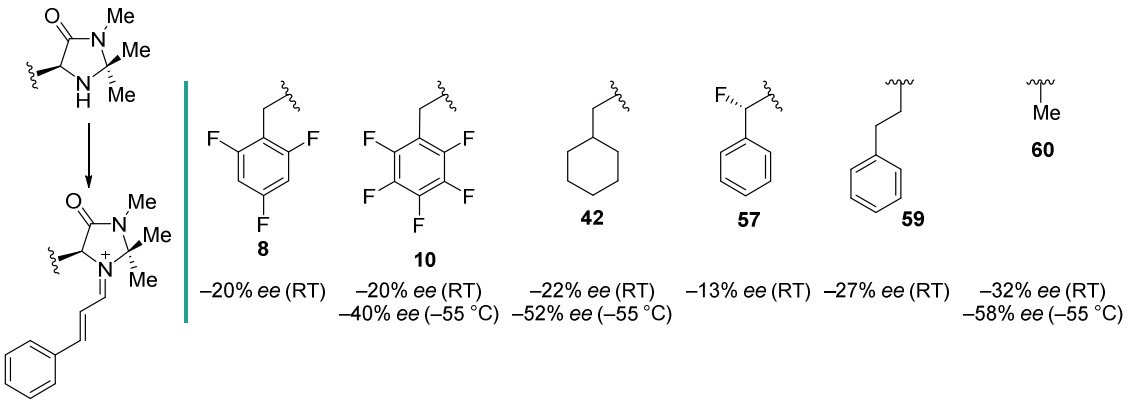

Figure 89 *Catalysts for which a 'reversal of selectivity' was observed in the Friedel-Crafts addition of N-Me-indole* ***96*** *and (E)-cinnamaldehyde* ***2****.*

It seems likely that a directing interaction must be key to the observed reversal of the stereochemical outcome in the Friedel-Crafts addition when using *N*-methyl-indole as the nucleophile. Since the substituent in the 5-position of the imidazolidinone ring is the only moiety discriminating the two faces of the iminium ion, a directing interaction must occur between this moiety and the nucleophile. It is proposed, that the hydrogen substituents in α-position undergo a CH-π interaction with the indole. An additional CH-π interaction could occur between the nucleophile and the *syn*-methyl group, leading to a pincer-like interaction (Figure 90, left). CH-π interactions of indole moieties (especially of tryptophan) are very common and well studied. Computational analysis by Macias and MacKerell has shown that CH-π interactions to the six-membered ring of tryptophan are the strongest of all for aromatic amino acid side chains.[158b] Similarly, Sherrill *et al.* computed the interaction between methane and the six-membered ring of indole to be more stable than the one between methane and the five-membered ring of indole.[159] A protein database study identified three quarters of all tryptophan moieties to be involved in a CH-π interaction, making it the most abundant CH-π interaction in proteins. Furthermore, interactions with the six-membered ring of tryptophan dominate over those with the five-membered ring.[119a] In the pincer hydrogen bond system proposed in this study, a CH-π interaction with the six-membered ring of *N*-methyl indole would allow the reacting π-bond of the nucleophile to be in proximity to the reaction center of the iminium chain. There could be an additional stabilising CH-π interaction between the hydrogen pointing towards the iminium chain and the five-membred ring of the indole. This pincer model would also offer a possible explanation for why reversal of the stereochemical outcome in the Friedel-Crafts addition was not observed for the nucleophile *N*-methyl pyrrole. Besides the fact that the five-membered ring of *N*-methyl pyrrole undergoes weaker CH-π interactions than the six-membered ring of *N*-methyl indole (Q_{zz} = –4.10 and –5.10, respectively, Figure 90, right), the pincer interaction proposed would not bring the pyrrole nucleophile in close enough proximity to the reaction center for an effective directing effect.

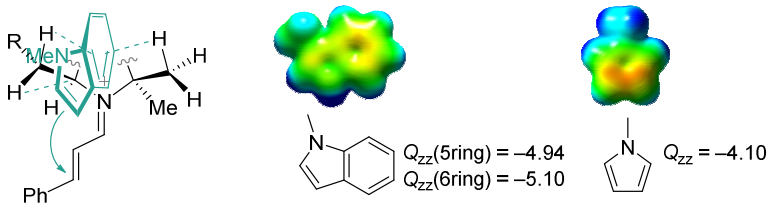

Figure 90 *Left: Proposed pincer-like interaction involving two CH-π interactions between indole and the iminium salt. Right: ESP maps and Q_{zz} of N-Me indole* ***96*** *and N-Me pyrrole* ***38****. Colour range of the electrostatic potential: −0.06 (red) to + 0.06 (blue).*

In addition, this model provides an explanation for why it was found beneficial to employ the 2nd generation MacMillan catalyst instead of the 1st generation MacMillan catalyst in the addition reaction of indoles but not of pyrroles: The introduction of a *tert*-butyl group in place of the *geminal*-dimethyl group prevents a directing CH-π interaction, thus, ensuring higher selectivity from the other face. This is presumably not required for the addition of pyrrole since, as proposed above, a directing effect is not functional. For "*conformer equivalent*" **57** a different interaction must be responsible for the observed reversal of the stereochemical outcome. A possible explanation is a directing CF-π interaction between the fluorine substituent positioned in proximity of the pendant iminium chain by virtue of a stabilising fluorine-iminium ion *gauche* effect and the indole. A similar CF-π interaction could also account for the increased selectivity of the MacMillan catalyst carrying a fluorine substituent on the *anti*-methyl group as compared to the parent catalyst **1** observed by Seebach *et al.* (62% as compared to 44% *ee*, see page 99 and Figure 91).[157]

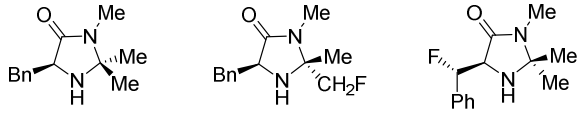

Figure 91 *Left: Parent catalyst **1**. Middle and right: Fluorinated derivatives suggested to undergo a directing CF-π interaction with the substrate in the Friedel-Crafts reaction of N-Me indole and (E)-cinnamaldehyde.*

4.6 Conclusions and Outlook

In this chapter, the organocatalytic Friedel-Crafts addition of *N*-methyl indole **96** to (*E*)-cinnamaldehyde **2** was studied using a large library of MacMillan catalyst derived imidazolidinones. Trends observed for the addition of *N*-methyl pyrrole (e.g., clear correlations between the obtained *ee* and the Q_{zz} and the NMR $\Delta\delta^1H_{syn/anti}$, respectively) were retained. Furthermore, an explanation for the observed reversal of the stereochemical outcome when using specific imidazolidinone catalysts in the addition reaction of indoles is presented. The working hypothesis also offers an explanation for the observation that enatioselectivities can be improved by using the 2nd generation MacMillan catalyst instead of the 1st generation MacMillan catalyst when indoles are used as the nucleophile in the Friedel-Crafts addition, but not when pyrroles are used. Experimental proof for the hypothesis presented in here is required. NMR studies to detect the proposed CH-π interactions are ongoing. For the purpose of these, a relatively unreactive iminium salt **98**

was prepared by condensation of the alanine-derived imidazolidinone **60** and (*E*)-(*para*-dimethylamino)cinnamaldehyde **91**. Due to the strong π-donor-character of the dimethylamino-substituent, the cation is stabilised by delocalisation. Mayr and Lakhdar found that the iminium ion derived from the benzyl catalyst **1** and (*E*)-(*para*-dimethylamino)cinnamaldehyde **91** is almost two orders of magnitude less reactive than the iminium ion of **1** and (*E*)-cinnamaldehyde **3** in the reaction with silyl ketene acetals **36** and **37** (Figure 92).[120]

	k_2 (**36**) [M^{-1} s^{-1}]	k_2 (**37**) [M^{-1} s^{-1}]
1a	9.06×10^3	5.23×10^2
95	2.07×10^1	1.31×10^0

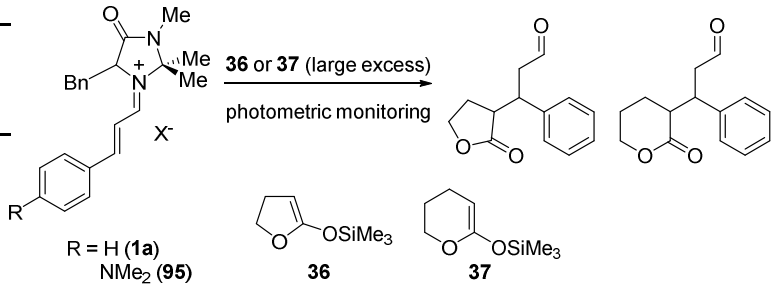

Figure 92 *By two orders of magnitude decreased reactivity of* ***95*** *as compared to* ***1a*** *reported by Mayr and Lakhdar.*

Thus, it is proposed that a mixture of **98** and *N*-methyl indole would be inert enough to observe CH-π interactions by low-temperature NMR spectroscopy (Figure 93).

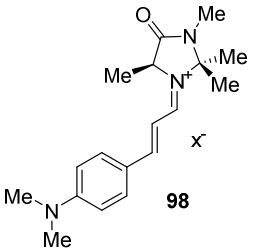

Figure 93 *Proposed model structure for NMR studies to verify CH-π interactions between the iminum salt and the substrate.*

5 Partial Cationic Character of the CH-π and the π-π Interactions in the MacMillan Catalyst Derived Iminium Ion

In the MacMillan catalyst derived α,β-unsaturated iminium ions, two stabilising non-covalent interactions involving the shielding aryl group have been identified to be important for high levels of enantioinduction: A CH-π interaction with the *syn*-methyl group and a π-π interaction with the pendant iminium chain (see Chapter 2.1.2). These interactions control the spacial arrangement of the shielding aryl group. Herein, it has been shown that disrupting these interactions by either electronic modifications or by geometric constraints, leads to diminished enantioselectivities in the Friedel-Crafts reaction using *N*-methyl pyrrole (Chapter 2) or *N*-methyl indole (Chapter 4). The interactions are predominantly treated as π-π and CH-π interactions in the literature. But the iminium cation can be delocalised into iminium chain (Figure 94), thus, raising the question whether the π-π interaction should not partially be treated as a cation-π interaction. A recent study by Mori and Yamada has suggested, that a cation-π interaction is operative in the iminium ion of the 2nd generation MacMillan catalyst and (*E*)-crotonaldehyde.[111] Furthermore, polarisation of the *syn*-methyl group through an inductive electron-withdrawing effect from the iminium ion might cause a partial positive charge on the hydrogen participating in the CH-π interaction. Thus, the CH-π interaction might also have a partial cationic character (Figure 94).

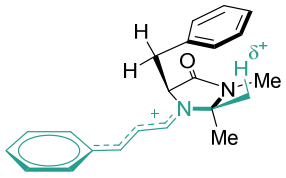

Figure 94 *Proposed charge delocalisation in iminium ion* ***1a****.*

To probe this hypothesis, a Mulliken population analysis of iminium ion **1a** in the CH-π conformation (global minimum, see chapter 2.2.7) and of **10a** forced into this conformation (not found to be a global minium, see chapter 2.2.7) was performed in collaboration with Dr. Mück-Lichtenfeld from WWU Münster (Figure 95).

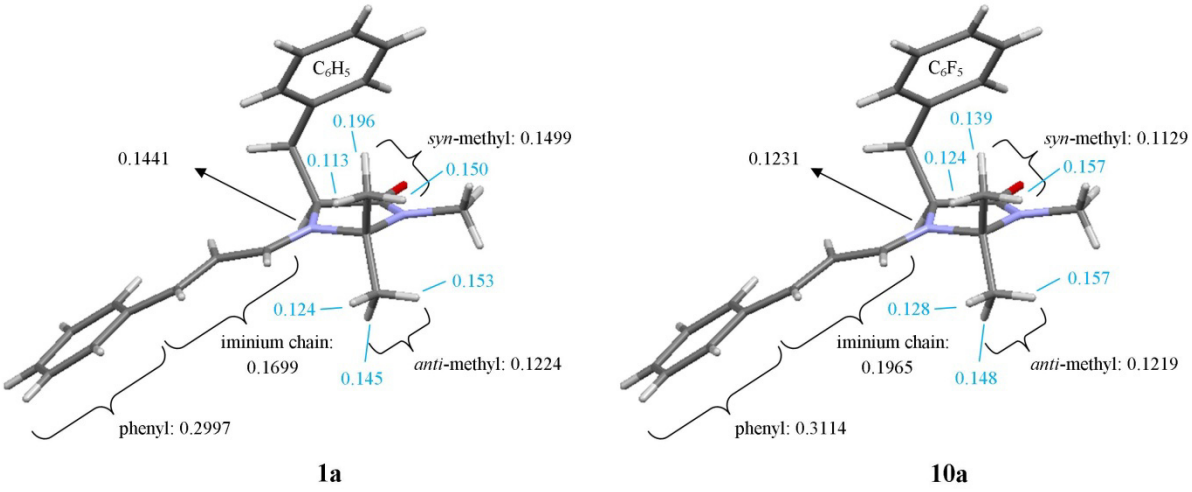

Figure 95 *Group electronegativities obtained from Mulliken population analyses of iminium salt* ***1a*** *and* ***10a*** *constrained in the CH-π conformation.*

It was found that only a small fraction of the positive charge is located on the iminium nitrogen (14.4% and 12.3% for **1a** and **10a**, respectively). A large portion of the charge is delocalised in the pendant aromatic system (47.0% and 50.8%, respectively). But also the methyl groups of the *geminal*-dimethyl moiety carry a significant partial positive charge. This is particularly pronounced for the *syn*-methyl group of the benzyl iminium ion **1a** (15.0%), whilst the *anti*-methyl group of **1a** only carries 12.2% of the positive charge. The same partial charge was found for the *anti*-methyl group of **10a**, but in contrast to the parent structure **1a**, the *syn*-methyl group of the pentafluoro-system **10a** is less positively charged than the *anti*-group (11.3%). The difference of partial charge in the *syn*-methyl group of 3.7% corresponds well to the difference of partial charge in the pendant aromatic system (3.8%). This suggest that in the CH-π conformation of **1a** the positive charge is located on the *syn*-methyl group to a greater extent, thus, stabilising this favourable interaction, while the opposite is observed when the electron-deficient pentafluorophenyl-ring is forced into proximity of the *syn*-methyl group. The difference might be even more obvious when comparing the partial charge of the interacting hydrogen-substituents. Whereas all the other hydrogen-substituents have similar partial charges for both iminium ions, the interacting hydrogen of the benzyl-iminium ion **1a** is 1.4 times as positively charged as the corresponding one in the fluorinated derivative **10a**.

To quantify the CH-π interaction, the two interacting moieties of the molecule (i.e., the aromatic ring and the rest of the molecule) were fragmented and the electronic distributions

calculated. The electron distribution changes resulting from bringing the two fragments into the CH-π contact are illustrated in Figure 96 for iminium ions **1a** (left) and **10a** (right). Green clouds correspond to increased electron-density, whilst orange clouds correspond to decreased electron-density. It was found that the two aryl rings are both polarised to a similar extent with increased electron-density towards the methyl-group. But the influence on the interacting methyl-group was found to be very different for the two systems. Whereas the *syn*-methyl group of the iminium fragment shows hardly any electronic redistribution when placed into close contact with the pentafluorophenyl, a strong redistribution is observed when the same fragment is put into contact with the electron-rich phenyl ring. Not only the interacting hydrogen-substituent, but also the iminium nitrogen show decreased electron-density, suggesting a strongly stabilising interaction. These differences are also reflected in the stabilisation energies resulting from combination of the fragments: The CH-π interaction of the iminium fragment with the phenyl-ring was computed to result in a stabilisation of 7.2 kcal/mol, while the interaction with the pentafluoro-ring only leads to a stabilisation of 3.4 kcal/mol.

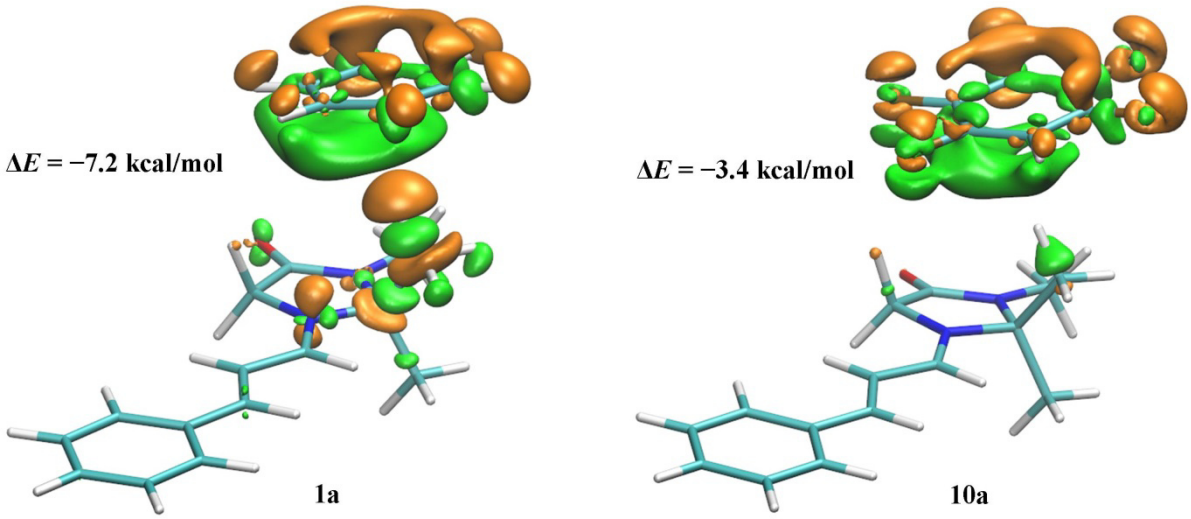

Figure 96 *Quantification of the stabilisation resulting from the combination of the two components of the CH-π interaction and illustration of the consequent redistribution of electron-density for iminium salts* ***1a*** *and* ***10a****. Isodensity value: 0.0005 a.u.*

6 Chiral Modifiers for Asymmetric Heterogeneous Catalysis

6.1 Introduction

Asymmetric heterogeneous catalysis is considerably less well established as a working horse for asymmetric synthesis compared to its homogeneous counterpart.[160] This is largely due to challenges in creating stable, active and highly enantioselective reaction sites on a solid surface.[160a] Nevertheless, the development of effective heterogeneous asymmetric catalysis processes is highly sought after because of their inherent advantages, i.e., easy separation and efficient recycling of the catalyst, very low catalyst loadings, and ease of transfer to continuous mode operation.[160c] Furthermore, the ever-growing demand for enantiopure compounds promotes research in this field and impressive progress has been reported in recent years. There are a number of strategies for the creation of asymmetric heterogeneous catalysts:[161]

The first, maybe most obvious, is the immobilisation of homogenous catalysts.[162] Examples for this include covalent tethering of the catalyst (e.g., on silica[163] and polymeric resins[164]), copolymerisation of monomers carrying the catalytic moiety,[165] encapsulation of the catalyst,[166] and fixation by electrostatic interactions.[160c]

Another strategy focuses on the use of chiral solids, which can e.g. be obtained by depositing the catalytically active particles (i.e., metals or metal oxides) on intrinsically chiral support materials, such as quartz and cellulose, or by developing enantiopure zeolites.[167] An additional research area in this category is the development of metal organic frameworks (MOFs) for heterogeneous asymmetric catalysis.[168]

Today, arguably the most successful strategy for the creation of an enantioselective heterogeneous catalyst is to chirally modify an achiral catalytic metal surface by adsorption of a chiral organic molecule, the so-called chiral modifier.[160a;169] Three general requirements for the chiral modifier have been identified to achieve efficient chiral modification of a metal catalyst: A strongly adsorbing anchor to rivet the modifier to the catalyst, a "*chiral pocket*" with specific stereochemical information to induce the desired facial discrimination, and an interacting moiety to guide the reactant to the chiral surface

site.[170] The three most successful systems so far have been the Pd/ and Pt/cinchona alkaloids[171] (especially cinchonidine) and Ni/tartaric acid.[172] Both systems have primarily been used in hydrogenation reactions. There are many critical parameters that have to be adjusted in order to develop a highly selective system for a specific substrate. The concentration and adsorption strength of the modifier are important. On the one hand, the modifier coverage should be sufficient to avoid background (stereounselective) reduction of the substrate. On the other hand, the substrate and hydrogen also require access to the metal surface, and so excess modifier molecules might block active hydrogenation surface sites. Furthermore, it has been reported, that some mobility is beneficial for formation of the modifier-substrate complex.[173] The adsorption strength is obviously strongly dependent on the anchoring unit, but also on the solvent and the hydrogen surface concentration as well as efficient mass transfer and the reaction temperature.[160a] In addition, the stereoselective surface reaction was found to be highly specific with regard to the molecular structures of the reactant and the chiral modifier. Pioneering work on the Pt/cinchona system for the reduction of alkyl pyruvates has been reported as early as 1979.[174] Nevertheless, continuous research efforts aimed at the elucidation of the surface phenomena (mechanistic studies) and at the optimisation of the catalytic performance (catalytic studies) have been reported in the literature, highlighting the complexity of the system and the great interest in achieving efficient asymmetric catalysis on chirally-modified metals.

6.2 MacMillan Catalyst-derived Imidazolidinones as Chiral Modifiers

It was envisaged, that due to common structural features in both imidazolidinones and cinchonidine (Figure 97), these species could be potentially good chiral modifiers for heterogeneous hydrogenation reactions. The imidazolidinones display all features which are essential for a chiral modifier: An anchoring moiety, a chiral centre, and, most importantly, a moiety that can interact with the substrate. The aromatic ring system of the molecule is expected to function as the anchoring unit, strongly adsorbing to the metal surface, as is the case for cinchonidine. Consequently, an asymmetric surface site could be formed by imidazolidinones in the heterogeneous hydrogenation of activated ketones. The enantioselectivity is proposed to originate from an N–H–O-type hydrogen bond involving the secondary amine moiety (Figure 97) or a covalent fixation.

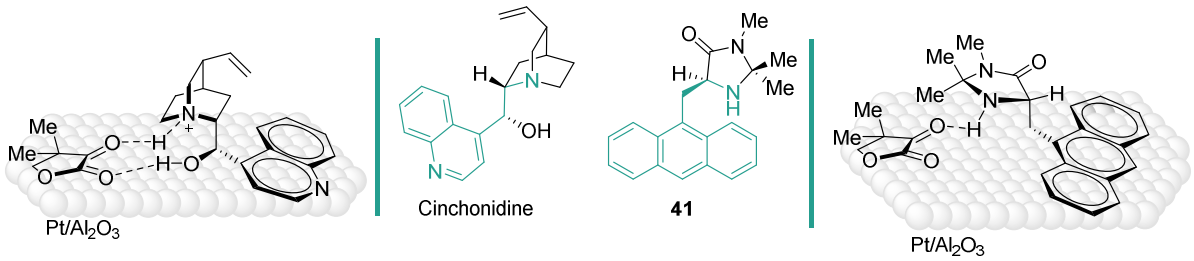

Figure 97 *Structural resemblance of cinchonidine with imidazolidinones (**41** shown as example). Left: Binding mode of cinchonidine and ketopantolactone (KPL) on Pt/Al_2O_3 as reported by Baiker et al.[2] Right: Proposed binding mode of **41**.*

The heterogeneous catalysis experiments reported in this thesis were carried out in collaboration with Prof. Alfons Baiker and Fabian Meemken at the ETH Zurich. For an initial structure-activity/enantioselectivity screening, a library of 20 different imidazolidinones (Figure 98) was tested in the reduction of ketopantolactone (KPL), which is the best-studied reaction for the chiral modification with cinchonidine. Afterwards, the modifiers were tested in the reduction of methylbenzoylformate (MBF) and trifluoroacetophenone (TFAP).

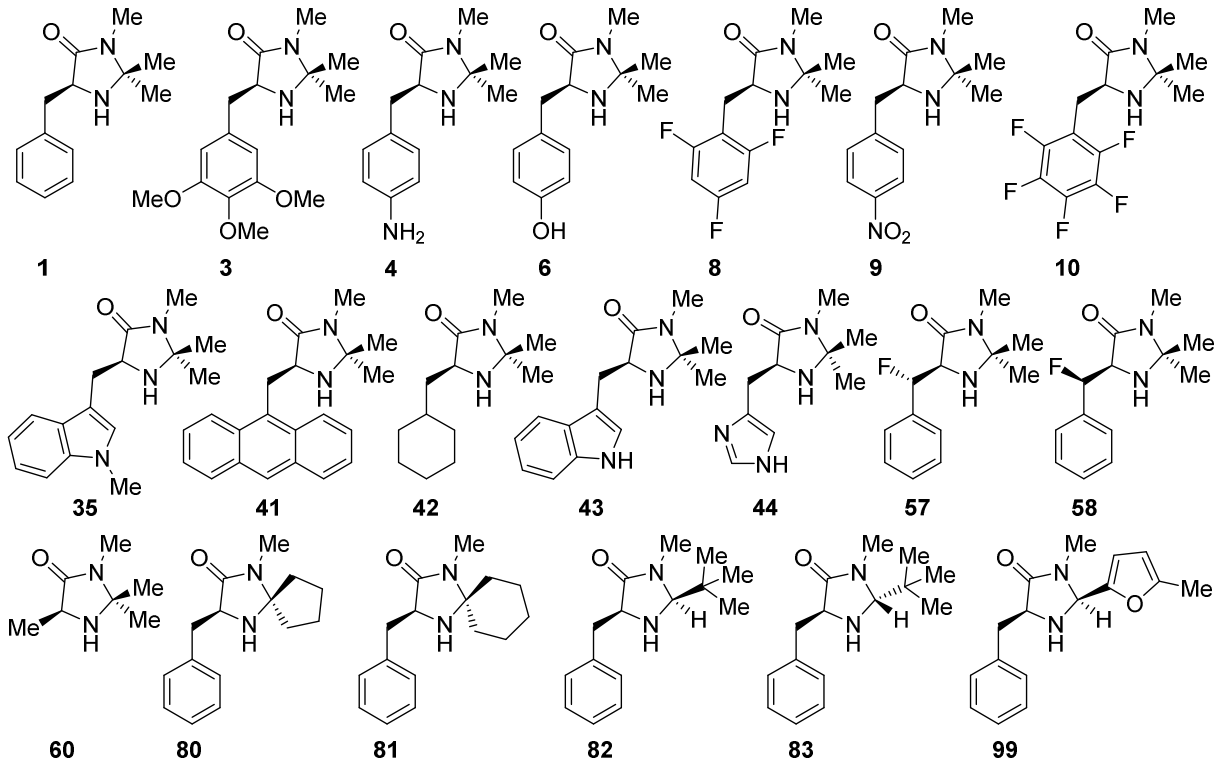

Figure 98 *Library of imidazolidinones tested for their efficiency as chiral surface modifiers of Pt/Al_2O_3 for the reduction of different ketones.*

6.2.1 Reduction of Ketopantolactone (KPL)

The modifiers were initially tested in the reduction of ketopantolactone (dihydro-4,4-dimethyl-2,3-furandione, Scheme 24) to complete a preliminary structure-activity/enantioselectivity screening (Table 18). The hydrogenations were performed in 10 mL of toluene at RT for 2 h with 50 mg pre-reduced Pt/Al_2O_3-catalyst (1 h under H_2-flow at 400 °C), 0.2 M substrate and 1 mM modifier under constant H_2-flow at atmospheric pressure with stirring of 500 rpm. The enantioselectivity and conversion were determined by chiral GC. First, as a reference, the performance of cinchonidine under the given reaction conditions was established, resulting in 40% enantiomeric excess (*R*).

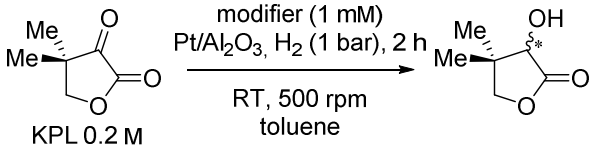

Scheme 24 *Reduction of ketopantolactone.*

Table 18 *Structure-activity screen of 20 different imidazolidinones as modifiers for the asymmetric reduction of ketopantolactone on Pt/Al_2O_3.*

Modifier	*ee* [%]	*e.r.*	Conversion [%]
Cinchonidine	40 (*R*)	70:30	Full
1	racemic	racemic	Full
3	11 (*R*)	55.5:44.5	Full
4	5 (*R*)	52.5:47.5	Full
6	9 (*R*)	54.5:45.5	Full
8	racemic	racemic	97
9	5 (*R*)	52.5:47.5	Full
10	7 (*R*)	53.5:46.5	Full
35	17 (*R*)	58.5:41.5	Full
41	21 (*R*)	60.5:39.5	Full
42	13 (*R*)	56.5:43.5	Full
43	16 (*R*)	58:42	Full
44	5 (*R*)	52.5:47.5	73
57	racemic	racemic	97
58	racemic	racemic	95
60	11 (*R*)	55.5:44.5	Full
80	racemic	racemic	98
81	racemic	racemic	99
82	racemic	racemic	97
83	racemic	racemic	97
99	5 (*R*)	52.5:47.5	62

Almost all reactions showed full conversion within the 2 h reaction time. Six imidazolidinones resulted in enantioselectivities over 10% [all (*R*)]. As expected, the best results were achieved with the modifiers carrying larger aromatic systems, namely the two indole-derivatives (**35** and **43** with 17% and 16% *ee*, respectively) and the anthracene

derivative (**41**, 21% *ee*). To our great surprise, modifier **60** without an anchoring group gave a small but notable *ee* of 11%, an observation that is currently not well understood and requires clarification. It was also surprising that the 1st generation MacMillan imidazolidinone **1** did not yield any selectivity, but the corresponding reduced modifier **42** gave an enantiomeric excess as high as 13%. For the lead compound **41**, a solvent screening with commonly used solvents for this kind of transformation was conducted (Table 19). All other reaction parameters were kept constant. Whereas employing acetic acid or ^{i}PrOH led to a drastic decrease of enantioselectivity, in THF comparable levels of stereocontrol as for toluene were reached.

Table 19 *Solvent screen in the asymmetric reduction of ketopantolactone on Pt/Al_2O_3 using **41** as chiral modifier.*

Modifier	Solvent	*ee* [%]	*e.r.*	Conversion [%]
41	Toluene	21 (*R*)	60.5:39.5	Full
41	Acetic acid	5 (*R*)	52.5:47.5	Full
41	THF	21 (*R*)	60.5:39.5	Full
41	^{i}PrOH	7 (*R*)	53.5:46.5	Full

6.2.2 Reduction of Methylbenzoylformate (MBF)

Next, a selection of imidazolidinone-derived modifiers was tested in the reduction of methylbenzoylformate (MBF, Scheme 25, Table 20). The reactions were performed using the same reaction parameters as for the reduction of KPL. The reaction, which already displayed low conversion when using cinchonidine (41% after 2 h), was even slower when using the imidazolidinones (8% after 2 h when using anthracene-derivative **41**). Again, the anthracene derivative **41** showed the highest levels of stereoselectivity (20% *ee* after 2 h) of the imidazolidinones tested, which is consistent with the observations discussed in chapter 6.2.1. However, the levels of enantioselectivity obtained are considerably worse compared to those obtained with cinchonidine (82% *ee*). To study the linearity of the reaction, the performance of three modifiers were monitored over several hours (GC-analysis after 2, 3, 4, and 5 h), showing an increase of both conversion and selectivity over time. Thus, the results for modifier **41** could be improved to 24% *ee* and 18% conversion after 5 h. Furthermore, to exclude problems with the reaction setup or the purity of the substrate, the reductions were run without addition of a modifier. In this control experiment, the MBF used in the discussed reactions (68% conversion) and freshly purified

methylbenzoylformate (85% conversion) were tested, showing that the quality of the substrate does influence the conversion but does not explain the very low conversion with the tested modifiers.

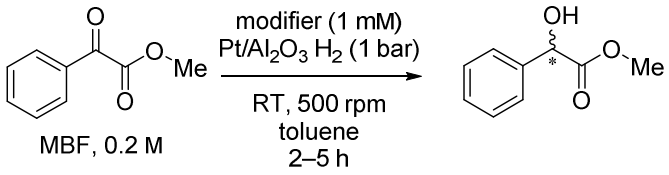

Scheme 25 *Reduction of methylbenzoylformate.*

Table 20 *Screen of different imidazolidinones as modifiers for the asymmetric reduction of methylbenzoylformate on Pt/Al_2O_3. (a) Freshly opened methylbenzoylformate was used.*

Modifier	Time [h]	*ee* [%]	*e.r.*	Conversion [%]
without	2	-	-	68
without[(a)]	2	-	-	85
Cinchonidine	2	82 (*R*)	91:9	41
3	2	2 (*R*)	51:49	57
6	2	2 (*R*)	51:49	44
6[(a)]	2	2 (*R*)	51:49	44
41	2	20 (*R*)	60:40	8
	3	22 (*R*)	61:39	11
	4	23 (*R*)	61.5:38.5	14
	5	24 (*R*)	62:38	18
43	2	7.1 (*R*)	53.5:46.5	11
	3	7.1 (*R*)	53.5:46.5	15
	4	7.2 (*R*)	53.6:46.4	18
	5	7.4 (*R*)	53.7:46.3	21
99	2	racemic	racemic	23
	3	racemic	racemic	31
	4	racemic	racemic	38
	5	racemic	racemic	45

In order to improve conversions and selectivities, a number of reactions were repeated at higher pressure (10 bar). Enantioselectivity of the Pt/cinchona-system for the hydrogenation of activated ketones is generally improved at higher hydrogen pressure.

Table 21 *Screen of different imidazolidinones as modifiers for the asymmetric reduction of MBF on Pt/Al_2O_3 using 10 bar H_2. (a) Freshly purified methylbenzoylformate was used.*

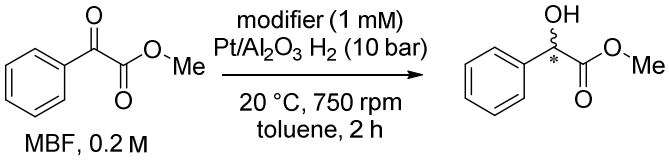

Modifier	*ee* [%]	*e.r.*	Conversion [%]
without	-	-	99
without[(a)]	-	-	99
1	racemic	racemic	73
35	11 (*R*)	55.5:44.5	27
41	47 (*R*)	73.5:26.5	39
43	21 (*R*)	60.5:39.5	28
44	racemic	racemic	62

This strategy proved successful and the results using the anthracene-derivative **41** could be improved to 47% *ee* and 39% conversion. The only other two imidazolidinones giving mentionable selectivities were the two indole-derivatives **35** and **43**. However, enantioselectivity and conversion were both much lower than for **41**. Interestingly, when employing either **1** (phenyl) or **44** (imidazole), the conversion was much better, but no selectivity was observed. The deterioration of enantioselectivity found for these two modifiers might be linked to their weaker adsorption, which might be expected for the phenyl- or imidazole-group due to the smaller size of the aromatic system as compared to the other compounds tested.

6.3 L-Proline-derived Chiral Modifiers

The L-proline-derived structures **100**, **101**, and **102** have previously been studied by Tungler and co-workers as chiral modifiers in the reduction of the C=C double bond of isophorone on Pd-catalysts (Scheme 26).[175] These structures feature all the prerequisites needed for a chiral modifier: A chiral centre, an anchoring moiety and a secondary amine as interacting group. For this reaction, the best results were achieved with **100** yielding enantioselectivities up to 42% *ee* and full conversion.

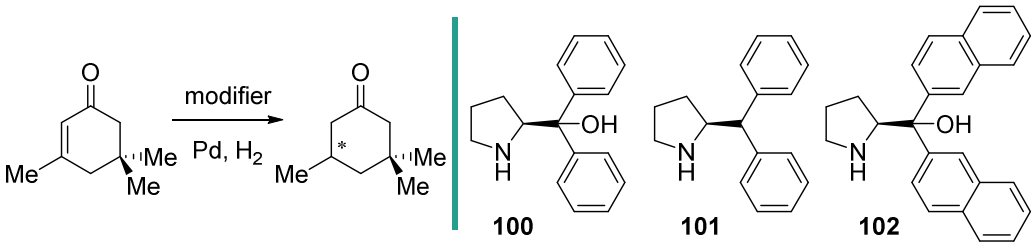

Scheme 26 *L-Proline-derivatives as modifiers in the asymmetric reduction of isophorone reported by Tungler et al.*

Motivated by this study, we envisaged to test **100** and a number of L-proline-derivatives **103-110** (Figure 99), previously synthesised in the group or commercially available, as modifiers in the reduction of different ketones.

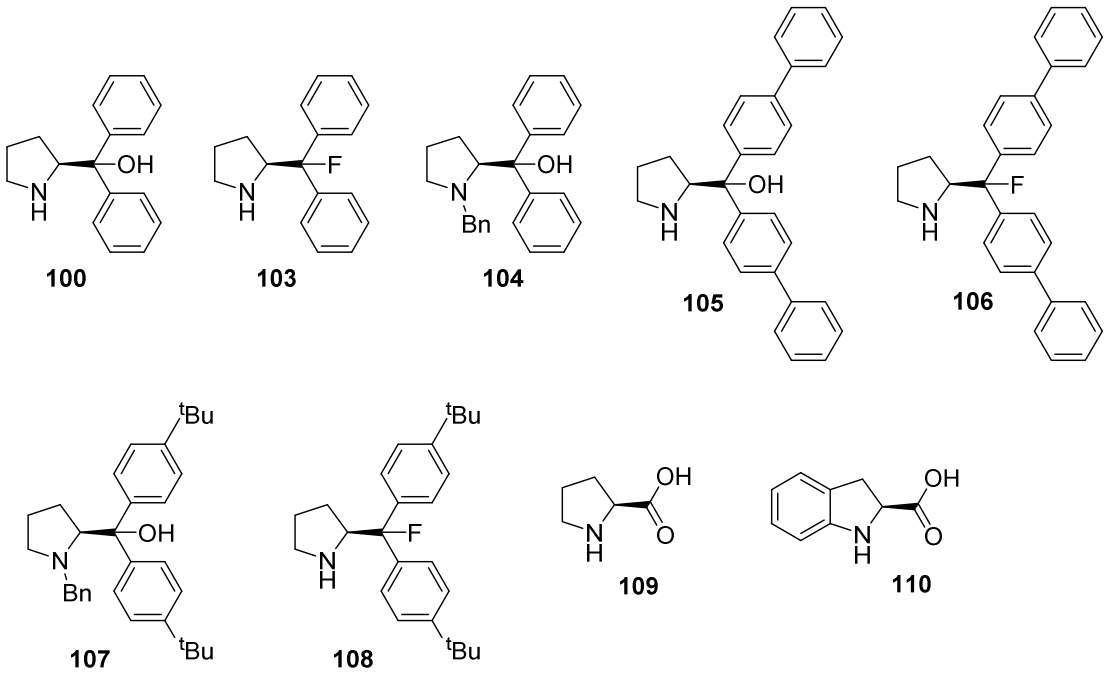

Figure 99 *Library of L-proline-derivatives investigated in the heterogeneous asymmetric reduction of various ketones.*

6.3.1 Reduction of Ketopantolactone (KPL)

First, the reduction of ketopantolactone, which gave promising results in the study using chiral imidazolidinones as modifiers (chapter 6.2.1), was investigated. The same reaction parameters were used as a starting point. Cinchonidine was used as reference compound which gave an enantiomeric excess of 40% and full conversion.

Table 22 *Structure-activity screen of L-proline-derivatives as modifiers for the asymmetric hydrogenation of ketopantolactone on Pt/Al_2O_3.*

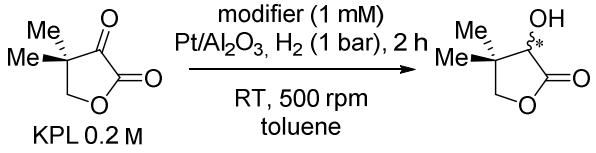

Modifier	*ee* [%]	*e.r.*	Conversion [%]
Cinchonidine	40 (*R*)	30:70	Full
100	racemic	racemic	Full
103	23 (*S*)	61.5:38.5	Full
104	2 (*R*)	49:51	Full
105	9 (*S*)	54.5:45.5	Full
106	22 (*S*)	61:39	Full
107	racemic	racemic	92
108	13 (*S*)	56.5:43.5	Full
109	racemic	racemic	Full
110	5 (*S*)	52.5:47.5	Full

Almost all reactions reached completion within two hours. The compound **100**, reported by Tungler *et al.*, did not give any stereoselectivity in this reaction. Interestingly, when substituting the hydroxyl group by fluorine, the selectivity went up to 23% *ee*. The same trend was preserved for the di-biphenyl-compounds: While **105** gave low levels of enantioselectivity (9% *ee*), the selectivity went up to 22% *ee* when using the fluorinated analogue **106**. Using the third fluorinated compound **108** as chiral modifier resulted in a lower selectivity of 13% *ee*, which is probably due to the large *tert*-butyl groups hindering successful anchoring. Results for the most successful compound **100** were tried to be improved by increasing the hydrogen pressure to 10 bar and increasing the stirring to 750 rpm, but no improvement could be achieved (22% *ee*, full conversion).

6.3.2 Reduction of Methylbenzoylformate (MBF)

The most promising L-proline-derived modifiers for the reduction of ketopantolactone proved to be the fluorinated compounds **103**, **106**, and **108**. Therefore, these structures and their non-fluorinated counterparts **100** and **105** were tested in the hydrogenation of MBF (Table 23). The reduction was found to be very slow when using this class of modifiers with conversions being between 16%-35% after two hours, indicating a competitive adsorption between these modifiers and the substrate on the same surface site.[176] The best selectivity was observed for **103** (17% *ee*), again much higher than the non-fluorinated counterpart (5% *ee*). Unfortunately, when increasing the reaction time to obtain higher conversion, the selectivity decreased (13% *ee* and 81% conversion after 13.5 h). The fluorinated biphenyl modifier **106** gave the best results after 13.5 h (14% *ee* and 99% conversion). Only marginally less effective was the non-fluorinated counterpart **105** (11% *ee* and 96% conversion).

Table 23 *Screening of several fluorinated and non-fluorinated L-proline-derivatives as modifiers for the asymmetric hydrogenation of methylbenzoylformate on Pt/Al_2O_3.*

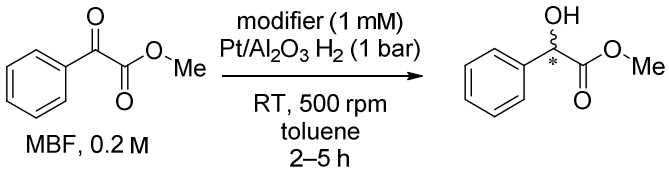

Modifier	Time [h]	*ee* [%]	*e.r.*	Conversion [%]
Cinchonidine	2	82 (*R*)	9:91	41
100	2	5 (*S*)	52.5:47.5	24
	13.5	4 (*S*)	52:48	99
103	2	17 (*S*)	58.5:41.5	16
	13.5	13 (*S*)	56.6:43.5	81
105	2	12 (*S*)	56:44	23
	13.5	11 (*S*)	55.5:44.5	96
106	2	12 (*S*)	56:44	23
	13.5	14 (*S*)	57:43	99
108	2	10 (*S*)	55:45	35

Increasing the hydrogen pressure (10 bar) and stirring rate (750 rpm) led to slightly increased performance of 19% *ee* and 34% conversion after 2 h.

6.3.3 Reduction of Trifluoroacetophenone (TFAP)

As a third reaction for investigation, the hydrogenation of TFAP was studied, again using the fluorinated L-proline-derivatives and their hydroxyl-counterparts (Table 24). The reference compound cinchonidine was found to give 36% *ee* and 90% conversion in this reaction after 2 h when employing the same reaction conditions as used in the reductions of KPL and MBF.

Table 24 *Screen of several fluorinated and non-fluorinated proline-derivatives as modifiers for the asymmetric hydrogenation of trifluoroacetophenone on Pt/Al_2O_3.*

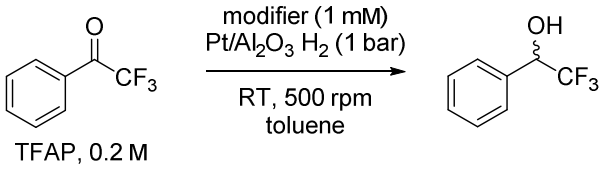

Modifier	Time [h]	*ee* [%]	*e.r.*	Conversion [%]
Cinchonidine	2	36 (*R*)	32:68	90
100	2	11 (*S*)	55.5:44.5	89
	3	10 (*S*)	55:45	97
	4	9 (*S*)	54.5:45.5	98
	5	9 (*S*)	54.5:45.5	99
103	2	13 (*S*)	56.6:43.5	35
	3	11 (*S*)	55.5:44.5	42
	4	11 (*S*)	55.5:44.5	47
	5	10 (*S*)	55:45	47
105	2	17 (*S*)	58.5:41.5	32
	3	14 (*S*)	57:43	44
	4	12 (*S*)	56:44	52
	5	11 (*S*)	55.5:44.5	59
106	2	20 (*S*)	60:40	37
	3	18 (*S*)	59:41	53
	4	17 (*S*)	58.5:41.5	68
	5	16 (*S*)	58:42	78
108	2	2 (*S*)	51:49	32
	3	1 (*S*)	50.5:49.5	50
	4	1 (*S*)	50.5:49.5	65

Consistent with previous findings, better results were found for the fluorinated modifiers than for the hydroxyl-analogues, even though the difference was less pronounced (**100** and **103** resulted in 11% *ee* and 13% *ee*, respectively, and **105** and **106** resulted in 17% *ee* and 20% *ee*, respectively). The fluorinated compound carrying a *tert*-butyl group on the anchoring moieties (**108**) was not an effective modifier in this reaction. The best results were obtained with modifier **106** (20% *ee*, 37% conversion). Unfortunately, increasing the reaction times to achieve higher conversion led to a loss of selectivity. Similarly, increasing the hydrogen pressure to 4 bar and stirring to 750 rpm resulted in deterioration of enantioselectivity to 12% *ee* while increasing conversion to 55% after 2 h.

6.4 Conclusions and Outlook

The performances of two classes of low molecular weight organic molecules as chiral modifiers in asymmetric heterogeneous hydrogenations of several activated ketones were tested. The first class of substances, which has so far not been tested on the performance as chiral modifier, included different imidazolidinones (Page 121, Figure 98). The second class of compounds represents L-proline-derivatives, mostly carrying aromatic moieties which can act as anchoring units on the metal catalyst (Page 127, Figure 99). In the context of heterogeneous catalysis, this type of compound has been subject to studies by Tungler *et al.* as modifiers for C=C bond reductions on Pd,[175c] but, to the best of our knowledge, have not been tested as chiral modifiers for C=O bond hydrogenations. At this early stage of exploring the potential of these compounds as novel chiral modifiers, these were not able to compete with the established cinchonidine. Nevertheless, a preliminary validation of their potential is presented. For example, application of the new modifiers in the reduction of KPL on Pt/Al_2O_3 resulted in stereoselectivities of 21% *ee* for the imidazolidinone carrying an anthracene anchor (**41**) and 23% *ee* for the fluorinated L-proline-derived modifier **103**, while the benchmark modifier cinchonidine provides 40% *ee* under the same reaction conditions. Furthermore, it was observed that the fluorinated L-proline-derivatives performed generally better than their hydroxyl-analogues, the most prominent example being 23% difference in the enantiomeric excess using **100** and **103** in the hydrogenation of MBF. It is believed that further optimisation studies will likely enhance the performance of these modifiers to a synthetically useful level. It is important to note that the optimisation of cinchonidine as a chiral modifier took decades to achieve and is still ongoing. Moreover, studies on the observed beneficial effect of fluorine in modifier design may assist in designing improved modifiers.

7 Conclusions and Outlook

In this thesis, the importance of non-covalent interactions for molecular pre-organisation in MacMillan catalyst-derived iminium ions were studied. In this intermediate, two of the three possible staggered conformations around the C–CPh bond are postulated to be stabilised by non-covalent interactions, and predominant population of these two conformers is believed to be crucial for high levels of enantioinduction. It is proposed that conformer **I** is stabilised by a partially cationic CH-π interaction with the *syn*-methyl group, and conformer **II** by a π-π interaction with the iminium chain (Figure 100, centre).[8a;47;49]

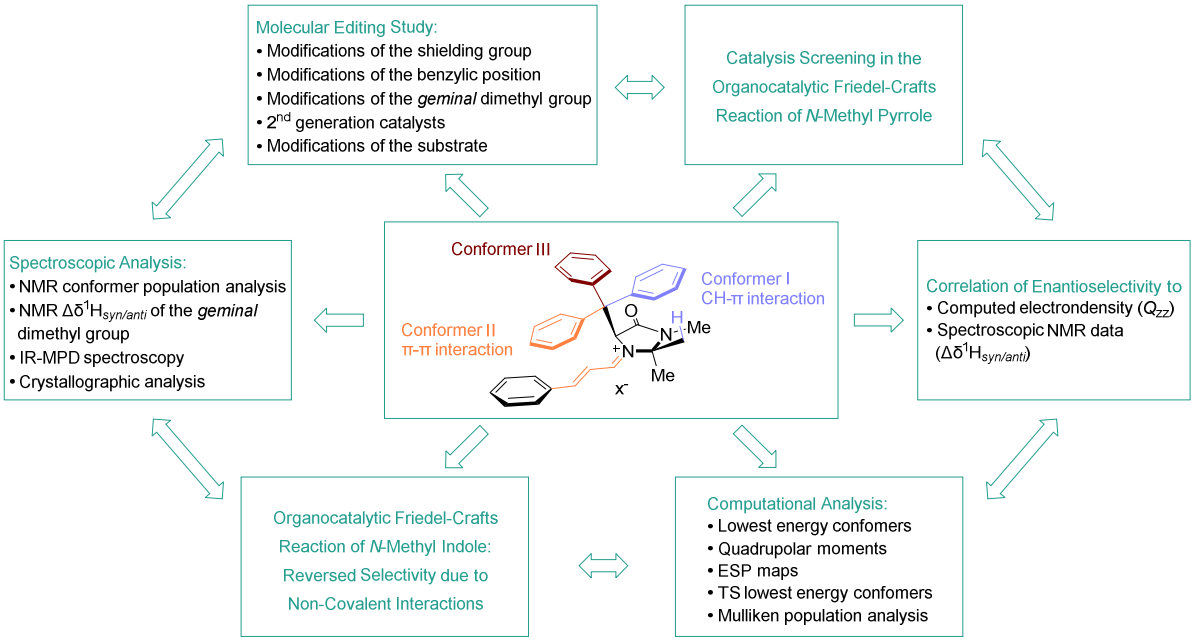

Figure 100 *Overview of the studies on non-covalent interactions in the MacMillan catalyst-derived reactive intermediate.*

A large library of imidazolidinones was prepared in an elaborate molecular editing study. Iminium salts of many of these catalysts were obtained by condensation with (*E*)-cinnamaldehyde, and studied by solution phase NMR. A conformer population analysis of a selection of iminium salts with electronically modified aryl shielding moieties (R) demonstrated that those with shielding group electron-densities similar to those of the parent phenyl structure predominantly populate conformer **I**. Increasing the electron-density of the shielding group by introduction of electron-donating substituents led to an increased

population of conformer **II**, while electron-deficient analogues preferentially populate conformer **III**, presumably due to destabilisation of the non-covalent interactions. The electron-densities were represented by the computed traceless quadrupole moment tensor component perpendicular to the aromatic ring (Q_{zz}). Gratifyingly, it was possible to obtain X-ray structures of one electron-rich (R = indole, $Q_{zz} = -5.10$, conformer **II**), one electron-deficient (R = C_6F_5, $Q_{zz} = +2.33$, conformer **III**), and one electronically intermediate iminium ion (R = C_6H_4OH, $Q_{zz} = -3.78$, conformer **I**) verifying the conformational diversity proposed by NMR studies. Moreover, it was observed that for the *geminal*-dimethyl moiety, the shift-differences of the *syn*- and the *anti*-methyl groups ($\Delta\delta^1H_{syn/anti}$) in the iminium salts vary greatly. This is likely directly related to the population of conformer **I**. Whilst a high population of conformer **I** was believed to lead to large $\Delta\delta^1H_{syn/anti}$ due to strong shielding of the *syn*-methyl group, the opposite effect was attributed to decreased population of conformer **I**. A computational lowest energy conformer analysis supported this supposition. In the molecular editing study it was also observed that the non-covalent interactions controlling the conformational behaviour of the iminium salts are not only sensitive towards electronic modifications of the aryl shielding group, but also to steric modifications and modifications in the benzylic position. The catalyst library was tested in the organocatalytic Friedel-Crafts reaction of *N*-methyl pyrrole and (*E*)-cinnamaldehyde. The electron-rich trimethoxyphenyl imidazolidinone was identified as an improved catalyst as compared to the parent MacMillan catalyst (94% as compared to 85% *ee* at RT after 3 h). Furthermore, a direct linear relationship between the enantioselectivities obtained and the Q_{zz} of the shielding group of a given imidazolidinone was observed for most of the catalysts. Because comparison of the Q_{zz} value was not always convenient for all imidazolidinones, and additionally because this analysis requires computation, the $\Delta\delta^1H_{syn/anti}$ was found to be a more amenanable quantity for all imidazolidinones. Fortunately, a clear correlation between the enantioselectivity obtained and the $\Delta\delta^1H_{syn/anti}$ was identified, providing a useful tool for future catalyst design. Due to the exothermicity of this reaction, it was assumed that the transition state resembles the iminium ion intermediate, thus observed enantioselectivity was rationalised based on the conformational behaviour of the iminium ion. To validate this working hypothesis, a computational lowest energy conformation analysis of the transition state was performed. Consistent with the results for the iminium ion, conformer **I** was identified as the global minimum structure. Subsequent application of the catalyst library in the organocatalytic Friedel-Crafts reaction of *N*-methyl indole and (*E*)-cinnamaldehyde replicated the trends observed for the reaction using *N*-methyl pyrrole. Interestingly, using

N-methyl indole, a reversal of selectivity was observed for catalysts predominantly populating conformer **III**. A pincer type model directing the indole nucleophile by the action of two CH-π interactions was proposed. Consequently, an explanation is offered for the observation that in the Friedel-Crafts reaction of indoles the 2nd generation MacMillan catalysts was found to be privileged, while when using pyrroles, the 1st and 2nd generation catalysts gave virtually the same enantioselectivities. Furthermore, it was suggested that the discussed CH-π and π-π interactions have a considerable cationic character due to delocalisation of the positive charge into not only the iminium chain, but also in the *geminal*-dimethyl group. Indeed, a Mulliken population analysis of the iminium ion derived from the 1st generation MacMillan catalyst showed that only 14.4% of the positive charge is localised on the nitrogen and that the rest of the charge is not only delocalised into the aromatic system but also into the *geminal*-dimethyl group. In an additional theoretical study, the molecule was partitioned into the two interacting fragments and the stabilisation energy resulting from bringing the two fragments into CH-π contact was found to be –7.2 kcal/mol. Comparison of this result to the interaction energy of NMe_4^+ and benzene (–9 kcal/mol)[104a] and of CH_4 and benzene (–1.45 kcal/mol)[98] supports the notion of a considerable cationic character of the CH-π interaction. A selection of iminium ions were studied by gas phase IR-MPD spectroscopy using the free electron laser FELIX at Radboud University in Nijmegen. It was proposed that conformational preferences in the gas phase could be detected by delicate characteristic shifts of fingerprint IR bands. A preliminary validation of this method is presented. Moreover, the efficiency of the studied imidazolidinones as chiral modifiers for asymmetric heterogeneous catalysis was examined and first promising results were obtained.

8 Experimental Section

8.1 Materials and Methods

All chemicals were purchased as reagent grade and used without further purification. Solvents for purification (extraction and chromatography) were purchased as technical grade and distilled on the rotary evaporator prior to use. All reactions using air or moisture sensitive compounds were carried out in flame-dried and evacuated glassware under an atmosphere of argon. Solvents for these reactions were dried according to standard procedures or were taken from the solvent drying system. For column chromatography SiO_2–60 (230–400 mesh ASTM; *Fluka*) was used as stationary phase. Analytical thin layer chromatography (TLC) was performed on glass plates pre-coated with SiO_2–60 F_{254} (*Merck*) and visualized with a UV-lamp (254 nm) or by dipping in cerium ammonium molybdate (CAM) stain, $KMnO_4$ stain, or ninhydrine stain, followed by heating. Flash column chromatography was carried out on *Fluka* silica gel 60 (230-400 mesh). Concentration *in vacuo* was performed at ~10 mbar and 40 °C, drying at ~10^{-2} mbar and RT. NMR spectra were measured at ETH Zurich on a *Varian AVANCE 300 MHz*, a *Bruker ARX 300 MHz*, a *Bruker DRX 400 MHz* or a *Bruker AV 400 MHz* spectrometer at ambient temperature or by the Laboratory for Organic Chemistry (ETH) NMR service on a *Bruker AV 600 MHz*, *DRX 600 MHz or DRX 500 MHz* spectrometer at ambient temperature. Or NMR spectra were measured by the NMR service of the Organisch-Chemisches Institut, Westfälische Wilhelms-Universität Münster on a *Bruker AV300* or an *Agilent DD2 600* spectrometer at ambient temperature. ^{1}H NMR spectra are reported as follows: chemical shift δ in ppm (multiplicity, number of protons, coupling constant *J* in Hz, assignment of proton). The deuterated solvent residual peak was used as internal reference: C*H*Cl_3 (δ_H 7.260), CD_2*H*OD (δ_H 3.310), C_2D_5*H*OS (δ_H 2.500) and CD_2*H*CN (δ_H 1.940). ^{13}C NMR spectra are reported as follows: chemical shift δ in ppm (multiplicity if different from s due to heteronuclear couplings to fluorine, number of carbons if different from 1, coupling constant $^xJ_{CF}$ in Hz, assignment of carbon). The solvent peak was used as internal reference: *C*DCl_3 (δ_C 77.16), *C*D_3OD (δ_C 49.000), *C*$_2D_6OS$ (δ_H 2.500) and *C*D_3CN (δ_C 1.32). ^{19}F NMR spectra are reported as follows: chemical shift δ in ppm (multiplicity, number of fluorines, coupling constant $^xJ_{YF}$ in Hz, assignment of fluorine). The resonance multiplicity is abbreviated as: s (singlet), d (doublet), t (triplet), q (quadruplet), m (multiplet) and b (broad). Assignments of

unknown compounds are based on DEPT, COSY (HH and FF), HMBC, HSQC, HOESY and/or NOESY spectra if required for assignment. Melting points were measured on a *Büchi B-545* melting-point apparatus in open capillaries and are uncorrected. IR spectra were recorded on a *Perkin-Elmer 100 FT-IR* spectrometer, selected adsorption bands are reported in wavenumbers (cm^{-1}) and intensities are reported as: w (weak), m (medium), s (strong) and b (broad). Optical rotations were measured on a *JASCO P-2000* polarimeter or a *Perkin-Elmer 341* polarimeter with 1 dm cell length and $\lambda = 589$ nm (Na D-line), concentrations are given as mg mL^{-1}. HPLC spectra were recorded on an *Agilent 1100* series (DAD, *Agilent technologies 1200* series) using a *Chiralcel* OJ-H (5 µm, 250·4.6 mm) or a *Reprosil* Chiral-OM (5 µm, 250·4.6 mm) column and *n*-hexane/*iso*-propanol as eluent. GC spectra were recorded on an *Agilent 7890A* chromatograph equipped with a flame ionization detector (FID) operated at 300 °C using hydrogen as fuel gas (30 mL/min) and air as oxidant (400 mL/min). Nitrogen was used as a make-up gas (25 mL/min) and helium as a carrier gas (1.623 mL/min), the injections with a split ratio of 20:1 were performed at 250 °C . Separation was achieved using a *CP-Chirasil-Dex CB* (0.25 µm, 25 m·0.25 mm) chiral capillary column. High-resolution mass spectra (HR ESI and EI MS) were measured by the MS service of the Laboratory for Organic Chemistry, ETH Zurich and by the MS service of the Organisch-Chemisches Institut, Westfälische Wilhelms-Universität Münster. Elemental analyses were performed at the Laboratory for Organic Chemistry, ETH Zurich on a *LECO CHN/900* instrument.

8.2 Synthetic Procedures

8.2.1 Synthesis of 1-Boc-2-(*tert*-butyl)-3-methyl-4-imidazolidinone (racemic and chiral)

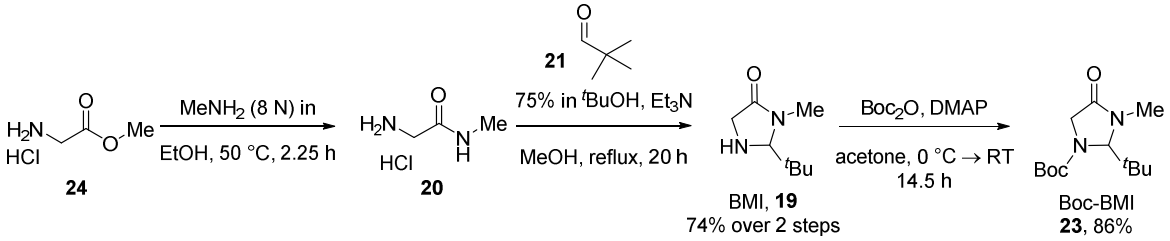

2-(*tert*-Butyl)-3-methyl-4-imidazolidinone (BMI) (19)[177]

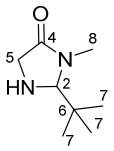

To glycine methyl ester hydrochloride (12.5 g, 99.6 mmol, 1.0 equiv.) was added $MeNH_2$ (8 N in EtOH, 50.0 mL, 398 mmol, 4.0 equiv.) at RT and the resulting solution was heated to 50 °C until complete conversion was observed on TLC after 2.25 h. The reaction was allowed to come to RT and evaporated *in vacuo* to give glycine methyl amide hydrochloride as a white solid. The product was dissolved in MeOH (150 mL) and pivalaldehyde (75% in ^{t}BuOH, 31.4 mL, 199 mmol, 2.0 equiv.) and Et_3N (11.1 mL, 79.7 mmol, 0.8 equiv.) were added at RT. The resulting solution was heated to reflux for 20 h. The mixture was concentrated *in vacuo*, CH_2Cl_2 was added to the residue and the insoluble white solid ($Et_3N{\cdot}HCl$) filtered off. The filtrate was concentrated *in vacuo* and purified by CC (SiO_2; CH_2Cl_2/MeOH/NH_3 (25% in H_2O) 20:1:0.1) to give imidazolidinone **19** as a yellow oil (11.4 g, 74%).

R_f = 0.74 (SiO_2; CH_2Cl_2/MeOH 10:1); ^{1}H NMR (400 MHz, $CDCl_3$): δ = 4.04 (d, 1H, J = 1.2, H–C2), 3.41 (d, J = 16.0, 1H, H–C5), 3.34 (d, J = 16.0, 1H, H–C5), 2.86 (s, 3H, H–C8), 2.32 (b, 1H, H–N), and 0.88 (s, 9H, H–C7) ppm; ^{13}C NMR (100 MHz, $CDCl_3$): δ = 174.7 (C4), 85.0 (C2), 49.1 (C5), 37.5 (C6), 31.1 (C8), and 25.5 (3C, C7) ppm; IR (ATR): $\tilde{\nu}$ = 3295m, 2962m, 2908w, 2868w, 1666s, 1485m, 1433m, 1405s, 1389m, 1363w, 1353w, 1319s,

1260m, 1210m, 1123w, 1105s, 1028m, 1003w, 957w, 886s, 825s, 747m, 681s, and 654w cm^{-1}; HR-ESI-MS: *m/z*: 157.1333 ([*M*+H]$^+$, calcd for $C_8H_{17}N_2O^+$: 157.1335); analytical data in agreement with the literature.[142;177]

1-Boc-2-(*tert*-butyl)-3-methyl-4-imidazolidinone (Boc-BMI, racemic) (23)

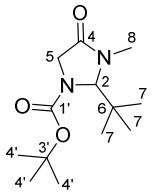

Boc-BMI
23

To a solution of imidazolidinone **19** (2.75 g, 17.6 mmol, 1.00 equiv.) in acetone (35.0 mL) were added Boc_2O (5.32 g, 24.3 mmol, 1.38 equiv.) and DMAP (0.24 g, 1.9 mmol, 0.11 equiv.) under Ar at 0 °C. The solution was allowed to come to RT and stirred for 14.5 h during which time it turned from yellow to an intense orange color. Et_3N (2.5 mL, 17.6 mmol, 1.0 equiv.) and, after another 7 h, H_2O (1.5 mL) were added. After stirring for an additional 1.0 h, the organic solvent was evaporated *in vacuo*. Et_2O (20 mL) and an aqueous solution of HCl (1 N, 20 mL) were added to the residue, the layers were separated and the organic layer was washed with an aqueous solution of HCl (1 N, 20 mL) and with a saturated aqueous solution of $NaHCO_3$ (20 mL). The organic layer was dried over $MgSO_4$ and concentrated *in vacuo*. The resulting oil was purified by CC (SiO_2; CH_2Cl_2/MeOH/NH_3 (25% in H_2O) 20:1:0.1) to give Boc-BMI (**23**) as an off-white solid (3.88 g, 86%).

R_f = 0.67 (SiO_2; CH_2Cl_2/MeOH 10:1); M.p. = 71.3–72.2 °C; ^{1}H NMR (400 MHz, $CDCl_3$): δ = 4.89 (bs, 1H, H–C2), 4.05 (bs, 1H, H–C5), 3.66 (bd, 1H, *J* = 16.0, H–C5), 2.93 (s, 3H, H–C8), 1.40 (s, 9H, H–C4'), and 0.91 (s, 9H, H–C7) ppm; ^{13}C NMR (100 MHz, $CDCl_3$): δ = 170.5 (C4), 154.6 (b, C1'), 82.3 (b, C2), 81.1 (b, C3'), 50.0 (b, C5), 39.5 (C6), 31.5 (C8), 28.2 (3C, C4'), and 25.9 (3C, C7) ppm; IR (ATR): $\tilde{\nu}$ = 3373w, 3344w, 3291w, 2940w, 2915w, 2877w, 1644s, 1524s, 1495m, 1455m, 1439w, 1399m, 1343w, 1322w, 1267w, 1230w, 1153m, 1109m, 1031w, 979w, 927m, 914m, 877m, 858m, 745s, 699s, and 661w cm^{-1}; HR-ESI-MS: *m/z*: 279.1678 ([*M*+Na]$^+$, calcd for $C_{13}H_{24}N_2O_3Na^+$: 279.1685); analytical data in agreement with the literature.[122b]

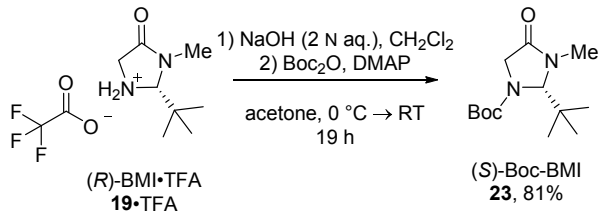

(*R*)-BMI•TFA
19•TFA

(*S*)-Boc-BMI
23, 81%

(2*S*)-1-Boc-2-(*tert*-butyl)-3-methyl-4-imidazolidinone (*S*-Boc-BMI) (23, chiral)[122b]

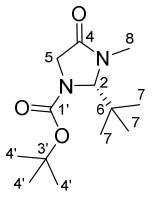

(*S*)-Boc-BMI
23

To a solution of (*R*)-BMI trifluoroacetic acid (2.00 g, 7.40 mmol, 1.00 equiv.) in CH_2Cl_2 (5.00 mL) was added aqueous NaOH (2 N, approx. 7 mL) to adjust the pH to approx. 8. The layers were separated and the aqueous phase extracted three times with CH_2Cl_2. The combined organic layers were dried over $MgSO_4$ and concentrated *in vacuo*. The residue was dissolved in acetone (14.0 mL) and Boc_2O (2.21 mL, 9.62 mmol, 1.3 equiv.) and DMAP (90.4 mg, 0.74 mmol, 0.1 equiv.) were added under Ar at 0 °C. The solution was allowed to come to RT and stirred for 19 h. Et_3N (1.0 mL, 7.4 mmol, 1.0 equiv.) and after another 2 h H_2O (0.7 mL) were added. After stirring for an additional 2 h, the organic solvent was evaporated *in vacuo*. Et_2O (10 mL) and an aqueous solution of HCl (1 N, 10 mL) were added to the residue, the layers were separated and the organic layer was washed with an aqueous solution of HCl (1 N, 10 mL) and with a saturated aqueous solution of $NaHCO_3$ (10 mL). The organic layer was dried over $MgSO_4$ and concentrated *in vacuo* give (*S*)-Boc-BMI (**23**) as a white solid (1.53 g, 81%).

$R_f = 0.69$ (SiO_2; CH_2Cl_2/MeOH 10:1); M.p. = 65.0–65.7 °C; $[\alpha]_D^{20}$: –11.6 (c = 1.05, CH_2Cl_2); ^{1}H NMR (400 MHz, $CDCl_3$): δ = 4.88 (bd, 1H, J = 55.0, H–C2), 4.08 (bd, 1H, J = 14.1, H–C5), 3.73 (bd, 1H, J = 16.0, H–C5), 2.98 (s, 3H, H–C8), 1.46 (s, 9H, H–C4'), and 0.96 (s, 9H, H–C7) ppm; ^{13}C NMR (100 MHz, $CDCl_3$): δ = 170.6 (C4), 154.7 (b, C1'), 82.3 (b, C2), 81.0 (b, C3'), 59.5 (b, C5), 39.5 (C6), 31.5 (C8), 28.2 (3C, C4'), and 25.9 (3C, C7) ppm; IR (ATR): $\tilde{\nu}$ = 2968w, 2951w, 1694s, 1480w, 1450w, 1434w, 1400m, 1362s, 1301s, 1288m, 1252s, 1162s, 1118m, 1104s, 1035w, 1007w, 939m, 928m, 877m, 868m, 776m, 762w, 728w, and 664w cm^{-1}; HR-ESI-MS: *m/z*: 257.1861 ([*M*+H]$^+$, calcd for $C_{13}H_{25}N_2O_3^+$: 257.1860); analytical data in agreement with the literature.[122b]

8.2.2 Syntheses of (5*S*)-5-Benzyl-2,2,3-trimethyl-4-imidazolidinone (1) and (5*S*)-5-Benzyl-2,2,3-trimethyl-4-oxo-1-[(*E*)-3-phenylallylidene]-imidazolidin-1-ium salt (1a)

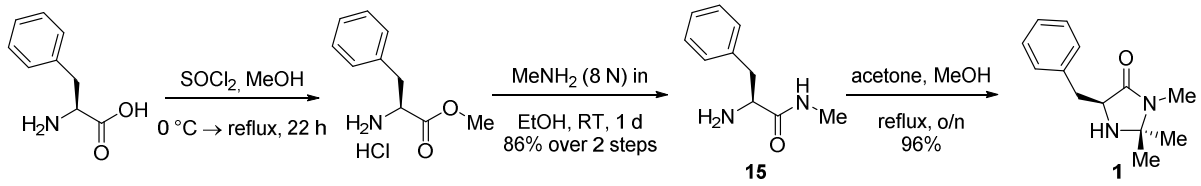

_L_-Phenylalanine methyl amide (15)[178]

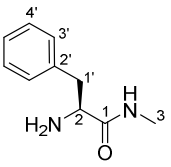

To a suspension of *L*-phenylalanine (6.98 g, 42.3 mmol, 1.0 equiv.) in MeOH (17.1 mL, 423 mmol, 10 equiv.) was added thionyl chloride (3.70 mL, 50.7 mmol, 1.2 equiv.) over 15 min at 0 °C and the resulting solution was allowed to come to RT before it was heated to reflux for 22 h. The solution was allowed to come to RT and evaporated *in vacuo* to give the *L*-phenylalanine methyl ester hydrochloride as a white solid. To the ester was added $MeNH_2$ (8 N in EtOH, 21.0 mL, 169 mmol, 4.0 equiv.) at RT and the solution stirred for 23 h. The reaction was concentrated *in vacuo* and a saturated aqueous solution of $NaHCO_3$ (45 mL) was added. The aqueous layer was extracted with CH_2Cl_2 (3 x 55 mL). The combined organic layers were dried over $MgSO_4$, filtrated and concentrated *in vacuo* to give amide **15** as a yellowish solid (6.44 g, 86%).

R_f = 0.37 (CH_2Cl_2/MeOH 10:1); M.p. = 58.5–59.6 °C; $[\alpha]_D^{20}$: –66.1 (*c* = 1.07, CH_2Cl_2); ^{1}H NMR (300 MHz, $CDCl_3$): δ = 7.32 (2H, t, *J* = 7.2, H–C4'), 7.28–7.19 (4H, m, H–C3', H–C5', H–N^{amide}), 3.61 (1H, dd, *J* = 9.4, 3.9, H–C2), 3.29 (1H, dd, *J* = 13.7, 3.9, H–C1'), 2.82 (3H, d, *J* = 5.0, H–C3), 2.68 (1H, dd, *J* = 13.7, 9.4, H–C1'), and 1.38 (2H, b, H–N^{amine}) ppm; ^{13}C NMR (75 MHz, $CDCl_3$): δ = 174.9 (C1), 138.2 (C2'), 129.4 (2C, C3'), 128.8 (2C, C4'), 126.9 (C5'), 56.6 (C2), 41.2 (C1'), and 26.0 (C3) ppm; IR (ATR): $\tilde{\nu}$ = 3343w, 3291w, 3033w, 2940w, 2915w, 2877w, 1644s, 1524s, 1455m, 1439m, 1399m, 1342w, 1322w, 1268w, 1229w, 1152w, 1109m, 978w, 927w, 913w, 877m, 858m, 834w, 745s, and

699s cm^{-1}, HR-ESI-MS: *m/z*: 179.1186 ([*M*+H]$^+$, calcd for $C_{10}H_{15}N_2O^+$: 179.1179); analytical data in agreement with the literature.[178]

(5*S*)-5-Benzyl-2,2,3-trimethyl-4-imidazolidinone (1)[179]

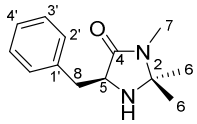

1

To a solution of amide **15** (1.00 g, 5.6 mmol, 1 equiv.) in MeOH (12.0 mL) was added acetone (2.1 mL, 28.1 mmol, 5.0 equiv.) and NEt_3 (0.6 mL, 4.5 mmol, 0.8 equiv.) at RT under an atmosphere of argon and the yellow solution was heated to reflux overnight. The reaction was allowed to come to RT and concentrated *in vacuo* to give **1** as a yellow oil (1.22 g, quant.).

R_f = 0.79 (CH_2Cl_2/MeOH 10:1); $[\alpha]_D^{20}$: –33.2 (*c* = 0.94, CH_3OH); ^{1}H NMR (400 MHz, $CDCl_3$): δ = 7.36–7.18 (5H, m, H–C2', H–C3', and H–C4'), 3.80 (1H, dd, *J* = 6.8, 4.5, H–C5), 3.15 (1H, dd, *J* = 14.2, 4.5, H–C8), 3.01 (1H, dd, *J* = 14.2, 6.8, H–C8), 2.76 (3H, s, H–C7), 1.70 (1H, b, H–N^{amine}), 1.27 (3H, s, H–C6), and 1.16 (3H, s, H–C6) ppm; ^{13}C NMR (101 MHz, $CDCl_3$): δ = 173.5 (C4), 137.3 (C1'), 129.7 (2C, C2'), 128.7 (2C, C3'), 126.9 (C4'), 75.7 (C2), 59.4 (C5), 37.4 (C8), 27.4 (C6), 25.5 (C6), and 25.4 (C7) ppm; IR (ATR): $\tilde{\nu}$ = 3317b, 2979w, 2931w, 1745w, 1680s, 1602w, 1496w, 1424s, 1398s, 1367m, 1269m, 1148m, 1089w, 1030w, 922w, 904w, 748s, 701s, and 673w cm^{-1}; HR-ESI-MS: *m/z*: 219.1492 ([*M*+H]$^+$, calcd for $C_{13}H_{19}N_2O^+$: 219.1492); analytical data in agreement with the literature.[179]

(5*S*)-5-Benzyl-2,2,3-trimethyl-4-imidazolidinone hydrochloride (1·HCl)

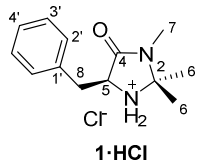

Imidazolidinone **1** (7.0 mg, 32 µmol, 1.0 equiv.) was dissolved in HCl in MeOH (1.25 N, 0.1 mL, 125 µmol, 3.9 equiv.) and stirred for 30 min at RT. The solution was concentrated *in vacuo* to give **1·HCl** as a white solid (8.2 mg, quant.).

^{1}H NMR (400 MHz, CD_3OD): δ = 7.47–7.29 (5H, m, H–C2', H–C3', and H–C4'), 4.66 (1H, dd, *J* = 10.7, 3.4, H–C5), 3.54 (1H, dd, *J* = 15.2, 3.4, H–C8), 3.07 (1H, dd, *J* = 15.2, 10.7, H–C8), 2.92 (3H, s, H–C7), 1.75 (3H, s, H–C6), and 1.60 (3H, s, H–C6) ppm; ^{13}C NMR (101 MHz, CD_3OD): δ = 167.7 (C4), 136.5 (C1'), 130.22 and 130.19 (2·2C, C2' and C3'), 128.8 (C4'), 79.0 (C2), 59.7 (C5), 35.0 (C8), 25.7 (C6), 24.3 (C6), and 22.1 (C7) ppm; analytical data in agreement with the literature.[3]

(5*S*)-5-Benzyl-2,2,3-trimethyl-4-oxo-1-[(*E*)-3-phenylallylidene]-imidazolidin-1-ium perchlorate (1a·ClO_4^-):

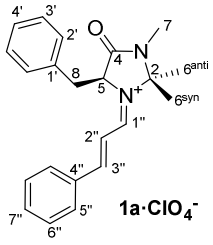

To imidazolidinone **1** (34.9 mg, 0.16 mmol, 1 equiv.) in Et_2O (0.20 mL) was added perchloric acid (60% in H_2O, 26.80 mg, 0.16 mmol, 1 equiv.) in EtOH/Et_2O (1:1, 0.40 mL) at RT and the resulting mixture stirred for 15 min before it was evaporated *in vacuo* to give the imidazolidinone salt. The salt was redissolved in MeOH (0.40 mL) and heated to 35 °C. (*E*)-cinnamaldehyde (40.2 µL, 0.32 mmol, 2 equiv.) was added and the yellow solution stirred for 1 h. The solvent was removed *in vacuo* and the residue dissolved in a minimum amount of MeOH. From this solution the iminium salt was crashed out with Et_2O and the supernatant solution taken off. The washing procedure was repeated and the iminium salt isolated as a yellow solid (31.9 mg, 46%).

M.p. = 189.9–191.9 °C; $[\alpha]_D^{20.5}$: +2.5 (c = 0.45, CH_3CN); ^{1}H NMR (300 MHz, CD_3CN): δ_H = 8.73 (1H, dd, J = 10.7, 1.9, H–C1''), 8.18 (1H, d, J = 15.0, H–C3''), 7.93 (2H, d, J = 7.3, H–C5''), 7.77–7.68 (1H, m, H–C7''), 7.62 (2H, t, J = 7.6, H–C6''), 7.38–7.20 (4H, m, H–C3', H–C4', H–C2''), 7.09 (2H, dd, J = 7.9, 1.7, H–C2'), 5.20 (1H, s, H–C5), 3.57 (1H, dd, J = 14.7, 5.7, H–C8), 3.47 (1H, dd, J = 14.7, 3.7, H–C8), 2.78 (3H, s, H–C7), 1.70 (3H, s, H–C6anti), and 0.79 (3H, s, H–C6syn) ppm; ^{13}C NMR (151 MHz, CD_3CN): δ_C = 168.2 (C1''), 166.7 (C3''), 165.2 (C4), 136.1 (C7''), 134.8 (C1'), 134.4 (C4''), 132.5 (2C, C5''), 131.1 (2C, C2'), 130.7 (2C, C6''), 130.1 (2C, C3'), 129.2 (C4'), 118.4 (C2''), 86.5 (C2), 65.2 (C5), 37.2 (C8), 27.5 (C6anti), 26.1 (C7), and 24.8 (C6syn) ppm; IR (ATR): $\tilde{\nu}$ = 2938b, 1712s, 1620s, 1601s, 1587s, 1455m, 1438m, 1420m, 1043m, 1335w, 1311w, 1281m, 1235w, 1197m, 1179m, 1151w, 1115m, 1081m, 1051w, 1012m, 999m, 955w, 933w, 872w, 756m, 750m, 705m, 684w, 642w, and 622s cm^{-1}; HR-ESI-MS: m/z: 333.19602 ([M-ClO_4^-]$^+$, calcd for $C_{22}H_{25}N_2O^+$: 333.19614); analytical data in agreement with the literature.[49]

(5*S*)-5-Benzyl-2,2,3-trimethyl-4-oxo-1-[(*E*)-3-phenylallylidene]-imidazolidin-1-ium hexafluoroantimonat (1a·SbF_6^-):

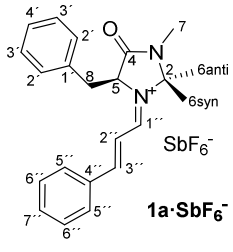

To imidazolidinone **1** (50.0 mg, 0.23 mmol, 1.0 equiv.) in MeOH (1.0 mL) was added fluoroantimonic acid (65% in H_2O, 135.0 mg, 0.25 mmol, 1.1 equiv.) in MeOH (1.0 mL) at RT and the resulting mixture stirred for 15 min before (*E*)-cinnamaldehyde (29.0 µL, 0.23 mmol, 1 equiv.) was added. The yellow solution was stirred overnight. The solvent was removed *in vacuo* and the residue dissolved in a minimum amount of MeOH. From this solution the iminium salt was crashed out with Et_2O and the supernatant solution taken off. This purification procedure was repeated two additional times to give **1a·SbF_6^-** as a red solid.

M.p. = 172.0–173.3 °C; $[\alpha]_D^{20}$ = +506.7 (c = 1.06 in MeOH); ^{1}H NMR (600 MHz, CD_3CN): δ_H = 8.73 (1H, dd, J = 10.7, 1.9, H–C1''), 8.20 (1H, d, J = 15.0, H–C3''), 7.93 (2H, dd, J = 8.4, 1.0, H–C5''), 7.74–7.69 (1H, m, H–C7''), 7.62 (2H, t, J = 7.8, H–C6''), 7.33–7.25

(4H, m, H–C3', H–C4', H–C2''), 7.11–7.07 (2H, m, H–C2'), 5.19 (1H, t, *J* = 5.4, H–C5), 3.57 (1H, dd, *J* = 14.8, 5.8, H–C8), 3.47 (1H, dd, *J* = 14.8, 3.6, H–C8), 2.79 (3H, d, *J* = 0.4, H–C7), 1.70 (3H, s, H–C6^{anti}), and 0.81 (3H, s, H–C6^{syn}) ppm; ^{13}C NMR (151 MHz, CD_3CN): δ_C = 168.2 (C1''), 166.8 (C3''), 165.2 (C4), 136.1 (C7''), 134.8 (C1'), 134.4 (C4''), 132.5 (2C, C5''), 131.2 (2C, C2'), 130.7 (2C, C6''), 130.1 (2C, C3'), 129.2 (C4'), 118.4 (C2''), 86.5 (C2), 65.2 (C5), 37.3 (C8), 27.6 (C6^{anti}), 26.1 (C7), and 24.8 (C6^{syn}) ppm; IR (ATR): $\tilde{\nu}$ = 3064b, 1712s, 1622s, 1603s, 1588s, 1455m, 1437m, 1402m, 1392m, 1309w, 1291m, 1235w, 1198m, 1179m, 1151m, 1118w, 1081w, 1050w, 1013w, 1000w, 935w, 862w, 755m, 703m, 687w, 655m, and 640s cm^{-1}; HR-ESI-MS: m/z: 333.19588 ([M-SbF_6-]$^+$, calcd for $C_{22}H_{25}N_2O^+$: 333.19614).

8.2.3 Syntheses of (5*S*)-2,2,3-Trimethyl-5-(3,4,5-trimethoxybenzyl)imidazolidin-4-one (3) and 5-(3',3',4'-Trimethoxybenzyl)-2,2,3-trimethyl-4-oxo-1-[(*E*)-3-phenylallylidene]-imidazolidin-1-ium salt (3a)

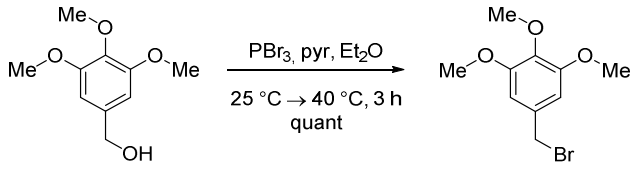

1-Bromomethyl-3,4,5-trimethoxybenzene[180]

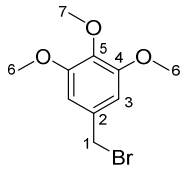

To a solution of 3,4,5-trimethoxybenzyl alcohol (4.00 g, 20.2 mmol, 1.00 equiv.) in Et_2O (1.00 L) were added successively PBr_3 (5.46 g, 20.2 mmol, 1.00 equiv.) and pyridine (79.8 mg, 1.01 mmol, 0.05 equiv.) slowly at RT. The mixture was heated to 40 °C and after completion was detected by TLC (3 h), it was allowed to cool to RT. H_2O was added and the aqueous layer extracted twice with Et_2O. The combined organic layers were dried over $MgSO_4$ and concentrated *in vacuo* to give 1-bromomethyl-3,4,5-trimethoxybenzene as a white solid (5.27 g, quant.), which should be kept in the freezer (turns first orange then brown at RT).

R_f = 0.76 (CH/EtOAc 1:1); M.p. = 72.3–73.4 °C (Lit. 74–75 ºC); ^{1}H NMR (300 MHz, $CDCl_3$): δ = 6.62 (2H, s, H–C3), 4.47 (2H, s, H–C1), 3.88 (6H, d, *J* = 0.7, H-C6), and 3.85 (3H, d, *J* = 0.8 Hz, H-C7) ppm; ^{13}C NMR (101 MHz, $CDCl_3$): δ = 153.5 (2C, C4), 138.3 (C5), 133.3 (C2), 106.3 (2C, C3), 61.0 (C7), 56.3 (2C, C6), and 34.4 (C1) ppm; HR-EI-MS: *m*/*z*: 181.0866 ([*M*-Br$^-$]$^+$, calcd for $C_{10}H_{13}O_3^+$: 181.0859); analytical data in agreement with the literature.[181]

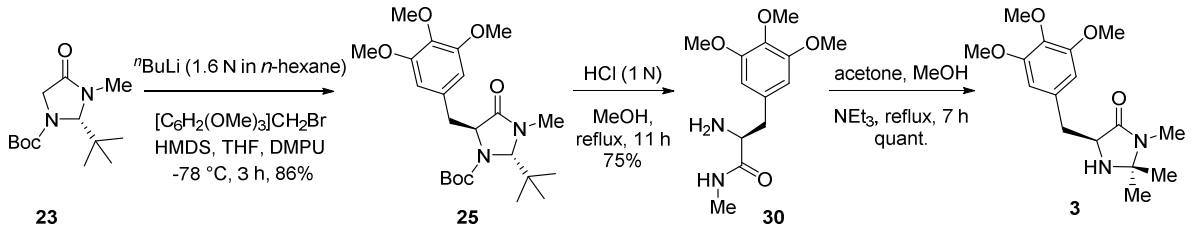

(2*S*,5*S*)-1-Boc-2-(*tert*-butyl)-3-methyl-5-(3,4,5-trimethoxybenzyl)-4-imidazolidinone (25)[122b]

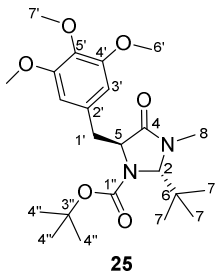

A solution of HMDS (1.28 mL, 6.16 mmol, 1.2 equiv.) in dry THF (4.00 mL) in a flame-dried Schlenck under an atmosphere of argon was cooled to 0 °C. ^{n}BuLi (1.6 N in ^{n}hexane, 3.85 mL, 6.16 mmol, 1.2 equiv.) was added dropwise and the solution stirred for 15 min before it was cooled to –78 °C. DMPU (1.86 mL, 15.4 mmol, 3.0 equiv.) and then (*S*)-Boc-BMI (**23**) (1.30 g, 5.13 mmol, 1.0 equiv.) in THF (4.00 mL) was added dropwise to the orange solution that turned darker upon addition. After 30 min, 1-bromomethyl-3,4,5-trimethoxybenzene (1.34 g, 5.13 mmol, 1.0 equiv.) in THF (4.00 mL) was added slowly and the resulting mixture stirred for 3 h during which time a brown solid formed. The reaction was quenched by addition of a saturated aqueous solution of NH_4Cl and extracted three times with CH_2Cl_2. The combined organic layers were dried over $MgSO_4$ and concentrated *in vacuo*. Purification by CC (SiO_2; CH/EtOAc 3:1) gave **25** as a white solid (1.93 g, 86%).

R_f = 0.40 (CH/EtOAc 1:1); M.p. = 69.6–71.2 °C; $[\alpha]_D^{23}$: +34.4 (*c* = 0.83, CH_3OH); ^{1}H NMR (300 MHz, $CDCl_3$): δ = 6.38 (2H, s, H–C3'), 4.65 (1H, d, *J* = 1.5, H–C2), 4.28 (1H, dd, *J* = 4.4, 2.2, H–C5), 3.80 (6H, s, H–C6'), 3.79 (3H, s, H–C7'), 3.65 (1H, bs, H–C1'), 3.13 (1H, bd, *J* = 12.8, H–C1'), 2.80 (s, 3H, H–C8), 1.47 (s, 9H, H–C4'), and 0.93 (s, 9H, H–C7) ppm; ^{13}C NMR (100 MHz, $CDCl_3$, racemic compound, C4 and C1" not visible): δ = 152.8 (C4'), 136.9 (C2'), 131.7 (b, C5'), 107.4 (2C, C3'), 81.1 (C2), 77.4 (C3"), 61.0 (C7'), 60.9 (C5), 56.4 (2C, C6'), 41.1 (C6), 32.0 (C1'), 28.4 (3C, C4"), 26.8 (3C, C7), and 25.9 (C8) ppm; IR (ATR): $\tilde{\nu}$ = 2966w, 2931w, 2840w, 1693s, 1588w, 1509w, 1456w, 1433w,

1407w, 1380m, 1363m, 1339w, 1325w, 1302w, 1254m, 1239m, 1165m, 1126s, 1112s, 1050w, 1019m, 966w, 956w, 930w, 889w, 859w, 835w, 787w, 764m, 713w, and 668w cm^{-1}; HR-ESI-MS: *m*/*z*: 459.2464 ([*M*+Na]$^+$, calcd for $C_{23}H_{36}N_2O_6Na^+$: 459.2466).

L-3,4,5-Trimethoxyphenylalanine *N*-methyl amide (30)[182]

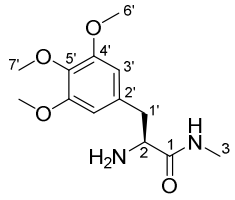

30

To a solution of **25** (1.75 g, 4.01 mmol, 1.0 equiv.) in MeOH (45.0 mL) was added an aqueous solution of HCl (1 N, 45.0 mL) at RT and the mixture heated to reflux for 11 h. The reaction was allowed to come to RT and basified to a pH of 10 with an aqueous solution of NaOH (2 N) and extracted three times with CH_2Cl_2. The combined organic layers were dried over $MgSO_4$ and concentrated *in vacuo* to give amide **30** as an off-white solid (812 mg, 75%).

R_f = 0.26 (CH_2Cl_2/MeOH 10:1); M.p. = 127.8–128.6 °C; $[\alpha]_D^{20}$: +16.6 (*c* = 0.98, CH_3OH); ^{1}H NMR (300 MHz, $CDCl_3$): δ = 7.30 (1H, b, H–N^{amide}), 6.43 (2H, s, H–C3'), 3.83 (6H, s, H–C6'), 3.81 (3H, s, H–C7'), 3.59 (1H, dd, *J* = 9.4, 3.9, H–C2), 3.19 (1H, dd, *J* = 13.6, 3.9, H–C1'), 2.82 (3H, d, *J* = 5.0, H–C3), 2.61 (1H, dd, *J* = 13.6, 9.4, H–C1'), and 1.48 (2H, bs, H–N^{amine}) ppm; ^{13}C NMR (101 MHz, $CDCl_3$): δ = 174.8 (C1), 153.3 (2C, C4´), 136.7 (C2'), 133.6 (C5'), 106.0 (2C, C3'), 60.8 (C7'), 56.6 (C2), 56.1 (2C, C6'), 41.4 (C1'), and 25.9 (C3) ppm; IR (ATR): $\tilde{\nu}$ = 3390w, 3311w, 2998w, 2945w, 2841w, 1648m, 1589m, 1507m, 1454m, 1420w, 1402w, 1328m, 1232s, 1185w, 1149w, 1123s, 1040w, 1002m, 972w, 920w, 857w, 812s, 783w, 760m, 739m, and 686w cm^{-1}; HR-ESI-MS: *m*/*z*: 269.1497 ([*M*+H]$^+$, calculated for $C_{13}H_{21}N_2O_4^+$: 269.1496).

(5*S*)-2,2,3-Trimethyl-5-(3,4,5-trimethoxybenzyl)imidazolidin-4-one (3)

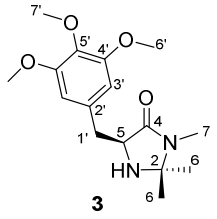

3

To a solution of amide **30** (300 mg, 1.12 mmol, 1.0 equiv.) in MeOH (5.0 mL) were added aceton (0.62 mL, 8.40 mmol, 7.5 equiv.) and NEt_3 (0.12 mL, 0.90 mmol, 0.8 equiv.) at RT under an atmosphere argon and the solution heated to reflux for 7 h. The reaction was allowed to come to RT and concentrated *in vacuo* to give imidazolidinone **3** as an off-white solid (345 mg, quant.).

R_f = 0.73 (CH_2Cl_2/MeOH 10:1); M.p. = 116.8–118.2 °C; $[\alpha]_D^{20}$: –37.2 (*c* = 0.94, CH_3OH); ^{1}H NMR (300 MHz, $CDCl_3$): δ = 6.44 (2H, s, H–C3'), 3.81 (6H, s, H–C6'), 3.80 (3H, s, H–C7'), 3.75 (1H, t, *J* = 5.3, H–C5), 3.02 (2H, d, *J* = 5.3, H–C1'), 2.74 (3H, s, H–C7), 1.26 (3H, s, H–C6), and 1.16 (3H, s, H–C6) ppm; ^{13}C NMR (75 MHz, $CDCl_3$): δ = 173.5 (C4), 153.3 (2C, C4'), 136.9 (C2'), 132.8 (C5'), 106.5 (2C, C3'), 75.7 (C2), 61.0 (C7'), 59.4 (C5), 56.2 (2C, C6'), 37.4 (C1'), 27.3 (C6), 25.4 (C6), and 25.4 (C7) ppm; IR (ATR): $\tilde{\nu}$ = 3291w, 2920w, 2686w, 2565w, 2432w, 1702s, 1673w, 1590m, 1508w, 1459m, 1424s, 1396s, 1385m, 1328m, 1315w, 1234m, 1154w, 1113s, 1064w, 1000m, 967w, 875w, 831w, 789w, and 771w cm^{-1}; HR-ESI-MS: *m*/*z*: 309.1814 ([*M*+H]$^+$, calcd for $C_{16}H_{25}N_2O_4^+$: 309.1809); elemental analysis calcd (%, racemic compound) for $C_{16}H_{24}N_2O_4$ (308.2): C 62.32, H 7.84, N 9.08, O 20.75; found: C 62.02, H 7.68, N 8.96, O 20.82.

2,2,3-Trimethyl-5-(3,4,5-trimethoxybenzyl)imidazolidin-4-one hydrochloride (3·HCl)

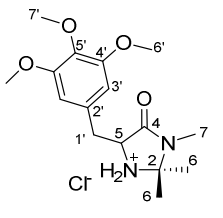

3·HCl

Imidazolidinone **3** (30.0 mg, 97 µmol, 1.0 equiv.) was dissolved in HCl in MeOH (1.25 N, 0.31 mL, 388 µmol, 4.0 equiv.) and stirred for 30 min at RT. The solution was concentrated *in vacuo* to give the hydrochloride salt **3·HCl** as a white powder (33 mg, quant.).

Crystals suitable for X-ray crystallographic analysis were achieved by vapour exchange of a methanolic solution of **3·HCl** with Et_2O.

M.p. = 85.2–86.0 °C; ^{1}H NMR (600 MHz, CD_3OD): δ = 6.77 (2H, s, H–C3'), 4.69 (1H, dd, *J* = 11.0, 3.0, H–C5), 3.87 (6H, s, H–C6'), 3.74 (3H, s, H–C7'), 3.50 (1H, dd, *J* = 15.1, 3.0, H–C1'), 2.97 (1H, dd, *J* = 15.1, 11.0, H–C1'), 2.93 (3H, s, H–C7), 1.77 (3H, s, H–C6), and 1.60 (3H, s, H–C6) ppm; ^{13}C NMR (151 MHz, CD_3OD): δ = 167.6 (C4), 155.0 (2C, C4'), 138.4 (C2'), 132.4 (C5'), 107.3 (2C, C3'), 78.9 (C2), 61.0 (C7'), 59.9 (C5), 56.7 (2C, C6'), 35.2 (C1'), 25.7 (C7), 24.2 (C6), and 21.9 (C6) ppm; IR (ATR): $\tilde{\nu}$ = 3309w, 2920w, 2684w, 2517w, 2431w, 1702s, 1614w, 1591m, 1507w, 1457m, 1425m, 1397m, 1385m, 1327w, 1315w, 1241m, 1181w, 1155w, 1111s, 1064w, 1034w, 999m, 968w, 875w, 831w, 789w, and 667m cm^{-1}.

^{1}H NMR counterion-effect study of 3·X in CD_3OD at RT

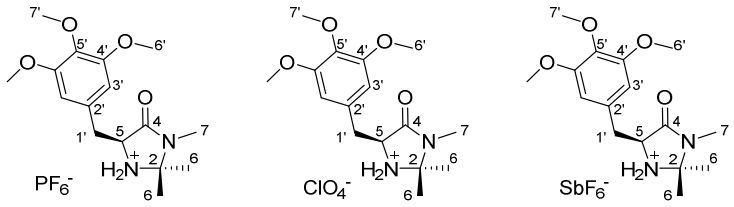

3·HPF$_6$ **3·HClO$_4$** **3·HSbF$_6$**

Imidazolidinone **3** (rac, 25.0 mg, 81 µmol, 1.0 equiv.) was dissolved in EtOH (0.5 mL), the corresponding acid was added (81 µmol, 1.0 equiv.) in Et_2O (0.5 mL) and the solution stirred for 30 min at RT. The solution was concentrated *in vacuo* to give the salt as a white solid in quant. yield.

3·HPF$_6$: HPF_6 (60% in H_2O, 20 mg)

^{1}H NMR (300 MHz, CD_3OD): δ = 6.74 (2H, s, H–C3'), 4.63 (1H, dd, *J* = 10.5, 3.5, H–C5), 3.87 (6H, s, H–C6'), 3.74 (3H, s, H–C7'), 3.47 (1H, dd, *J* = 15.0, 3.5, H–C1'), 3.01–2.89 (4H, m, H–C1', H–C7), 1.74 (3H, s, H–C6), and 1.60 (3H, s, H–C6) ppm.

3·HClO$_4$: $HClO_4$ (70% in H_2O, 12 mg)

^{1}H NMR (300 MHz, CD_3OD): δ = 6.73 (2H, s, H–C3'), 4.68 (1H, ddd, *J* = 10.8, 3.5, 0.5, H–C5), 3.87 (6H, s, H–C6'), 3.74 (3H, s, H–C7'), 3.51 (1H, dd, *J* = 15.1, 3.5, H–C1'), 2.92 (3H, d, *J* = 0.6, H–C7), 2.90 (1H, dd, *J* = 15.2, 10.9, H–C1'), 1.76 (3H, s, H–C6), and 1.61 (3H, s, H–C6) ppm.

3·HSbF$_6$: $HSbF_6$ (65% in H_2O, 43 mg)

^{1}H NMR (300 MHz, CD_3OD): δ = 6.72 (2H, s, H–C3'), 4.64 (1H, ddd, *J* = 10.8, 3.5, 0.6, H–C5), 3.87 (6H, s, H–C6'), 3.74 (3H, s, H–C7'), 3.51 (1H, dd, *J* = 15.2, 3.5, H–C1'), 2.94–2.83 (4H, m, H–C1', H–C7), 1.74 (3H, s, H–C6), and 1.60 (3H, s, H–C6) ppm.

5-(3',3',4'-Trimethoxybenzyl)-2,2,3-trimethyl-4-oxo-1-[(*E*)-3-phenylallylidene]-imidazolidin-1-ium perchlorate (3a·ClO$_4^-$):

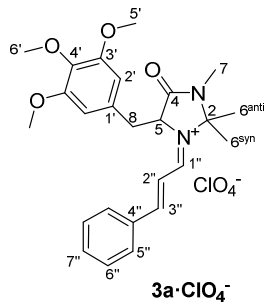

3a·ClO$_4^-$

To racemic imidazolidinone **3** (49.6 mg, 0.16 mmol, 1.0 equiv.) in Et_2O (0.2 mL) was added $HClO_4$ (60% in H_2O, 26.8 mg, 0.16 mmol, 1.0 equiv.) in EtOH/Et_2O (1:1, 0.4 mL) at RT and stirred for 10 min, before the yellow solution was evaporated *in vacuo* to give the off-white $HClO_4$ salt as a solid. The solid was dissolved in MeOH (0.4 mL) and *E*-cinnamaldehyde (40.2 µL, 0.32 mmol, 2.0 equiv.) was added at 35 °C and the yellow solution stirred for 1 h. The solvent was evaporated *in vacuo*. The residue was dissolved in a minimum amount of MeOH, the iminium salt was crashed out with Et_2O and the supernatant solution taken off. This purification procedure was repeated two additional times to give iminium salt **3a·ClO$_4^-$** as a yellow solid.

M.p. = 116.1 °C decomp.; ^{1}H NMR (600 MHz, CD_3CN): δ_H = 8.77 (1H, dd, *J* = 10.7, 1.9, H–C1''), 8.13 (1H, d, *J* = 15.0, H–C3''), 7.87–7.83 (2H, m, H–C5''), 7.71–7.67 (1H, m, H–C7''), 7.59 (2H, t, *J* = 7.9, H–C6''), 7.11 (1H, dd, *J* = 15.0, 10.7, H–C2''), 6.38 (2H, s, H–

C2'), 5.17 (1H, td, *J* = 5.3, 1.6, H–C5), 3.73 (6H, s, H–C5'), 3.52 (1H, dd, *J* = 14.7, 5.4, H–C8), 3.47 (3H, s, H–C6'), 3.31 (1H, dd, *J* = 14.7, 5.2, H–C8), 2.86 (3H, d, *J* = 0.5, H–C7), 1.75 (3H, s, H–C6^{anti}), and 1.13 (3H, s, H–C6^{syn}) ppm; ^{13}C NMR (151 MHz, CD_3CN): δ_C = 168.2 (C1''), 165.9 (C4), 165.4 (C3''), 154.8 (2C, C3'), 139.0 (C4'), 136.0 (C7''), 134.4 (C4''), 132.4 (2C, C5''), 130.6 (2C, C6''), 130.3 (C1'), 118.6 (C2''), 108.2 (2C, C2'), 86.6 (C2), 65.1 (C5), 60.7 (C6'), 56.8 (2C, C5'), 38.2 (C8), 27.3 (C6^{anti}), 26.2 (C7), and 25.5 (C6^{syn}) ppm; IR (ATR): $\tilde{\nu}$ = 3382br, 3068w, 2984w, 1704s, 1622s, 1588s, 1517m, 1441m, 1403m, 1392m, 1325w, 1277w, 1233w, 1198m, 1178m, 1153w, 1073s, 999s, 931m, 852w, 813w, 756m, 726w, 684m, and 621s cm^{-1}; HR-ESI-MS: *m*/*z*: 423.22755 ([*M*-ClO_4^-]$^+$, calcd for $C_{25}H_{31}N_2O_4^+$: 423.22838).

^{1}H NMR counterion-effect study of 3a·X in CD_3CN at RT

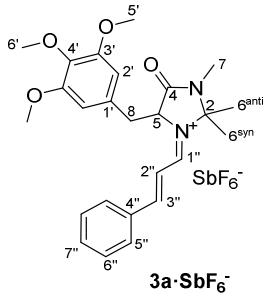

3a·SbF_6^-

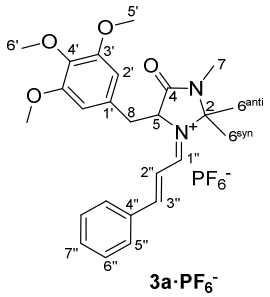

3a·PF_6^-

5-(3',3',4'-Trimethoxybenzyl)-2,2,3-trimethyl-4-oxo-1-[(*E*)-3-phenylallylidene]-imidazolidin-1-ium hexafluoroantimonat (3a·SbF_6^-)

To imidazolidinone **3** (rac, 9.6 mg, 31 µmol, 1.0 equiv.) in MeOH (0.5 mL) was added fluoroantimonic acid (65% in H_2O, 11.5 mg, 33 µmol, 1.1 equiv.) RT and the resulting mixture stirred for 30 min before (*E*)-cinnamaldehyde (4 µL, 31 µmol, 1.0 equiv.) was added. The yellow solution was stirred for 3 h. The solvent was removed *in vacuo* and the residue dissolved in a minimum amount of MeOH. From this solution the iminium salt was crashed out with Et_2O and the supernatant solution taken off. This purification procedure was repeated two additional times to give iminium salt **3a·SbF_6^-** as a yellow solid.

^{1}H NMR (400 MHz, CD_3CN): δ_H = 8.71 (1H, dd, *J* = 10.7, 1.8, H–C1''), 8.09 (1H, d, *J* = 15.0, H–C3''), 7.84 (2H, dd, *J* = 8.2, 1.0, H–C5''), 7.70 (1H, tt, *J* = 7.4, 1.9, H–C7''), 7.59 (2H, t, *J* = 7.6, H–C6''), 7.10 (1H, dd, *J* = 15.0, 10.7, H–C2''), 6.38 (2H, s, H–C2'), 5.15 (1H,

td, *J* = 4.9, 0.9, H–C5), 3.73 (6H, s, H–C5'), 3.52 (1H, dd, *J* = 14.6, 5.4, H–C8), 3.48 (3H, s, H–C6'), 3.31 (1H, dd, *J* = 14.6, 5.2, H–C8), 2.86 (3H, d, *J* = 0.4, H–C7), 1.74 (3H, s, H–$C6^{anti}$), and 1.12 (3H, s, H–$C6^{syn}$) ppm.

5-(3',3',4'-Trimethoxybenzyl)-2,2,3-trimethyl-4-oxo-1-[(*E*)-3-phenylallylidene]-imidazolidin-1-ium hexafluorophosphat (3a·PF_6^-)

To imidazolidinone **3** (rac, 25 mg, 81 µmol, 1.0 equiv.) was added fluorophosphoric acid (60% in H_2O, 19.7 mg, 81 µmol, 1.0 equiv.) in EtOH (0.5 mL) at RT and the resulting mixture stirred for 10 min before it was concentrated *in vacuo*. The salt was dissolved in EtOH (0.3 mL) and (*E*)-cinnamaldehyde (11.2 µL, 89 µmol, 1.1 equiv.) was added. The yellow solution was stirred overnight during which time the product precipitated from the solution as a yellow solid. The supernatant solution was taken off and the solid washed with EtOH to give iminium salt **3a·PF_6^-** as a yellow solid.

^{1}H NMR (300 MHz, CD_3CN): δ_H = 8.72 (1H, dd, *J* = 10.7, 1.8, H–C1''), 8.08 (1H, d, *J* = 15.1, H–C3''), 7.86 (2H, d, *J* = 7.3, H–C5''), 7.76–7.67 (1H, m, H–C7''), 7.61 (2H, t, *J* = 7.5, H–C6''), 7.12 (1H, dd, *J* = 15.0, 10.7, H–C2''), 6.40 (2H, s, H–C2'), 5.17 (1H, t, *J* = 4.7, H–C5), 3.75 (6H, s, H–C5'), 3.54 (1H, dd, *J* = 14.6, 5.3, H–C8), 3.50 (3H, s, H–C6'), 3.33 (1H, dd, *J* = 14.6, 5.2, H–C8), 2.88 (3H, s, H–C7), 1.76 (3H, s, H–$C6^{anti}$), and 1.14 (3H, s, H–$C6^{syn}$) ppm.

8.2.4 Syntheses of (5*S*)-5-*para*-Aminobenzyl-2,2,3-trimethyl-4-imidazolidinone (4) and 5-(4'-Aminobenzyl)-2,2,3-trimethyl-4-oxo-1-[(*E*)-3-phenylallylidene]-imidazolidin-1-ium salt (4a)

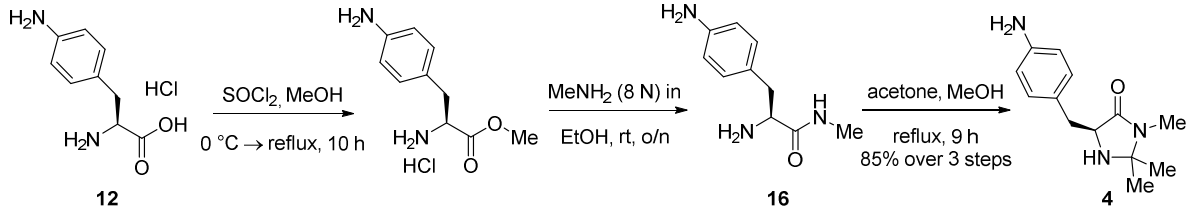

(5*S*)-5-*para*-Aminobenzyl-2,2,3-trimethyl-4-imidazolidinone (4)

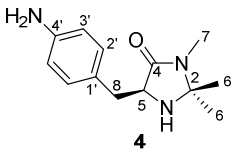

To 4-amino-*L*-phenylalanine hydrochloride (**12**) (500 mg, 2.31 mmol, 1.0 equiv.) in MeOH (2.5 mL, 61.7 mmol, 26.7 equiv.) was added thionyl chloride (0.2 mL, 2.77 mmol, 1.2 equiv.) over 5 min at 0 °C and the resulting solution was allowed to come to RT before it was heated to reflux for 10 h. The solution was allowed to come to RT and evaporated *in vacuo* to give the *L*-tyrosine methyl ester hydrochloride as a white powder. To the ester was added $MeNH_2$ (8 N in EtOH, 1.20 mL, 9.24 mmol, 4.0 equiv.) at RT and the solution stirred overnight. After evaporation *in vacuo*, the residue was dissolved in MeOH (5.0 mL), acetone (0.85 mL, 11.6 mmol, 5.0 equiv.) was added at RT under an atmosphere of argon and the yellow solution was heated to reflux overnight. The reaction was allowed to come to RT and concentrated *in vacuo*. Purification by CC (SiO_2; CH_2Cl_2/MeOH/NH_3 (33% aqueous) 10:1:0.1) gave imidazolidinone **6** as a brown oil (458 mg, 85%).

R_f = 0.41 (CH_2Cl_2/MeOH 10:1); $[\alpha]_D^{23}$: –55.6 (c = 0.78, CH_3OH); ^{1}H NMR (300 MHz, $CDCl_3$): δ = 6.98 (2H, d, J = 8.3, H–C2'), 6.60 (2H, d, J = 8.3, H–C3'), 3.70 (1H, t, J = 5.3, H–C5), 2.97 (2H, dd, J = 5.2, 1.8, H–C8), 2.72 (3H, s, H–C7), 1.23 (3H, s, H–C6), and 1.13 (3H, s, H–C6) ppm; ^{13}C NMR (75 MHz, $CDCl_3$): δ = 173.7 (C4), 145.3 (C4'), 130.5 (2C, C2'), 126.4 (C1'), 115.4 (2C, C3'), 75.6 (C2), 59.4 (C5), 35.9 (C8), 27.1 (C7), and 25.3 (2C, C6) ppm; IR (ATR): $\tilde{\nu}$ = 3343w, 2973w, 2925w, 1673s, 1516s, 1428m, 1399s, 1319w, 1274m, 1206w, 1180m, 1147m, 1089w, 1018w, 921w, 805m, and 728w cm^{-1}; HR-ESI-MS: *m*/*z*: 234.1611 ([*M*+H]$^+$, calcd for $C_{14}H_{19}N_3O^+$: 234.1601).

8.2.5 Syntheses of (5*S*)-2,2,3-Trimethyl-5-(3,5-dimethoxybenzyl)imidazolidin-4-one (5) and 5-(3',3'-Dimethoxybenzyl)-2,2,3-trimethyl-4-oxo-1-[(*E*)-3-phenylallylidene]-imidazolidin-1-ium salt (5a)

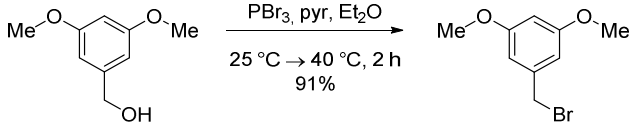

1-Bromomethyl-3,5-dimethoxybenzene[180]

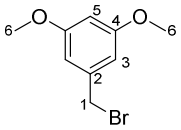

To a solution of 3,5-dimethoxybenzyl alcohol (500m g, 2.97 mmol, 1.00 equiv.) in Et_2O (14 mL) were added successively PBr_3 (0.28 mL, 2.97 mmol, 1.00 equiv.) and pyridine (12 µL, 0.15 mmol, 0.05 equiv.) slowly at RT. The mixture was heated to 40 °C and after completion was detected by TLC (2 h), it was allowed to cool to RT. H_2O (20 mL) was added slowly and the aqueous layer extracted Et_2O (3·15 mL). The combined organic layers were washed with H_2O and brine and dried over $MgSO_4$. Concentration *in vacuo* gave 1-bromomethyl-3,5-dimethoxybenzene as a white crystalline solid (625 mg, 91%), which should be kept in the freezer (turns first orange then brown at RT).

R_f = 0.88 (CH/EtOAc 1:1); M.p. = 71.2–71.8 °C; ^{1}H NMR (400 MHz, $CDCl_3$): δ = 6.55 (2H, d, *J* = 2.3, H–C3), 6.41 (1H, d, *J* = 2.3, H–C5), 4.42 (2H, s, H–C1), and 3.79 (6H, s, H-C6) ppm; ^{13}C NMR (101 MHz, $CDCl_3$): δ = 161.0 (2C, C4), 139.8 (C2), 107.0 (2C, C3), 100.6 (C5), 55.4 (2C, C6), and 33.7 (C1) ppm; HR-EI-MS: *m*/*z*: 151.0758 ([*M*-Br$^-$]$^+$, calcd for $C_9H_{11}O_2^+$: 151.0759); analytical data in agreement with the literature.[180]

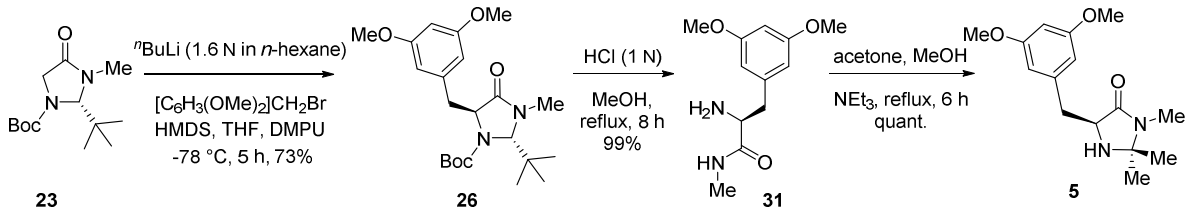

(2*S*,5*S*)-1-Boc-2-(*tert*-butyl)-3-methyl-5-(3,5-dimethoxybenzyl)-4-imidazolidinone (26)[122b]

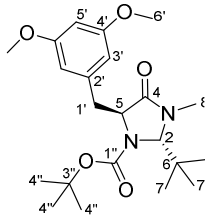

A solution of HMDS (0.3 mL, 1.42 mmol, 1.2 equiv.) in dry THF (1.00 mL) in a flame-dried Schlenck under an atmosphere of argon was cooled to 0 °C. ^{n}BuLi (1.6 N in ^{n}hexane, 0.9 mL, 1.42 mmol, 1.2 equiv.) was added dropwise and the solution stirred for 15 min before it was cooled to -78 °C. DMPU (0.43 mL, 3.54 mmol, 3.0 equiv.) and then (*S*)-Boc-BMI (**23**) (300 g, 1.18 mmol, 1.0 equiv.) in THF (1.00 mL) was added dropwise, the solution turned yellow during the addition. After 30 min, 1-bromomethyl-3,5-dimethoxybenzene (273 g, 1.18 mmol, 1.0 equiv.) in THF (1.00 mL) was added slowly and the resulting mixture stirred for 5 h. The reaction was quenched by addition of a saturated aqueous solution of $NaHCO_3$ (4 mL) and extracted with CH_2Cl_2 (3·5 mL). The combined organic layers were dried over $MgSO_4$ and concentrated *in vacuo*. Purification by CC (SiO_2; CH/EtOAc 3:1) gave **26** as a colourless oil (352 mg, 73%).

R_f = 0.53 (CH/EtOAc 1:1); $[\alpha]_D^{20}$: +40.0 (*c* = 1.00, CH_3OH); ^{1}H NMR (400 MHz, $CDCl_3$): δ = 6.31 (2H, s, H–C3'), 6.27 (1H, bt, *J* = 2.1, H–C5'), 4.63 (1H, bs, H–C2), 4.27 (1H, bs, H–C5), 3.71 (6H, s, H–C6'), 3.66 (1H, bs, H–C1'), 3.13 (1H, dd, *J* = 14.2, 1.2, H–C1'), 2.81 (s, 3H, H–C8), 1.47 (s, 9H, H–C4'), and 0.91 (s, 9H, H–C7) ppm; ^{13}C NMR (101 MHz, $CDCl_3$): δ = 171.5 (C4), 160.3 (2C, C4'), 152.8 (C1''), 138.0 (C2'), 108.0 (b, 2C, C3'), 99.0 (b, C5'), 81.0 (C2), 81.0 (C3''), 60.5 (C5), 55.3 (2C, C6'), 40.9 (C6), 34.4 (b, C1'), 31.9 (C8), 28.3 (3C, C4'), and 26.6 (3C, C7) ppm; IR (ATR): $\tilde{\nu}$ = 2966w, 2838w, 1698s, 1595s, 1457m, 1431m, 1407m, 1397s, 1366s, 1312w, 1251m, 1204m, 1151s, 1127s, 1067m, 1033w, 960w, 887w, 862w, 774w, 755w, 736w, and 696w cm^{-1}; HR-ESI-MS: *m*/*z*: 407.2542 ([*M*+H]$^+$, calcd for $C_{22}H_{35}N_2O_5^+$: 407.2540).

L-3,5-Dimethoxyphenylalanine *N*-methyl amide (31)[182]

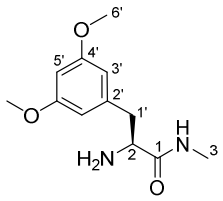

31

To a solution of **26** (300 mg, 0.74 mmol, 1.0 equiv.) in MeOH (7.0 mL) was added an aqueous solution of HCl (1 N, 7.0 mL) at RT and the mixture heated to reflux for 8 h. The reaction was allowed to come to RT and basified to a pH of 10 with an aqueous solution of NaOH (2 N, circa 4 mL) and extracted three times with CH_2Cl_2. The combined organic layers were dried over $MgSO_4$ and concentrated *in vacuo* to give amide **31** as a white solid (175 mg, 99%).

M.p. = 61.7–63.6 °C; $[\alpha]_D^{23}$: +15.1 (*c* = 0.60, CH_3OH); ^{1}H NMR (400 MHz, $CDCl_3$): δ = 7.33 (1H, bd, *J* = 5.5, H–N^{amide}), 6.34 (2H, s, H–C3'), 6.31 (1H, s, H–C5'), 3.74 (6H, d, *J* = 1.2, H–C6'), 3.56 (1H, dd, *J* = 9.7, 3.9, H–C2), 3.19 (1H, dd, *J* = 13.6, 3.9, H–C1'), 2.79 (3H, d, *J* = 5.0, H–C3), 2.56 (1H, dd, *J* = 13.6, 9.6, H–C1'), and 1.45 (2H, bs, H–N^{amine}) ppm; ^{13}C NMR (101 MHz, $CDCl_3$): δ = 174.9 (C1), 161.0 (2C, C4´), 140.4 (C2'), 107.2 (2C, C3'), 98.8 (C5'), 56.4 (C2), 55.4 (2C, C6'), 41.4 (C1'), and 25.9 (C3) ppm; IR (ATR): $\tilde{\nu}$ = 3379w, 3314w, 2958w, 2935w, 2865w, 1636m, 1595s, 1524m, 1463m, 1446m, 1428m, 1400m, 1346m, 1332w, 1291m, 1205s, 1147s, 1147s, 1097w, 1081w, 1057s, 994w, 955w, 907w, 877w, 838w, 822m, 786w, 742m, 690m, and 657w cm^{-1}; HR-ESI-MS: *m*/*z*: 239.1397 ([*M*+H]$^+$, calcd for $C_{12}H_{19}N_2O_3^+$: 239.1390).

(5*S*)-2,2,3-Trimethyl-5-(3,4,5-trimethoxybenzyl)imidazolidin-4-one (5)

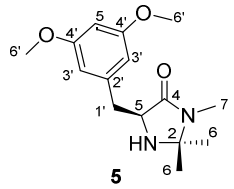

5

To a solution of amide **31** (100 mg, 0.42 mmol, 1.0 equiv.) in MeOH (2.0 mL) were added aceton (0.23 mL, 3.15 mmol, 7.5 equiv.) and NEt_3 (47 µL, 0.34 mmol, 0.8 equiv.) at RT under an atmosphere argon and the solution heated to reflux for 6 h. The reaction was allowed to come to RT and concentrated *in vacuo* to give imidazolidinone **5** as a yellow oil (122 mg, quant.).

$[\alpha]_D^{23}$: –39.3 (*c* = 1.02, CH_3OH); ^{1}H NMR (400 MHz, $CDCl_3$): δ = 6.37 (2H, d, *J* = 2.3, H–C3'), 6.31 (1H, d, *J* = 2.3, H–C5'), 3.73 (7H, m, H–C5, H–C6'), 3.06 (1H, dd, *J* = 14.1, 4.5, H–C1'), 2.91 (1H, dd, *J* = 14.0, 6.9, H–C1'), 2.74 (3H, s, H–C7), 1.24 (3H, s, H–C6), and 1.18 (3H, s, H–C6) ppm; ^{13}C NMR (101 MHz, $CDCl_3$): δ = 173.5 (C4), 160.9 (2C, C4'), 139.6 (C2'), 107.4 (2C, C3'), 99.0 (C5'), 75.6 (C2), 59.2 (C5), 55.4 (2C, C6'), 37.7 (C1'), 27.4 (C6), 25.4 (C6), and 25.3 (C7) ppm; IR (ATR): $\tilde{\nu}$ = 2933w, 2839w, 1684s, 1595s, 1461m, 1429s, 1398m, 1368w, 1315w, 1294w, 1205s, 1151s, 1066m, 931w, 832w, and 698w cm^{-1}; HR-ESI-MS: *m/z*: 279.1708 ($[M+H]^+$, calcd for $C_{15}H_{23}N_2O_3^+$: 279.1703).

5-(3',3'-Dimethoxybenzyl)-2,2,3-trimethyl-4-oxo-1-[(*E*)-3-phenylallylidene]-imidazolidin-1-ium perchlorate (5a·ClO_4^-):

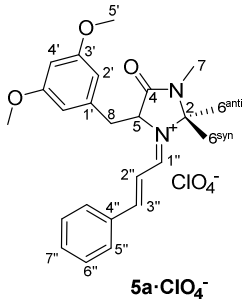

5a·ClO_4^-

To racemic imidazolidinone **5** (3.3 mg, 12 µmol, 1.0 equiv.) in Et_2O (20 µL) was added $HClO_4$ (70% in H_2O, 1.7 mg, 12 µmol, 1.0 equiv.) in EtOH/Et_2O (1:1, 40 µL) at RT and stirred for 10 min, before the yellow solution was evaporated *in vacuo* to give the off-white

$HClO_4$ salt as a solid. The solid was dissolved in MeOH (20 µL) and (*E*)-cinnamaldehyde (3.0 µL, 24 µmol, 2.0 equiv.) was added at 35 °C and the yellow solution stirred for 1 h. The solvent was evaporated *in vacuo*. The residue was dissolved in a minimum amount of MeOH, the iminium salt was crashed out with Et_2O and the supernatant solution taken off. The iminium salt **5a·ClO$_4^-$** was isolated as a yellowish solid contaminated with (*E*)-cinnamaldehyde (P/(*E*)-cinnamaldehyde 1:1.3).

^{1}H NMR (300 MHz, CD_3CN): δ_H = 8.73 (1H, dd, *J* = 10.7, 1.7, H–C1''), 8.10 (1H, d, *J* = 14.8, H–C3''), 7.88–7.82 (2H, m, H–C5''), 7.72–7.58 (3H, m, H–C7'', H–C6''), 7.11 (1H, dd, *J* = 15.1, 10.6, H–C2''), 6.34–6.27 (3H, m, H–C2', H–C4'), 5.16 (1H, b, H–C5), 3.67 (6H, s, H–C5'), 3.50 (1H, dd, *J* = 14.5, 5.3, H–C8), 3.30 (1H, dd, *J* = 14.5, 5.1, H–C8), 2.84 (3H, d, *J* = 0.7, H–C7), 1.74 (3H, s, H–C6^{anti}), and 1.13 (3H, s, H–C6^{syn}) ppm; HR-ESI-MS: *m*/*z*: 393.2170 ([*M*–ClO_4^-]$^+$, calcd for $C_{24}H_{29}N_2O_3^+$: 393.2173).

8.2.6 Syntheses of (5*S*)-5-*para*-Hydroxybenzyl-2,2,3-trimethyl-4-imidazolidinone (6) and 5-(4'-Hydroxybenzyl)-2,2,3-trimethyl-4-oxo-1-[(*E*)-3-phenylallylidene]-imidazolidin-1-ium salt (6a)

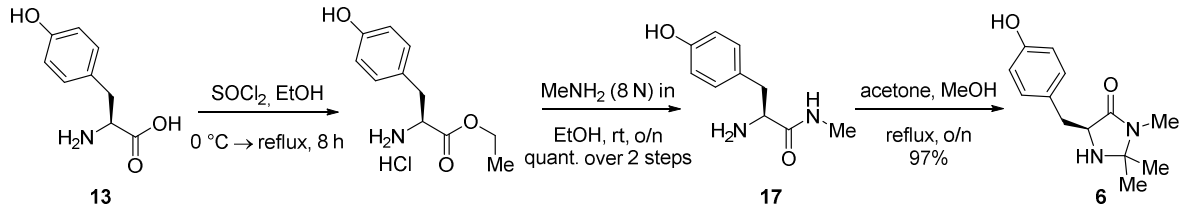

***L*-Tyrosine methyl amide (17)**

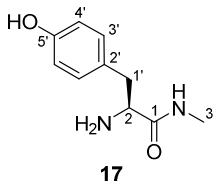

To *L*-tyrosine (1.00 g, 5.52 mmol, 1.0 equiv.) in EtOH (3.4 mL, 82.8 mmol, 15 equiv.) was added thionyl chloride (0.6 mL, 8.28 mmol, 1.5 equiv.) over 5 min at 0 °C and the resulting solution was allowed to come to RT before it was heated to reflux for 8 h. The solution was allowed to come to RT and evaporated *in vacuo* to give the *L*-tyrosine ethyl ester hydrochloride as a white powder. To the ester was added $MeNH_2$ (8 N in EtOH, 2.80 mL, 22.1 mmol, 4.0 equiv.) at RT and the solution stirred overnight. After evaporation *in vacuo*, THF was added and the remaining white solid filtered off ($MeNH_2 \cdot HCl$). The filtrate was concentrated *in vacuo* to give amide **17** as an orange oil (1.09 g, quant.).

R_f = 0.21 (CH_2Cl_2/MeOH 10:1); $[\alpha]_D^{20}$: +23.2 (*c* = 1.02, CH_3OH); ^{1}H NMR (300 MHz, CD_3OD): δ = 7.00 (2H, d, *J* = 8.5, H–C3'), 6.71 (2H, d, *J* = 8.6, H–C4'), 3.44 (1H, t, *J* = 6.8, H–C2), 2.87 (1H, dd, *J* = 13.4, 6.5, H–C1'), 2.71 (1H, dd, *J* = 13.4, 7.1, H–C1'), and 2.67 (3H, s, H–C3) ppm; ^{13}C NMR (75 MHz, CD_3OD): δ = 177.1 (C1), 157.4 (C5'), 131.3 (2C, C3'), 129.3 (C2'), 116.3 (2C, C4'), 57.9 (C2), 41.6 (C1'), and 26.1 (C3) ppm; IR (ATR): $\tilde{\nu}$ = 3275b, 2939w, 1644s, 1612s, 1592s, 1540m, 1513s, 1447m, 1410m, 1309w, 1234s, 1170m, 1105w, 1022w, 942w, 821s, and 696w cm^{-1}; HR-ESI-MS: *m*/*z*: 195.1133 ($[M+H]^+$, calculated for $C_{10}H_{15}N_2O_2^+$: 195.1128); analytical data in agreement with the literature.[183]

(5*S*)-5-*para*-hydroxybenzyl-2,2,3-trimethyl-4-imidazolidinone (6)

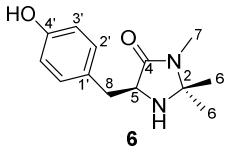

6

To a solution of amide **17** (985 mg, 5.07 mmol, 1.0 equiv.) in MeOH (10.0 mL) was added acetone (1.9 mL, 25.4 mmol, 5.0 equiv.) at RT under an atmosphere of argon and the yellow solution was heated to reflux overnight. The reaction was allowed to come to RT and concentrated *in vacuo* to give imidazolidinone **6** as an off-white solid (1.15 g, 97%).

R_f = 0.64 (CH_2Cl_2/MeOH 10:1); M.p. = 94.5–95.8 °C; $[\alpha]_D^{20.5}$: –57.0 (*c* = 1.00, CH_3OH); ^{1}H NMR (300 MHz, CD_3OD): δ = 7.06 (2H, d, *J* = 8.5, H–C2'), 6.72 (2H, d, *J* = 8.6, H–C3'), 3.73 (1H, dd, *J* = 6.8, 4.4, H–C5), 3.00 (1H, dd, *J* = 14.3, 4.3, H–C8), 2.85 (1H, dd, *J* = 14.3, 7.1, H–C8), 2.75 (3H, d, *J* = 0.4, H–C7), 1.26 (3H, s, H–C6), and 1.20 (3H, s, H–C6) ppm; ^{13}C NMR (101 MHz, CD_3OD): δ = 175.5 (C4), 157.4 (C4'), 131.5 (2C, C2'), 129.0 (C1'), 116.3 (2C, C3'), 77.4 (C2), 60.9 (C5), 37.0 (C8), 26.8 (C6), 25.6 (C7), and 24.8 (C6) ppm; IR (ATR): $\tilde{\nu}$ = 3276w, 2974w, 2939w, 1661s, 1479w, 1447m, 1427m, 1400s, 1384s, 1370s, 1331w, 1262m, 1243m, 1210w, 1147s, 1076m, 1037m, 1004w, 993w, 936s, 916m, 847s, and 757s cm^{-1}; HR-ESI-MS: *m/z* (%): 235.1444 ([*M*+H]$^+$, calculated for $C_{13}H_{19}N_2O_2^+$: 235.1441); analytical data in agreement with the literature.[184]

5-*para*-hydroxybenzyl-2,2,3-trimethyl-4-imidazolidinone hydrochloride (6·HCl, racemic)

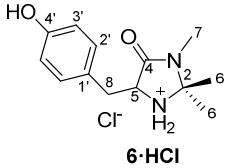

6·HCl

Imidazolidinone **6** (18.7 mg, 80 µmol, 1.0 equiv.) was dissolved in HCl in MeOH (1.25 N, 0.25 mL, 313 µmol, 3.9 equiv.) and stirred for 30 min at RT. The solution was concentrated *in vacuo* to give **6·HCl** as a white solid (19 mg, quant.).

M.p. = 84.7–85.6 °C; ^{1}H NMR (400 MHz, CD_3OD): δ = 7.21 (2H, d, *J* = 8.5, H–C2'), 6.81 (2H, d, *J* = 8.6, H–C3'), 4.57 (1H, dd, *J* = 10.7, 3.5, H–C5), 3.45 (1H, dd, *J* = 15.3, 3.5, H–C8), 2.91 (3H, s, H–C7), 2.95–2.85 (1H, m, H–C8), 1.70 (3H, s, H–C6), and 1.58 (3H, s, H–C6) ppm; ^{13}C NMR (101 MHz, CD_3OD): δ = 167.8 (C4), 158.4 (C4'), 131.2 (2C, C2'), 126.6 (C1'), 116.9 (2C, C3'), 78.9 (C2), 60.0 (C5), 34.3 (C8), 25.6 (C7), 24.2 (C6), and 22.0 (C6) ppm; IR (ATR): $\tilde{\nu}$ = 2924w, 2702m, 2493w, 1696s, 1614w, 1594m, 1516m, 1423s, 1394s, 1309w, 1264m, 1217s, 1174m, 1160m, 1101w, 1038w, 938w, 826m, 794w, 732w, and 668m cm^{-1}.

^{1}H NMR counterion-effect study of 6·X in CD_3OD at RT

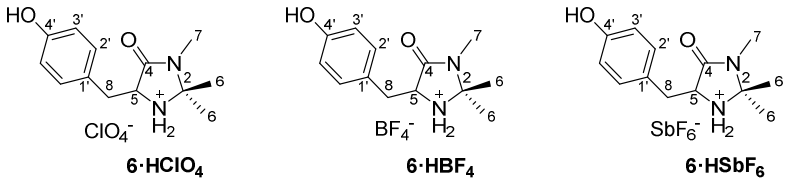

6·HClO$_4$ **6·HBF$_4$** **6·HSbF$_6$**

Imidazolidinone **6** (10.0 mg, 43 µmol, 1.0 equiv.) was dissolved in MeOH (0.5 mL), the corresponding acid was added (47 µmol, 1.1 equiv.) and the solution stirred for 30 min at RT. The solution was concentrated *in vacuo* to give the corresponding salt as a white solid in quant. yield.

6·HClO$_4$: $HClO_4$ (70% in H_2O, 6.7 mg)

^{1}H NMR (300 MHz, CD_3OD): δ = 7.22 (2H, d, *J* = 8.5, H–C2'), 6.81 (2H, d, *J* = 8.6, H–C3'), 4.57 (1H, ddd, *J* = 10.7, 3.3, 0.5, H–C5), 3.44 (1H, dd, *J* = 15.3, 3.5, H–C8), 2.91 (3H, d, *J* = 0.5, H–C7), 2.89 (1H, dd, *J* = 15.4, 10.6, H–C8), 1.71 (3H, s, H–C6), and 1.59 (3H, s, H–C6) ppm.

6·HBF$_4$: HBF_4 (50% in H_2O, 8.2 mg)

^{1}H NMR (300 MHz, CD_3OD): δ = 7.21 (2H, d, *J* = 8.5, H–C2'), 6.81 (2H, d, *J* = 8.6, H–C3'), 4.56 (1H, dd, *J* = 10.6, 3.4, H–C5), 3.44 (1H, dd, *J* = 15.4, 3.5, H–C8), 2.91 (3H, s, H–C7), 2.88 (1H, dd, *J* = 15.3, 10.6, H–C8), 1.70 (3H, s, H–C6), and 1.58 (3H, s, H–C6) ppm.

6·HSbF$_6$: $HSbF_6$ (65% in H_2O, 24.9 mg)

^{1}H NMR (300 MHz, CD_3OD): δ = 7.21 (2H, d, *J* = 8.5, H–C2'), 6.81 (2H, d, *J* = 8.6, H–C3'), 4.55 (1H, dd, *J* = 10.7, 3.6, H–C5), 3.43 (1H, dd, *J* = 15.2, 3.6, H–C8), 2.90 (3H, d, *J* = 0.6, H–C7), 2.88 (1H, dd, *J* = 15.3, 10.6, H–C8), 1.70 (3H, s, H–C6), and 1.58 (3H, s, H–C6) ppm.

5-(4'-Hydroxybenzyl)-2,2,3-trimethyl-4-oxo-1-[(*E*)-3-phenylallylidene]-imidazolidin-1-ium perchlorate (6a·ClO$_4^-$)

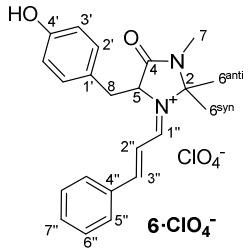

6·ClO$_4^-$

To imidazolidinone **6** (37.5 mg, 0.16 mmol, 1 equiv.) in Et_2O (0.20 mL) was added perchloric acid (60% in H_2O, 26.80 mg, 0.16 mmol, 1 equiv.) in EtOH/Et_2O (1:1, 0.40 mL) at RT and the resulting mixture stirred for 10 min before it was evaporated *in vacuo* to give the imidazolidinone salt. The salt was dissolved in MeOH (0.40 mL) and heated to 35 °C. (*E*)-cinnamaldehyde (40.2 µL, 0.32 mmol, 2 equiv.) was added and the yellow solution stirred for 1 h. The solvent was removed *in vacuo* and the residue dissolved in a minimum amount of MeOH. From this solution the iminium salt was crashed out with Et_2O and the supernatant solution taken off. The washing procedure was repeated and the iminium salt **6a·ClO$_4^-$** isolated as a yellow solid (50.3 mg, 70%).

Crystals suitable for X-ray crystallographic analysis were obtained from a solution in CH_3CN by vapor diffusion with Et_2O.

M.p. = 117.3 °C decomp.; ^{1}H NMR (600 MHz, CD_3CN): δ_H = 8.71 (1H, dd, *J* = 10.7, 1.9, H–C1''), 8.14 (1H, d, *J* = 15.0, H–C3''), 7.90 (2H, dd, *J* = 8.4, 1.1, H–C5''), 7.73–7.69 (1H, m, H–C7''), 7.63–7.59 (2H, m, H–C6''), 7.23 (1H, dd, *J* = 15.0, 10.7, H–C2''), 6.92 (2H, d, *J* = 8.5, H–C2'), 6.72 (2H, d, *J* = 8.6, H–C3'), 5.13 (1H, t, *J* = 4.8, H–C5), 3.49 (1H, dd, *J* = 14.9, 5.6, H–C8), 3.36 (1H, dd, *J* = 14.9, 4.0, H–C8), 2.80 (3H, d, *J* = 0.5, H–C7), 1.71

(3H, s, H–C6anti), and 0.93 (3H, s, H–C6syn) ppm; ^{13}C NMR (151 MHz, CD_3CN): δ_C = 168.0 (C1''), 166.3 (C3''), 165.4 (C4), 158.0 (C4'), 136.0 (C7''), 134.4 (C4''), 132.4 (2C, C5''), 132.4 (2C, C2'), 130.7 (2C, C6''), 125.6 (C1'), 118.5 (C2''), 116.8 (2C, C3'), 86.6 (C2), 65.4 (C5), 36.7 (C8), 27.5 (C6anti), 26.1 (C7), and 25.1 (C6anti) ppm; IR (ATR): $\tilde{\nu}$ = 3370br, 3070w, 2985w, 1704s, 1603s, 1588s, 1517m, 1441m, 1403m, 1392m, 1325w, 1276w, 1233w, 1199m, 1178m, 1153m, 1076s, 999s, 931w, 852w, 813w, 756m, 726s, 684w, and 621s cm^{-1}; HR-ESI-MS: *m*/*z*: 349.19106 ([*M*-ClO_4^-]$^+$, calcd for $C_{22}H_{25}N_2O_2^+$: 349.19105).

8.2.7 Synthesis of (5*S*)-2,2,3-Trimethyl-5-(*para*-fluorobenzyl)-4-imidazolidinone (7)

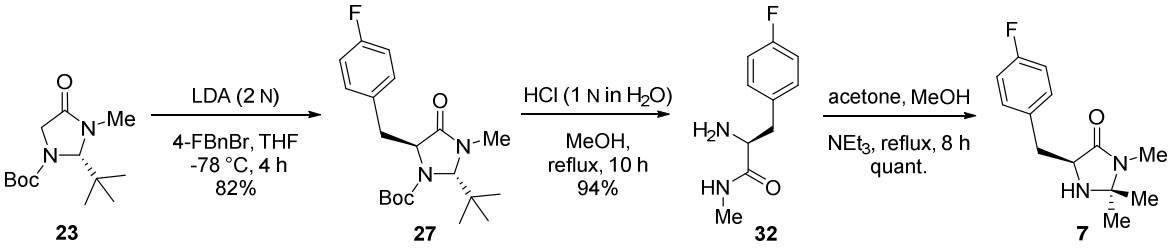

(2*S*,5*S*)-1-Boc-2-(*tert*-butyl)-3-methyl-5-(*para*-fluoro)benzyl-4-imidazolidinone (27)[122a]

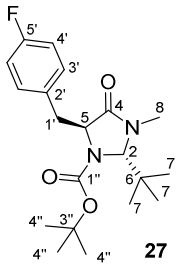

A solution of (*S*)-Boc-BMI (**23**) (570 mg, 2.22 mmol, 1.0 equiv.) in dry THF (3.00 mL) in a flame-dried Schlenck under an atmosphere of argon was cooled to –78 °C. LDA (2.0 N in THF/^{n}heptane/ethylbenzene, 1.22 mL, 2.44 mmol, 1.1 equiv.) was added dropwise and the solution stirred for 30 min before 4-fluorobenzylbromide (420 mg, 2.22 mmol, 1.0 equiv.) in THF (1.00 mL) was added slowly. After 4 h, the reaction was quenched by addition of a sat. aqueous solution of NH_4Cl (2 mL), diluted with water (3 mL) and extracted with CH_2Cl_2 (3 x 5 mL). The combined organic layers were dried over $MgSO_4$ and concentrated *in vacuo*. Purification by CC (SiO_2; CH/EtOAc 8:1) gave **27** as a white solid (667 mg, 82%).

R_f = 0.49 (SiO_2; hexane/EtOAc 2:1); M.p. = 126.8 °C decomp.; $[\alpha]_D^{20}$: +26.8 (c = 0.91, CH_3OH); ^{1}H NMR (400 MHz, $CDCl_3$): δ = 7.12 (2H, dd, J = 8.2, 5.8, H–C3'), 6.87 (2H, t, J = 8.7, H–C4'), 4.54 (1H, b, H–C2), 4.29 (1H, s, H–C5), 3.81 (1H, b, H–C1'), 3.15 (1H, dd, J = 14.1, 2.2, H–C1'), 2.78 (3H, b, H–C8), 1.49 (9H, s, H–C4''), and 0.91 (9H, s, H–C7) ppm; ^{13}C NMR (101 MHz, $CDCl_3$): δ = 171.4 (C4), 162.0 (d, $^1J_{CF}$ = 252.4, C5'), 152.7 (C1''), 131.8 (C2´), 131.6 (2C, d, $^3J_{CF}$ = 3.1, C3'), 114.8 (2C, d, $^2J_{CF}$ = 20.9, C4'), 81.2 (C3''), 81.2 (C2), 60.8 (C5), 41.0 (C6), 32.8 (C1'), 31.9 (C8), 28.4 (C4''), and 26.7 (C7) ppm; ^{19}F NMR (282 MHz, $CDCl_3$): δ = –116.55 (1F, b, F–C5') ppm; IR (ATR): $\tilde{\nu}$ = 2975w, 2933w, 1694s, 1602w, 1512w, 1478w, 1457w, 1440w, 1400m, 1377s, 1364s, 1302m, 1258m, 1236w, 1216m, 1179m, 1160m, 1116s, 1098w, 1934w, 1010w, 981w, 948w, 886m,

867w, 841w, 822w, 786m, 770m, 717m, and 705w cm^{-1}; HR-ESI-MS: *m/z* (%): 387.2059 ([*M*–Na]$^+$, calcd for $C_{20}H_{29}FN_2O_3Na^+$: 387.2060). Analytical data in agreement with the literature.[122a]

L-(*para*-Fluoro)-phenylalanine *N*-methyl amide (32)

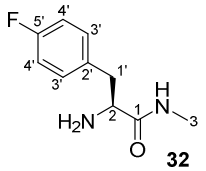

32

To a solution of **27** (575 mg, 1.58 mmol, 1.0 equiv.) in MeOH (15.0 mL) was added an aqueous solution of HCl (1 N, 15.0 mL) at RT and the mixture heated to reflux for 10 h. The reaction was allowed to come to RT and basified to a pH of 10 with an aqueous solution of NaOH (2 N) and extracted with CH_2Cl_2 (3·20.0 mL). The combined organic layers were dried over $MgSO_4$ and concentrated *in vacuo* to give amide **32** as a white solid (290 mg, 94%).

M.p. = 133.7–134.5 °C; $[\alpha]_D^{23}$: +28.1 (*c* = 1.04, CH_3OH); ^{1}H NMR (300 MHz, $CDCl_3$): δ = 7.23 (1H, b, H–N^{amide}), 7.16 (2H, dd, *J* = 8.6, 5.5, H–C3'), 6.98 (2H, t, *J* = 8.7, H–C4'), 3.56 (1H, dd, *J* = 9.1, 4.1, H–C2), 3.20 (1H, dd, *J* = 13.8, 4.0, H–C1'), 2.79 (3H, d, *J* = 5.0, H–C3), 2.69 (1H, dd, *J* = 13.8, 9.1, H–C1'), and 1.32 (2H, b, H–N^{amine}) ppm; ^{13}C NMR (75 MHz, $CDCl_3$): δ = 174.7 (C1), 161.9 (d, $^1J_{CF}$ = 244.9, C5'), 133.7 (d, $^4J_{CF}$ = 3.3, C2'), 130.8 (2C, d, $^3J_{CF}$ = 7.9, C3'), 115.6 (2C, d, $^2J_{CF}$ = 21.2, C4'), 56.5 (d, $^5J_{CF}$ = 0.7, C1'), 40.3 (C2), and 25.9 (C3) ppm; ^{19}F NMR (382 MHz, $CDCl_3$): δ = –116.20 (1F, tt, $^3J_{HF}$ = 8.7, $^4J_{HF}$ = 5.4, F–C4´) ppm; IR (ATR): $\tilde{\nu}$ = 3375w, 3300m, 2943w, 1637s, 1600m, 1530m, 1507s, 1443w, 1406m, 1339w, 1311w, 1272w, 1222s, 1154m, 1110m, 1093m, 1016w, 983w, 927w, 884w, 867w, 816s, 797m, 751m, 710w, 693m, and 658w cm^{-1}; HR-ESI-MS: *m/z*: 197.1085 ([*M*+H]$^+$, calcd for $C_{10}H_{14}FN_2O^+$: 197.1085).

(5*S*)-2,2,3-Trimethyl-5-(*para*-fluorobenzyl)-4-imidazolidinone (7)

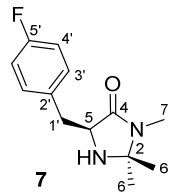

7

To a solution of amide **32** (141 mg, 0.72 mmol, 1.0 equiv.) in MeOH (4.00 mL) were added aceton (0.40 mL, 5.33 mmol, 7.5 equiv.) and NEt_3 (0.08 mL, 0.58 mmol, 0.8 equiv.) at RT under an atmosphere argon and the solution heated to reflux for 8 h. The reaction was allowed to come to RT and concentrated *in vacuo* to give imidazolidinone **7** as an orange sticky solid (172 mg, quant.).

$[\alpha]_D^{23}$: –44.0 (c = 0.50, CH_3OH); ^{1}H NMR (300 MHz, $CDCl_3$): δ = 7.12 (2H, dd, J = 8.6, 5.5, H–C3'), 6.89 (2H, t, J = 8.7, H–C4'), 3.68 (1H, dd, J = 6.7, 4.6, H–C5), 3.02 (1H, dd, J = 14.2, 4.4, H–C1'), 2.87 (1H, dd, J = 14.2, 6.8, H–C1'), 2.66 (3H, s, H–C7), 1.71 (1H, b, H–N), 1.19 (3H, s, H–C6), and 1.10 (3H, s, H–C6) ppm; ^{13}C NMR (75 MHz, $CDCl_3$): δ = 173.1 (C4), 161.7 (d, $^1J_{CF}$ = 244.7, C5'), 132.9 (d, $^4J_{CF}$ = 3.2, C2'), 130.9 (2C, d, $^3J_{CF}$ = 7.8, C3'), 115.2 (2C, d, $^2J_{CF}$ = 21.1, C4'), 75.5 (C2), 59.2 (C5), 36.4 (C1'), 27.2 (C6), 25.2 (C6), and 25.1 (C7) ppm; 19F NMR (75 MHz, $CDCl_3$): δ = –116.28 (1F, s, F–C4´) ppm; IR (ATR): $\tilde{\nu}$ = 3315w, 2978w, 2927w, 1683s, 1602w, 1509s, 1426m, 1399s, 1220s, 1158m, 1098w, 1017w, 824m, and 722w cm^{-1}; HR-ESI-MS: m/z: 237.1398 ($[M+H]^+$, calcd for $C_{13}H_{18}FN_2O^+$: 237.1398).

8.2.8 Syntheses of (5*S*)-2,2,3-Trimethyl-5-(2,4,6-trifluorobenzyl)-4-imidazolidinone (8) and (*S*)-5-(2',4',6'-Trifluorobenzyl)-2,2,3-trimethyl-4-oxo-1-[(*E*)-3-phenylallylidene]-imidazolidin-1-ium salt (8a)

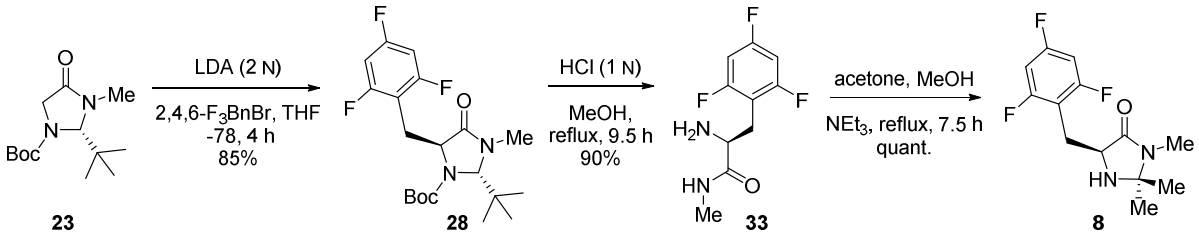

(2*S*,5*S*)-1-Boc-2-(*tert*-butyl)-3-methyl-5-(2,4,6-trifluorobenzyl)-4-imidazolidinone (28)

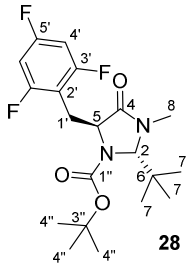

A solution of (*S*)-Boc-BMI (**23**) (570 mg, 2.22 mmol, 1.0 equiv.) in dry THF (3.00 mL) in a flame-dried Schlenck under an atmosphere of argon was cooled to –78 °C. LDA (2.0 N in THF/*n*heptane/ethylbenzene, 1.22 mL, 2.44 mmol, 1.1 equiv.) was added dropwise and the solution stirred for 30 min before 2,4,6-trifluorobenzylbromide (500 mg, 2.22 mmol, 1.0 equiv.) in THF (1.00 mL) was added slowly. After 5 h, the reaction was quenched by addition of saturated aqueous solution of NH_4Cl (2 mL), diluted with water (3 mL) and extracted with CH_2Cl_2 (3 · 5 mL). The combined organic layers were dried over $MgSO_4$ and concentrated *in vacuo*. Purification by CC (SiO_2; CH/EtOAc 10:1) gave **28** as an orange oil (757 mg, 85%).

R_f = 0.51 (SiO_2; CH/EtOAc 2:1); $[\alpha]_D^{23}$: –1.1 (*c* = 0.89, CH_3OH); ^{1}H NMR (300 MHz, $CDCl_3$): δ = 6.62 (2H, t, *J* = 8.3, H–C4'), 4.99 (1H, s, H–C2), 4.22 (1H, d, *J* = 5.6, H–C5), 3.79 (1H, dd, *J* = 13.9, 3.4, H–C1'), 2.93 (4H, s, H–C8, H–C1'), 1.49 (9H, s, H–C4''), and 0.95 (9H, s, H–C7) ppm; ^{13}C NMR (75 MHz, $CDCl_3$): δ = 171.1 (C4), 161.5 (2C, ddd, $^1J_{CF}$ = 248.4, $^3J_{CF}$ = 15.5, $^3J_{CF}$ = 14.7, C3'), 161.4 (dt, $^1J_{CF}$ = 247.4, $^4J_{CF}$ = 15.7, C5'), 152.9 (b, C1''), 109.3 (t, $^2J_{CF}$ = 21.3, C2'), 99.7 (2C, ddd, $^2J_{CF}$ = 28.4, $^2J_{CF}$ = 25.4, $^4J_{CF}$ = 2.6, C4'), 81.2 (C2), 80.6 (C3''), 57.1 (C5), 40.9 (C6), 31.8 (C1'), 28.2 (3C, C4''), 26.5 (3C, C7), and

23.9 (b, C8) ppm; ^{19}F NMR (75 MHz, $CDCl_3$): δ = –110.4 (2F, b, F–C3'), and –110.8 (b, F–C5') ppm; IR (ATR): $\tilde{\nu}$ = 3331w, 2976w, 2928w, 1682s, 1602w, 1508s, 1425m, 1398s, 1368w, 1219s, 1158m, 1098m, 1016w, 922w, 823m, and 731m cm^{-1}; HR-EI-MS: *m/z* : 423.1867 ([*M*–Na]$^+$, calculated for $C_{20}H_{27}F_3N_2O_3Na^+$: 423.1866).

L-2,4,6-Trifluorophenylalanine *N*-methyl amide (33)

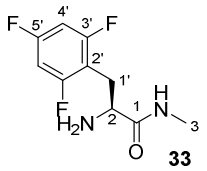

33

To a solution of **28** (680 mg, 1.70 mmol, 1.0 equiv.) in MeOH (10.0 mL) was added an aq. solution of HCl (1 N, 10.0 mL) at RT and the mixture heated to reflux overnight. The reaction was allowed to come to RT and basified to a pH of 10 with an aqueous solution of NaOH (2 N) and extracted with CH_2Cl_2 (3 · 35 mL). The combined organic layers were dried over $MgSO_4$ and concentrated *in vacuo* to give amide **33** as a white solid (355 mg, 90%).

R_f = 0.56 (CH_2Cl_2/MeOH 10:1); M.p. = 50.7–52.1 °C; $[\alpha]_D^{23}$: +30.3 (*c* = 0.95, CH_3OH); ^{1}H NMR (300 MHz, $CDCl_3$): δ = 7.26 (1H, b, H–N^{amide}), 6.65 (2H, dd, *J* = 8.7, 7.8, H–C4'), 3.54 (1H, dd, *J* = 9.6, 4.3, H–C2), 3.29 (1H, dd, *J* = 14.1, 4.3, H–C1'), 2.81 (3H, d, *J* = 5.0, H–C3), 2.74 (1H, dd, *J* = 14.1, 9.7, H–C1'), and 1.42 (2H, bs, H–N^{amine}) ppm; ^{13}C NMR (75 MHz, $CDCl_3$): δ = 174.2 (C1), 161.9 (2C, ddd, $^1J_{CF}$ = 247.8, $^3J_{CF}$ = 14.7, $^3J_{CF}$ = 11.5, C3'), 161.6 (dt, $^1J_{CF}$ = 248.4, $^3J_{CF}$ = 15.7, H-C5'), 110.4 (td, $^2J_{CF}$ = 20.4, $^4J_{CF}$ = 4.6, C2'), 101.3–99.6 (2C, m, C4'), 55.0 (C2), 28.0 (C1'), and 26.0 (C3) ppm; ^{19}F NMR (282 MHz, $CDCl_3$): δ = –109.84 (1F, tt, $^3J_{FH}$ = 22.6, $^4J_{FF}$ = 5.8, F–C5'), and –111.26 (2F, dd, $^3J_{FH}$ = 7.4, $^4J_{FF}$ = 5.9, F–C3') ppm; IR (ATR): $\tilde{\nu}$ = 3302w, 3077w, 2941w, 1625s, 1601s, 1538m, 1493m, 1436m, 1412w, 1345w, 1305w, 1272w, 1224w, 1157w, 1138w, 1114s, 1021m, 993m, 950w, 838m, 779w, 723w, 707w, and 659w cm^{-1}; HR-ESI-MS: *m/z*: 233.0902 ([*M*+H]$^+$, calcd for $C_{10}H_{12}F_3N_2O^+$: 233.0896).

(5*S*)-2,2,3-Trimethyl-5-(2,4,6-trifluorobenzyl)-4-imidazolidinone (8)

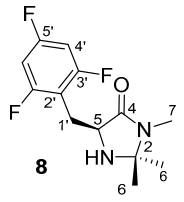

8

To a solution of amide **33** (320 mg, 1.38 mmol, 1.0 equiv.) in MeOH (8.00 mL) were added aceton (0.76 mL, 10.3 mmol, 7.5 equiv.) and NEt_3 (0.15 mL, 1.10 mmol, 0.8 equiv.) at RT under an atmosphere argon and the solution heated to reflux overnight. The reaction was allowed to come to RT and concentrated *in vacuo* to give imidazolidinone **8** as yellow oil (682 mg, quant.).

$[\alpha]_D^{23}$: –32.2 (*c* = 0.48, CH_3OH); ^{1}H NMR (300 MHz, $CDCl_3$): δ = 6.60 (2H, dd, *J* = 8.8, 7.7, H–C4'), 3.69 (1H, dd, *J* = 10.2, 4.1, H–C5), 3.22 (1H, dd, *J* = 14.1, 4.2, H–C1'), 2.75 (3H, s, H–C7), 2.68 (1H, dd, *J* = 14.1, 10.4, H–C1'), 1.74 (1H, b, H–N), 1.35 (3H, s, H–C6), and 1.23 (3H, s, H–C6) ppm; ^{13}C NMR (101 MHz, $CDCl_3$): δ = 172.9 (C4), 161.7 (2C, ddd, $^1J_{CF}$ = 247.7, $^3J_{CF}$ = 14.8, $^3J_{CF}$ = 11.6, C3'), 161.4 (dt, $^1J_{CF}$ = 248.0, $^3J_{CF}$ = 15.7, C5'), 110.3 (td, $^2J_{CF}$ = 20.5, $^4J_{CF}$ = 4.7, C2'), 100.1 (2C, ddd, $^2J_{CF}$ = 28.7, $^2J_{CF}$ = 25.5, $^4J_{CF}$ = 2.1, C4'), 75.7 (C2), 58.0 (C5), 27.6 (C6), 25.8 (C8), 25.3 (C6), and 25.3 (C7) ppm; ^{19}F NMR (75 MHz, $CDCl_3$): δ = –110.35 (1F, t, $^3J_{FF}$ = 5.7, F–C5'), and –111.45 (2F, d, $^3J_{FF}$ = 5.7, F–C3') ppm; IR (ATR): $\tilde{\nu}$ = 3326w, 2976w, 1687s, 1641m, 1622m, 1605s, 1497m, 1440s, 1400m, 1268w, 1167m, 1149w, 1116s, 1058m, 998m, 940w, 839m, and 737w cm^{-1}; HR-ESI-MS: *m*/*z*: 273.1207 ($[M+H]^+$, calcd for $C_{13}H_{16}F_3N_2O^+$: 273.1209).

(*S*)-5-(2',4',6'-Trifluorobenzyl)-2,2,3-trimethyl-4-oxo-1-[(*E*)-3-phenylallylidene]-imidazolidin-1-ium perchlorate (8a ClO_4^-):

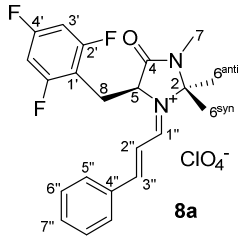

To imidazolidinone **8** (43.6 mg, 0.16 mmol, 1.0 equiv.) in Et_2O (0.2 mL) was added $HClO_4$ (60% in H_2O, 26.8 mg, 0.16 mmol, 1.0 equiv.) in EtOH/Et_2O (1:1, 0.4 mL) at RT and stirred for 10 min, before the sovent was evaporated *in vacuo* to give the off-white $HClO_4$ salt as a solid. The solid was dissolved in MeOH (0.4 mL) and (*E*)-cinnamaldehyde (40.2 µL, 0.32 mmol, 2.0 equiv.) was added at 35 °C and the yellow solution stirred for 1 h. The solvent was evaporated *in vacuo*. The residue was dissolved in a minimum amount of MeOH, the iminium salt was crashed out with Et_2O and the supernatant solution taken off. This purification procedure was repeated two additional times to give **8a·ClO_4^-** as a yellow solid.

M.p. = 198.5 °C decomp.; $[\alpha]_D^{20} = +122.5$ ($c = 0.83$ in CH_3CN); ^{1}H NMR (600 MHz, CD_3CN): $\delta_H = 8.87$ (1H, dd, $J = 10.7, 1.7$, H–C1''), 8.20 (1H, d, $J = 15.0$, H–C3''), 7.83 (2H, dd, $J = 8.2, 1.0$, H–C5''), 7.73–7.69 (1H, m, H–C7''), 7.60 (2H, t, $J = 7.9$, H–C6''), 7.16 (1H, dd, $J = 15.0, 10.7$, H–C2''), 6.87 (2H, dd, $J = 8.9, 7.9$, H–C3'), 5.06 (1H, t, $J = 6.0$, H–C5), 3.48 (1H, dd, $J = 15.0, 7.6$, H–C8), 3.42 (1H, dd, $J = 15.1, 5.8$, H–C8), 2.89 (3H, d, $J = 0.5$, H–C7), 1.82 (3H, s, H–C6anti), and 1.64 (3H, s, H–C6syn) ppm; ^{13}C NMR (151 MHz, CD_3CN, C1', C2' and C4' assigned in CFdec spectrum): $\delta_C = 168.7$ (C1''), 166.6 (C3''), 164.5 (C4), 163.6 (C4'), 162.9 (2C, C2'), 136.2 (C7''), 134.3 (C4''), 132.2 (2C, C5''), 130.8 (2C, C6''), 118.1 (C2''), 108.2 (C1'), 101.7 (2C, dd, $^2J_{CF} = 31.2$, $^2J_{CF} = 26.0$, C3'), 86.8 (C2), 61.9 (C5), 26.9 (C6syn), 26.9 (C6anti), 26.4 (C8), and 26.3 (C7) ppm; 19F NMR (564 MHz, CD_3CN): $\delta_F = -108.7$ (1F, tt, $^2J_{HF} = 9.0$, $^3J_{FF} = 6.7$, F–C4'), and –110.4 (2F, dd, $^2J_{HF} = 7.8$, $^3J_{FF} = 6.6$, F–C2') ppm; IR (ATR): $\tilde{\nu}$ = 3376br, 3071w, 2985w, 1705s, 1619s, 1604s, 1588s, 1517m, 1442m, 1403m, 1392m, 1325w, 1276w, 1233w, 1198m, 1178m, 1153m, 1075s, 998s, 931w, 852w, 813w, 756m, 684w, and 621s cm^{-1}; HR-ESI-MS: *m/z*: 387.16776 ([*M*-ClO_4^-]$^+$, calcd for $C_{22}H_{22}F_3N_2O^+$: 387.16787).

8.2.9 Syntheses of (5*S*)-2,2,3-Trimethyl-5-(*para*-ntirobenzyl)-4-imidazolidinone (9) and 5-(4'-Nitrobenzyl)-2,2,3-trimethyl-4-oxo-1-[(*E*)-3-phenylallylidene]-imidazolidin-1-ium salt (9a)

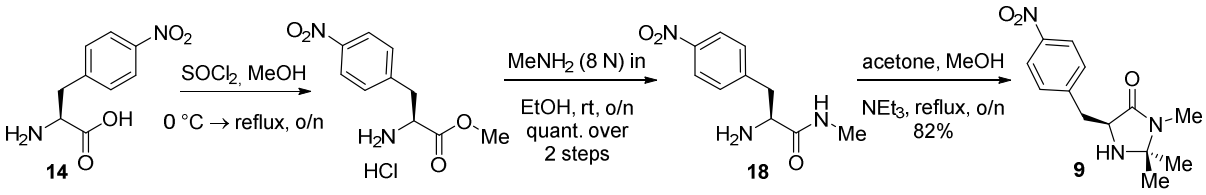

L-(*para*-Nitro)-phenylalanine *N*-methyl amide (18)

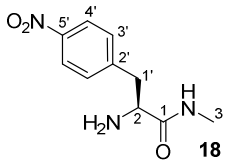

To L-(*para*-nitro)-phenylalanine (**14**) (500 mg, 2.38 mmol, 1.0 equiv.) in EtOH (2.00 mL) was added thionyl chloride (0.40 mL, 5.47 mmol, 2.3 equiv.) over 5 min at 0 °C and the resulting solution was allowed to come to RT before it was heated to reflux for 1 d. The solution was allowed to come to RT and evaporated *in vacuo* to give the L-(*para*-nitro)-phenylalanine methyl ester hydrochloride as a yellow solid. To the ester was added $MeNH_2$ (8 N in EtOH, 1.20 mL, 9.52 mmol, 4.0 equiv.) at RT and the solution stirred overnight. After evaporation *in vacuo*, a saturated aqueous solution of $NaHCO_3$ (5 mL) was added and the aqueous layer extracted with CH_2Cl_2 (3 · 5 mL). The combined organic layers were dried over $MgSO_4$, filtrated concentrated *in vacuo* to give amide **18** as a yellow solid (483 mg, 91%), which was used without characterisation in the next step.

^{1}H NMR (300 MHz, $CDCl_3$): δ = 8.18 (2H, d, *J* = 8.7, H–C4´), 7.39 (2H, d, *J* = 8.6, H–C3´), 7.22 (1H, b, H–N^{amide}), 3.66 (1H, dd, *J* = 8.7, 4.2, H–C2), 3.34 (1H, dd, *J* = 13.7, 4.2, H–C1´), 2.91 (1H, dd, *J* = 13.7, 8.7, H–C1´), 2.82 (3H, d, *J* = 5.0, H–C3), and 1.36 (2H, b, H–N^{amine}) ppm.

(5*S*)-2,2,3-Trimethyl-5-(*para*-ntirobenzyl)-4-imidazolidinone (9)

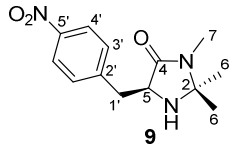

9

To a solution of amide **18** (450 mg, 2.02 mmol, 1 equiv.) in MeOH (10.0 mL) was added acetone (1.10 mL, 15.1 mmol, 7.5 equiv.) at RT under an atmosphere of argon and the yellow solution was heated to reflux for 8 h. The reaction was allowed to come to RT and concentrated *in vacuo* to give imidazolidinone **9** as a yellow oil (533 mg, quant.).

$[\alpha]_D^{23}$: –57.1 (*c* = 1.25, CH_3OH); ^{1}H NMR (400 MHz, $CDCl_3$): δ = 8.13 (2H, d, *J* = 8.8, H–C4'), 7.42 (2H, d, *J* = 8.9, H–C3'), 3.84 (1H, ddd, *J* = 7.7, 4.2, 0.8, H–C5), 3.25 (1H, dd, *J* = 14.1, 4.2, H–C1'), 2.96 (1H, dd, *J* = 14.1, 7.8, H–C1'), 2.76 (3H, d, *J* = 0.7, H–C7), 1.81 (1H, b, H–N^{amine}), 1.28 (3H, s, H–C6), and 1.21 (3H, s, H–C6) ppm; ^{13}C NMR (75 MHz, $CDCl_3$): δ = 172.4 (C4), 146.8 (C5'), 145.8 (C2'), 130.4 (2C, C3'), 123.6 (2C, C4'), 75.7 (C2), 59.1 (C5), 38.0 (C1'), 27.8 (C6), 25.5 (C6), and 25.2 (C7) ppm; IR (ATR): $\tilde{\nu}$ = 3326w, 2976w, 1681s, 1601m, 1515s, 1427m, 1399m, 1368w, 1343s, 1265w, 1205w, 1182w, 1148w, 1108w, 1086w, 1017w, 907w, 861w, 819w, 746w, and 700w cm^{-1}; HR-ESI-MS: *m*/*z*: 264.1345 ($[M+H]^+$, calcd for $C_{13}H_{18}N_3O_3^+$: 264.1343).

5-(4'-Nitrobenzyl)-2,2,3-trimethyl-4-oxo-1-[(*E*)-3-phenylallylidene]-imidazolidin-1-ium perchlorate (9a·ClO_4^-)

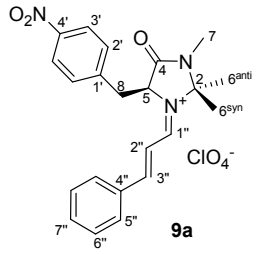

9a

To imidazolidinone **9** (21.1 mg, 0.08 mmol, 1 equiv.) was added perchloric acid (60% in H_2O, 13.4 mg, 0.16 mmol, 1 equiv.) in EtOH/Et_2O (1:1, 0.40 mL) at RT and the resulting mixture stirred for 10 min before it was evaporated *in vacuo* to give the imidazolidinone salt. The salt was dissolved in MeOH (0.20 mL) and (*E*)-cinnamaldehyde (20.1 µL, 0.16 mmol, 1 equiv.) was added and the yellow solution stirred overnight during which time the product precipitated as a yellow solid. Iminium salt **9a** was filtered off, washed with Et_2O and dried *in vacuo*.

M.p. = 117.3 °C decomp.; $[\alpha]_D^{23}$: +587.5 (*c* = 0.59, CH_3CN); ^{1}H NMR (400 MHz, CD_3CN): δ_H = 8.82 (1H, dd, *J* = 10.7, 2.0, H–C1''), 8.24 (1H, d, *J* = 15.0, H–C3''), 8.13 (2H, d, *J* = 8.7, H–C3′), 7.92 (2H, d, *J* = 8.7, H–C5''), 7.72 (1H, t, *J* = 7.4, H–C7''), 761 (2H, t, *J* = 7.6, H–C6''), 7.36 (2H, d, *J* = 8.7, H–C2'), 7.28 (1H, dd, *J* = 15.0, 10.7, H–C2''), 5.28 (1H, bs, H–C5), 3.70 (1H, dd, *J* = 14.6, 5.9, H–C8), 3.57 (1H, dd, *J* = 14.7, 4.1, H–C8), 2.80 (3H, s, H–C7), 1.73 (3H, s, H–C6^{anti}), and 0.99 (3H, s, H–C6^{syn}) ppm; ^{13}C NMR (101 MHz, CD_3CN): δ_C = 168.7 (C1''), 167.4 (C3''), 164.8 (C4), 148.7 (C4'), 142.5 (C1'), 136.2 (C7''), 134.3 (C4''), 132.6 (2C, C5''), 132.5 (2C, C2'), 130.7 (2C, C6''), 124.9 (2C, C3'), 118.1 (C2''), 86.5 (C2), 64.3 (C5), 37.0 (C8), 27.4 (C6^{anti}), 26.2 (C7), and 25.6 (C6^{syn}) ppm; IR (ATR): $\tilde{\nu}$ = 3375w, 2978w, 1714m, 1672m, 1629w, 1603w, 1590w, 1520s, 1500s, 1434w, 1419w, 1395m, 1345s, 1300w, 1201w, 1180w, 1109s, 1056s, 1035m, 1014w, 997s, 971s, 946s, 893w, 857w, 822w, 799w, 757w, 743w, 696w, and 683w cm^{-1}.

8.2.10 Syntheses of (5*S*)-2,2,3-Trimethyl-5-(pentafluorobenzyl)-4-imidazolidinone (10) and 5-Pentafluorobenzyl-2,2,3-trimethyl-4-oxo-1-[(*E*)-3-phenylallylidene]-imidazolidin-1-ium salt (10a)

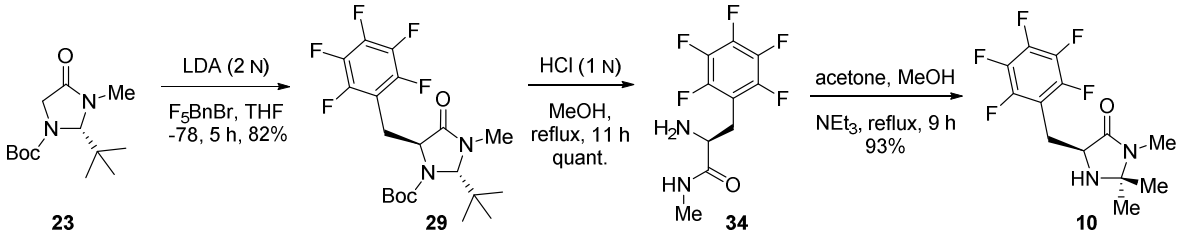

(2*S*,5*S*)-1-Boc-2-(*tert*-butyl)-3-methyl-5-(pentafluorobenzyl)-4-imidazolidinone (29)[122a]

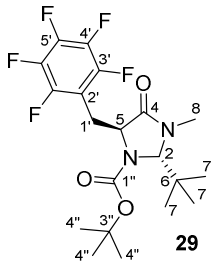

A solution of (*S*)-Boc-BMI (**23**) (128 mg, 0.50 mmol, 1.0 equiv.) in dry THF (0.70 mL) in a flame-dried Schlenck under an atmosphere of argon was cooled to –78 °C. LDA (0.28 mL, 0.55 mmol, 1.1 equiv.) was added resulting in a dark red solution. After 30 min, pentafluorobenzylbromide (131 mg, 0.50 mmol, 1.0 equiv.) in dry THF (0.25 mL) was added slowly upon which the solution turned purple. The reaction was stirred at –78 °C for 5 h and then quenched by addition of saturated aqueous solution of NH_4Cl (2 mL) and extracted with CH_2Cl_2 (3 · 5 mL). The combined organic layers were dried over $MgSO_4$ and concentrated *in vacuo*. Purification by CC (SiO_2; CH/EtOAc 8:1) gave **29** as an off-white solid (179 mg, 82%).

R_f = 0.66 (SiO_2; CH/EtOAc 2:1); M.p. = 65.9–69.6°C; $[\alpha]_D^{23}$: –0.7 (*c* = 0.95, CH_3OH); ^{1}H NMR (300 MHz, $CDCl_3$): δ = 4.99 (1H, bs, H–C2), 4.22 (1H, bs, H–C5), 3.89 (1H, dd, *J* = 13.9, 3.0, H–C1'), 2.95 (3H, s, H–C8), 2.91 (1H, bs, H–C1'), 1.48 (9H, s, H–C4''), and 0.95 (9H, s, H–C7) ppm; ^{13}C NMR (75 MHz, $CDCl_3$): δ = 170.8 (C4), 152.8 (C1''), 145.6 (2C, dm, $^1J_{CF}$ = 246.8, C^{Ar}), 137.2 (dm, $^1J_{CF}$ = 268.6, C5'), 137.0 (2C, dm, $^1J_{CF}$ = 205.2, C^{Ar}), 111.1 (b, C2'), 81.8 (C2), 80.9 (C3''), 56.8 (C5), 41.1 (C6), 32.1 (C1'), 28.3 (3C, C4''), 26.6 (3C, C7), and 24.7 (b, C8) ppm; ^{19}F NMR (282 MHz, $CDCl_3$): δ = –141.7 (2F, bs, F–C3'),

–157.3 (1F, bs, F–C5'), and –163.2 (2F, bs, F–C4') ppm; IR (ATR): $\tilde{\nu}$ = 2973w, 2932w, 1695s, 1658w, 1602w, 1511m, 1506m, 1478w, 1457w, 1400m, 1376s, 1364s, 1302m, 1257m, 1216m, 1178m, 1160m, 1116s, 1098m, 1035w, 1010w, 980m, 948w, 934w, 912w, 886m, 840w, 821w, 786m, 771m, and 717m cm^{-1}; HR-ESI-MS: *m/z*: 459.1662 ([*M*+Na]$^+$, calcd for $C_{20}H_{25}F_5N_2O_3Na^+$: 459.1678). Analytical data in agreement with the literature.[122a]

L-Pentafluorophenylalanine *N*-methyl amide (34)

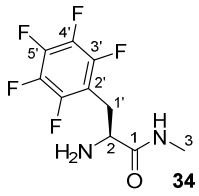

To a solution of **29** (100 mg, 0.23 mmol, 1.0 equiv.) in MeOH (3.0 mL) was added an aqueous solution of HCl (1 N, 3.0 mL) at RT and the mixture heated to reflux for 11 h. The reaction was allowed to come to RT and basified to a pH of 10 with an aqueous solution of NaOH (2 N) and extracted with CH_2Cl_2. The combined organic layers were dried over $MgSO_4$ and concentrated *in vacuo* to give amide **34** as a white solid (62 mg, quant.).

M.p. = 98.4–99.3 °C; $[\alpha]_D^{22}$ = –0.263 (c = 0.039 in $CHCl_3$); ^{1}H NMR (300 MHz, $CDCl_3$): δ = 7.21 (1H, bs, H–N^{amide}), 3.58 (1H, dd, J = 9.1, 4.9, H–C2), 3.37 (1H, dd, J = 14.1, 4.4, H–C1'), 2.91–2.74 (4H, m, H–C3, H–C1'), and 1.50 (2H, s, H–N^{amine}) ppm; ^{13}C NMR (75 MHz, $CDCl_3$): δ = 173.5 (C1), 145.6 (dm, $^1J_{CF}$ = 247.3, C^{Ar}), 139.8 (dm, $^1J_{CF}$ = 252.1, C^{Ar}), 137.3 (dm, $^1J_{CF}$ = 250.5, C^{Ar}), 111.9 (td, $^2J_{CF}$ = 18.5, $^3J_{CF}$ = 3.7, C2'), 54.8 (C2), 28.5 (C1'), and 26.1 (C3) ppm; ^{19}F NMR (377 MHz, $CDCl_3$): δ = –142.4 (2F, dd, $^3J_{FF}$ = 22.6, $^4J_{FF}$ = 8.4, F–C3'), –156.0 (1F, t, $^3J_{FF}$ = 20.9, F–C5'), and –162.1 (2F, dt, $^3J_{FF}$ = 22.5, $^4J_{FF}$ = 8.4, F–C4') ppm; IR (ATR): $\tilde{\nu}$ = 3379w, 3330m, 3298w, 2953w, 2910w, 1649s, 1540m, 1520s, 1500s, 1445m, 1423m, 1407m, 1298m, 1116s, 1098s, 1000s, 972s, 932s, 914s, 890m, 849m, 805s, 735m, 710s, and 664m cm^{-1}; HR-ESI-MS: *m/z*: 269.0718 ([*M*+H]$^+$, calcd for $C_{10}H_{10}F_5N_2O^+$: 269.0708).

(5*S*)-2,2,3-Trimethyl-5-(pentafluorobenzyl)-4-imidazolidinone (10)

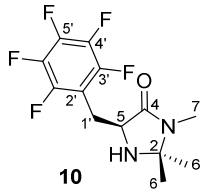

10

To a solution of amide **34** (181 mg, 0.68 mmol, 1.0 equiv.) in MeOH (4.0 mL) were added acetone (0.37 mL, 5.06 mmol, 7.5 equiv.) and NEt_3 (0.08 mL, 0.54 mmol, 0.8 equiv.) at RT under an atmosphere argon and the solution heated to reflux for 9 h. The reaction was allowed to come to RT and concentrated *in vacuo* to give imidazolidinone **10** as an off-white solid (194 mg, 93%).

M.p. = 73.0–75.3 °C; $[\alpha]_D^{20} = -31.5$ ($c = 0.91$ in CH_3OH); ^{1}H NMR (300 MHz, $CDCl_3$): $\delta = 3.78$ (1H, dd, $J = 10.3$, 4.6, H–C5), 3.31 (1H, d, $J = 14.1$, H–C1'), 2.86–2.75 (4H, m, H–C1', H–C7), 1.72 (2H, b, H–N), 1.40 (3H, s, H–C6), and 1.30 (3H, s, H–C6) ppm; ^{13}C NMR (101 MHz, $CDCl_3$, racemic compound): $\delta = 172.3$ (C4), 145.6 (2C, dm, $^1J_{CF} = 245.6$, C^{Ar}), 139.6 (dm, $^1J_{CF} = 245.0$, C5'), 137.4 (2C, dm, $^1J_{CF} = 251.8$, C^{Ar}), 111.9 (td, $^2J_{CF} = 18.4$ $^3J_{CF} = 3.8$, C2'), 76.0 (C2), 57.7 (C5), 28.0 (C6), 26.6 (C1'), 25.6 (C6), and 25.4 (C7) ppm; ^{19}F NMR (282 MHz, $CDCl_3$): $\delta = (-142.3)–(-142.7)$ (2F, m, F-C3'), –157.2 (1F, t, $^3J_{FF} = 20.8$, F–C5'), and –163.0 (2F, td, $^3J_{FF} = 22.6$, $^4J_{FF} = 8.3$, F–C4') ppm; IR (ATR): $\tilde{\nu}$ = 3318m, 2982w, 1676s, 1519s, 1499s, 1441m, 1404s, 1384m, 1371m, 1303w, 1279w, 1202w, 1182m, 1156w, 1119s, 1099m, 1042m, 1012m, 977m, 964s, 937s, 885w, 795w, 768w, 736w, and 681w cm^{-1}; HR-EI-MS: *m*/*z*: 309.1018 ($[M+H]^+$, calcd for $C_{13}H_{14}F_5N_2O^+$: 309.1021); elemental analysis (racemic compound) calcd (%) for $C_{13}H_{13}F_5N_2O$ (308.2): C 50.65, H 4.25, N 9.09, F 30.82; found: C 50.74, H 4.43, N 8.87, F 31.06.

2,2,3-Trimethyl-5-(pentafluorobenzyl)-4-imidazolidinone hydrochloride (10·HCl)

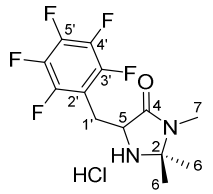

10•HCl

Racemic imidazolidinone **10** (30 mg, 97.0 µmol, 1.0 equiv.) was dissolved in HCl in MeOH (1.25 N, 0.31 mL) and stirred for 30 min at RT. The solvent was evaporated *in vacuo* to give **10·HCl** as a white solid. Crystals suitable for crystallographic analysis were obtained by vapor diffusion of a methanolic solution of the solid with Et_2O.

M.p. = 184.1–186.2 °C; ^{1}H NMR (600 MHz, CD_3OD): δ = 4.52 (1H, t, *J* = 7.3, H–C5), 3.55 (1H, dd, *J* = 14.9, 6.8, H–C1'), 3.29 (1H, dd, *J* = 15.0, 7.1, H–C1'), 2.90 (3H, *J* = 0.5, H–C7), 1.82 (3H, s, H–C6), and 1.64 (3H, s, H–C6) ppm; ^{13}C NMR (151 MHz, CD_3OD): δ = 166.8 (C4), 147.0 (2C, dqd, $^{1}J_{CF}$ = 246.1, $^{3}J_{CF}$ = 8.0, $^{4}J_{CF}$ = 3.7, C^{Ar}), 142.1 (dm, $^{1}J_{CF}$ = 251.9, C5'), 140.0 (2C, dm, $^{1}J_{CF}$ = 249.8, C^{Ar}), 110.7 (td, $^{2}J_{CF}$ = 18.1 $^{3}J_{CF}$ = 3.5, C2'), 79.1 (C2), 56.4 (C5), 25.7 (C7), 24.4 (C6), 22.6 (C1'), and 22.2 (C6) ppm; ^{19}F NMR (282 MHz, $CDCl_3$): δ = –143.33 (2F, m, F-C3'), –158.4 (1F, t, $^{3}J_{FF}$ = 20.0, F–C5'), and –165.1 (2F, m, F–C4') ppm; IR (ATR): $\tilde{\nu}$ = 2935w, 2661w, 2512w, 2460w, 2400w, 1715s, 1662w, 1562w, 1520m, 1506s, 1435m, 1418m, 1396m, 1355m, 1299w, 1271w, 1238w, 1197w, 1181w, 1156m, 1127m, 1059s, 1003w, 988w, 970m, 954s, 919m, 847w, 780w, and 667w cm^{-1}.

5-Pentafluorobenzyl-2,2,3-trimethyl-4-oxo-1-[(*E*)-3-phenylallylidene]-imidazolidin-1-ium perchlorate (10a·ClO_4^-):

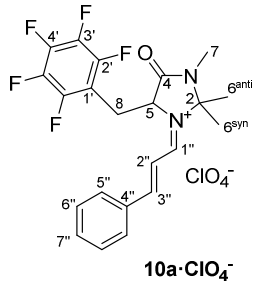

10a·ClO_4^-

To imidazolidinone **10** (24.7 mg, 0.08 mmol, 1.0 equiv.) in Et_2O (0.10 mL) was added perchloric acid (60% in H_2O, 11.5 mg, 0.08 mmol, 1 equiv.) in Et_2O/EtOH (1:1, 0.2 mL) at RT and the resulting mixture stirred for 10 min before it was evaporated *in vacuo* to give the imidazolidinone salt. The salt was redissolved in MeOH (0.20 mL) and heated to 35 °C. (*E*)-cinnamaldehyde (20.1 µL, 0.16 mmol, 2 equiv.) was added and the yellow solution stirred for 1 h. The solvent was removed *in vacuo* and the residue dissolved in a minimum amount of MeOH. From this solution the iminium salt **10a·ClO_4^-** was crashed out as a yellow solid with Et_2O and the supernatant solution taken off. Crystals suitable for X-ray crystallographic analysis were obtained from a solution in MeOH/CH_3CN (2:1) by vapour diffusion with Et_2O.

M.p. = 185.1–186.3 °C; ^{1}H NMR (600 MHz, CD_3CN): δ_H = 8.87 (1H, dd, J = 10.7, 1.8, H–C1''), 8.24 (1H, d, J = 15.0, H–C3''), 7.89 (2H, dd, J = 8.2, 1.0, H–C5''), 7.76–7.71 (1H, m, H–C7''), 7.63 (2H, t, J = 7.9, H–C6''), 7.22 (1H, dd, J = 15.0, 10.7, H–C2''), 5.09–5.04 (1H, m, H–C5), 3.54 (1H, dd, J = 15.0, 5.2, H–C8), 3.49 (1H, dd, J = 15.0, 8.3, H–C8), 2.90 (3H, d, J = 0.5, H–C7), 1.83 (3H, s, H–C6anti), and 1.70 (3H, s, H–C6syn) ppm; ^{13}C NMR (151 MHz, CD_3CN, C1', C2', C3' and C4' not visible): δ_C = 168.8 (C1''), 167.2 (C3''), 164.1 (C4), 136.5 (C7''), 134.2 (C4''), 132.3 (2C, C5''), 130.9 (2C, C6''), 117.9 (C2''), 86.8 (C2), 61.1 (C5), 27.2 (C6syn), 26.8 (C6anti), 26.5 (C8), and 26.3 (C7) ppm; ^{19}F NMR (564 MHz, CD_3CN): δ_F = (–141.1)–(–141.2) (2F, m, F–C2'), –155.6 (1F, t, $^2J_{FF}$ = 20.1, F-C4'), and (–163.6)–(–163.7) (2F, m, F–C3') ppm; IR (ATR): $\tilde{\nu}$ = 2997b, 1712s, 1661w, 1617m, 1603m, 1588s, 1523m, 1506s, 1455m, 1434m, 1405m, 1396m, 1334w, 1277m, 1236w, 1215w, 1181m, 1161m, 1125m, 1093s, 1074s, 1039s, 1012m, 1004m, 976m, 964m, 935m, 865m, 823w, 765s, 700w, 685w, and 621m cm^{-1}; HR-ESI-MS: m/z: 423.1484 ([M-ClO_4^-]$^+$, calcd for $C_{22}H_{20}F_5N_2O^+$: 423.1496).

^{1}H NMR counterion-effect study of 10a·X in CD_3CN at RT:

5-Pentafluorobenzyl-2,2,3-trimethyl-4-oxo-1-[(*E*)-3-phenylallylidene]-imidazolidin-1-ium hexafluoroantimonat (10a·SbF_6^-)

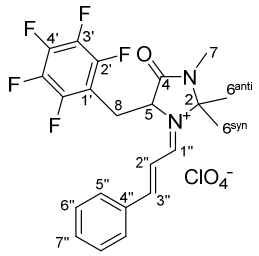

10a·SbF_6^-

^{1}H NMR (400 MHz, CD_3CN): δ_H = 8.85 (1H, dd, *J* = 10.7, 1.7, H–C1''), 8.22 (1H, d, *J* = 15.0, H–C3''), 7.89 (2H, d, *J* = 7.3, H–C5''), 7.74 (1H, tt, *J* = 7.4, 1.2, H–C7''), 7.63 (2H, t, *J* = 7.6, H–C6''), 7.22 (1H, dd, *J* = 15.0, 10.7, H–C2''), 5.05 (1H, t, *J* = 6.3, H–C5), 3.54 (1H, dd, *J* = 15.2, 5.6, H–C8), 3.48 (1H, dd, *J* = 15.0, 8.2, H–C8), 2.90 (3H, s, H–C7), 1.82 (3H, s, H–C6anti), and 1.70 (3H, s, H–C6syn) ppm.

8.2.11 Syntheses of (*S*)-5-(1-Methylindol-3-ylmethyl)-2,2,3-trimethylimidazolidin-4-one and (*S*)-5-(1-Methylindol-3-ylmethyl)-2,2,3-trimethyl-4-oxo-1-[(*E*)-3-phenylallylidene]-imidazolidin-1-ium salt

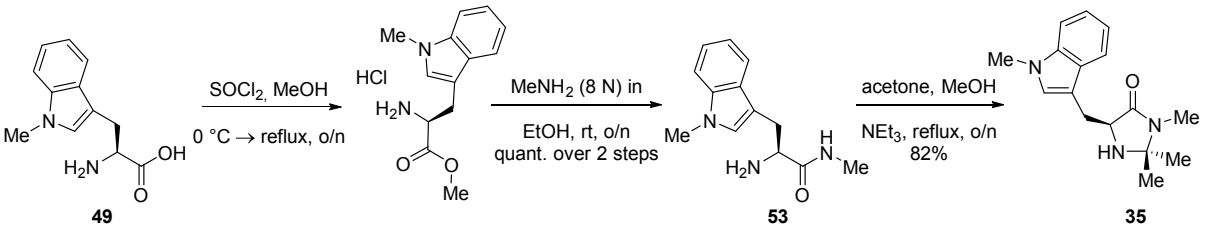

1-Methyl-L-tryptophan methyl ester

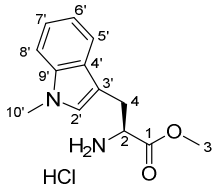

To 1-methyl-L-tryptophan (500 mg, 2.29 mmol, 1.0 equiv.) in MeOH (1.86 mL, 45.8 mmol, 20 equiv.) was added thionyl chloride (0.20 mL, 2.75 mmol, 1.2 equiv.) over 10 min at 0 °C and the resulting mixture was allowed to come to RT before it was heated to reflux overnight. The solution was allowed to come to RT and evaporated *in vacuo* to give 1-methyl-L-tryptophan methyl ester hydrochloride as an off-white solid (615 mg, quant.).

M.p. = 197.6–198.4 °C; $[\alpha]_D^{23}$: +14.5 (*c* = 0.89, CH_3OH); ^{1}H NMR (300 MHz, CD_3OD): δ = 7.54 (1H, dt, *J* = 7.9, 1.0, H–C5'), 7.39 (1H, dt, *J* = 8.3, 0.8, H–C8'), 7.21 (1H, ddd, *J* = 8.2, 7.1, 1.1, H–C7'), 7.14–7.07 (2H, m, H–C6', H–C2'), 4.32 (1H, dd, *J* = 7.3, 5.5, H–C2), 3.80 (6H, s, H–C3, H–C10'), 3.45 (1H, ddd, *J* = 15.1, 5.5, 0.6, H–C4), and 3.36 (1H, dd, *J* = 9.6, 5.6, H–C4) ppm; ^{13}C NMR (75 MHz, CD_3OD): δ = 170.8 (C1), 138.8 (C9'), 129.9 (C2'), 128.7 (C4'), 123.1 (C7'), 120.4 (C6'), 119.1 (C5'), 110.7 (C8'), 106.8 (C3'), 54.6 (C2), 53.7 (C3), 32.9 (C10'), and 27.4 (C4) ppm; IR (ATR): $\tilde{\nu}$ = 3009w, 2837m, 2637w, 2010w, 1746s, 1613w, 1575w, 1542w, 1505m, 1474m, 1445m, 1377w, 1359w, 1327w, 1284w, 1251w, 1228s, 1186w, 1159w, 1123w, 1074m, 1047w, 1011w, 9909w, 945w, 919w, 890w, 864w, 833w, 739m, 727s, and 657w cm^{-1}; HR-ESI-MS: *m*/*z*: 233.1283 ([*M*–Cl]$^+$, calcd for $C_{13}H_{17}N_2O_2^+$: 233.1285); analytical data in agreement with the literature.[185]

1-Methyl-L-tryptophan methyl amide (53)

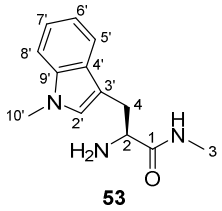

53

To 1-methyl-L-tryptophan methyl ester (584 mg, 2.17 mmol, 1.0 equiv.) was added $MeNH_2$ (8 N in EtOH, 1.10 mL, 8.70 mmol, 4.0 equiv.) at RT and the solution stirred overnight. After evaporation *in vacuo*, the crude product was dissolved in a saturated aqueous solution of $NaHCO_3$ (20 mL) and $CHCl_3$ (15 mL), the aqueous layer was extracted twice with $CHCl_3$ ($2 \cdot 15$ mL), the combined organic layers were dried over $MgSO_4$ and concentrated *in vacuo* to give amide **53** as a sticky oil (502 mg, quant.).

$[\alpha]_D^{23}$: +6.7 (c = 0.95, CH_3OH); ^{1}H NMR (300 MHz, CDCl3): δ = 7.67 (1H, dt, *J* = 7.9, 1.1, H–C5'), 7.31 (1H, dt, *J* = 8.2, 1.2, H–C8'), 7.23 (1H, dd, *J* = 8.2, 1.1, H–C7'), 7.12 (1H, ddd, *J* = 8.0, 6.8, 1.2, H–C6'), 6.92 (1H, s, H–C2'), 3.76 (3H, s, H–C10'), 3.70 (1H, dd, *J* = 8.9, 4.1, H–C2), 3.38 (1H, ddd, *J* = 14.4, 4.1, 0.6, H–C4), 2.90 (1H, dd, *J* = 14.4, 9.0, H–C4), 2.81 (3H, d, *J* = 5.0, H–C3), and 1.46 (2H, bs, H–N^{amine}) ppm; ^{13}C NMR (75 MHz, CD_3OD): δ = 175.4 (C1), 137.2 (C9'), 128.1 (C4'), 127.9 (C2'), 121.9 (C7'), 119.2 (2C, C5', C6'), 110.3 (C3'), 109.4 (C8'), 55.8 (C2), 32.8 (C10'), 30.7 (C3), and 25.9 (C4) ppm; IR (ATR): $\tilde{\nu}$ = 3300w, 3052w, 2934w, 1652s, 1532m, 1471m, 1409w, 1375w, 1326m, 1250w, 1156w, 1130w, 1012w, 909w, 846w, and 735s cm^{-1}; HR-ESI-MS: *m*/*z*: 232.1445 ($[M+H]^+$, calcd for $C_{13}H_{18}N_3O^+$: 232.1444).

(*S*)-5-(1-Methylindol-3-ylmethyl)-2,2,3-trimethylimidazolidin-4-one (35):

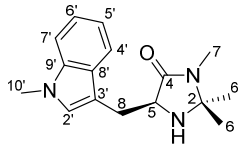

35

To a solution of amide **53** (502 mg, 2.17 mmol, 1.0 equiv.) in MeOH (10.0 mL) was added acetone (1.20 mL, 16.3 mmol, 7.5 equiv.) and NEt_3 (0.24 mL, 1.74 mmol, 0.8 equiv.) at RT under an atmosphere of argon and the yellow solution was heated to reflux overnight. The reaction was allowed to come to RT and concentrated *in vacuo*. Purification by CC (SiO_2; CH_2Cl_2/MeOH/NH_3 (25% in H_2O) 20:1:0.2) gave imidazolidinone **35** as a yellow oil (484 mg, 82%).

R_f = 0.46 (CH_2Cl_2/MeOH 10:1); $[\alpha]_D^{23}$: –37.8 (*c* = 0.31, CH_3OH); ^{1}H NMR (600 MHz, $CDCl_3$): δ = 7.64 (1H, dt, *J* = 7.8, 0.9, H–C4'), 7.27 (1H, dt, *J* = 8.2, 0.9, H–C7'), 7.21 (1H, ddd, *J* = 8.2, 7.0, 1.1, H–C6'), 7.10 (1H, ddd, *J* = 8.0, 7.0, 1.0, H–C5'), 6.95 (1H, s, H–C2'), 3.82 (1H, ddd, *J* = 5.9, 4.7, 0.5, H–C5), 3.73 (3H, s, H–C10'), 3.32 (1H, ddd, *J* = 15.1, 4.6, 0.7, H–C8), 3.17 (1H, ddd, *J* = 15.1, 6.1, 0.7, H–C8), 2.73 (3H, d, *J* = 0.6, H–C7), 1.25 (3H, s, H–C6), and 1.09 (3H, s, H–C6) ppm; ^{13}C NMR (151 MHz, $CDCl_3$): δ = 174.1 (C4), 136.9 (C9'), 128.4 (C8'), 128.0 (C2'), 121.6 (C6'), 119.1 (C5'), 119.0 (C4'), 109.1 (C7'), 109.0 (C3'), 75.4 (C2), 59.1 (C5), 32.7 (b, C10'), 27.0 (C6), 26.3 (C8), 25.2 (C7), and 25.1 (C6) ppm; IR (ATR): $\tilde{\nu}$ = 3295b, 2921w, 2239w, 1682s, 1615w, 1526w, 1472m, 1425m, 1397m, 1379m, 1327w, 1253w, 1205w, 1150w, 1086w, 1013w, 921w, 799w, and 738s cm^{-1}; HR-ESI-MS: *m*/*z*: 272.1763 ($[M+H]^+$, calcd for $C_{16}H_{22}N_3O^+$: 272.1757).

(*S*)-5-(1-Methylindol-3-ylmethyl)-2,2,3-trimethyl-4-oxo-1-[(*E*)-3-phenylallylidene]-imidazolidin-1-ium perchlorate (35a·ClO_4^-):

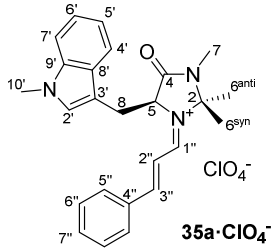

To imidazolidinone **35** (43.4 mg, 0.16 mmol, 1.0 equiv.) in Et_2O (0.2 mL) was added $HClO_4$ (60% in H_2O, 26.8 mg, 0.16 mmol, 1.0 equiv.) in EtOH/Et_2O (1:1, 0.4 mL) at RT and stirred for 10 min, before the solution was evaporated *in vacuo* to give the $HClO_4$ salt as a solid. The solid was dissolved in MeOH (0.4 mL) and (*E*)-cinnamaldehyde (40.2 µL, 0.32 mmol, 2.0 equiv.) was added at 35 °C and the solution stirred for 1 h. The solvent was evaporated *in vacuo*. The residue was dissolved in a minimum amount of MeOH, the iminium salt was crashed out with Et_2O and the supernatant solution taken off. This purification procedure was repeated two additional times to give iminium salt **35a·ClO_4^-** as a red solid.

M.p. = 137.8 °C decomp.; $[\alpha]_D^{20}$ = +195.3 (c = 0.43 in CD_3CN); ^{1}H NMR (600 MHz, CD_3CN): δ_H = 8.67 (1H, d, J = 10.7, H–C1''), 7.94 (1H, d, J = 15.1, H–C3''), 7.66–7.62 (1H, m, H–C7''), 7.59 (1H, dt, J = 8.0, 0.9, H–C4'), 7.50 (2H, t, J = 7.8, H–C6''), 7.40 (2H, dd, J = 8.2, 1.0, H–C5''), 7.24–7.18 (2H, m, H–C6', H–C7'), 7.14 (1H, ddd, J = 8.0, 6.5, 1.5, H–5'), 6.93 (1H, s, H–C2'), 6.68 (1H, dd, J = 15.0, 10.6, H–C2''), 5.08 (1H, t, J = 5.0, H–C5), 3.81 (1H, dd, J = 15.5, 5.0, H–C8), 3.59 (3H, s, H–C10'), 3.43 (1H, dd, J = 17.8, 6.6, H–C8), 2.78 (3H, d, J = 0.4, H–C7), 1.72 (3H, s, H–C6^{anti}), and 1.14 (3H, s, H–C6^{syn}) ppm; ^{13}C NMR (151 MHz, CD_3CN): δ_C = 167.7 (C1''), 166.0 (C4), 164.6 (C3''), 138.1 (C9'), 135.5 (C7''), 134.2 (C4''), 131.9 (2C, C5''), 130.8 (C2'), 130.6 (2C, C6''), 128.3 (C3'), 123.4 (C8'), 120.6 (C5'), 119.6 (C4'), 118.5 (C2''), 111.0 (C7'), 107.0 (C3'), 86.5 (C2), 64.7 (C5), 33.1 (C10'), 29.3 (C8), 27.3 (C6^{anti}), 26.1 (C7), and 25.6 (C6^{syn}) ppm; IR (ATR): $\tilde{\nu}$ = 3058w, 2939w, 1712s, 1621m, 1604m, 1589s, 1474m, 1455m, 1429m, 1390m, 1324w, 1282w, 1197m, 1180m, 1073s, 1011m, 999m, 932w, 743s, 686m, and 621s cm^{-1}; HR-ESI-MS: m/z: 386.22284 ([M-ClO_4^-]$^+$, calcd for $C_{25}H_{28}N_3O^+$: 386.22324).

8.2.12 Synthesis of (5*S*)-2,2,3-Trimethyl-5-[4-(1*H*-pyrrol-1-yl)benzyl]imidazolidin-4-one (40)

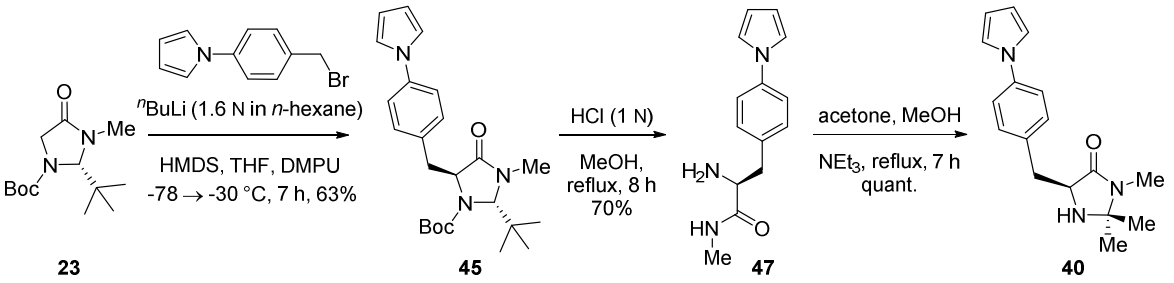

(2*S*,5*S*)-1-Boc-2-(*tert*-butyl)-3-methyl-5-[4-(1*H*-pyrrol-1-yl)benzyl]-4-imidazolidinone (45)

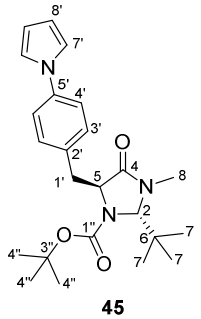

A solution of HMDS (0.42 mL, 2.03 mmol, 1.2 equiv.) in dry THF (1.50 mL) in a flame-dried Schlenck under an atmosphere of argon was cooled to 0 °C. ^{n}BuLi (1.6 N in ^{n}hexane, 1.27 mL, 2.03 mmol, 1.2 equiv.) was added dropwise and the solution stirred for 15 min before it was cooled to –78 °C. DMPU (0.61 mL, 5.08 mmol, 3.0 equiv.) and then (*S*)-Boc-BMI (**23**) (429 mg, 1.69 mmol, 1.0 equiv.) in THF (1.50 mL) was added dropwise to the orange solution that turned darker upon addition. After 30 min, the reaction was diluted with THF (1.50 mL) and 1-[4-(Bromomethyl)phenyl]-1H-pyrrole (400 mg, 1.69 mmol, 1.0 equiv.) was added in small portions over 2 min. The resulting suspension was gradually warmed to –30 °C over 7 h. The reaction was quenched by addition of a saturated aqueous solution of $NaHCO_3$ and extracted three times with CH_2Cl_2. The combined organic layers were dried over $MgSO_4$ and concentrated *in vacuo*. Purification by CC (SiO_2; CH/EtOAc 5:1) gave **45** as a white solid (440 mg, 63%).

R_f = 0.76 (CH/EtOAc 1:1); M.p. = 137.0–138.4 °C; $[\alpha]_D^{20}$: +57.3 (c = 0.94, CH_3OH); ^{1}H NMR (600 MHz, $CDCl_3$): δ = 7.22 (4H, bs, H–C3', H–C4'), 7.06 (2H, t, J = 2.2, H–C8'),

6.33 (2H, t, *J* = 2.2, H–C7'), 4.58 (1H, bs, H–C2), 4.32 (1H, bs, H–C5), 3.86 (1H, bs, H–C1'), 3.21 (1H, dd, *J* = 14.0, 2.2, H–C1'), 2.81 (3H, bs, H–C8), 1.50 (9H, s, H–C4''), and 0.93 (9H, s, H–C7); ^{13}C NMR (151 MHz, $CDCl_3$): δ = 171.4 (C4), 152.8 (C1''), 139.4 (C5'), 133.4 (C2'), 131.4 (2C, C3'), 119.8 (2C, C4'), 119.2 (2C, C7'), 110.4 (2C, C8'), 81.2 (C3''), 81.2 (C2), 60.8 (C5), 41.0 (C6), 33.2 (C1'), 32.0 (C8), 28.4 (3C, C4''), and 26.7 (3C, C7) ppm; IR (ATR): $\tilde{\nu}$ = 2970w, 2932w, 1691s, 1612w, 1522m, 1482w, 1458w, 1437w, 1405w, 1378s, 1362m, 1327m, 1299m, 1254m, 1180m, 1163m, 1118m, 1071m, 1024w, 984w, 944w, 923w, 884w, 867w, 847w, 832w, 792w, 766w, and 722s cm^{-1}; HR-ESI-MS: *m*/*z*: 412.2604 ([*M*+H]$^+$, calcd for $C_{24}H_{34}N_3O_3^+$: 412.2595).

L-4-(1*H*-pyrrol-1-yl)phenylalanine *N*-methyl amide (47)

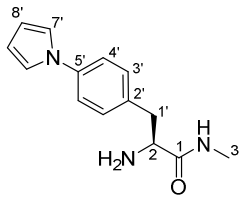

47

To a solution of **45** (339 mg, 0.82 mmol, 1.0 equiv.) in MeOH (7.5 mL) was added an aqueous solution of HCl (1 N, 7.5 mL) at RT and the mixture heated to reflux for 8 h. The reaction was allowed to come to RT and basified to a pH of 10 with an aqueous solution of NaOH (2 N, circa 3.5 mL) and extracted four times with CH_2Cl_2. The combined organic layers were dried over $MgSO_4$ and concentrated *in vacuo* to give as a yellow solid. Filtration over silica (CH_2Cl_2/MeOH 10:1, 300 mL) gave amide **47** as an off-white solid (139 mg, 70%).

R_f = 0.30 (CH_2Cl_2/MeOH 10:1); M.p. = 158.1–159.1 °C; $[\alpha]_D^{23}$: +16.9 (*c* = 0.85, CH_3OH); ^{1}H NMR (400 MHz, $CDCl_3$): δ = 7.33 (2H, d, *J* = 8.5, H–C3'), 7.25 (2H, d, *J* = 8.5, H–C4'), 7.25 (1H, bs, H–C^{amide}), 7.05 (2H, t, *J* = 2.2, H–C8'), 6.33 (2H, t, *J* = 2.2, H–C7'), 3.61 (1H, dd, *J* = 9.1, 4.1, H–C2), 3.26 (1H, dd, *J* = 13.8, 4.1, H–C1'), 2.81 (3H, d, *J* = 5.0, H–C3), 2.73 (1H, dd, *J* = 13.8, 9.1, H–C1'), and 1.59 (2H, bs, H–C^{amine}) ppm; ^{13}C NMR (100 MHz, $CDCl_3$): δ = 174.7 (C4), 139.7 (C5'), 135.4 (C2'), 130.5 (2C, C3'), 120.8 (2C, C4'), 119.4 (2C, C7'), 110.5 (2C, C8'), 56.5 (C5), 40.5 (C1'), and 26.0 (C3) ppm; IR (ATR): $\tilde{\nu}$ = 3365w, 3288w, 2940w, 1640s, 1614m, 1520s, 1479m, 1408m, 1326s, 1255w, 1228w, 1194w,

1152w, 1109w, 1071m, 1017w, 979w, 921m, 880w, 863w, 814s, and 717s cm^{-1}; HR-ESI-MS: *m*/*z*: 269.1497 ([*M*+H]$^+$, calculated for $C_{13}H_{21}N_2O_4^+$: 269,1496).

(5*S*)-2,2,3-Trimethyl-5-[4-(1*H*-pyrrol-1-yl)benzyl]imidazolidin-4-one (40)

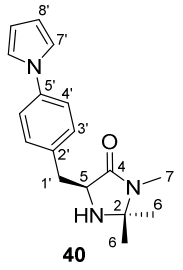

40

To a solution of amide **47** (100 mg, 0.41 mmol, 1.0 equiv.) in MeOH (2.0 mL) were added acetone (0.23 mL, 3.08 mmol, 7.5 equiv.) and NEt_3 (45 µL, 0.33 mmol, 0.8 equiv.) at RT and the solution heated to reflux for 5.5 h. The reaction was allowed to come to RT and concentrated *in vacuo* to give imidazolidinone **40** as a yellow sticky solid (120 mg, quant.).

$[\alpha]_D^{23}$: –45.8 (*c* = 1.03, CH_3OH); ^{1}H NMR (300 MHz, $CDCl_3$): δ = 7.37–7.23 (4H, m, H–C3', H–C4'), 7.06 (2H, t, *J* = 2.2, H–C8'), 6.33 (2H, t, *J* = 2.2, H–C7'), 3.90–3.75 (1H, m, H–C2), 3.16 (1H, dd, *J* = 14.2, 4.4, H–C1'), 3.00 (1H, dd, *J* = 14.3, 6.9, H–C1'), 2.76 (3H, s, H–C3), 1.28 (3H, s, H–C6), and 1.19 (3H, s, H–C6) ppm; ^{13}C NMR (75 MHz, $CDCl_3$): δ = 173.3 (C4), 139.6 (C5'), 134.7 (C2'), 130.7 (2C, C3'), 120.6 (2C, C4'), 119.3 (2C, C7'), 110.4 (2C, C8'), 75.7 (C2), 59.4 (C5), 36.8 (C1'), 27.5 (C7), and 25.4 (2C, C6) ppm; IR (ATR): $\tilde{\nu}$ = 3320w, 2974w, 2928w, 1683s, 1612w, 1520s, 1479m, 1424m, 1397m, 1327s, 1256w, 1183w, 1147w, 1118w, 1070m, 1020w, 923w, 810m, and 727s cm^{-1}; HR-ESI-MS: *m*/*z*: 284.1762 ([*M*+H]$^+$, calcd for $C_{18}H_{21}N_3O^+$: 284.1757).

8.2.13 Syntheses of (5*S*)-2,2,3-Trimethyl-5-(anthracen-3-ylmethyl)-imidazolidin-4-one (41) and 5-(Anthracen-3-ylmethyl)-2,2,3-trimethyl-4-oxo-1-[(*E*)-3-phenylallylidene]-imidazolidin-1-ium salt (41a)

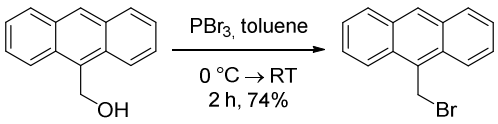

9-Bromomethylanthracene[186]

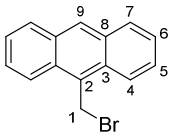

To 9-anthrylmethanol in toluene was added PBr_3 at 0 °C and the yellow solution stirred for 1 h at 0 °C and 1 h at RT. An aqueous solution of Na_2CO_3 (2 N) was added, the organic layer was washed with H_2O and brine, dried over $MgSO_4$ and the solvent evaporated to circa 10 mL. The product crystallized from the solution and the solvent was evaporated *in vacuo*. The product was suspended in Et_2O, filtered off and dried on HV, resulting in bright yellow needles (1.93 g, 74%).

R_f = 0.82 (CH/EtOAc 2:1); 136.3 –139.3 °C; ^{1}H NMR (300 MHz, $CDCl_3$): δ = 8.49 (1H, s, H–C9), 8.30 (2H, d, *J* = 8.9, H–C4), 8.04 (2H, d, *J* = 8.5, H–C7), 7.65 (2H, ddd, *J* = 8.9, 6.5, 1.4, H–C5), 7.51 (2H, ddd, *J* = 8.4, 6.6, 1.2, H–C6), and 5.54 (2H, s, H–C1) ppm; HR-ESI-MS: *m*/*z*: 191.0859 ([*M*–Br]$^+$, calcd for $C_{15}H_{11}^+$: 191.0855); analytical data in agreement with the literature.[186]

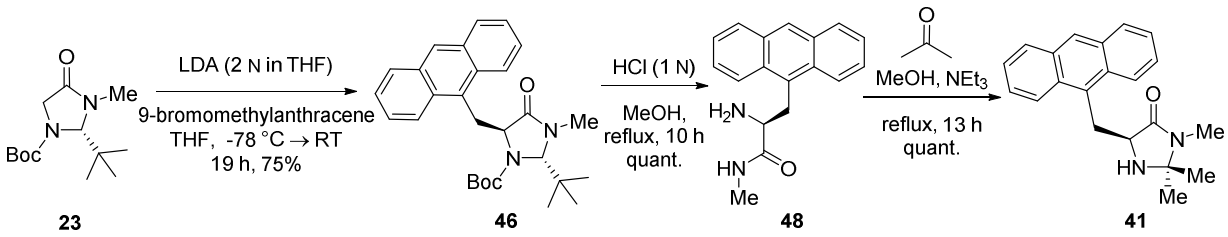

(2*S*,5*S*)-1-Boc-2-(*tert*-butyl)-3-methyl-5-(anthracen-3-ylmethyl)-4-imidazolidinone (46)

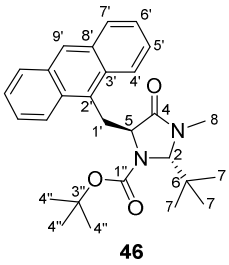

46

A solution of (*S*)-Boc-BMI (**23**) (512 mg, 2.00 mmol, 1.0 equiv.) in dry THF (3.00 mL) in a flame-dried Schlenck under an atmosphere of argon was cooled to –78 °C. LDA (2 N in THF, 1.30 mL, 2.60 mmol, 1.3 equiv.) was added resulting in a dark red solution. After 30 min, 9-bromomethylanthracene (650 mg, 2.40 mmol, 1.2 equiv.) suspended in dry THF (4.00 mL) was added slowly upon which the solution turned orange and precipitate formed slowly. The reaction was gradually warmed from –78 °C to RT over 20 h. The reaction was quenched by addition of saturated aqueous solution of $NaHCO_3$, extracted three times with CH_2Cl_2. The combined organic layers were dried over $MgSO_4$ and concentrated *in vacuo*. Purification by CC (SiO_2; CH/EtOAc 10:1→8:1) gave **46** as an off-white solid (670 mg, 75%).

R_f = 0.37 (CH/EtOAc 3:1); M.p. = 178.7 °C decomp.; $[\alpha]_D^{23}$: –196.2 (*c* = 0.87, CH_3OH); ^{1}H NMR (300 MHz, $CDCl_3$): δ = 8.38 (1H, s, H–C9'), 8.30 (2H, d, *J* = 8.6, H–C4'), 8.00 (2H, d, *J* = 7.5, H–C7'), 7.55–7.39 (4H, m, H–C5', H–C6'), 5.21 (1H, bs, H–C2), 4.93 (1H, dd, *J* = 13.8, 3.1, H–C5), 4.59 (1H, dd, *J* = 10.4, 3.5, H–C1'), 3.67 (1H, dd, *J* = 14.0, 10.4, H–C1'), 2.94 (3H, bs, H–C8), 1.63 (9H, s, H–C4''), and 0.96 (9H, s, H–C7) ppm; ^{13}C NMR (101 MHz, $CDCl_3$, C1'' not visible): δ = 170.7 (C4), 131.6 (3C, C2', C8'), 131.0 (2C, C3'), 129.4 (2C, C4'), 126.9 (C9'), 125.5 (2C, C5' or C6'), 125.0 (2C, C7'), 124.7 (2C, C5' or C6'), 81.8 (C3''), 80.7 (C2), 58.5 (C5), 41.2 (C6), 31.9 (C8), 30.1 (C8), 28.6 (3C, C4''), and 26.5 (3C, C7) ppm; IR (ATR): $\tilde{\nu}$ = 2974w, 2911w, 2261w, 2240w, 1702s, 1690s, 1625w, 1479w, 1456w, 1401w, 1353w, 1378m, 1368m, 1301w, 1252m, 1204w, 1139w, 1117m, 1033w,

966w, 911m, 883w, 850w, 841w, 775w, 722s, and 657w cm^{-1}; HR-ESI-MS: *m*/*z*: 447.2648 ([*M*+H]$^+$, calcd for $C_{28}H_{35}N_2O_3^+$: 447.2642).

(*S*)-2-Amino-3-(anthracen-9-yl)-*N*-methylpropanamide (48)

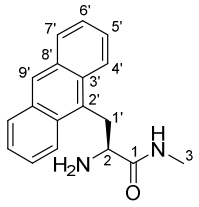

48

To a solution of **46** (600 mg, 1.34 mmol, 1.0 equiv.) in MeOH (15 mL) was added an aqueous solution of HCl (1 N, 15 mL) at RT and the mixture heated to reflux for 10 h. The reaction was allowed to come to RT and basified to a pH of 10 with an aqueous solution of NaOH (2 N) and extracted three times with CH_2Cl_2. The combined organic layers were dried over $MgSO_4$ and concentrated *in vacuo* to give amide **48** as a white solid (374 mg, quant.). The amide was used without purification in the next step.

(5*S*)-2,2,3-Trimethyl-5-(anthracen-3-ylmethyl)-imidazolidin-4-one (41)

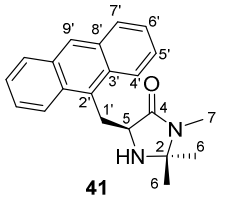

41

To a solution of amide **48** (300 mg, 1.08 mmol, 1.0 equiv.) in MeOH (3.0 mL) was added acetone (0.60 mL, 8.08 mmol, 7.5 equiv.) at RT and the solution heated to reflux for 13 h. The reaction was allowed to come to RT and concentrated *in vacuo* to give imidazolidinone **41** as a white solid (344 mg, quant.).

M.p. = 54.5–55.3 °C; $[\alpha]_D^{23}$: +23.8 (*c* = 0.59, CH_3OH); ^{1}H NMR (300 MHz, $CDCl_3$): δ = 8.45 (2H, d, *J* = 8.9, H–C4'), 8.38 (1H, s, H–C9'), 8.01 (2H, d, *J* = 8.0, H–C7'), 7.55–7.44 (4H, m, H–C5', H–C6'), 4.33 (1H, dd, *J* = 14.6, 3.1, H–C5), 4.10 (1H, dd, *J* = 9.6, 3.1,

H–C1'), 3.81 (1H, dd, *J* = 14.6, 9.7, H–C1'), 2.86 (3H, s, H–C7), 1.36 (3H, s, H–C6), and 1.16 (3H, s, H–C6) ppm; ^{13}C NMR (101 MHz, $CDCl_3$): δ = 173.4 (C4), 134.2 (2C, C2'), 131.7 (2C, C8'), 130.4 (2C, C3'), 129.3 (2C, 74'), 126.7 (C9'), 125.9 (2C, C5' or C6'), 125.1 (2C, C5' or C6'), 124.9 (2C, C4'), 75.8 (C2), 60.1 (C5), 31.1 (C1'), 28.3 (C6), 25.6 (C6), and 25.3 (C7) ppm; IR (ATR): $\tilde{\nu}$ = 3294w, 3056w, 2976w, 2930w, 1667s, 1599m, 1425m, 1398m, 1314m, 1284m, 1197m, 1148m, 1090w, 1039w, 932w, 885w, 841w, 817w, 765w, 732s, and 694m cm^{-1}; HR-ESI-MS: *m/z*: 319.1810 ([*M*+H]$^+$, calcd for $C_{21}H_{23}N_2O^+$: 319.1805).

5-(Anthracen-3-ylmethyl)-2,2,3-trimethyl-4-oxo-1-[(*E*)-3-phenylallylidene]-imidazolidin-1-ium perchlorate (41a·ClO_4^-):

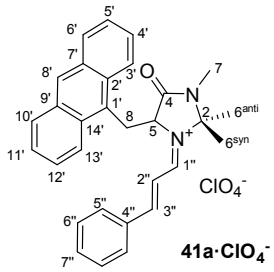

41a·ClO_4^-

To imidazolidinone **41** (25.5 mg, 0.16 mmol, 1.0 equiv.) in Et_2O/EtOH (1:1, 0.40 mL) was added perchloric acid (60% in H_2O, 26.80 mg, 0.16 mmol, 1.0 equiv.) at RT and the resulting mixture stirred for 10 min before it was evaporated *in vacuo* to give the imidazolidinone salt. The salt was redissolved in MeOH (0.40 mL) and (*E*)-cinnamaldehyde (40.2 µL, 0.32 mmol, 2.0 equiv.) was added and the yellow solution stirred for 12 h at RT during which time the colour changed. The solvent was removed *in vacuo* and the residue dissolved in a minimum amount of MeOH. From this solution the iminium salt **41a·ClO_4^-** was crashed out as a yellow solid with Et_2O and the supernatant solution taken off and the product dried on HV.

M.p. = 239–242 °C decomp.; $[\alpha]_D^{23}$ = –53.1 (*c* = 1.01 in CD_3CN); ^{1}H NMR (600 MHz, CD_3CN): δ_H = 8.61 (1H, dd, *J* = 3.4, 2.2, H–C1''), 7.62 (1H, dd, *J* = 7.7, 0.6, H–C3'), 7.52 (1H, dd, *J* = 7.3, 1.1, H–C10')´, 7.34 (1H, td, *J* = 7.6, 1.3, H–C5'), 7.26 (1H, td, *J* = 7.5, 1.1, H–C11'), 7.22–7.20 (3H, m, H–C6'', H–C7''), 7.18 (1H, td, *J* = 7.6, 1.3, H–C12'), 7.16 (1H, td, *J* = 7.5, 1.1, H–C4'), 6.99 (1H, dd, *J* = 7.3, 1.1, H–C6'), 6.91 (1H, dd, *J* = 7.6, 0.5, H–

C13'), 6.75–6.70 (2H, m, H–C5''), 5.08–5.01 (1H, m, H–C5), 4.53 (1H, d, *J* = 2.8, H–C8'), 3.93 (1H, dd, *J* = 4.9, 2.8, H–C3''), 3.79 (1H, dd, *J* = 14.6, 11.7, H–C8), 3.38 (1H, dd, *J* = 14.4, 4.5, H–C8), 3.31 (1H, dt, *J* = 4.9, 2.4, H–C2''), 2.99 (3H, d, *J* = 0.8, H–C7), 1.67 (3H, s, H–C6^{anti}), and 1.41 (3H, s, H–C6^{syn}) ppm; ^{13}C NMR (151 MHz, CD_3CN): δ_C = 182.4 (C1''), 165.1 (C4), 144.9 (C9'), 142.1 (C7'), 142.0 (C2'), 141.9 (C4''), 141.4 (C14'), 129.3 (C6''), 128.6 (C11'), 128.5 (C5''), 128.2 (C7''), 127.9 (C4'), 127.6 (C5'), 127.5 (C6'), 127.4 (C12'), 126.2 (C10'), 123.0 (C3'), 122.8 (C13'), 87.2 (C2), 57.6 (C5), 52.5 (C2''), 52.4 (C8'), 52.2 (C3''), 45.6 (C1'), 26.4 (C7), 25.2 (C6^{syn}), 25.1 (C6^{anti}), and 23.2 (C8) ppm; IR (ATR): $\tilde{\nu}$ = 3011w, 2919w, 1721s, 1681w, 1455m, 1435w, 1403m, 1381w, 1290w, 1219w, 1191w, 1168w, 1072s, 1019w, 984w, 964w, 767m, 758m, 749w, 707m, 726w, 675w, and 660w cm^{-1}; HR-ESI-MS: *m*/*z*: 433.2270 ([*M*-ClO_4^-]$^+$, calcd for $C_{30}H_{29}N_2O^+$: 433.2274).

8.2.14 Syntheses of (5*S*)-5-Cyclohexylmethyl-2,2,3-trimethyl-4-imidazolidinone (42) and (5*S*)-5- Cyclohexylmethyl -2,2,3-trimethyl-4-oxo-1-[(*E*)-3-phenylallylidene]-imidazolidin-1-ium salt (42a)

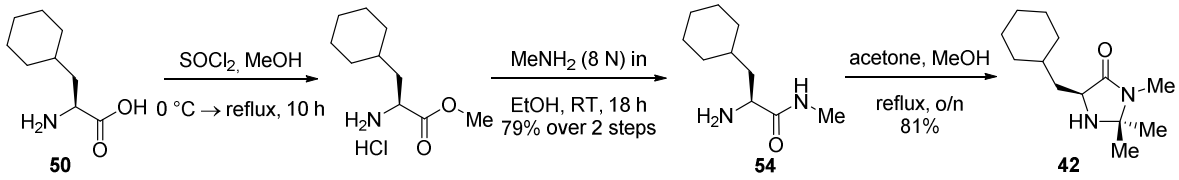

(*S*)-2-Amino-3-cyclohexyl-*N*-methylpropanamide (54)

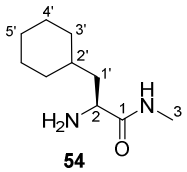

To a suspension of (2*S*)-2-amino-3-cyclohexylpropanoic acid hydrate (2.50 g, 14.6 mmol, 1.0 equiv.) in MeOH (12.0 mL, 292 mmol, 20 equiv.) was added thionyl chloride (1.30 mL, 17.5 mmol, 1.2 equiv.) over 5 min at 0 °C and the resulting solution was allowed to come to RT before it was heated to reflux for 10 h. The solution was allowed to come to RT and evaporated *in vacuo* to give the methyl ester hydrochloride as a white solid. To the ester was added $MeNH_2$ (8 N in EtOH, 7.30 mL, 58.4 mmol, 4.0 equiv.) at RT and the solution stirred for 18 h. The reaction was concentrated *in vacuo* and a saturated aqueous solution of $NaHCO_3$ was added. The aqueous layer was extracted three times with CH_2Cl_2 and the combined organic layers were dried over $MgSO_4$, filtrated and concentrated *in vacuo* to give amide **54** as a white solid (2.06 g, 77%).

M.p. = 77.3–79.1 °C; $[\alpha]_D^{23}$: +15.1 (*c* = 1.00, CH_3OH); ^{1}H NMR (300 MHz, $CDCl_3$): δ = 7.31 (1H, b, H–N^{amide}), 3.41 (1H, dd, *J* = 9.8, 3.9, H–C2),2.80 (3H, d, *J* = 5.0, H–C3), 1.91–1.55 (6H, m, H–C1', 5·H–$C^{cyclohexyl}$), 1.49 (2H, b, H–N^{amine}), 1.41–1.12 (5H, m, H–C1', H–C2', 5·H–$C^{cyclohexyl}$), and 1.06–0.82 (2H, m, 2·H–$C^{cyclohexyl}$) ppm; ^{13}C NMR (101 MHz, $CDCl_3$): δ = 176.5 (C1), 52.9 (C2), 42.9 (C1'), 34.5 (C2'), 34.3 ($C^{cyclohexyl}$), 32.2 ($C^{cyclohexyl}$), 26.6 ($C^{cyclohexyl}$), 26.5 ($C^{cyclohexyl}$), 26.2 ($C^{cyclohexyl}$) and 25.9 (C3) ppm; IR (ATR): $\tilde{\nu}$ = 3395w, 3311m, 2921s, 2844m, 17332w, 1636s, 1531s, 1452m, 1400m, 1348w, 1309w, 1284w, 1220w, 1171w, 1156m, 1092w, 984w, 963w, 912w, 890w, 879w, 843m, 819m,

785w, 760.2w, 709m, and 674 cm^{-1}; HR-ESI-MS: *m*/*z*: 185.1648 ([*M*+H]$^+$, calcd for $C_{10}H_{21}N_2O^+$: 185.1648).

(5*S*)-5-Cyclohexylmethyl-2,2,3-trimethyl-4-imidazolidinone (42)

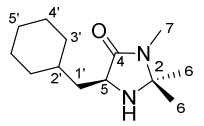

42

To a solution of amide **54** (1.96 g, 10.6 mmol, 1.0 equiv.) in MeOH (20.0 mL) was added acetone (4.0 mL, 53.2 mmol, 5.0 equiv.) at RT under an atmosphere of argon and the solution heated to reflux overnight. The reaction was allowed to come to RT and concentrated *in vacuo* to give imidazolidinone **42** as a white solid (1.94 g, 81%).

M.p. = 101.3–101.9 °C; $[\alpha]_D^{20}$: –22.2 (*c* = 1.02, CH_3OH); ^{1}H NMR (400 MHz, $CDCl_3$): δ = 3.48 (1H, dd, *J* = 10.1, 3.4, H–C5), 2.74 (3H, s, H–C7), 1.89–1.73 (2H, m, H–C1', H–C^{cyclohexyl}), 1.72–1.56 (5H, m, H–N^{amine}, H–C^{cyclohexyl}), 1.54–1.42 (1H, m, H–C2'), 1.37 (3H, s, H–C6), 1.26 (3H, s, H–C6), 1.30–1.04 (4H, m, H–C1', H–C^{cyclohexyl}), and 1.03–0.79 (2H, m, H–C^{cyclohexyl}) ppm; ^{13}C NMR (101 MHz, $CDCl_3$): δ = 175.3 (C4), 75.6 (C2), 59.1 (C5), 40.6 (C1'), 34.7 (C2'), 34.3 (C^{cyclohexyl}), 32.2 (C^{cyclohexyl}), 27.5 (C6), 26.5 (C^{cyclohexyl}), 26.3 (C^{cyclohexyl}), 26.1 (C^{cyclohexyl}), 25.3 (C7), and 24.8 (C6) ppm; IR (ATR): $\tilde{\nu}$ = 3324w, 3267w, 2970w, 2918s, 2847m, 1677s, 1475w, 1445m, 1424m, 1398s, 1333w, 1260w, 1208w, 1150m, 1082w, 997w, 919w, 857w, 810w, 794w, 744w, and 666w cm^{-1}; HR-ESI-MS: *m*/*z*: 225.1958 ([*M*+H]$^+$, calcd for $C_{14}H_{25}N_2O^+$: 225.1961).

(5*S*)-5-Cyclohexylmethyl-2,2,3-trimethyl-4-oxo-1-[(*E*)-3-phenylallylidene]-imidazolidin-1-ium salt (42a·ClO_4^-):

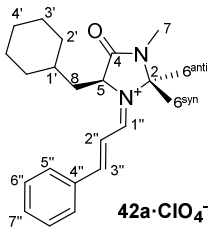

To imidazolidinone **42** (18.0 mg, 0.08 mmol, 1 equiv.) was added perchloric acid (60% in H_2O, 14.4 mg, 0.08 mmol, 1 equiv.) in EtOH/Et_2O (1:1, 0.40 mL) at RT and the resulting mixture stirred for 10 min before it was evaporated *in vacuo* to give the imidazolidinone salt. The salt was redissolved in MeOH (0.20 mL) and heated to 35 °C. (*E*)-cinnamaldehyde (20.1 µL, 0.16 mmol, 2 equiv.) was added and the yellow solution stirred for 1 h. The solvent was removed *in vacuo* and the residue dissolved in a minimum amount of MeOH. From this solution the iminium salt was crashed out with Et_2O and the supernatant solution taken off. The washing procedure was repeated and the iminium salt **42a·ClO_4^-** isolated as a yellow solid.

^{1}H NMR (600 MHz, CD_3CN): δ_H = 8.77 (1H, dd, *J* = 10.6, 1.8, H–C1''), 8.15 (1H, d, *J* = 15.1, H–C3''), 7.87 (2H, d, *J* = 7.2, H–C5''), 7.71 (1H, tt, *J* = 7.3, 1.2, H–C7''), 7.61 (2H, t, *J* = 7.6, H–C6''), 7.11 (1H, dd, *J* = 15.1, 10.6, H–C2''), 4.82 (1H, d, *J* = 9.4, H–C5), 2.90 (3H, d, *J* = 0.6, H–C7), 1.82 (3H, s, H–C6), 1.78 (3H, s, H–C6), 2.10–1.55 (7H, m, H–C8, H–$C^{cyclohexyl}$), and 1.40–0.93 (6H, m, H–$C^{cyclohexyl}$) ppm; ^{13}C NMR (151 MHz, CD_3CN): δ_C = 168.2 (C1''), 166.7 (C3''), 165.2 (C4), 136.1 (C7''), 134.8 (C1'), 134.4 (C4''), 132.5 (2C, C5''), 131.1 (2C, C2'), 130.7 (2C, C6''), 130.1 (2C, C3'), 129.2 (C4'), 118.4 (C2''), 86.5 (C2), 65.2 (C5), 37.2 (C8), 27.5 ($C6^{anti}$), 26.1 (C7), and 24.8 ($C6^{syn}$) ppm; HR-ESI-MS: *m*/*z*: 339.2426 ([*M*-ClO_4^-]$^+$, calcd for $C_{22}H_{31}N_2O^+$: 339.2431).

8.2.15 Syntheses of (5*S*)-5-(Indol-3-ylmethyl)-2,2,3-trimethyl-4-imidazolidinone (43) and (*S*)-5-(Indol-3-ylmethyl)-2,2,3-trimethyl-4-oxo-1-[(*E*)-3-phenylallylidene]-imidazolidin-1-ium salt (43a)

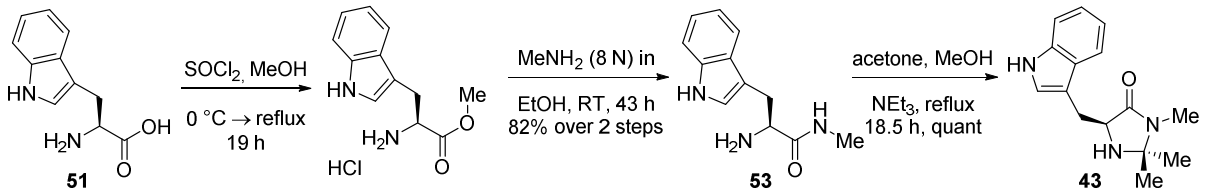

_L_-Tryptophan methyl amide (53)

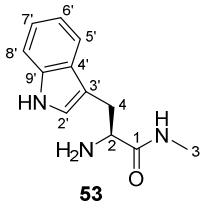

To *L*-tryptophan (1.00 g, 4.90 mmol, 1.0 equiv.) in MeOH (5.00 mL, 123 mmol, 25 equiv.) was added thionyl chloride (0.43 mL, 5.88 mmol, 1.2 equiv.) over 10 min at 0 °C and the resulting mixture was allowed to come to RT before it was heated to reflux for 19 h. The solution was allowed to come to RT and evaporated *in vacuo* to give the tryptophan methyl ester hydrochloride as an off-white solid. To the ester was added $MeNH_2$ (8 N in EtOH, 2.50 mL, 19.6 mmol, 4.0 equiv.) at RT and the solution stirred for 42.5 h. After evaporation *in vacuo*, the crude product was dissolved in sat. aq. solution of $NaHCO_3$ (20 mL) and $CHCl_3$, the aqueous layer was extracted with $CHCl_3$ (3·30 mL), the combined organic layers were dried over $MgSO_4$ and concentrated *in vacuo* to give amide **53** as an orange sticky solid (868 mg, 82%).

M.p. = 96.2–99.1 °C; $[\alpha]_D^{23}$: +11.0 (c = 0.75, CH_3OH); ^{1}H NMR (400 MHz, CDCl3): δ = 8.31 (1H, b, H–N^{Ar}), 7.67 (1H, d, *J* = 7.6, H–C5'), 7.38 (1H, d, *J* = 7.9, H–C8'), 7.26 (1H, b, H–N^{amide}), 7.20 (1H, t, *J* = 7.4, H–C7'), 7.12 (1H, t, *J* = 7.2, H–C6'), 7.06 (1H, s, H–C2'), 3.72 (1H, dd, *J* = 8.4, 3.4, H–C2), 3.40 (1H, dd, *J* = 14.4, 3.2, H–C4), 2.92 (1H, dd, *J* = 14.3, 9.1, H–C4), 2.81 (3H, d, *J* = 4.4, H–C3), and 1.45 (2H, b, H–N^{amine}) ppm; ^{13}C NMR (101 MHz, $CDCl_3$): δ = 175.59 (C1), 136.56 (C9'), 127.67 (C4'), 123.18 (C2'), 122.38 (C7'), 119.72 (C6'), 119.12 (C5'), 112.03 (C3'), 111.38 (C8'), 55.78 (C2), 30.95 (C4), and 25.97 (C3) ppm; IR (ATR): $\tilde{\nu}$ = 3274m, 2922w, 1643s, 1533s, 1456m, 1436m, 1409m,

1232w, 1158w, 1101w, 1010w, 908w, 848, and 739s cm^{-1}; HR-EI-MS: *m/z*: 218.1278 ([*M*+H]$^+$, calcd for $C_{12}H_{16}N_3O^+$: 218.1288); analytical data in agreement with the literature.[142]

(5*S*)-5-(Indol-3-ylmethyl)-2,2,3-trimethyl-4-imidazolidinone (43)

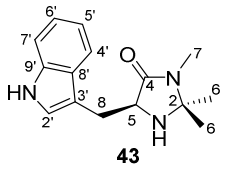

43

To a solution of amide **53** (432 mg, 2.0 mmol, 1.0 equiv.) in MeOH (8.0 mL) was added acetone (1.1 mL, 14.9 mmol, 7.5 equiv.) and NEt_3 (0.22 mL, 1.59 mmol, 0.8 equiv.) at RT under an atmosphere of argon and the yellow solution was heated to reflux overnight. The reaction was allowed to come to RT and concentrated *in vacuo* to give imidazolidinone **43** as a yellow sticky solid (516 mg, quant.).

M.p. = 109.6–110.8 °C; $[\alpha]_D^{20}$: – 66.3 (c = 0.98, CH_3OH); ^{1}H NMR (400 MHz, $CDCl_3$): δ = 8.07 (1H, b, H–N^{Ar}), 7.67 (1H, d, *J* = 7.8, H–C4'), 7.36 (1H, d, *J* = 8.1, H–C7'), 7.19 (1H, dd, *J* = 7.5, 0.9, H–C6'), 7.16–7.09 (2H, m, H–C5', H–C2'), 3.85 (1H, t, *J* = 5.2, H–C5), 3.33 (1H, dd, *J* = 15.1, 4.6, H–C8), 3.21 (1H, dd, *J* = 15.0, 5.8, H–C8), 2.73 (3H, s, H–C7), 1.25 (3H, s, H–C6), and 1.07 (3H, s, H–C6) ppm; ^{13}C NMR (101 MHz, $CDCl_3$): δ = 174.2 (C4), 136.3 (C9'), 128.1 (C8'), 123.4 (C2'), 122.3 (C6'), 119.8 (C5'), 119.1 (C4'), 111.2 (C7'), 110.9 (C3'), 75.6 (C2), 59.1 (C5), 27.1 (C6), 26.5 (C8), 25.4 (C7), and 25.3 (C6); IR (ATR): $\tilde{\nu}$ = 3262bw, 2976w, 2926w, 1668s, 1429m, 1400m, 1367w, 1339w, 1257w, 1208w, 1185w, 1148w, 1090w, 1010w, 923w, 878w, 796w, and 739s cm^{-1}; HR-ESI-MS: *m/z*: 258.1597 ([*M*+H]$^+$, calculated for $C_{15}H_{20}N_3O^+$: 258.1601).

(5*S*)-5-(Indol-3-ylmethyl)-2,2,3-trimethyl-4-imidazolidinone hydrochloride (43·HCl)

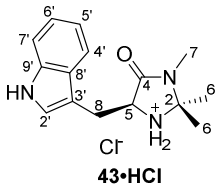

43•HCl

Imidazolidinone **43** (50 mg, 194 µmol, 1.0 equiv.) was dissolved in HCl in MeOH (1.25 N, 0.62 mL, 775 µmol, 4.0 equiv.) and stirred for 30 min at RT. The solution was concentrated *in vacuo* to give **43·HCl** as a red sticky oil (57 mg, quant.).

Crystals suitable for X-ray crystallographic analysis were achieved by vapour exchange of a methanolic solution of **43·HCl** with Et_2O.

M.p. = 64.4 °C decomp.; $[\alpha]_D^{23}$: –78.1 (c = 0.64, CH_3OH); ^1H NMR (400 MHz, $CDCl_3$): δ = 7.65 (1H, d, *J* = 7.9, H–C4'), 7.44–7.37 (2H, m, H–C7', H–C2'), 7.15 (1H, t, *J* = 7.2, H–C6'), 7.07 (1H, t, *J* = 7.1, H–C5'), 4.67 (1H, dd, *J* = 10.5, 3.5, H–C5), 3.65 (1H, dd, *J* = 15.7, 3.4, H–C8), 3.31 (1H, m, H–C8), 2.89 (3H, s, H–C7), 1.69 (3H, s, H–C6), and 1.56 (3H, s, H–C6) ppm; ^{13}C NMR (101 MHz, $CDCl_3$): δ = 168.1 (C4), 138.4 (C9'), 127.8 (C8'), 125.5 (C2'), 123.0 (C6'), 120.3 (C5'), 119.1 (C4'), 112.7 (C7'), 108.4 (C3'), 79.0 (C2), 58.8 (C5), 25.7 (C7 or C8), 25.6 (C7 or C8), 24.3 (C6), and 22.4 (C6); IR (ATR): $\tilde{\nu}$ = 3256b, 2920w, 2698b, 1695s, 1621w, 1423m, 1393m, 1265w, 1234w, 1157w, 1101w, 1071w, 1010w, 928w, 850w, 791w, 744s, and 668 cm^{-1}.

(*S*)-5-(Indol-3-ylmethyl)-2,2,3-trimethyl-4-oxo-1-[(*E*)-3-phenylallylidene]-imidazolidin-1-ium perchlorate (43a·ClO_4^-)

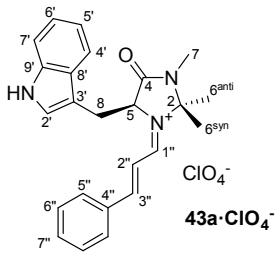

43a·ClO_4^-

To imidazolidinone **43** (20.3 mg, 0.08 mmol, 1.0 equiv.) in Et_2O (0.1 mL) was added $HClO_4$ (70% in H_2O, 11.5 mg, 0.08 mmol, 1.0 equiv.) in EtOH/Et_2O (1:1, 0.2 mL) at RT and stirred

for 10 min, before the solution was evaporated *in vacuo* to give the $HClO_4$ salt as a solid. The solid was dissolved in MeOH (0.2 mL) and (*E*)-cinnamaldehyde (20.1 µL, 0.16 mmol, 2.0 equiv.) was added at 35 °C and the solution stirred for 1 h. The solvent was evaporated *in vacuo*. The residue was dissolved in a minimum amount of MeOH, the iminium salt was crashed out with Et_2O and the supernatant solution taken off. This purification procedure was repeated two additional times to give iminium salt **43a·ClO$_4^-$** as a red solid.

M.p. = 135.1 °C decomp.; $[\alpha]_D^{23}$ = +522.9 (*c* = 0.77 in CH_3CN); ^{1}H NMR (400 MHz, CD_3CN): δ_H = 9.30 (1H, bs, H–N^{Ar}), 8.65 (1H, dd, *J* = 10.7, 1.8, H–C1''), 7.95 (1H, d, *J* = 15.1, H–C3''), 7.67–7.57 (2H, m, H–C7'', H–C4'), 7.50 (2H, t, *J* = 7.8, H–C6''), 7.43 (2H, d, *J* = 7.4, H–C5''), 7.29 (1H, d, *J* = 8.0, H–7'), 7.21–7.10 (2H, m, H–C6', H–C5'), 7.00 (1H, d, *J* = 2.5, H–2'), 6.78 (1H, dd, *J* = 15.0, 10.7, H–C2''), 5.11 (1H, t, *J* = 5.0, H–C5), 3.83 (1H, dd, *J* = 15.4, 5.1, H^{si}–C8), 3.47 (1H, dd, *J* = 15.4, 6.0, H^{re}–C8), 2.78 (3H, s, H–C7), 1.71 (3H, s, H–C6^{anti}), and 1.07 (3H, s, H–C6^{syn}) ppm; ^{13}C NMR (151 MHz, CD_3CN): δ_C = 167.7 (C1''), 166.0 (C4), 164.9 (C3''), 137.5 (C9'), 135.6 (C7''), 134.2 (C4''), 132.0 (2C, C5''), 130.6 (2C, C6''), 127.9 (C8'), 126.7 (C2'), 123.5 (C7'), 120.8 (C5'), 119.4 (C4'), 118.3 (C2''), 112.9 (C7'), 108.0 (C3'), 86.5 (C2), 64.6 (C5), 29.3 (C8), 27.3 (C6^{anti}), 26.1 (C7), and 25.5 (C6^{syn}) ppm; IR (ATR): $\tilde{\nu}$ = 3359w, 3059w, 1709m, 1621m, 1603m, 1588s, 1456w, 1429w, 1390m, 1341w, 1312w, 1281w, 1233w, 1155w, 1197m, 1179m, 1071s, 999m, 931w, 866w, 745s, and 684w cm^{-1}; HR-ESI-MS: *m/z*: 372.2073 ([*M*–ClO_4^-]$^+$, calcd for $C_{24}H_{26}N_3O^+$: 372.2070).

^{1}H NMR and ^{13}C NMR counterion-effect study in CD_3CN at RT

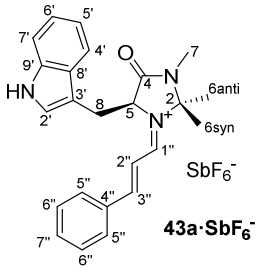

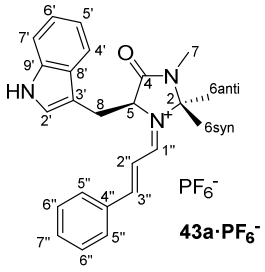

(*S*)-5-(Indol-3-ylmethyl)-2,2,3-trimethyl-4-oxo-1-[(*E*)-3-phenylallylidene]-imidazolidin-1-ium hexafluorophosphat (43a·SbF$_6^-$):

^{1}H NMR (400 MHz, CD_3CN): δ_H = 9.31 (1H, bs, H–N^{Ar}), 8.63 (1H, dd, *J* = 10.6, 1.1, H–C1''), 7.94 (1H, d, *J* = 15.0, H–C3''), 7.64 (1H, t, *J* = 7.3, H–C7''), 7.59 (1H, d, *J* = 7.8, H–C4'), 7.50 (2H, t, *J* = 7.7, H–C6''), 7.43 (2H, d, *J* = 7.4, H–C5''), 7.29 (1H, d, *J* = 8.0, H–7'), 7.20–7.11 (2H, m, H–C6', H–C5'), 7.00 (1H, d, *J* = 2.1, H–2'), 6.77 (1H, dd, *J* = 15.0, 10.7, H–C2''), 5.11 (1H, t, *J* = 4.7, H–C5), 3.83 (1H, dd, *J* = 15.4, 5.0, H^{si}–C8), 3.47 (1H, dd, *J* = 15.4, 6.0, H^{re}–C8), 2.78 (3H, s, H–C7), 1.71 (3H, s, H–$C6^{anti}$), and 1.08 (3H, s, H–$C6^{syn}$) ppm; ^{13}C NMR (151 MHz, CD_3CN): δ_C = 167.6 (C1''), 166.0 (C4), 164.8 (C3''), 137.4 (C9'), 135.5 (C7''), 134.2 (C4''), 132.0 (2C, C5''), 130.5 (2C, C6''), 127.9 (C8'), 126.6 (C2'), 123.5 (C7'), 120.8 (C5'), 119.3 (C4'), 118.3 (C2''), 112.8 (C7'), 107.9 (C3'), 86.5 (C2), 64.6 (C5), 29.2 (C8), 27.2 ($C6^{anti}$), 26.1 (C7), and 25.4 ($C6^{syn}$) ppm.

(*S*)-5-(Indol-3-ylmethyl)-2,2,3-trimethyl-4-oxo-1-[(*E*)-3-phenylallylidene]-imidazolidin-1-ium hexafluoroantimonat (43a·PF_6^-)

Crystals suitable for X-ray crystallographic analysis were achieved by vapour exchange of a solution of **43·PF_6^-** in CH_2Cl_2/^{n}heptane/CH_3CN (2:1:1) with Et_2O.

M.p. = 179.7–180.5 °C; ^{1}H NMR (400 MHz, CD_3CN): δ_H = 9.31 (1H, bs, H–N^{Ar}), 8.63 (1H, dd, *J* = 10.7, 1.7, H–C1''), 7.94 (1H, d, *J* = 15.1, H–C3''), 7.64 (1H, t, *J* = 7.5, H–C7''), 7.59 (1H, d, *J* = 7.9, H–C4'), 7.50 (2H, t, *J* = 7.8, H–C6''), 7.43 (2H, d, *J* = 7.3, H–C5''), 7.29 (1H, d, *J* = 7.9, H–7'), 7.19–7.13 (2H, m, H–C6', H–C5'), 7.00 (1H, d, *J* = 2.5, H–2'), 6.77 (1H, dd, *J* = 15.0, 10.7, H–C2''), 5.11 (1H, t, *J* = 4.8, H–C5), 3.83 (1H, dd, *J* = 15.4, 5.0, H^{si}–C8), 3.47 (1H, dd, *J* = 15.4, 6.0, H^{re}–C8), 2.78 (3H, s, H–C7), 1.71 (3H, s, H–$C6^{anti}$), and 1.08 (3H, s, H–$C6^{syn}$) ppm; ^{13}C NMR (151 MHz, CD_3CN): δ_C = 167.6 (C1''), 166.1 (C4), 164.9 (C3''), 137.5 (C9'), 135.6 (C7''), 134.2 (C4''), 132.0 (2C, C5''), 130.6 (2C, C6''), 127.9 (C8'), 126.7 (C2'), 123.5 (C7'), 120.8 (C5'), 119.4 (C4'), 118.3 (C2''), 112.9 (C7'), 108.0 (C3'), 86.6 (C2), 64.7 (C5), 29.3 (C8), 27.3 ($C6^{anti}$), 26.1 (C7), and 25.5 ($C6^{syn}$) ppm.

8.2.16 Synthesis of (5S)-5-[(1H-Imidazol-5-yl)methyl]-2,2,3-trimethylimidazolidin-4-one (44)

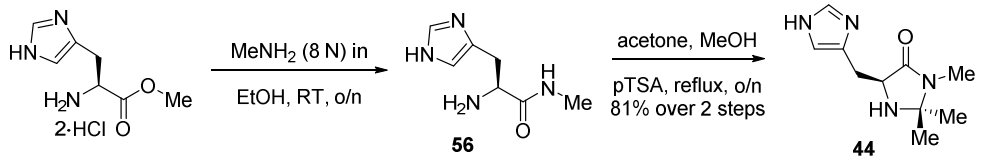

(5*S*)-5-[(1*H*-Imidazol-5-yl)methyl]-2,2,3-trimethylimidazolidin-4-one (44)[135a]

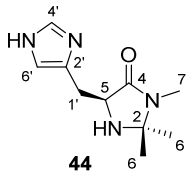

To L-histidine methyl ester dihydrochloride (1.00 g, 4.13 mmol, 1.0 equiv.) was added $MeNH_2$ (8 N in EtOH, 2.1 mL, 16.8 mmol, 4.1 equiv.) at RT and the solution stirred overnight. After concentration *in vacuo*, the residue was redissolved in H_2O (10 mL) and CH_2Cl_2 (10 mL), and $NaHCO_3$ (3.5 g) was added. The aqueous layer was washed twice with CH_2Cl_2 (2·10 mL) and evaporated to dryness. The product was dissolved in MeOH and the insoluble inorganic salts filtered of. Evaporation to dryness gave the product, which was used without further purification in the next step. Amide **56** was dissolved in MeOH (8.0 mL) and acetone (1.50 mL, 20.7 mmol, 5.0 equiv.) and pTSA·H_2O (7.9 mg, 0.04 mmol, 0.01 equiv.) were added at RT under an atmosphere of argon. The suspension was heated to reflux overnight, allowed to come to RT and concentrated *in vacuo*. To the residue was added CH_2Cl_2, the remaining inorganic salts removed by filtration, and the orange solution concentrated *in vacuo* to give imidazolidinone **44** as an orange oil (696 mg, 81%).

$[\alpha]_D^{23}$ = –37.5 (*c* = 1.25 in CD_3CN); ^{1}H NMR (300 MHz, $CDCl_3$): δ = 7.55 (1H, s, H–C4'), 6.88 (1H, s, H–C6'), 3.76 (1H, d, *J* = 5.3, H–C5), 3.10 (1H, dd, *J* = 15.3, 4.4, H–C1'), 2.98 (1H, dd, *J* = 14.9, 6.4, H–C1'), 2.87 (3H, s, H–C7), 1.32 (3H, s, H–C6), and 1.31 (3H, s, H–C6) ppm; IR (ATR): $\tilde{\nu}$ = 3223b, 2976m, 1666s, 1432m, 1403m, 1259w, 1208w, 1149m, 1086w, 1032w, 987w, 936w, 824w, and 661w cm^{-1}; HR-ESI-MS: *m*/*z*: 209.1398 ([*M*+*H*]$^+$, calcd for $C_{10}H_{17}N_4O^+$: 209.1397); analytical data in agreement with the literature.[135a]

8.2.17 Synthesis of (5*S*)-2,2,3-Trimethyl-5-(phenylethyl)imidazolidin-4-one (59)

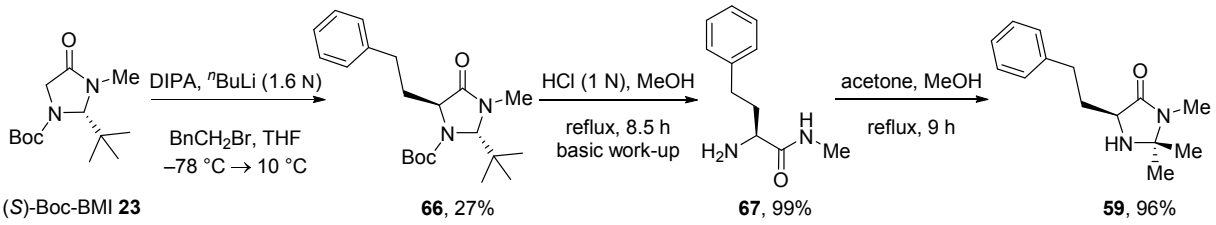

(2*S*,5*S*)-1-Boc-2-(*tert*-butyl)-3-methyl-5-(phenylethyl)-4-imidazolidinone (66)

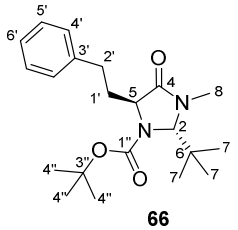

66

To a solution of DIPA (0.47 mL, 3.32 mmol, 1.2 equiv.) in dry THF (4.00 mL) in a flame-dried Schlenck under an atmosphere of argon at –78 °C was added ^{n}BuLi (1.6 N in ^{n}hexane, 2.10 mL, 3.32 mmol, 1.2 equiv.) and the solution stirred for 30 min. Then (*S*)-Boc-BMI **23** (700 mg, 2.76 mmol, 1.0 equiv.) in THF (4.00 mL) was added dropwise to the solution that turned red upon addition. After 30 min, (2-bromomethyl)benzene (0.38 mL, 2.76 mmol, 1.0 equiv.) was added slowly and the resulting mixture stirred for 6 h at –78 °C before it was gradually warmed to 10 °C and stirred overnight at 10 °C. The reaction was quenched by addition of a saturated aqueous solution of $NaHCO_3$ (4 mL) and extracted with CH_2Cl_2 (3·10 mL). The combined organic layers were dried over $MgSO_4$ and concentrated *in vacuo*. Purification by CC (SiO_2; CH/EtOAc 3:1) gave **66** as an off-white solid (269 mg, 27%).

R_f = 0.42 (CH/EtOAc 3:1); M.p. = 111.2–112.9 °C; $[\alpha]_D^{20}$: +11.7 (*c* = 0.91, CH_3OH); ^{1}H NMR (400 MHz, $CDCl_3$): δ = 7.25 (2H, t, *J* = 7.4, H–C5'), 7.21–7.10 (3H, m, H–C4', H–C6'), 5.01 (1H, bs, H–C52), 4.13 (1H, d, *J* = 2.8, H–C5), 2.99 (3H, s, H–C8), 2.73 (1H, bs, H–C1'), 2.34 (1H, d, *J* = 11.2, C2'), 2.30–2.13 (2H, m, H–C1', H–C2'), 1.52 (s, 9H, H–C4'), and 0.98 (s, 9H, H–C7) ppm; ^{13}C NMR (100 MHz, $CDCl_3$): δ = 172.0 (C4), 153.5 (b, C1''), 141.3 (C3'), 128.6 (2C, C4'), 128.4 (2C, C5'), 126.0 (C6'), 81.1 (C2), 76.6 (C3''), 59.5 (C5), 40.9 (C6), 31.9 (C8), 31.1 (b, C1'), 29.5 (C2'), 28.4 (3C, C4''), and 26.6 (3C, C7) ppm; IR (ATR): $\tilde{\nu}$ = 2972w, 2933w, 1693s, 1603w, 1477w, 1454w, 1407m, 1362m, 1378m, 1330w, 1294w, 1257m, 1166m, 1133m, 1087w, 1066w, 1032w, 996w, 896w, 868w,

784w, 771w, 754w, 721w, 706w, and 696w cm^{-1}; HR-ESI-MS: *m*/*z*: 361.2487 ([*M*+H]$^+$, calcd for $C_{21}H_{33}N_2O_3^+$: 361.2486).

(*S*)-2-Amino-*N*-methyl-4-phenylbutanamide (67)

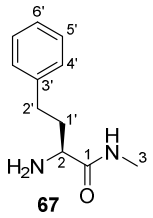

67

To a solution of **66** (220 mg, 0.61 mmol, 1.0 equiv.) in MeOH (5.0 mL) was added an aqueous solution of HCl (1 N, 5.0 mL) at RT and the mixture heated to reflux for 8.5 h. The reaction was allowed to come to RT and basified to a pH of 10 with an aqueous solution of NaOH (2 N) and extracted three times with CH_2Cl_2. The combined organic layers were dried over $MgSO_4$ and concentrated *in vacuo* to give amide **67** as an yellowish oil (120 mg, quant).

$[\alpha]_D^{23}$: +12.0 (*c* = 0.92, CH_3OH); ^{1}H NMR (400 MHz, $CDCl_3$, racemic compound): δ = 7.34 (1H, b, H–N^{amide}), 7.30–7.24 (2H, m, H–C4'), 7.21–7.15 (3H, m, H–C5', H–C6'), 3.34 (1H, dd, *J* = 8.2, 4.5, H–C2), 2.80 (3H, d, *J* = 5.0, H–C3), 2.75–2.65 (2H, m, H–C2'), 2.18 (1H, dddd, *J* = 11.5, 9.7, 7.1, 4.5, H–C1'), 1.79 (1H, dddd, *J* = 14.1, 9.7, 8.3, 6.1, H–C1'), and 1.50 (2H, bs, H–N^{amine}) ppm; ^{13}C NMR (101 MHz, $CDCl_3$): δ = 175.5 (C1), 141.2 (C3'), 128.4 (2C, C4´), 128.4 (2C, C5'), 126.0 (C6'), 54.8 (C2), 36.6 (C1'), 32.1 (C2'), and 25.8 (C3) ppm; IR (ATR): $\tilde{\nu}$ = 3307m, 2922w, 1650s, 1610m, 1548s, 1481s, 1454m, 1417w, 1384m, 1344s, 1300m, 1246m, 1155w, 1101w, 1078w, 1030w, 992w, 908w, 813w, 784w, 746m, 698s, and 669m cm^{-1}; HR-ESI-MS: *m*/*z*: 193.1340 ([*M*+H]$^+$, calcd for $C_{11}H_{17}N_2O^+$: 193.1335).

(5*S*)-2,2,3-Trimethyl-5-(phenylethyl)imidazolidin-4-one (59)

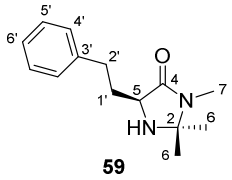

59

To a solution of amide **67** (100 mg, 0.52 mmol, 1.0 equiv.) in MeOH (3.0 mL) was added acetone (0.29 mL, 3.90 mmol, 7.5 equiv.) at RT under an atmosphere argon and the solution heated to reflux for 5 h. The reaction was allowed to come to RT and concentrated *in vacuo* to give imidazolidinone **59** as a yellow oil (110 mg, 91%).

$[\alpha]_D^{23}$: +2.2 (*c* = 1.01, CH_3OH); ^{1}H NMR (300 MHz, $CDCl_3$): δ = 7.35–7.09 (5H, m, H–C4', H–C5', H–C6'), 3.49 (1H, dd, *J* = 8.5, 4.3, H–C5), 2.89–2.68 (2H, m, H–C2'), 2.77 (3H, s, H–C7), 2.31–2.15 (1H, m, H–C1'), 1.89–1.66 (1H, m, H–C1'), 1.39 (3H, s, H–C6), and 1.29 (3H, s, H–C6) ppm; ^{13}C NMR (75 MHz, $CDCl_3$): δ = 174.2 (C4), 141.4 (C3'), 128.6 (2C, C4'), 128.5 (2C, C5'), 126.1 (C6'), 75.7 (C2), 57.7 (C5), 34.1 (C1'), 32.3 (C2'), 27.6 (C6), 25.3 (C7), and 25.1 (C6) ppm; IR (ATR): $\tilde{\nu}$ = 2972w, 2932w, 1688s, 1523w, 1477w, 1454m, 1426m, 1367m, 1397s, 1382s, 1327w, 1300w, 1255m, 1180m, 1160m, 1120m, 1071m, 1030w, 983w, 945w, 923w, 885w, 832w, 792w, 723s, and 701s cm^{-1}; HR-ESI-MS: *m*/*z*: 233.1654 ($[M+H]^+$, calcd for $C_{14}H_{21}N_2O^+$: 233.1648).

8.2.18 Syntheses of (5*S*)-2,2,3,5-Tetramethyl-4-imidazolidinone (60) and (5*S*)-2,2,3,5-Tetramethyl-4-oxo-1-[(*E*)-3-phenylallylidene]-imidazolidin-1-ium salt (60a)

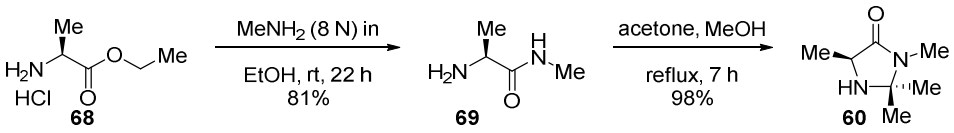

L-Alanine methyl amide (69)

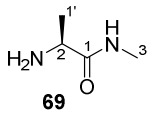

To *L*-alanine ethyl ester hydrochloride (4.00 g, 26 mmol, 1.0 equiv.) was added $MeNH_2$ (8 N in EtOH, 13 mL, 104 mmol, 4.0 equiv.) at RT and the solution was stirred for 22 h. After concentration *in vacuo* an aq. solution of K_2CO_3 (2 N) was added and the aqueous layer extracted twice with CH_2Cl_2. The combined organic layers were dried over $MgSO_4$, filtrated and concentrated *in vacuo* to give amide **69** as a colourless liquid (2.16 g, 81%).

$[\alpha]_D^{20}$: +3.7 (*c* = 1.00, CH_3OH); ^{1}H NMR (400 MHz, $CDCl_3$): δ = 7.30 (1H, b, H–N^{amide}), 3.43 (1H, q, *J* = 7.0, H–C2), 2.75 (3H, d, *J* = 5.0, H–C3), 1.45 (2H, b, H–N^{amine}), and 1.27 (3H, d, *J* = 7.0, H–C1') ppm; ^{13}C NMR (100 MHz, $CDCl_3$): δ = 176.4 (C1), 50.8 (C2), 25.8 (C3), and 21.8 (C1') ppm; IR (ATR): $\tilde{\nu}$ = 3296m, 3086w, 2968w, 1646s, 1532s, 1452w, 1409m, 1367w, 1321w, 1262w, 1157w, 1131w, 1074w, 1039w, 930w, and 842m cm^{-1}; HR-ESI-MS: *m/z*: 103.0849 ($[M+H]^+$, calcd for $C_4H_{11}N_2O^+$: 103.0866); analytical data in agreement with the literature.[187]

(5*S*)-2,2,3,5-Tetramethyl-4-imidazolidinone (60)

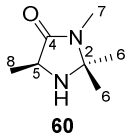

To a solution of amide **69** (366 mg, 3.58 mmol, 1.0 equiv.) in MeOH (8.00 mL) was added acetone (1.32 mL, 17.9 mmol, 5.0 equiv.) at RT under an atmosphere of argon and the

yellow solution was heated to reflux for 7 h. The reaction was allowed to come to RT and concentrated *in vacuo* to give imidazolidinone **60** as an off-white solid (496 mg, 98%).

M.p. = 83.8–84.7 °C; $[\alpha]_D^{20}$: +20.2 (*c* = 1.03, CH_3OH); ^1H NMR (300 MHz, $CDCl_3$): δ = 3.51 (1H, q, *J* = 6.8, H–C5), 2.75 (3H, d, *J* = 0.4, H–C7), 1.68 (1H, b, H–N^{amine}), 1.39 (3H, s, H–C6), 1.32 (3H, d, *J* = 6.9, H–C8), and 1.27 (3H, s, H–C6) ppm; ^{13}C NMR (75 MHz, $CDCl_3$): δ = 175.1 (C4), 75.5 (C2), 54.1 (C5), 27.5 (C6), 25.4 (C7), 24.7 (C6), and 17.7 (C8) ppm; IR (ATR): $\tilde{\nu}$ = 3276w, 2975m, 2939w, 1661s, 1479m, 1448m, 1427m, 1400s, 1384s, 1370s, 1331w, 1262m, 1243m, 1210w, 1148m, 1115w, 1077m, 1038m, 1004w, 993w, 936m, 917m, 847s, and 758m cm^{-1}; HR-ESI-MS: *m*/*z*: 143.1180 ($[M+H]^+$, calcd for $C_7H_{15}N_2O^+$: 143.1179); analytical data in agreement with the literature.[187]

2,2,3,5-Tetramethyl-4-imidazolidinone hydrochloride (60·HCl, racemic)

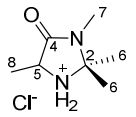

60•HCl

Imidazolidinone **60** (10.0 mg, 70 µmol, 1.0 equiv.) was dissolved in HCl in MeOH (1.25 N, 0.22 mL, 280 µmol, 3.9 equiv.) and stirred for 30 min at RT. The solution was concentrated *in vacuo* to give **60·HCl** as a white solid (12.5 mg, quant.).

M.p. = 165.9 °C decomp.; ^1H NMR (400 MHz, CD_3OD): δ = 4.35 (1H, q, *J* = 7.1, H–C5), 2.89 (3H, s, H–C7), 1.78 (3H, s, H–C6), 1.67 (3H, s, H–C6), and 1.57 (3H, d, *J* = 7.1, H–C8) ppm; ^{13}C NMR (101 MHz, CD_3OD): δ = 168.8 (C4), 78.6 (C2), 53.9 (C5), 25.6 (C7), 24.7 (C6), 22.6 (C6), and 13.9 (C8) ppm; IR (ATR): $\tilde{\nu}$ = 2925m, 2790w, 2701m, 2494m, 2414w, 2066w, 1720s, 1593m, 1472m, 1444m, 1423s,1395s, 1373s, 1307m, 1335w, 1267w, 1215w, 1196w, 1160w, 1098w, 1082w, 1037m, 957w, 935w, 745w, and 668w cm^{-1}; analytical data in agreement with the literature.[49]

(5*S*)-2,2,3,5-Tetramethyl-4-oxo-1-[(*E*)-3-phenylallylidene]-imidazolidin-1-ium perchlorate (60a·ClO_4^-)

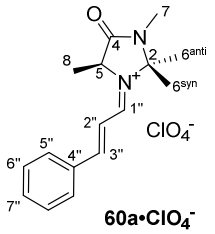

60a•ClO_4^-

To imidazolidinone **60** (22.7 mg, 0.16 mmol, 1 equiv.) in Et_2O (0.20 mL) was added perchloric acid (60% in H_2O, 26.8 mg, 0.16 mmol, 1 equiv.) in EtOH/Et_2O (1:1, 0.40 mL) at RT and the resulting mixture stirred for 15 min before it was evaporated *in vacuo* to give the imidazolidinone salt. The salt was redissolved in MeOH (0.40 mL) and heated to 35 °C. (*E*)-cinnamaldehyde (40.2 µL, 0.32 mmol, 2 equiv.) was added and the solution stirred for 1 h. The solvent was removed *in vacuo* and the residue dissolved in a minimum amount of MeOH. From this solution the iminium salt was crashed out with Et_2O and the supernatant solution taken off. The washing procedure was repeated and the iminium salt **60a·ClO_4^-** isolated as a yellow solid (28.3 mg, 50%).

M.p. = 105.7–107.2 °C; $[\alpha]_D^{20.5}$: –14.2 (*c* = 0.49, CH_3CN); ^{1}H NMR (600 MHz, CD_3CN): δ = 8.80 (1H, dd, *J* = 10.6, 1.8, H–C1''), 8.18 (1H, d, *J* = 15.1, H–C3''), 7.93 (2H, dd, *J* = 8.4, 1.0, H–C5''), 7.69 (1H, t, *J* = 7.4, H–C7''), 7.60 (2H, t, *J* = 7.8, H–C6''), 7.30 (1H, ddd, *J* = 15.1, 10.6, 0.6, H–C2''), 4.88 (1H, q, *J* = 7.1, H–C5), 2.92 (3H, d, *J* = 0.5, H–C7),1.83 (1H, s, H–C6), 1.80 (3H, s, H–C6), and 1.70 (3H, d, *J* = 7.2, H–C8) ppm; ^{13}C NMR (151 MHz, CD_3CN): δ = 167.4 (C1''), 166.5 (C4), 165.9 (C3''), 135.8 (C7''), 134.5 (C4''), 132.2 (2C, C5''), 130.7 (2C, C6''), 118.2 (C2''), 86.3 (C2), 59.5 (C5), 27.8 (C6), 26.4 (C6), 26.2 (C7), and 18.9 (C8) ppm; IR (ATR): $\tilde{\nu}$ = 3492b, 2975b, 1710s, 1621m, 1604m, 1590s, 1575m, 1474w, 1455w, 1429w, 1391m, 1324w, 1282w, 1197w, 1180w, 1074s, 1012m, 999m, 932w, 876w, 866w, 744s, 686w, and 621s cm^{-1}; HR-ESI-MS: *m*/*z*: 257.16572 ([*M*-ClO_4^-]$^+$, calcd for $C_{16}H_{21}N_2O^+$: 257.16484); analytical data in agreement with the literature.[49]

^{1}H NMR counterion-dependence comparison in CD_3CN at RT

2,2,3,5-Tetramethyl-4-oxo-1-[(*E*)-3-phenylallylidene]-imidazolidin-1-ium hexafluoridoantimonate (60a·SbF_6^-, racemic)

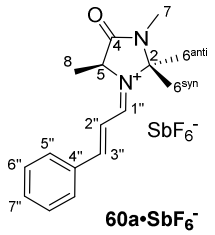

60a•SbF_6^-

^{1}H NMR (300 MHz, CD_3CN): δ_H = 8.76 (1H, dd, *J* = 10.6, 1.8, H–C1''), 8.14 (1H, d, *J* = 15.1, H–C3''), 7.97–7.88 (2H, m, H–C5''), 7.75–7.66 (1H, m, H–C7''), 7.64–7.55 (2H, m, H–C6''), 7.29 (1H, dd, *J* = 15.1, 10.6, H–C2''), 4.86 (1H, qd, *J* = 7.3, 1.7, H–C5), 2.92 (3H, d, *J* = 0.6, H–C7),1.82 (1H, s, H–C6), 1.80 (3H, s, H–C6), and 1.69 (3H, d, *J* = 7.2, H–C8) ppm.

8.2.19 Syntheses of (5*S*)-5-Benzhydryl-2,2,3-trimethyl-4-imidazolidinone (61) and (5*S*)-5-Benzhydryl-2,2,3-trimethyl-4-oxo-1-[(*E*)-3-phenylallylidene]-imidazolidin-1-ium salt (61a)

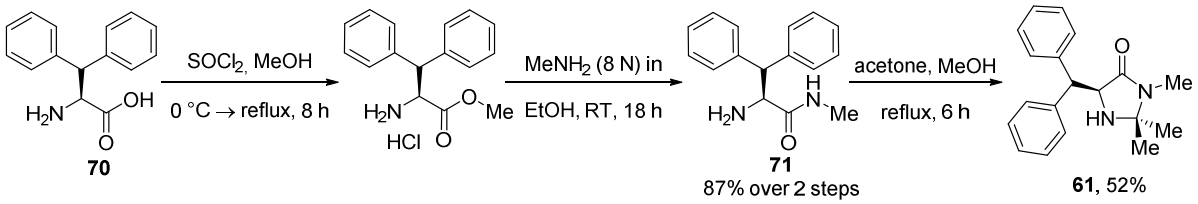

_L_-Diphenylalanine methyl amide (71)

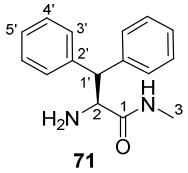

To a suspension of *L*-diphenylalanine (250 mg, 1.04 mmol, 1.0 equiv.) in MeOH (0.84 mL, 20.7 mmol, 20 equiv.) was added thionyl chloride (0.09 mL, 1.24 mmol, 1.2 equiv.) over 5 min at 0 °C and the resulting solution was allowed to come to RT before it was heated to reflux for 8 h. The solution was allowed to come to RT and evaporated *in vacuo* to give the *L*-diphenylalanine methyl ester hydrochloride as a white solid. To the ester was added $MeNH_2$ (8 N in EtOH, 0.52 mL, 1.04 mmol, 4.0 equiv.) at RT and the solution stirred for 18 h. The reaction was concentrated *in vacuo* and a saturated aqueous solution of $NaHCO_3$ was added. The aqueous layer was extracted three times with CH_2Cl_2. The combined organic layers were dried over $MgSO_4$, filtrated and concentrated *in vacuo* to give amide **71** as a yellow oil (229 mg, 87%).

$[\alpha]_D^{23}$: +71.6 (c = 0.32, CH_3OH); ^{1}H NMR (300 MHz, $CDCl_3$): δ = 7.28–7.10 (10H, m, H–C3', H–C4', H–C5'), 6.47 (1H, bs, H–N^{amide}), 4.51 (1H, d, J = 6.2, H–C2), 4.03 (1H, b, H–C1'), 2.56 (3H, d, J = 4.8, H–C3), and 1.67 (2H, b, H–N^{amine}) ppm; ^{13}C NMR (75 MHz, $CDCl_3$): δ = 174.0 (C1), 141.8 (C2'), 140.2 (C2'), 129.3 (C^{Ar}), 128.8 (C^{Ar}), 128.8 (C^{Ar}), 128.6 (C^{Ar}), 128.6 (C^{Ar}), 128.5 (C^{Ar}), 128.2 (C^{Ar}), 128.1 (C^{Ar}), 127.0 (C5'), 126.7 (C5'), 59.2 (C1'), 54.9 (C2), and 25.9 (C3) ppm; IR (ATR): $\tilde{\nu}$ = 3296w, 3060w, 3028w, 2941w, 1736w, 1652m, 1599w, 1539m, 1494m, 1450m, 1410w, 1277w, 1157w, 1080w, 1031w, 1002w, 856w, 747m, and 697s cm^{-1}; HR-ESI-MS: *m/z*: 255.1506 ([*M*+H]$^+$, calcd for $C_{16}H_{19}N_2O^+$: 255.1492).

(5*S*)-5-Benzhydryl-2,2,3-trimethyl-4-imidazolidinone (61)

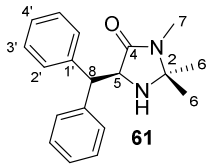

61

To a solution of amide **71** (200 mg, 0.79 mmol, 1 equiv.) in MeOH (2.00 mL) was added acetone (0.29 mL, 3.93 mmol, 5.0 equiv.) at RT under an atmosphere of argon and the solution was heated to reflux for 6 h. The reaction was allowed to come to RT and concentrated *in vacuo*. Purification by CC (SiO_2; CH/EtOAc 8:1→5:1) gave imidazolidinone **61** as a white solid (121 mg, 52%).

R_f = 0.13 (CH/EtOAc 3:1); M.p. = 106.8–108.8 °C; $[\alpha]_D^{23}$: –107.8 (*c* = 1.30, CH_3OH); ^{1}H NMR (300 MHz, $CDCl_3$): δ = 7.49 (2H, d, *J* = 7.3, H–C^{Ar}), 7.40–7.14 (6H, m, H–C^{Ar}), 7.12–7.02 (2H, m, H–C^{Ar}), 5.02 (1H, d, *J* = 1.2, H–C8), 4.16 (1H, d, *J* = 1.3, H–C8), 2.71 (3H, s, H–C7), 1.75 (1H, b, H–N^{amine}), 1.28 (3H, s, H–C6), and 0.87 (3H, s, H–C6) ppm; ^{13}C NMR (75 MHz, $CDCl_3$): δ = 173.3 (C4), 142.2 (C1'), 139.8 (C1'), 129.8 (C^{Ar}), 129.0 (C^{Ar}), 128.9 (C^{Ar}), 128.9 (C^{Ar}), 128.6 (C^{Ar}), 128.3 (C^{Ar}), 127.1 (C^{Ar}), 126.9 (C^{Ar}), 126.7 (C^{Ar}), 75.9 (C2), 62.2 (C5), 50.6 (C8), 26.6 (C6), 25.7 (C6), and 25.5 (C7) ppm; IR (ATR): $\tilde{\nu}$ = 3337w, 3028w, 2976w, 1734m, 1674m, 1600w, 1494m, 1450m, 1435w, 1403m, 1382w, 1367w, 1271w, 1184m, 1091w, 1030w, 1002w, 950w, 845w, 789w, 764m, 746m, and 703s cm^{-1}; HR-ESI-MS: *m*/*z*: 295.1807 ($[M+H]^+$, calcd for $C_{19}H_{23}N_2O^+$: 295.1805).

(5*S*)-5-Benzhydryl-2,2,3-trimethyl-4-oxo-1-[(*E*)-3-phenylallylidene]-imidazolidin-1-ium perchlorate (61a·ClO_4^-)

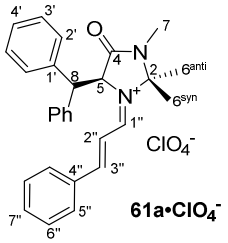

To imidazolidinone **61** (23.6 mg, 0.08 mmol, 1.0 equiv.) was added perchloric acid (60% in H_2O, 13.4 mg, 0.08 mmol, 1.0 equiv.) in EtOH/Et_2O (1:1, 0.40 mL) at RT and the resulting mixture stirred for 15 min before it was evaporated *in vacuo* to give the imidazolidinone salt. The salt was redissolved in MeOH (0.20 mL) and heated to 35 °C. (*E*)-cinnamaldehyde (20.1 µL, 0.16 mmol, 2.0 equiv.) was added and the brown solution stirred for 1 h. The solvent was removed *in vacuo* and the residue dissolved in a minimum amount of MeOH. From this solution the iminium salt **61a·ClO_4^-** was crushed out with Et_2O and the supernatant solution taken off. The washing procedure was repeated and the iminium salt contaminated with starting material **61** (circa 3:1 product:SM) was isolated as a brown solid.

^{1}H NMR (300 MHz, CD_3CN): δ_H = 8.75 (1H, d, *J* = 10.9, H–C1''), 8.08 (1H, d, *J* = 15.1, H–C3''), 7.78 (2H, d, *J* = 7.0, H–C5''), 7.74–7.27 (12H, m, H–C^{Ar}), 7.20 (1H, t, H–C7''), 7.05 (1H, dd, *J* = 14.9, 10.7, H–C2''), 5.73 (1H, d, *J* = 5.8, H–C5), 4.81 (1H, d, *J* = 5.9, H–C8), 2.77 (3H, s, H–C7), 1.75 (3H, s, H–$C6^{anti}$), and 1.18 (3H, s, H–$C6^{syn}$) ppm; HR-ESI-MS: *m*/*z*: 409.2266 ([*M*-ClO_4^-]$^+$, calcd for $C_{28}H_{29}N_2O^+$: 409.2274).

8.2.20 Attempted Syntheses of (5*S*)-5-Trityl-2,2,3-trimethyl-4-imidazolidinone (62)

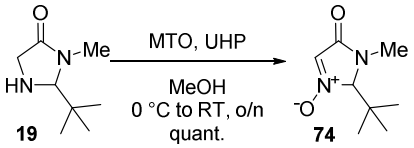

2-*tert*-Butyl-3-methyl-2,3-dihydroimidazol-4-one-N-oxide (74)[138]

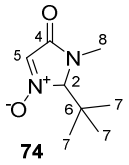

To a solution of MTO (26 mg, 0.11 mmol, 0.05 equiv.) and UHP (1.00 g, 10.6 mmol, 5 equiv.) in MeOH (3 mL) at 0 °C under an atmosphere of argon was added imidazolidinone **19** (333 mg, 2.13 mmol, 1.0 equiv.) in MeOH (7.0 mL) over 10 min. The solution was slowly warmed to RT and stirred for 24 h. After concentration *in vacuo*, the product was taken up in CH_2Cl_2, the remaining white solid was filtered of and the filtrate washed with a saturated aqueous solution of $NaHCO_3$. The organic layer was dried over $MgSO_4$ and concentrated *in vacuo* to give the product at a white solid (253 mg, 70%).

^{1}H NMR (300 MHz, $CDCl_3$): δ = 7.05 (1H, s, H–C5), 4.63 (1H, s, H–C2), 3.04 (3H, s, H–C8), and 1.08 (9H, s, H–C9) ppm; ^{13}C NMR (75 MHz, $CDCl_3$): δ = 165.9 (C4), 126.4 (C5), 94.7 (C2), 37.5 (C6), 32.2 (C8), and 25.4 (3C, C7) ppm. Analytical data in agreement with the literature.[138]

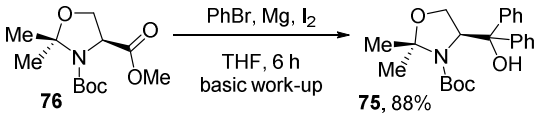

^{t}Butyl (*S*)-4-(hydroxydiphenylmethyl)-2,2-dimethyloxazolidine-3-carboxylate (75)[188]

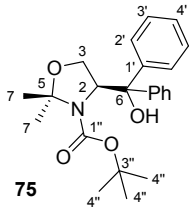

75

A flame dried flask under argon was charged with Mg swarfs (94 mg, 3.86 mmol, 2.5 equiv.) and I_2 (0.4 mg). THF (2 mL) and PhBr (135 µL, 1.29 mmol, 0.83 equiv.) and the reaction initiated with the heat gun. PhBr (270 µL, 2.58 mmol, 1.67 equiv.) was added over 10 min. After complete addition, the reaction was stirred for another 15 min, before it was cooled to 0 °C, and **76** (400 mg, 1.54 mmol, 1.0 equiv.) in dry THF (1 mL) was added over 5 min. The reaction was warmed to RT and stirred for 6 h during which time it turned from yellow to red. A saturated aqueous solution of NH_4Cl was added and the mixture was extracted three times with Et_2O. The combined organic layers were dried over $MgSO_4$ and concentrated *in vacuo* to give a brown liquid. Purification by CC ($SiO2_;$ CH/EtOAc 8:1) gave the product as a white foam (521 mg, 88%). The product was observed to be unstable and decompose to the ring-opened product (2:3 product/opened product after 1 d).

R_f = 0.63 (CH/EtOAc 3:1) ^{1}H NMR (300 MHz, $CDCl_3$): δ = 7.54–7.47 (2H, m, H–C^{Ar}), 7.37–7.18 (8H, m, H–C^{Ar}), 4.96 (1H, dd, *J* = 7.0, 1.8, H–C2), 4.11 (1H, dd, *J* = 9.9, 7.1, H–C3), 4.01 (1H, dd, *J* = 9.9, 1.8, H–C3), 1.42 (9H, s, H–C4"), and 1.35 (6H, b, H–C7) ppm; HR-ESI-MS: *m*/*z*: 406.1993 ([*M*+Na]$^+$, calcd for $C_{23}H_{29}NO_4Na^+$: 406.1989). Analytical data in agreement with the literature.[188]

8.2.21 Synthesis of (*S*)-5-Benzyl-3-methylimidazolidin-4-one (78)

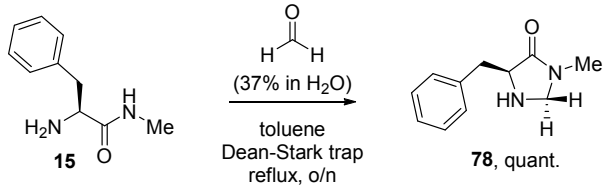

(*S*)-5-Benzyl-3-methylimidazolidin-4-one (78)

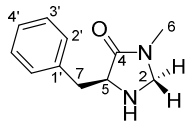

78

To a solution of amide **15** (220 mg, 1.23 mmol, 1.0 equiv.) in toluene (4.0 mL) was added formaldehyde (37% in H_2O, 0.25 mL, 3.09 mmol, 2.5 equiv.) and the flask equipped with a Dean-Stark trap. The solution was heated to reflux overnight. The solvent was removed *in vacuo* to give imidazolidinone **78** as an orange solid (235 mg, quant.).

M.p. = 65.3–65.8 °C; $[\alpha]_D^{23}$: –71.2 (*c* = 0.52, CH_3OH); ^{1}H NMR (300 MHz, $CDCl_3$): δ = 7.32–7.27 (5H, m, H–C^{Ar}), 4.67 (1H, d, *J* = 15.2, H–C2), 4.37 (1H, d, *J* = 15.4, H–C2), 3.80 (1H, dd, *J* = 9.0, 5.5, H–C5), 3.38 (1H, dd, *J* = 14.7, 5.5, H–C7), 2.94 (3H, s, H–C6), and 2.92 (1H, dd, *J* = 14.8, 8.9, H–C7) ppm; ^{13}C NMR (75 MHz, $CDCl_3$): δ = 174.6 (C4), 139.6 (C1'), 129.2 (2C, C^{Ar}), 128.4 (2C, C^{Ar}), 126.3 (C5'), 82.6 (C5), 64.5 (C2), 37.2 (C7), and 34.7 (C6) ppm; IR (ATR): $\tilde{\nu}$ = 3321w, 2934w, 1634s, 1496w, 1453m, 1397w, 1358m, 1306w, 1228w, 1144w, 1064m, 1030w, 992m, 954w, 875w, 814w, 725s, and 697s cm^{-1}; HR-ESI-MS: *m/z*: 415.2099 ($[(M)_2$+NaC$]^+$, calcd for $C_{23}H_{28}N_4O_2Na^+$: 415.2104).

8.2.22 Synthesis of (*S*)-7-Benzyl-5-methyl-2-oxa-5,8-diazaspiro[3.4]octan-6-one (79)

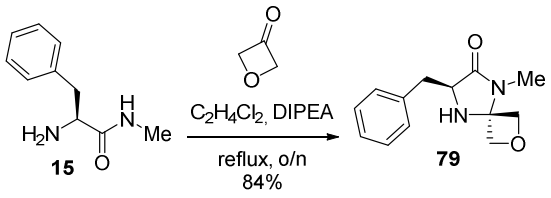

(*S*)-7-Benzyl-5-methyl-2-oxa-5,8-diazaspiro[3.4]octan-6-one (79)

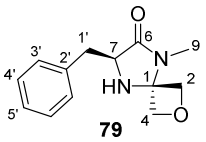

To a solution of amide **15** (1.00 g, 5.61 mmol, 1.0 equiv.) in $C_2H_4Cl_2$ (30 mL) was added oxetane-3-one (0.33 mL, 5.61 mmol, 1.0 equiv.) and DIPEA (0.77 mL, 4.49 mmol, 0.8 equiv.) and the solution heated to 60 °C for 15 h. The solvent was removed *in vacuo* and purification by CC (SiO_2; CH_2Cl_2/MeOH 20:1) gave imidazolidinone **79** as a yellow solid (1.09 g, 84%).

M.p. = 143.6–144.3 °C; $[\alpha]_D^{20}$: –8.7 (*c* = 1.00, CH_3OH); ^{1}H NMR (300 MHz, $CDCl_3$): δ = 7.37–7.26 (3H, m, H–C4', H–C5'), 7.19–7.11 (2H, m, H–C3'), 6.79 (1H, bs, H–N^{amine}), 5.15 (2H, t, *J* = 2.8, H–C4), 4.81 (1H, dt, *J* = 13.0, 2.4, H–C2), 3.71–3.54 (2H, m, H–C2, H–C7), 3.39 (1H, dd, *J* = 13.2, 2.7, H–C1'), 2.87 (3H, d, *J* = 5.0, H–C9), and 2.73 (1H, dd, *J* = 13.2, 10.6, H–C1') ppm; ^{13}C NMR (75 MHz, $CDCl_3$): δ = 171.8 (C6), 167.8 (C1), 137.9 (C2'), 129.8 (2C, C3'), 128.7 (2C, C4'), 127.0 (C5'), 84.0 (C4), 82.4 (C2), 68.2 (C7), 40.5 (C1'), and 25.9 (C9) ppm; IR (ATR): $\tilde{\nu}$ = 3300m, 3028w, 2931w, 1754w, 1651s, 1533m, 1496m, 1454m, 1410m, 1157w, 972w, 848w, 748m, and 702s cm^{-1}; HR-ESI-MS: *m*/*z*: 233.1284 ([*M*+H]$^+$, calcd for $C_{13}H_{17}N_2O_2^+$: 233.1285).

8.2.23 Syntheses of (2*S*)-2-Benzyl-4-methyl-1,4-diaza-spiro[4.4]nonan-3-one (80) and (2*S*)-2-Benzyl-1-methyl-1,4-diaza-1-[(*E*)-3-phenylallylidene]-spiro[4.4]nonan-3-one salt (80a)

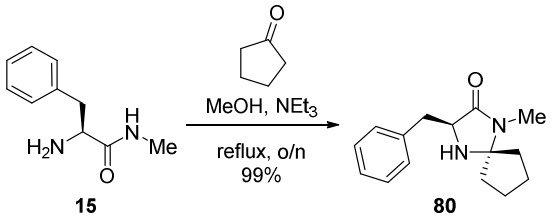

(2*S*)-2-Benzyl-4-methyl-1,4-diaza-spiro[4.4]nonan-3-one (80)[140]

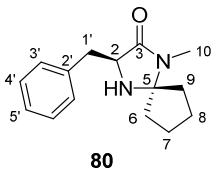

To a solution of **15** (1.00 g, 5.61 mmol, 1.0 equiv.) in MeOH (12.0 mL) was added cyclopentanone (2.48 mL, 28.1 mmol, 5.0 equiv.) and NEt_3 (0.62 mL, 4.49 mmol, 0.8 equiv.) at RT under an atmosphere of argon and the yellow solution was heated to reflux overnight. The reaction was allowed to come to RT and concentrated *in vacuo*. Purification by CC (SiO_2; CH_2Cl_2/MeOH/NH_3 (25% in H_2O) 20:1:0.1) gave **80** as a yellow oil (1.36 g, 99%).

R_f = 0.64 (CH_2Cl_2/MeOH 10:1); $[\alpha]_D^{20}$: –57.7 (*c* = 1.05, $CHCl_3$); ^{1}H NMR (300 MHz, $CDCl_3$): δ = 7.33–7.26 (2H, m, H–C4'), 7.26–7.18 (3H, m, H–C3', and H–C5'), 3.77 (1H, dd, *J* = 6.8, 4.4, H–C2), 3.12 (1H, dd, *J* = 14.0, 4.4, H–C1'), 2.99 (1H, dd, *J* = 14.0, 6.7, H–C1'), 2.75 (3H, s, H–C10), 1.69–1.40 (8H, m, H–C6, H–C7, H–C8, H–C9, H–N^{amine}), and 0.95 (1H, d, *J* = 12.4, H–C9 or H–C6) ppm; ^{13}C NMR (101 MHz, CD_3OD): δ = 174.1 (C3), 137.3 (C2'), 129.6 (2C, C3'), 128.6 (2C, C4'), 126.8 (C5'), 85.8 (C5), 59.5 (C2), 36.9 (C9), 36.9 (C1'), 34.7 (C6), 25.5 (C10), 23.9 (C7 or C8), and 23.9 (C7 or C8) ppm; IR (ATR): $\tilde{\nu}$ = 3306bw, 2955m, 1682s, 1496w, 1425m, 1401m, 1332w, 1260w, 1095m, 1030w, 806w, 748m, and 701m cm^{-1}; HR-ESI-MS: *m*/*z*: 245.1657 ([*M*+H]$^+$, calcd for $C_{15}H_{21}N_2O^+$: 245.1648); analytical data in agreement with the literature.[140]

(2*S*)-2-Benzyl-4-methyl-1,4-diaza-spiro[4.4]nonan-3-one hydrochloride (80·HCl)

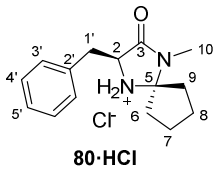

80·HCl

Imidazolidinone **80** (7.9 mg, 32 µmol, 1.0 equiv.) was dissolved in HCl in MeOH (1.25 N, 0.2 mL, 250 µmol, 7.8 equiv.) and stirred for 30 min at RT. The solution was concentrated *in vacuo* to give **80·HCl** as a white solid (9.0 mg, quant.).

Crystals suitable for X-ray crystallographic analysis were achieved by vapour exchange of a methanolic solution of **80·HCl** with Et_2O.

^{1}H NMR (400 MHz, CD_3OD): δ = 7.46–7.37 (4H, m, H–C3', H–C4'), 7.32 (1H, t, *J* = 6.9, H–C5'), 4.60 (1H, dd, *J* = 10.3, 3.6, H–C2), 3.52 (1H, dd, *J* = 15.1, 3.4, H–C1'), 3.07 (1H, dd, *J* = 15.2, 10.3, H–C1'), 2.93 (3H, s, H–C10), 2.40–2.33 (1H, m, H–C9 or H–C6), 2.19–1.95 (3H, m, H–C9, H–C6), and 1.94–1.73 (4H, m, H–C7, H–C8) ppm; ^{13}C NMR (101 MHz, CD_3OD): δ = 167.9 (C3), 136.5 (C2'), 130.3 (2C, C4'), 130.2 (2C, C3'), 128.8 (C5'), 88.4 (C5), 60.0 (C2), 35.2 (C9), 35.1 (C1´), 33.4 (C6), 26.0 (C10), 25.2 (C7 or C8), and 24.8 (C7 or C8) ppm.

(2*S*)-2-Benzyl-1-methyl-1,4-diaza-1-[(*E*)-3-phenylallylidene]-spiro[4.4]nonan-3-one hexafluorophosphate (80a·PF_6^-):

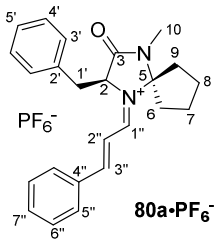

80a·PF_6^-

To imidazolidinone **80** (25.0 mg, 0.10 mmol, 1.0 equiv.) in EtOH (0.3 mL) was added hexafluorophosphoric acid (60% in H_2O, 25.0 mg, 0.10 mmol, 1.0 equiv.) at RT and the resulting mixture stirred for 10 min before it was evaporated *in vacuo* to give the imidazolidinone salt. The residue was dissolved in EtOH (0.5 mL) and (*E*)-cinnamaldehyde

(29.0 µL, 0.23 mmol, 1 equiv.) was added. The red solution was stirred overnight at RT during which time a white solid crushed out. The solid was filtered of and dried *in vacuo* to give the iminium salt **80a·PF_6^-** as a yellow solid.

M.p. = 136.1 °C decomp.; $[\alpha]_D^{23}$ = +466.5 (*c* = 0.65 in CH_3CN); ^{1}H NMR (400 MHz, CD_3CN): δ_H = 8.53 (1H, dd, *J* = 10.7, 1.8, H–C1''), 8.21 (1H, d, *J* = 15.0, H–C3''), 7.91 (2H, d, *J* = 7.3, H–C5''), 7.72 (1H, t, *J* = 7.4, H–C7''), 7.62 (2H, t, *J* = 7.6, H–C6''), 7.41–7.21 (4H, m, H–C4', H–C5', H–C2''), 7.08 (2H, d, *J* = 6.2, H–C3'), 5.17 (1H, bs, H–C2), 3.53 (1H, dd, *J* = 14.6, 5.7, H–C1´), 3.45 (1H, dd, *J* = 14.6, 3.6, H–C1´), 2.79 (3H, s, H–C10), 2.36 (1H, dt, *J* = 16.4, 8.4, H–C6 or H–C9), 2.15 (1H, dt, *J* = 16.1, 6.9, H–C6 or H–C9), 1.92–1.83 (2H, m, H–C7 or H–C8), 1.75 (1H, tt, *J* = 14.7, 7.4, H–C7 or H–C8), 1.64 (1H, tt, *J* = 16.1, 8.1, H–C7 or H–C8), and 1.14 (2H, t, *J* = 7.5, H–C6 or H–C9) ppm; ^{13}C NMR (101 MHz, CD_3CN): δ_C = 167.4 (C1''), 166.5 (C3''), 165.2 (C3), 136.1 (C7''), 134.6 (C2'), 134.4 (C4''), 132.4 (2C, C5''), 131.1 (2C, C3'), 130.7 (2C, C6''), 130.1 (2C, C4'), 129.2 (C5'), 118.5 (C2''), 95.7 (C5), 65.5 (C2), 41.2 (C6 or C9), 39.6 (C6 or C9), 37.3 (C1'), 26.8 (C7 or C8), 26.7 (C7 or C8) and 26.1 (C10) ppm; IR (ATR): $\tilde{\nu}$ = 2977w, 1695s, 1627w, 1590m, 1512w, 1479w, 1457w, 1440w, 1400m, 1377m, 1364m, 1337w, 1302m, 1258w, 1234w, 1216w, 1197m, 1180s, 1160m, 1116m, 1099m, 1034w, 1014w, 982w, 948w, 886w, 868w, 842s, 822s, 786m, and 771m cm^{-1}; HR-ESI-MS: m/z: 359.2112 ($[M–PF_6^-]^+$, calcd for $C_{22}H_{25}N_2O^+$: 359.2118); analytical data in agreement with the literature.[53]

8.2.24 Synthesis of (2*S*)-2-Benzyl-4-methyl-1,4-diaza-spiro[4.5]decan-3-one (81)

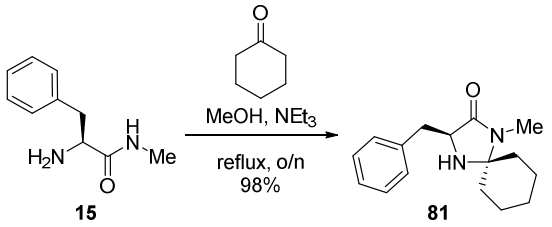

(2*S*)-2-Benzyl-4-methyl-1,4-diaza-spiro[4.5]decan-3-one (81)[140]

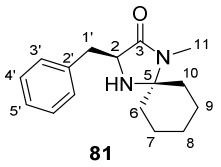

To a solution of amide **15** (1.00 g, 5.61 mmol, 1 equiv.) in MeOH (12.0 mL) was added cyclohexanone (2.90 mL, 28.1 mmol, 5.0 equiv.) and NEt_3 (0.62 mL, 4.49 mmol, 0.8 equiv.) at RT under an atmosphere of argon and the yellow solution was heated to reflux overnight. The reaction was allowed to come to RT and concentrated *in vacuo*. Purification by CC (SiO_2; CH_2Cl_2/MeOH/NH_3 (25% in H_2O) 20:1:0.1) gave imidazolidinone **81** as an orange oil (1.43 g, 98%).

R_f = 0.48 (CH_2Cl_2/MeOH 10:1); $[\alpha]_D^{20}$: –56.5 (*c* = 1.05, $CHCl_3$); ^{1}H NMR (300 MHz, $CDCl_3$): δ = 7.32–7.27 (2H, m, H–C4'), 7.26–7.11 (3H, m, H–C3', H–C5'), 3.76 (1H, dd, *J* = 6.8, 4.5, H–C2), 3.11 (1H, dd, *J* = 14.1, 4.4, H–C1'), 2.99 (1H, dd, *J* = 14.1, 6.8, H–C1'), 2.74 (3H, s, H–C11), 1.74–1.38 (9H, m, H–C6, H–C7, H–C8, H–C9, H–C10, H–N^{amine}), 1.13–0.98 (1H, m, H–C8), and 0.94 (1H, d, *J* = 12.3, H–C6 or H–C10) ppm; ^{13}C NMR (101 MHz, CD_3OD): δ = 173.7 (C3), 137.7 (C2'), 129.8 (2C, C3'), 128.6 (2C, C4'), 126.8 (C5'), 77.4 (C5), 59.3 (C2), 38.0 (C1'), 36.5 (C6 or C10), 33.8 (C6 or C10), 25.4 (C11), 25.0 (C8), 22.7 (C7 or C9), and 22.2 (C7 or C9) ppm; IR (ATR): $\tilde{\nu}$ = 3329bw, 2929m, 2856w, 1682s, 1496w, 1425m, 1403m, 1347w, 1242w, 1097m, 1075m, 907w, 805w, 744m, and 700m cm^{-1}; HR-ESI-MS: *m*/*z*: 259.1807 ($[M+H]^+$, calcd for $C_{16}H_{23}N_2O^+$: 259.1805); analytical data in agreement with the literature.[140]

(2*S*)-2-Benzyl-4-methyl-1,4-diaza-spiro[4.5]decan-3-one hydrochloride (81·HCl)

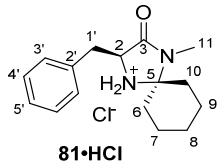

81•HCl

81 (8.4 mg, 32 µmol, 1.0 equiv.) was dissolved in HCl in MeOH (1.25 N, 0.2 mL, 250 µmol, 7.8 equiv.) and stirred for 30 min at RT. The solution was concentrated *in vacuo* to give **81·HCl** as a white solid (9.6 mg, quant.).

Crystals suitable for X-ray crystallographic analysis were achieved by vapour exchange of a methanolic solution of **81·HCl** with Et_2O.

M.p. = 158.3 °C decomp.; $[\alpha]_D^{20}$: –35.9 (*c* = 0.48, CH_3OH); ^{1}H NMR (400 MHz, CD_3OD): δ = 7.43 (2H, d, *J* = 7.1, H–C3'), 7.37 (2H, t, *J* = 7.3, H–C4'), 7.31 (1H, t, *J* = 7.1, H–C5'), 4.61 (1H, dd, *J* = 7.3, 5.4, H–C2), 3.44 (1H, dd, *J* = 15.1, 5.2, H–C1'), 3.19 (1H, dd, *J* = 15.1, 7.5, H–C1'), 2.91 (3H, s, H–C11), 2.07 (1H, td, *J* = 13.8, 4.1, H–C7 or H–C9), 1.96 (1H, dd, *J* = 11.9, 4.5, H–C8), 1.91–1.81 (2H, m, H–C7 or H–C9), 1.78–1.65 (3H, m, H–C6, H–C10, and H–C7 or H–C9), 1.50 (1H, dd, *J* = 27.0, 13.5, H–C6 or H–C10), and 1.34 (1H, t, *J* = 13.0, H–C6 or H–C10) ppm; ^{13}C NMR (101 MHz, CD_3OD): δ = 167.8 (C3), 136.5 (C2'), 130.6 (2C, C3'), 130.0 (2C, C4'), 128.7 (C5'), 82.0 (C5), 60.0 (C2), 35.6 (C1'), 33.4 (C7 or C9), 31.2 (C8), 26.4 (C11), 24.4 (C6 or C10), 22.5 (C7 or C9) and 24.8 (C6 or C10) ppm; IR (ATR): $\tilde{\nu}$ = 2915m, 2869w, 2599w, 2171w, 2003w, 1717s, 1665w, 1605w, 1574w, 1443w, 1457m, 1421m, 1398m, 1378m, 1362m, 1259w, 1244w, 1170w, 1113w, 1090m, 1033w, 954w, 914w, 895w, 752s, 703s, and 677m cm^{-1}.

(2*S*)-2-Benzyl-1-methyl-1,4-diaza-1-[(*E*)-3-phenylallylidene]-spiro[4.4]nonan-3-one hexafluorophosphate (81a·PF_6^-)

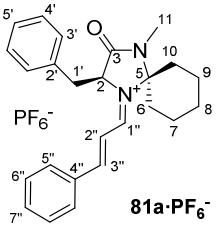

81a·PF_6^-

To **81** (26.4 mg, 0.10 mmol, 1.0 equiv.) in EtOH (0.3 mL) was added hexafluorophosphoric acid (60% in H_2O, 25.0 mg, 0.10 mmol, 1.0 equiv.) at RT and the resulting mixture stirred for 10 min before it was evaporated *in vacuo* to give the imidazolidinone salt. The residue was dissolved in EtOH (0.5 mL) and (*E*)-cinnamaldehyde (29.0 μL, 0.23 mmol, 1 equiv.) was added. The red solution was stirred overnight at RT and evaporated to dryness. The solvent was removed *in vacuo* and the residue dissolved in a minimum amount of MeOH. From this solution the iminium salt was crashed out with Et_2O and the supernatant solution taken off. This purification procedure was repeated two additional times to give a mixture of **81a·PF_6^-**, **81a**, and (*E*)-cinnamaldehyde (1:1.4:0.06) as a white solid which could not be separated.

^{1}H NMR (400 MHz, CD_3CN, **81a·PF_6^-**): δ = 8.82 (1H, dd, *J* = 10.6, 1.8, H–C1''), 8.24 (1H, d, *J* = 15.0, H–C3''), 7.87 (2H, d, *J* = 7.2, H–C5''), 7.75–7.69 (1H, m, H–C7''), 7.61 (2H, t, *J* = 7.6, H–C6''), 7.35–7.29 (3H, m, H–C4', H–C5'), 7.17 (1H, dd, *J* = 15.0, 10.6, H–C2''), 7.11 (2H, d, *J* = 6.8, H–C3'), 5.18 (1H, t, *J* = 4.3, H–C2), 3.57 (1H, dd, *J* = 14.7, 5.7, H–C1´), 3.43 (1H, dd, *J* = 14.5, 4.9, H–C1´), 2.96 (3H, s, H–C11), 2.25–2.14 (1H, m, H–C6 or H–C10), 2.05–1.97 (1H, m, H–C6 or H–C10), 1.90–1.20 (6H, m, H–C7, H–C8 and H–C9), 1.19–1.10 (1H, m, H–C6 or H–C10), and 0.94–0.88 (1H, m, H–C6 or H–C10) ppm; ^{13}C NMR (101 MHz, CD_3CN): δ = 168.1 (C1''), 167.0 (C3''), 165.9 (C3), 136.1 (C7''), 136.1 (C2'), 134.4 (C4''), 132.4 (2C, C5''), 131.1 (2C, C3'), 130.7 (2C, C6''), 130.1 (2C, C4'), 129.2 (C5'), 118.5 (C2''), 87.3 (C5), 65.3 (C2), 37.8 (C1'), 36.4 and 34.7 (C6 and C10), 28.2 (C11), 23.4, 23.1, and 21.9 (C7, C8, and C9) ppm.

8.2.25 Syntheses of 2nd Generation Catalysts 82-87[142]

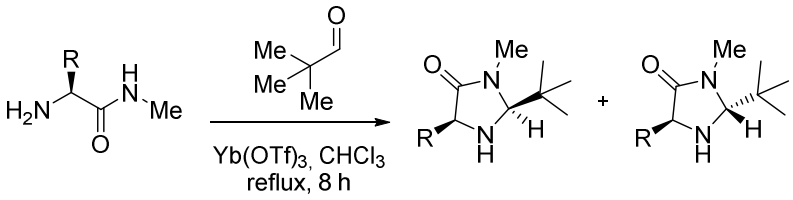

The 2nd generation MacMillan catalysts were prepared following the procedure reported by Tomkinson and co-workers.[142]

(2*S*,5*S*)-5-Benzyl-2-*tert*-butyl-3-methyl-4-imidazolidinone (82) and (2*R*,5*S*)-5-Benzyl-2-*tert*-butyl-3-methyl-4-imidazolidinone (83)

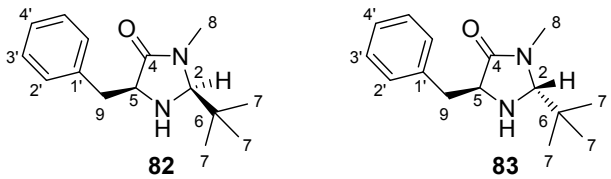

To amide **15** (2.00 g, 11.2 mmol, 1.00 equiv.) and pivaldehyde (1.93 g, 22.4 mmol, 2.00 equiv.) in $CHCl_3$ (100 mL) under an atmosphere of argon was added $Yb(OTf)_3$ (70 mg, 0.11 mmol, 0.01 equiv.) and the resulting mixture heated to reflux for 8 h. The reaction was allowed to come to RT and the two diastereomers separated by CC (SiO_2; CH/EtOAc 2:1). The *trans*-diastereomer elutes from the column prior to the *cis*-diastereomer.

(2*S*,5*S*)-5-Benzyl-2-*tert*-butyl-3-methyl-4-imidazolidinone (**82**): yellow oil (314 mg, 11%).

R_f = 0.32 (CH/EtOAc 1:1); M.p. = 69.5–73.0 °C; $[\alpha]_D^{23}$: –34.6 (*c* = 0.85, CH_3OH); ^1H NMR (300 MHz, $CDCl_3$): δ = 7.39–7.15 (5H, m, H–C^{Ar}), 4.06 (1H, d, *J* = 1.4, H–C2), 3.76–3.64 (1H, m, H–C5), 3.15 (1H, dd, *J* = 13.7, 4.0, H–C9), 3.00–2.89 (1H, m, H–C9), 2.91 (3H, s, H–C8), and 0.83 (9H, s, H–C7) ppm; IR (ATR): $\tilde{\nu}$ = 3368w, 3355w, 2961w, 1674s, 1495w, 1472w, 1453w, 1419w, 1393m, 1360w, 1340w, 1261w, 1205w, 1106m, 1078w, 1052w, 1028w, 1009w, 974w, 946w, 913w, 891w, 827w, 793w, 764w, 755m, 737m, 710m, and 699m cm^{-1}; HR-ESI-MS: *m*/*z*: 515.3356 ($[2M+Na]^+$, calcd for $C_{30}H_{44}N_4O_2Na^+$: 515.3356). Analytical data in agreement with the literature.[142]

(2*R*,5*S*)-5-Benzyl-2-*tert*-butyl-3-methyl-4-imidazolidinone (**83**): off-white solid (1.60 g, 58%).

R_f = 0.39 (CH/EtOAc 1:1); M.p. = 69.5–73.0 °C; $[\alpha]_D^{23}$: –55.6 (*c* = 1.00, CH_3OH); ^1H NMR (300 MHz, $CDCl_3$): δ = 7.33–7.20 (5H, m, H–C^{Ar}), 3.89–3.82 (1H, m, H–C5), 3.80 (1H, d, *J* = 1.8, H–C2), 3.11 (1H, dd, *J* = 14.1, 4.2, H–C9), 2.89 (1H, dd, *J* = 14.0, 7.1, H–C9), 2.89 (3H, d, *J* = 0.5, H–C8), 1.88 (1H, b, H–N^{amine})and 0.90 (9H, s, H–C7) ppm; IR (ATR): $\tilde{\nu}$ = 2956w, 1677s, 1603w, 1456m, 1431m, 1396m, 1355w, 1330w, 1307w, 1283w, 1260w, 1204w, 1160w, 1102m, 1025w, 902w, 848w, 755m, 735m, and 701s cm^{-1}; HR-ESI-MS: *m*/*z*: 515.3357 ($[2M+Na]^+$, calcd for $C_{30}H_{44}N_4O_2Na^+$: 515.3356). Analytical data in agreement with the literature.[142]

(2*S*,5*S*)-5-(3,4,5-Trimethoxybenzyl)-2-*tert*-butyl-3-methyl-4-imidazolidinone (84) and (2*R*,5*S*)-5-(3,4,5-Trimethoxybenzyl)-2-*tert*-butyl-3-methyl-4-imidazolidinone (85)

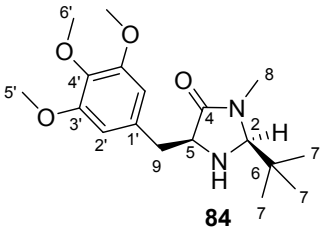

84

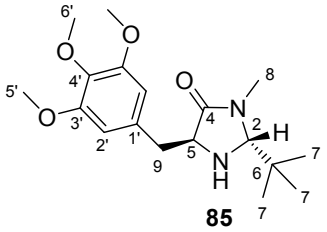

85

To amide **30** (600 mg, 2.24 mmol, 1.0 equiv.) and pivaldehyde (385 mg, 4.47 mmol, 2.0 equiv.) in $CHCl_3$ (25 mL) under an atmosphere of argon was added $Yb(OTf)_3$ (136 mg, 0.22 mmol, 0.1 equiv.) and the resulting mixture heated to reflux for 8 h. The reaction was allowed to come to RT and the two diastereomers separated by CC (SiO_2; CH/EtOAc 1:1→1:2). The *trans*-diastereomer elutes from the column prior to the *cis*-diastereomer.

(2*S*,5*S*)-5-(3,4,5-Trimethoxybenzyl)-2-*tert*-butyl-3-methyl-4-imidazolidinone (**84**): yellow oil (248 mg, 33%).

R_f = 0.19 (CH/EtOAc 1:1); $[\alpha]_D^{23}$: –16.8 (*c* = 1.00, CH_3OH); ^1H NMR (300 MHz, $CDCl_3$): δ = 6.47 (2H, s, H–C2'), 4.05 (1H, d, *J* = 1.4, H–C2), 3.80 (6H, s, H–C5'), 3.77 (3H, s, H–C6'), 3.65 (1H, t, *J* = 5.5, H–C5), 3.08–2.91 (2H, m, H–C9), 2.89 (3H, s, H–C8), and 0.82 (9H, s, H–C7) ppm; ^{13}C NMR (101 MHz, $CDCl_3$): δ = 175.3 (C4), 153.4 (2C, C3'), 136.9 (C4'), 133.4 (C1'), 106.6 (2C, C2'), 82.4 (C2), 60.9 (C6'), 59.4 (C5), 56.2 (C5'), 38.3 (C9),

35.0 (C6), 30.8 (C8), and 25.4 (3C, C7) ppm; IR (ATR): $\tilde{\nu}$ = 3363w, 2956w, 2838w, 1692m, 1589m, 1506w, 1456m, 1421m, 1396w, 1325w, 1238m, 1185w, 1123s, 1008w, 898w, 781w, 743w, and 675w cm^{-1}; HR-ESI-MS: *m*/*z*: 695.3990 ([2*M*+Na]$^+$, calcd for $C_{36}H_{56}N_4O_8Na^+$: 695.3990).

(2*R*,5*S*)-5-(3,4,5-Trimethoxybenzyl)-2-*tert*-butyl-3-methyl-4-imidazolidinone (**85**): off-white solid (307 mg, 41%).

R_f = 0.10 (CH/EtOAc 1:1); M.p. = 84.9–88.5 °C; $[\alpha]_D^{23}$: –42.2 (*c* = 1.07, CH_3OH); ^{1}H NMR (300 MHz, $CDCl_3$): δ = 6.46 (2H, s, H–C2'), 3.82 (6H, s, H–C5'), 3.85–3.75 (5H, m, H–C2, H–C5, H–C6'), 2.99 (1H, dd, *J* = 14.0, 4.5, H–C9), 2.92 (1H, dd, *J* = 14.1, 6.3, H–C9), 2.90 (3H, s, H–C8), 1.87 (1H, b, H–N^{amine}) and 0.91 (9H, s, H–C7) ppm; ^{13}C NMR (101 MHz, $CDCl_3$): δ = 175.4 (C4), 153.3 (2C, C3'), 136.8 (C4'), 133.0 (C1'), 106.4 (2C, C2'), 83.6 (C2), 61.0 (C6'), 59.7 (C5), 56.2 (C5'), 38.4 (C9), 37.9 (C6), 31.6 (C8), and 25.8 (3C, C7) ppm; IR (ATR): $\tilde{\nu}$ = 3320w, 2941w, 2877w, 1682s, 1593m, 1507m, 1453s, 1426s, 1400m, 1390m, 1357w, 1328m, 1314w, 1282w, 1233s, 1208w, 1181w, 1117s, 1105s, 1049w, 1006m, 978m, 910w, 853w, 809s, 780w, 755w, 729m, 679w, and 656m cm^{-1}; HR-ESI-MS: *m*/*z*: 359.1945 ([*M*+Na]$^+$, calcd for $C_{18}H_{28}N_2O_4Na^+$: 359.1941).

(2*S*,5*S*)-5-(Pentafluorobenzyl)-2-*tert*-butyl-3-methyl-4-imidazolidinone (86) and (2*R*,5*S*)-5-(Pentafluorobenzyl)-2-*tert*-butyl-3-methyl-4-imidazolidinone (87)

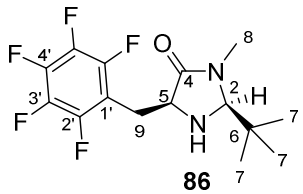

86

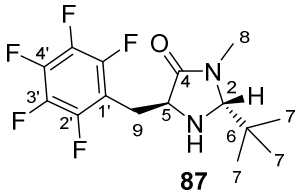

87

To amide **34** (500 mg, 1.86 mmol, 1.0 equiv.) and pivaldehyde (321 mg, 3.73 mmol, 2.0 equiv.) in $CHCl_3$ (20 mL) under an atmosphere of argon was added $Yb(OTf)_3$ (115 mg, 0.19 mmol, 0.1 equiv.) and the resulting mixture heated to reflux for 8 h. The reaction was allowed to come to RT and the two diastereomers separated by CC (SiO_2; CH/EtOAc 8:1→3:1). The *trans*-diastereomer elutes from the column prior to the *cis*-diastereomer.

(2*S*,5*S*)-5-(Pentafluorobenzyl)-2-*tert*-butyl-3-methyl-4-imidazolidinone (**86**): off-white solid (309 mg, 49%).

R_f = 0.38 (CH/EtOAc 1:1); M.p. = 79.0–85.8 °C; $[\alpha]_D^{23}$ = –21.8 (c = 1.518 in CH_3OH); ^{1}H NMR (300 MHz, $CDCl_3$): δ = 4.13 (1H, d, J = 1.3,H–C2), 3.83 (1H, dd, J = 9.2, 4.7, H–C5), 3.21 (1H, dd, J = 13.8, 4.5, H–C9), 2.93 (3H, s, H–C8), 2.88 (1H, dd, J = 13.9, 9.1, H–C9), 2.03 (1H, b, H–N^{amine}), and 0.92 (9H, s, H–C7) ppm; ^{13}C NMR (151 MHz, $CDCl_3$): δ = 173.4 (C4), 145.6 (2C, dm, $^1J_{CF}$ = 244.9, C^{Ar}), 140.1 (dm, $^1J_{CF}$ = 252.0, C4'), 137.6 (2C, dm, $^1J_{CF}$ = 250.4, C^{Ar}), 112.0 (t, $^2J_{CF}$ = 17.5, C1'), 82.4 (C2), 57.1 (C5), 35.6 (C6), 30.9 (C8), and 25.3 (C7) ppm; ^{19}F NMR (282 MHz, $CDCl_3$): δ = –141.8 (2F, dd, $^3J_{FF}$ = 20.8, $^4J_{FF}$ = 8.0, F–C3'), –156.8 (1F, t, $^3J_{FF}$ = 20.9, F–C5'), and –162.8 (2F, td, $^3J_{FF}$ = 22.2, $^4J_{FF}$ = 8.3, F–C4') ppm; IR (ATR): $\tilde{\nu}$ = 3375w, 2976w, 1729w, 1673s, 1520m, 1499s, 1435w, 1422w, 1396m, 1347w, 1300w, 1259w, 1202w, 1121m, 1110m, 1056w, 1034w, 995m, 971m, 946m, 893w, 850w, 799w, 763w, 743w, 719w and 667w cm^{-1}; HR-EI-MS: *m*/*z*: 359.1152 ([*M*+Na]$^+$, calcd for $C_{15}H_{17}F_5N_2ONa^+$: 359.1153).

Crystals suitable for X-ray crystallographic analysis were achieved by vapour exchange of a methanolic solution of the hydrochloride salt **80·HCl** with Et_2O.

(2*R*,5*S*)-5-(Pentafluorobenzyl)-2-*tert*-butyl-3-methyl-4-imidazolidinone (**87**): off-white solid (186 mg, 30%).

R_f = 0.51 (CH/EtOAc 1:1); M.p. = 52.8–55.2 °C; $[\alpha]_D^{23}$ = –21.2 (c = 1.14 in CH_3OH); ^{1}H NMR (300 MHz, $CDCl_3$): δ = 4.09 (1H, d, J = 1.7,H–C2), 3.83 (1H, dd, J = 9.2, 4.8, H–C5), 3.27–3.13 (1H, m, H–C9), 2.96 (3H, s, H–C8), 2.77 (1H, dd, J = 13.7, 9.2, H–C9), and 0.93 (9H, s, H–C7) ppm; ^{13}C NMR (151 MHz, $CDCl_3$): δ = 174.2 (C4), 145.7 (2C, dm, $^1J_{CF}$ = 246.7, C^{Ar}), 140.1 (dm, $^1J_{CF}$ = 252.4, C4'), 137.6 (2C, dm, $^1J_{CF}$ = 250.6, C^{Ar}), 111.8 (td, $^2J_{CF}$ = 18.0, $^3J_{CF}$ = 3.1, C1'), 83.4 (C2), 57.6 (C5), 37.5 (C6), 31.5 (C8), and 25.7 (C7) ppm; ^{19}F NMR (282 MHz, $CDCl_3$): δ = (–142.3)–(–142.6) (2F, m, F-C3'), –156.8 (1F, t, $^3J_{FF}$ = 20.9, F–C5'), and (–162.6)–(–162.8) (2F, m, F–C4') ppm; IR (ATR): $\tilde{\nu}$ = 3353w, 2971w, 2872w, 1683s, 1519m, 1499s, 1444w, 1418w, 1401m, 1366w, 1344w, 1305w, 1258w, 1205w, 1121m, 1075w, 1040m, 985m, 954m, 939m, 884w, 855w, 792w, 753w, and 737w cm^{-1}; HR-EI-MS: *m*/*z*: 695.2417 ([2*M*+Na]$^+$, calcd for $C_{30}H_{34}F_{10}N_4O_2Na^+$: 695.2414).

8.2.26 ^{1}H NMR Study of Iminium Salts 92-95 and 98

(5*S*)-5-Benzyl-2,2,3-trimethyl-4-oxo-1-[(*E*)-3-(*para*-chlorophenylallylidene]-imidazolidin-1-ium perchlorate (92·ClO_4^-):

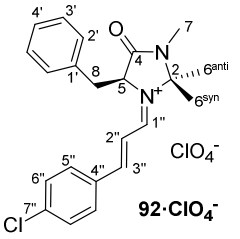

To imidazolidinone **1** (17.5 mg, 0.08 mmol, 1.0 equiv.) was added perchloric acid (60% in H_2O, 13.4 mg, 0.08 mmol, 1.0 equiv.) in EtOH/Et_2O (1:1, 0.40 mL) at RT and the resulting mixture stirred for 30 min before it was evaporated *in vacuo* to give the imidazolidinone salt. The salt was redissolved in MeOH (0.20 mL) and heated to 35 °C. (*E*)-(*para*-chloro)cinnamaldehyde (26.7 mg, 0.16 mmol, 2.0 equiv.) was added and the orange solution stirred for 1 h during which time the solution turned red. The solvent was removed *in vacuo* and the residue dissolved in a minimum amount of MeOH. From this solution the iminium salt was crashed out with Et_2O and the supernatant solution taken off. The washing procedure was repeated and the iminium salt isolated as a yellow solid.

Crystals suitable for X-ray crystallographic analysis were achieved by vapour exchange of a methanolic solution of **92·** ClO_4^- with Et_2O.

M.p. = 123.5–125.6 °C; $[\alpha]_D^{23}$: +561.9 (c = 0.70, CH_3CN); ^{1}H NMR (300 MHz, CD_3CN): δ_H = 8.73 (1H, dd, J = 10.6, 1.9, H–C1''), 8.13 (1H, d, J = 15.1, H–C3''), 7.89 (2H, d, J = 8.6, H–C5''), 7.63 (2H, d, J =8.6, H–C6''), 7.41–7.37 (1H, m, H–C4'), 7.32–7.26 (3H, m, H–C3', H–C2''), 7.09 (2H, dd, J = 7.7, 1.7, H–C2'), 5.19 (1H, s, H–C5), 3.57 (1H, dd, J = 14.6, 5.6, H–C8), 3.46 (1H, dd, J = 14.6, 3.8, H–C8), 2.78 (3H, d, J = 0.7, H–C7), 1.69 (3H, s, H–$C6^{anti}$), and 0.80 (3H, s, H–$C6^{syn}$) ppm; IR (ATR): $\tilde{\nu}$ = 2985w, 1699m, 1619m, 1603m, 1581m, 1489w, 1427w, 1402w, 1333w, 1311w, 1274w, 1238w, 1199w, 1177w, 1154w, 1076s, 1023w, 1011m, 963w, 928w, 867w, 816w, 747w, 705w, and 671w cm^{-1}; HR-EI-MS: m/z: 367.1567 ($[M–ClO_4^-]^+$, calcd for $C_{22}H_{24}ClN_2O^+$: 367.1572).

(5*S*)-5-Benzyl-2,2,3-trimethyl-4-oxo-1-[(*E*)-3-(*para*-fluorophenylallylidene]-imidazolidin-1-ium perchlorate (93·ClO_4^-):

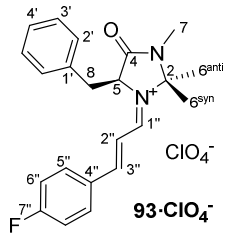

To imidazolidinone **1** (17.5 mg, 0.08 mmol, 1.0 equiv.) was added perchloric acid (60% in H_2O, 13.4 mg, 0.08 mmol, 1.0 equiv.) in EtOH/Et_2O (1:1, 0.40 mL) at RT and the resulting mixture stirred for 30 min before it was evaporated *in vacuo* to give the imidazolidinone salt. The salt was redissolved in MeOH (0.20 mL) and heated to 35 °C. (*E*)-(*para*-fluoro)cinnamaldehyde (22.4 mg, 0.16 mmol, 2.0 equiv.) was added and the solution stirred for 1 h. The solvent was removed *in vacuo* and the residue dissolved in a minimum amount of MeOH. From this solution the iminium salt was crashed out with Et_2O and the supernatant solution taken off. The washing procedure was repeated and the iminium salt isolated as an orange solid.

M.p. = 71.2–73.0 ; $[\alpha]_D^{23}$: +462.7 (*c* = 0.30, CH_3CN); ^{1}H NMR (300 MHz, CD_3CN): δ_H = 8.70 (1H, dd, *J* = 10.7, 1.8, H–C1''), 8.14 (1H, d, *J* = 15.0, H–C3''), 7.98 (2H, dd, *J* = 8.8, 5.5, H–C5''), 7.42–7.26 (5H, m, H–C3', H–C4', H–C6''), 7.22 (1H, dd, *J* = 15.0, 10.7, H–C2''), 7.09 (2H, dd, *J* = 7.7, 1.9, H–C2'), 5.18 (1H, b, H–C5), 3.57 (1H, dd, *J* = 14.7, 5.6, H–C8), 3.47 (1H, dd, *J* = 10.8, 4.0, H–C8), 2.78 (3H, s, H–C7), 1.69 (3H, s, H–C6^{anti}), and 0.79 (3H, s, H–C6^{syn}) ppm; ^{19}F NMR (282 MHz, CD_3CN) = –102.9 (1F, tt, $^3J_{HF}$ = 8.8, $^4J_{HF}$ = 5.6); IR (ATR): $\tilde{\nu}$ = 3076w, 1705m, 1625m, 1610m, 1583s, 1508w, 1434w, 1392m, 1404m, 1310w, 1281w, 1226m, 1197m, 1158m, 1076s, 1009m, 931w, 831m, 776w, 747m,and 703m cm^{-1}; HR-EI-MS: *m*/*z*: 351.1870 ([*M*–ClO_4^-]$^+$, calcd for $C_{22}H_{24}FN_2O^+$: 351.1867).

(5*S*)-5-Benzyl-2,2,3-trimethyl-4-oxo-1-[(*E*)-3-(*para*-methoxyphenylallylidene]-imidazolidin-1-ium perchlorate (94·ClO_4^-):

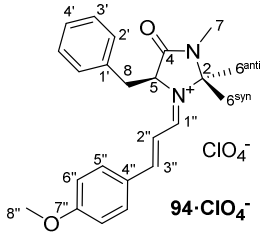

To imidazolidinone **1** (17.5 mg, 0.08 mmol, 1.0 equiv.) was added perchloric acid (60% in H_2O, 13.4 mg, 0.08 mmol, 1.0 equiv.) in EtOH/Et_2O (1:1, 0.40 mL) at RT and the resulting mixture stirred for 30 min before it was evaporated *in vacuo* to give the imidazolidinone salt. The salt was redissolved in MeOH (0.20 mL) and heated to 35 °C. (*E*)-(*para*-methoxy)cinnamaldehyde (26.0 mg, 0.16 mmol, 2.0 equiv.) was added and the solution stirred for 1 h. The solvent was removed *in vacuo* and the residue dissolved in a minimum amount of MeOH. From this solution the iminium salt was crashed out with Et_2O and the supernatant solution taken off. The washing procedure was repeated and the iminium salt isolated as a dark red solid.

M.p. = 111.5 °C decomp.; $[\alpha]_D^{23}$: +672.6 (*c* = 0.34, CH_3CN); ^{1}H NMR (400 MHz, CD_3CN): δ_H = 8.57 (1H, dd, *J* = 10.9, 1.8, H–C1''), 8.09 (1H, d, *J* = 14.7, H–C3''), 7.93 (2H, d, *J* = 8.9, H–C5''), 7.34–7.25 (3H, m, H–C3', H–C4'), 7.21–7.12 (3H, m, H–C2'', H–C6''), 7.11–7.05 (2H, m, H–C2'), 5.11 (1H, b, H–C5), 3.95 (3H, s, H–C8''), 3.57 (1H, dd, *J* = 14.6, 5.7, H–C8), 3.47–3.41 (1H, m, H–C8), 2.77 (3H, s, H–C7), 1.65 (3H, s, H–$C6^{anti}$), and 0.73 (3H, s, H–$C6^{syn}$) ppm; ^{13}C NMR (101 MHz, CD_3CN): δ_C = 167.1 (C7''), 166.6 (C1''), 166.5 (C3''), 165.5 (C4), 116.5 (2C, C6''), 115.6 (C2''), 85.8 (C2), 64.7 (C5), 56.9 (C8''), 36.8 (C8), 27.5 ($C6^{anti}$), 26.0 (C7), and 24.7 ($C6^{syn}$) ppm; IR (ATR): $\tilde{\nu}$ = 2938w, 1710m, 1626w, 1562s, 1511m, 1436w, 1402m, 1312w, 1265m, 1240m, 1207w, 1166s, 1075s, 1013s, 934w, 831m, 746w, and 702w cm^{-1}; HR-ESI-MS: *m*/*z*: 363.2069 ([*M*-ClO_4^-]$^+$, calcd for $C_{23}H_{27}N_2O_2^+$: 363.2067).

(5*S*)-5-Benzyl-2,2,3-trimethyl-4-oxo-1-[(*E*)-3-(*para*-dimethylaminophenylallylidene]-imidazolidin-1-ium perchlorate (95·ClO_4^-):

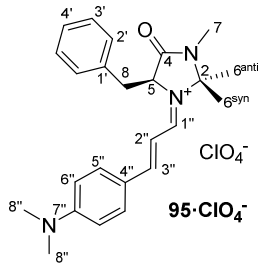

To imidazolidinone **1** (17.5 mg, 0.08 mmol, 1.0 equiv.) was added perchloric acid (60% in H_2O, 13.4 mg, 0.08 mmol, 1.0 equiv.) in EtOH/Et_2O (1:1, 0.40 mL) at RT and the resulting mixture stirred for 30 min before it was evaporated *in vacuo* to give the imidazolidinone salt. The salt was redissolved in MeOH (0.20 mL) and heated to 35 °C. (*E*)-(*para*-dimethylamino)cinnamaldehyde (28.0 mg, 0.16 mmol, 2.0 equiv.) was added and the red solution stirred for 1 h. The solvent was removed *in vacuo* and the residue dissolved in a minimum amount of MeOH. From this solution the iminium salt was crashed out with Et_2O and the supernatant solution taken off. The washing procedure was repeated and the iminium salt isolated as a dark green solid.

M.p. = 136.5 °C; $[\alpha]_D^{23}$: +1168.7 (c = 0.12, CH_3CN); ^{1}H NMR (300 MHz, CD_3CN): δ_H = 8.21 (1H, dd, J = 11.4, 1.3, H–C1''), 7.90 (1H, d, J = 14.0, H–C3''), 7.80 (2H, b, H–C6''), 7.29–7.27 (3H, m, H–C^{Ar}), 7.15–7.03 (2H, m, H–C^{Ar}), 6.92–6.83 (3H, m, H–C2'', H–C^{Ar}), 4.94 (1H, s, H–C5), 3.56 (1H, dd, J = 14.4, 5.7, H–C8), 3.36 (1H, dd, J = 14.5, 2.8, H–C8), 3.21 (6H, s, H–C8''), 2.73 (3H, s, H–C7), 1.58 (3H, s, H–$C6^{anti}$), and 0.64 (3H, s, H–$C6^{syn}$) ppm; ^{13}C NMR (75 MHz, CD_3CN): δ_C = 165.0 (C4), 163.9 (C1''), 160.1 (C3''), 155.9 (C7''), 134.3 (C1'), 129.8 (2C, C^{Ar}), 128.4 (2C, C^{Ar}), 127.4 (C^{Ar}), 121.5 (C^{Ar}), 112.4 (2C, b C6''), 108.8 (C2''), 82.7 (C2), 62.2 (C5), 39.5 (C8''), 34.7 (C8), 26.2 ($C6^{anti}$), 24.4 (C7), and 23.3 ($C6^{syn}$) ppm; IR (ATR): $\tilde{\nu}$ = 2938w, 1706m, 1627w, 1587m, 1551m, 1439w, 1379m, 1313w, 1227w, 1158m, 1074s, 1008m, 933m, 872w, 819w, 746w, 725w, and 702w cm^{-1}; HR-ESI-MS: m/z: 376.2381 ([M-ClO_4^-]$^+$, calcd for $C_{24}H_{30}N_3O^+$: 376.2381).

(5*S*)-2,2,3,5-tetramethyl-4-oxo-1-[(*E*)-3-(*para*-dimethylaminophenylallylidene]-imidazolidin-1-ium perchlorate (96·ClO_4^-):

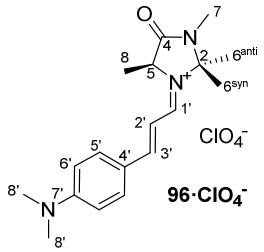

To imidazolidinone **1** (100 mg, 0.70 mmol, 1.0 equiv.) was added perchloric acid (60% in H_2O, 118 mg, 0.70 mmol, 1.0 equiv.) in MeOH (2.00 mL) at RT and the resulting mixture stirred for 30 min before (*E*)-(*para*-dimethylamino)cinnamaldehyde (136 mg, 0.77 mmol, 1.1 equiv.) was added and the red solution stirred overnight. The solvent was removed *in vacuo* and the residue dissolved in a minimum amount of MeOH. From this solution the iminium salt was crashed out with Et_2O and the supernatant solution taken off. The washing procedure was repeated and the iminium salt isolated as a red/purple solid.

M.p. = 193.0 °C decomp.; $[\alpha]_D^{23}$: +2731.2 (c = 0.46, CH_3CN); ^{1}H NMR (600 MHz, CD_3CN): δ_H = 8.29 (1H, dd, J = 11.3, 1.5, H–C1'), 7.86 (1H, d, J = 14.1, H–C3'), 7.77 (2H, b, H–C5'), 6.85 (2H, d, J = 9.4, H–C6'), 6.78 (1H, dd, J = 14.1, 11.3, H–C2'), 4.62 (1H, q, J = 7.1, H–C5), 3.18 (6H, s, H–C8'), 2.88 (3H, d, J = 0.6, H–C7), 1.73 (3H, s, H–C6), 1.70 (3H, s, H–C6), and 1.61 (3H, d, J = 7.0, H–C8) ppm; 13C NMR (151 MHz, CD3CN, C5' not visible): δ_C = 167.7 (C4), 164.9 (C3'), 161.1 (C1'), 157.1 (C7'), 122.6 (C4'), 113.7 (2C, C6'), 109.8 (2C, C2'), 84.0 (C2), 57.8 (C5), 40.8 (2C, C8'), 27.7 (C6), 26.4 (C6), 25.9 (C7), and 18.1 (C8) ppm; IR (ATR): $\tilde{\nu}$ = 2921w, 1716m, 1625w, 1549s, 1526s, 1486w, 1444w, 1411w, 1378s, 1307m, 1243m, 1151s, 1076s, 1008m, 972m, 939m, 856w, 821m, 723m and 695w cm^{-1}; HR-ESI-MS: m/z: 300.2076 ([M-ClO_4^-]$^+$, calcd for $C_{18}H_{26}N_3O^+$: 300.2070).

8.3 General Procedures for Catalysis Screening

8.3.1 General Procedure for the Conjugate Addition of 1-Methyl-1*H*-pyrrole (38) and (*E*)-cinnamaldehyde (2) to give 3-(1-Methyl-1*H*-pyrrol-2-yl)-3-phenylpropan-1-ol (39)

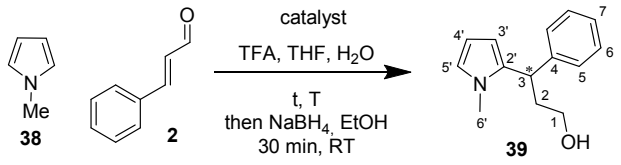

To the corresponding imidazolidinone catalyst (33.0 µmol, 0.2 equiv.) was added TFA (3.76 mg, 33.0 µmol, 0.2 equiv.) in THF (0.33 mL) and H_2O (0.05 mL) and the solution was stirred for 5 min at the given temperature before (*E*)-cinnamaldehyde was added (63 µL, 0.50 mmol, 3.0 equiv.). After an additional 30 min, 1-methyl-1*H*-pyrrole (15 µL, 0.17 mmol, 1.0 equiv.) was added and the yellow solution stirred for the given time, after which complete conversion of the starting material was observed by TLC. EtOH (0.5 mL) and $NaBH_4$ (19.0 mg, 0.50 mmol, 3.0 equiv.) were added (and the mixture warmed to RT). The reduction was quenched with aqueous saturated $NaHCO_3$ after 30 min and extracted three times with CH_2Cl_2. The combined organic layers were dried over $MgSO_4$ and evaporated *in vacuo*. The crude product **39** was purified by column chromatography (CH/EtOAc 4:1). The enantioselectivities were determined by chiral HPLC on a *Chiracel OJ-H* column, using *n*-hexane/*i*-PrOH 85:15 as eluent (1.0 mL/min). Retention times of the two enantiomers are: 11.30 min (*R*) and 18.31 min (*S*).

R_f = 0.58 (CH/EtOAc 1:1); ^{1}H NMR (300 MHz, $CDCl_3$): δ = 7.33–7.23 (2H, m, H–C6), 7.23–7.09 (3H, m, H–C5, H–C7), 6.53 (1H, t, *J* = 2.3, H–C5'), 6.19–6.14 (1H, m, H–C3'), 6.14–6.07 (1H, m, H–C4'), 4.12 (1H, t, *J* = 7.5, H–C3), 3.75–3.56 (2H, m, H–C1), 3.30 (3H, s, H–C6'), 2.34 (1H, dq, *J* = 13.4, 7.1, H–C2), 2.10 (1H, ddt, *J* = 14.0, 8.5, 5.7, H–C2), and 1.45 (1H, b, H–O) ppm; ^{13}C NMR (75 MHz, $CDCl_3$): δ = 143.6 (C4), 135.0 (C2'), 128.7 (2C, C6), 128.0 (2C, C5), 126.5 (C7), 122.0 (C5'), 106.4 (C4'), 105.8 (C3'), 60.8 (C1), 39.6 (C2), 39.1 (C6'), and 34.0 (C3) ppm; HR-ESI-MS: *m*/*z*: 238.1208 ([*M*+Na]$^+$, calcd for $C_{14}H_{17}NONa^+$: 238.1202); analytical data in agreement with the literature.[112b]

8.3.2 General Procedure for the Conjugate Addition of 1-Methyl-1*H*-indole (96) and (*E*)-cinnamaldehyde (2) to give 3-(1-Methyl-1*H*-indole-3-yl)-3-phenylpropan-1-ol (97)

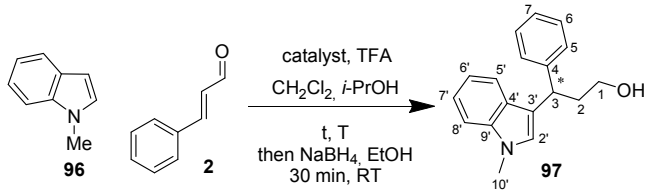

To the corresponding imidazolidinone catalyst (33.0 µmol, 0.2 equiv.) was added TFA (3.76 mg, 33.0 µmol, 0.2 equiv.) in CH_2Cl_2 (0.28 mL) and *i*-PrOH (0.05 mL) and the solution was stirred for 5 min at the given temperature before (*E*)-cinnamaldehyde (**2**) was added (63 µL, 0.50 mmol, 3.0 equiv.). After an additional 30 min, 1-methyl-1*H*-indole (**96**) (15 µL, 0.17 mmol, 1.0 equiv.) was added and the yellow solution stirred for the given time, after which complete conversion of the starting material was observed by TLC. EtOH (0.5 mL) and $NaBH_4$ (19.0 mg, 0.50 mmol, 3.0 equiv.) were added (and the mixture warmed to RT). The reduction was quenched with aqueous saturated $NaHCO_3$ after 30 min and extracted three times with CH_2Cl_2. The combined organic layers were dried over $MgSO_4$ and evaporated *in vacuo*. The crude product **97** was purified by column chromatography (CH/EtOAc 5:1). The enantioselectivities were determined by chiral HPLC on a *Reprosil Chiral-OM* column, using *n*-hexane/*i*-PrOH 85:15 as eluent (1.0 mL/min). Retention times of the two enantiomers are: 15.45 min (*R*) and 20.97 min (*S*).

R_f = 0.17 (CH/EtOAc 3:1); ^{1}H NMR (300 MHz, $CDCl_3$): δ = 7.39 (1H, d, *J* = 7.8, H–C5'), 7.28–7.16 (5H, m, H–C5, H–C6, H–C7), 7.14–7.05 (2H, m, H–C7', H–C8'), 6.94 (1H, t, *J* = 7.8, H–C6'), 6.82 (1H, s, H–C2'), 4.31 (1H, t, *J* = 7.8, H–C3), 3.67 (3H, s, H–C10'), 3.59 (2H, td, *J* = 6.4, 2.2, H–C1), 2.48–2.30 (1H, m, H–C2), 2.27–2.13 (1H, m, H–C2), and 1.46 (1H, s, H–O) ppm; HR-ESI-MS: *m*/*z*: 288.1361 ([*M*+Na]$^+$, calcd for $C_{18}H_{19}NONa^+$: 288.1359); analytical data in agreement with the literature.[52]

8.3.3 General Procedure for the Heterogeneous Hydrogenation Reactions of Ketopantolactone (KPL), Methylbenzoylformate (MBF) and Trifluoroacetophenone (TFAP)

The catalyst Pt/Al_2O_3 was pre-reduced (purge 10 min with He, change to H_2-flow, heat to 400 °C, keep at 400 °C for 1 h, let come to RT). The reaction vessel was charged with the pre-reduced Pt/Al_2O_3 (50 mg) and the solvent (5 mL), an atmosphere of H_2 was created and the mixture stirred for 1 h before the modifier (1 mM) and the substrate (0.2 M) in the solvent (5 mL) were added and the reaction stirred for the given time. Analysis (conversion and enantioselectivity) was performed using chiral GC (*CP-Chirasil-Dex CB*, 25 m length, 0.25 mm internal diameter, 0.25 μm film thickness).

GC details for the analysis of KPL hydrogenations: Temperature program: Start at 80 °C, increased to 140 °C at 10 °C min^{-1}, increased to 180 °C at 20 °C min^{-1} , held for 2 min. Retention times and elution temperatures: KPL (5.84 min, 138.4 °C), (*S*)-PL (7.38 min, 167.6 °C), and (*R*)-PL (7.51 min, 170.2 °C).

GC details for the analysis of MBF hydrogenations: Temperature program: Start at 120 °C, increased to 180 °C at 20 °C min^{-1}, held for 2 min. Retention times and elution temperatures: MBF (6.09 min, 145.5 °C), (*R*)-MM (7.38 min, 155.2 °C), and (*S*)-MM (7.51, 155.7 °C).

GC details for the analysis of TFAP hydrogenations: Temperature program: Start at 120 °C, held for 1 min, increased to 130 °C at 1 °C min^{-1}, held for 1 min, increased to 140 °C at 10 °C min^{-1}, held for 1 min, increased to 150 °C at 1 °C min^{-1}, held for 1 min, increased to 180 °C at 40 °C min^{-1}. Retention times and elution temperatures: TFAP (1.75 min, 120.8 °C), (*S*)-PTFE (10.7 min, 130.0 °C), and (*R*)-PTFE (11.1 min, 130.1 °C).

8.4 X-Ray Crystallographic Data

2,2,3-Trimethyl-5-(3,4,5-trimethoxybenzyl)-4-imidazolidinone hydrochloride (3·HCl)

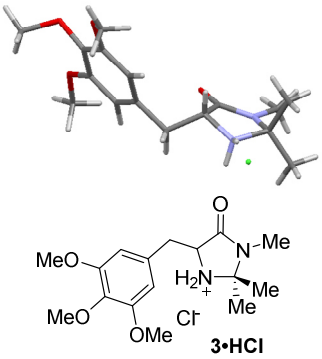

$C_{16}H_{25}ClN_2O_4$, M = 344.83; monoclinic; space group P121/n1;

a = 13.994(3) Å, b = 6.9573(14) Å, c = 19.006(4) Å;

α = 90°, β = 106.868(7)°, γ = 90°;

V = 1770.8(6) Å^3; Z = 4; T = 100(2) K;

reflections collected: 13330, independent reflections: 3657;

R_{int} = 0.1118, $R1$ = 0.0557, $wR2$ = 0.0893.

(5*S*)-2,2,3-Trimethyl-5-(2,4,6-trifluorobenzyl)-4-imidazolidinone hydrochloride (8·HCl)

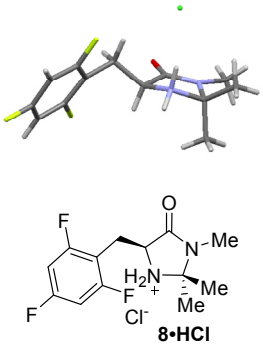

$C_{13}H_{16}ClF_3N_2O$, M = 308.73; monoclinic; space group $P2_1$;

a = 10.9270(7) Å, b = 5.8988(4) Å, c = 11.8970(7) Å;

α = 90°, β = 113.156(5)°, γ = 90°;

V = 705.06(8) Å^3; Z = 2; T = 223(2) K;

reflections collected: 4468, independent reflections: 2184;

R_{int} = 0.041, $R1$ = 0.0449, $wR2$ = 0.1248, Flack parameter = –0.02(2).

(5*S*)-2,2,3-Trimethyl-5-(*para*-nitrobenzyl)-4-imidazolidinone hydrochloride (9·HCl)

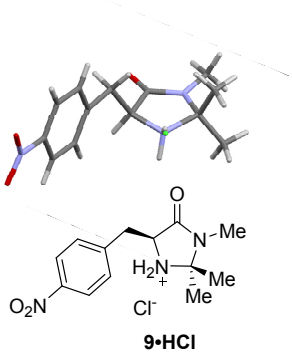

$C_{13}H_{18}ClN_3O_3$, M = 299.75; monoclinic; space group $P2_1$;

a = 5.9962(3) Å, b = 11.9908(10) Å, c = 20.1033(6) Å;

α = 90°, β = 95.649(5)°, γ = 90°;

V = 1438.39(15) Å^3; Z = 4; T = 223(2) K;

reflections collected: 10131, independent reflections: 4024;

R_{int} = 0.079, $R1$ = 0.0656, $wR2$ = 0.1676, Flack parameter = 0.03(3).

2,2,3-Trimethyl-5-(pentafluorobenzyl)-4-imidazolidinone hydrochloride (10·HCl)

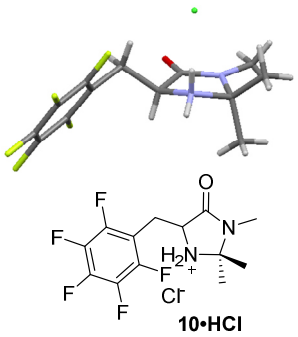

$C_{13}H_{15}ClF_5N_2O$, M = 344.71; monoclinic; space group P121/c1;

a = 11.0689(5) Å, b = 11.9396(4) Å, c = 11.0229(5) Å;

α = 90°, β = 108.3820(10)°, γ = 90°;

V = 1382.44(10) Å^3; Z = 4; T = 100(2) K;

reflections collected: 10797, independent reflections: 3184;

R_{int} = 0.0216, $R1$ = 0.0295, $wR2$ = 0.0813.

5-(4'-Hydroxybenzyl)-2,2,3-trimethyl-4-oxo-1-[(*E*)-3-phenylallylidene]-imidazolidin-1-ium perchlorate (6a·ClO_4^-)

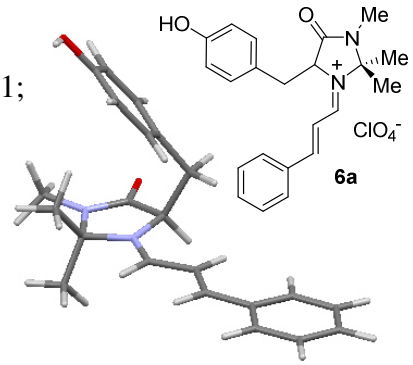

$C_{24}H_{28}ClN_3O_6$, M = 489.94; monoclinic; space group P121/c1;

a = 8.8543(16) Å, b = 23.147(5) Å, c = 12.154(3) Å;

α = 90°, β = 109.935(6)°, γ = 90°;

V = 2341.7(9) Å^3; Z = 4; T = 100(2) K;

reflections collected: 20623, independent reflections: 5372;

R_{int} = 0.1022, $R1$ = 0.0586, $wR2$ = 0.1087.

5-Pentafluorobenzyl-2,2,3-trimethyl-4-oxo-1-[(*E*)-3-phenylallylidene]-imidazolidin-1-ium perchlorate (10a·ClO_4^-)

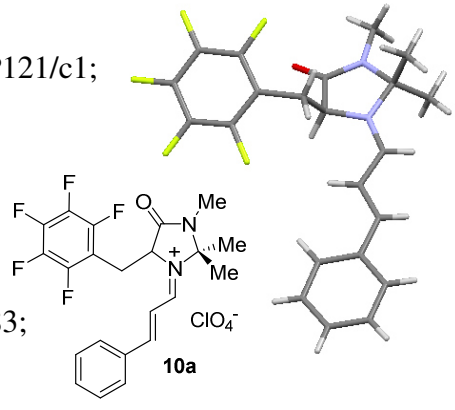

$C_{22}H_{20}ClF_5N_2O_5$, M = 521.85; monoclinic; space group P121/c1;

a = 7.0387(7) Å, b = 18.0680(19) Å, c = 17.673(2) Å;

α = 90°, β = 95.013(5)°, γ = 90°;

V = 2239.0(4) Å^3; Z = 4; T = 100(2) K;

reflections collected: 23237, independent reflections: 5183;

R_{int} = 0.0600, $R1$ = 0.0869, $wR2$ = 0.0963.

(5*S*)-5-Cyclohexylmethyl-2,2,3-trimethyl-4-imidazolidinone hydrochloride (42·HCl)

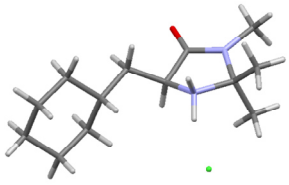

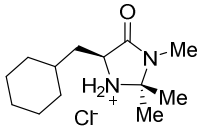

42•HCl

$C_{13}H_{25}ClN_2O$, M = 260.80; orthorombic; space group $P2_12_12_1$;

a = 6.9301(1) Å, b = 10.2438(1) Å, c = 20.7565(1) Å;

α = 90°, β = 90°, γ = 90°;

V = 1473.52(3) Å^3; Z = 4; T = 223(2) K;

reflections collected: 5853, independent reflections: 2447;

R_{int} = 0.054, $R1$ = 0.0480, $wR2$ = 0.1102, Flack parameter = –0.02(3).

(5*S*)-5-(Indol-3-ylmethyl)-2,2,3-trimethyl-4-imidazolidinone hydroperchlorate (43·$HClO_4$)

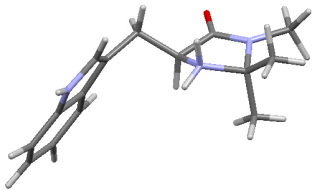

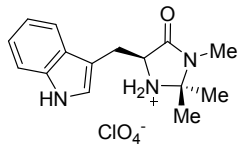

43•ClO_4^-

$C_{15}H_{20}ClN_3O_5$, M = 357.79; orthorhombic; space group Pna21;

a = 11.8766(4) Å, b = 11.5769(5) Å, c = 12.4657(5) Å;

α = 90°, β = 90°, γ = 90°;

V = 1713.96(12) Å^3; Z = 4; T = 100(2) K;

reflections collected: 26282, independent reflections: 3950;

R_{int} = 0.0291, $R1$ = 0.0390, $wR2$ = 0.1003, Flack parameter = 0.0(1).

(5*S*)-5-[(1*H*-Imidazol-5-yl)methyl]-2,2,3-trimethyl-4-imidazolidinone dihydrochloride (44·2HCl)

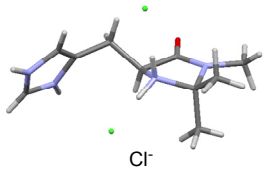

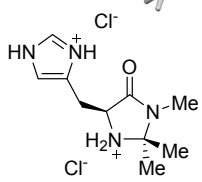

44•2HCl

$C_{11}H_{22}Cl_2N_4O_2$, M = 313.23; monoclinic; space group P1211;

a = 7.4452(4) Å, b = 7.3042(3) Å, c = 14.5434(7) Å;

α = 90°, β = 101.326(2)°, γ = 90°;

V = 775.49(6) Å^3; Z = 2; T = 100(2) K;

reflections collected: 7370, independent reflections: 3122;

R_{int} = 0.0396, $R1$ = 0.0376, $wR2$ = 0.0652, Flack parameter = –0.0(1).

5-(Indol-3-ylmethyl)-2,2,3-trimethyl-4-oxo-1-[(*E*)-3-phenylallylidene]-imidazolidin-1-ium perchlorate (43a·PF_6^-)

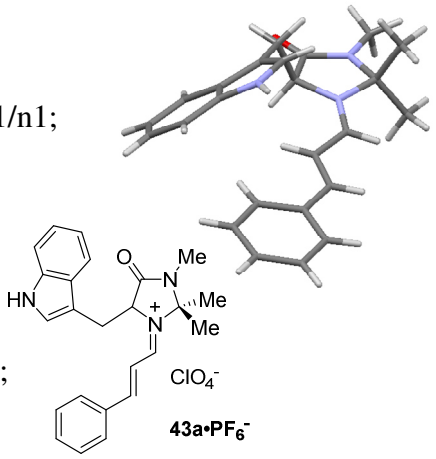

$C_{24}H_{26}F_6N_3OP$, M = 517.45; monoclinic; space group P121/n1;

a = 9.2146(4) Å, b = 22.4643(10) Å, c = 11.9453(5) Å;

α = 90°, β = 109.230(2)°, γ = 90°;

V = 2334.71(17) Å^3; Z = 4; T = 100(2) K;

reflections collected: 37211, independent reflections: 5352;

R_{int} = 0.0421, $R1$ = 0.0389, $wR2$ = 0.1053.

2,2,3,5-Tetramethyl-4-imidazolidinone hydrochloride (60·HCl)

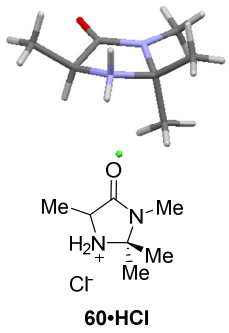

$C_7H_{15}ClN_2O$, M = 178.66; monoclinic; space group C2/c;

a = 21.2327(6) Å, b = 6.8342(5) Å, c = 14.6064(8) Å;

α = 90°, β = 115.692(3)°, γ = 90°;

V = 1909.97(18) Å^3; Z = 8; T = 223(2) K;

reflections collected: 10318, independent reflections: 1636;

R_{int} = 0.043, $R1$ = 0.0359, $wR2$ = 0.1023.

(2*S*)-2-Benzyl-4-methyl-1,4-diaza-spiro[4.4]nonan-3-one hydrochloride (80·HCl)

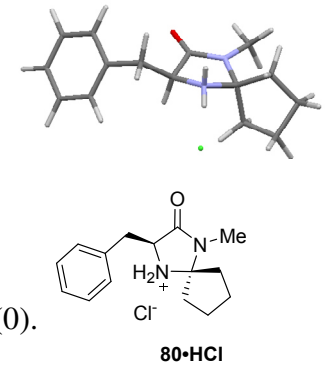

$C_{15.25}H_{21.5}Cl_{1.5}N_2O$, M = 302.02; monoclinic; space group P1211;

a = 14.9864(3) Å, b = 6.9196(2) Å, c = 31.2073(7) Å;

α = 90°, β = 100.410(2)°, γ = 90°;

V = 3182.93(13) Å^3; Z = 8; T = 100(2) K;

reflections collected: 12021, independent reflections: 6300;

R_{int} = 0.0320, $R1$ = 0.0392, $wR2$ = 0.0932, Flack parameter = 0.0(0).

(2*S*)-2-Benzyl-4-methyl-1,4-diaza-spiro[4.5]decan-3-one hydrochloride (81·HCl)

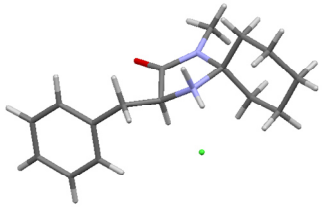

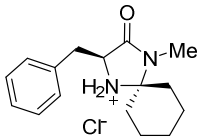

81•HCl

$C_{16}H_{23}ClN_2O$, M = 294.81; monoclinic; space group P1211;

a = 10.7535(4) Å, b = 6.7205(2) Å, c = 10.9429(4) Å;

α = 90°, β = 102.4400(10)°, γ = 90°;

V = 772.26(5) Å^3; Z = 2; T = 100(2) K;

reflections collected: 11633, independent reflections: 3461;

R_{int} = 0.0223, $R1$ = 0.0277, $wR2$ = 0.0756, Flack parameter = 0.0(0).

(2*S*,5*S*)-5-(Pentafluorobenzyl)-2-*tert*-butyl-3-methyl-4-imidazolidinone hydrochloride (86·HCl)

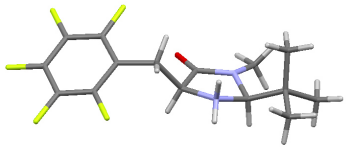

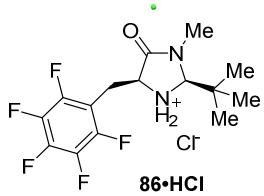

86•HCl

$C_{15}H_{18}ClF_5N_2O$, M = 372.76; orthorombic; space group $P2_12_12_1$;

a = 6.9225(2) Å, b = 22.0213(9) Å, c = 23.4008(9) Å;

α = 90°, β = 90°, γ = 90°;

V = 3567.30(2) Å^3; Z = 8; T = 223(2) K;

reflections collected: 21684, independent reflections: 5504;

R_{int} = 0.080, $R1$ = 0.0472, $wR2$ = 0.1010, Flack parameter = –0.01(2).

(5*S*)-5-Benzyl-2,2,3-trimethyl-4-oxo-1-[(*E*)-3-(*para*-chlorophenylallylidene]-imidazolidin-1-ium perchlorate (92·ClO_4^-)

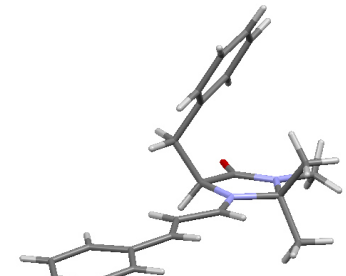

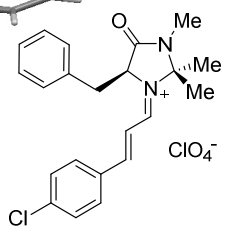

92•ClO_4^-

$C_{22}H_{24}Cl_2N_2O_5$, M = 467.33; triclinic; space group P1;

a = 9.3902(1) Å, b = 11.1396(1) Å, c = 13.2246(1) Å;

α = 68.627(1)°, β = 84.585(1)°, γ = 85.411(1)°;

V = 1280.90(2) Å^3; Z = 2; T = 223(2) K;

reflections collected: 15552, independent reflections: 6344;

R_{int} = 0.036, $R1$ = 0.0888, $wR2$ = 0.2455, Flack parameter = 0.042(18).

9 Bibliography

[1] a) R. Gordillo, K. N. Houk, *J. Am. Chem. Soc.* **2006**, *128*, 3543-3553.; b) W. Langenbeck, *Justus Liebigs Ann. Chem.* **1929**, *469*, 16-25.; c) G. Lelais, D. W. C. MacMillan, *Aldrichimica Acta* **2006**, *39*, 79-87.; d) D. Seebach, B. Amatsch, R. Amstutz, A. K. Beck, M. Doler, M. Egli, R. Fitzi, M. Gautschi, B. Herradön, P. C. Hidber, J. J. Irwin, R. Locher, M. Maestro, T. Maetzke, A. Mouriño, E. Pfammatter, D. A. Plattner, C. Schickli, W. B. Schweizer, P. Seiler, G. Stucky, W. Petter, J. Escalante, E. Juaristi, D. Quintana, C. Miravitlles, E. Molins, *HCA* **1992**, *75*, 913-934.

[2] F. Meemken, N. Maeda, K. Hungerbühler, A. Baiker, *Angew. Chem. Int. Ed.* **2012**, *51*, 8212-8216.

[3] J. C. Burley, R. Gilmour, T. J. Prior, G. M. Day, *Acta Crystallogr C* **2008**, *64*, o10-14.

[4] C. Sparr, R. Gilmour, *Angew. Chem. Int. Ed.* **2010**, *49*, 6520-6523.

[5] U. Grošelj, D. Seebach, D. M. Badine, W. B. Schweizer, A. K. Beck, I. Krossing, P. Klose, Y. Hayashi, T. Uchimaru, *HCA* **2009**, *92*, 1225-1259.

[6] R. L. Davis, K. L. Jensen, B. Gschwend, K. A. Jørgensen, *Chem. Eur. J.* **2014**, *20*, 64-67.

[7] C. Sparr, W. B. Schweizer, H. M. Senn, R. Gilmour, *Angew. Chem. Int. Ed.* **2009**, *48*, 3065-3068.

[8] a) K. A. Ahrendt, C. J. Borths, D. W. C. MacMillan, *J. Am. Chem. Soc.* **2000**, *122*, 4243-4244.; b) B. List, R. A. Lerner, C. F. Barbas, *J. Am. Chem. Soc.* **2000**, *122*, 2395-2396.

[9] Wöhler, Liebig, *Ann. Pharm.* **1832**, *3*, 249-282.

[10] a) W. Langenbeck, *Angew. Chem.* **1928**, *41*, 740-745.; b) W. Langenbeck, *Angew. Chem.* **1932**, *45*, 97-99.; c) F. Lynen, *Angew. Chem.* **1950**, *62*, 150-150.

[11] C. F. Barbas, *Angew. Chem. Int. Ed.* **2008**, *47*, 42-47.

[12] J. von Liebig, *Justus Liebigs Ann. Chem.* **1860**, *113*, 246-247.

[13] a) E. Knoevenagel, *Ber. Dtsch. Chem. Ges.* **1894**, *27*, 2345-2346.; b) E. Knoevenagel, *Ber. Dtsch. Chem. Ges.* **1898**, *31*, 2596-2619.

[14] M. Dennstedt, J. Zimmermann, *Ber. Dtsch. Chem. Ges.* **1886**, *19*, 75-78.

[15] a) A. Verley, F. Bölsing, *Ber. Dtsch. Chem. Ges.* **1901**, *34*, 3359-3362.; b) A. Verley, F. Bölsing, *Ber. Dtsch. Chem. Ges.* **1901**, *34*, 3354-3358.

[16] H. D. Dakin, *J. Biol. Chem.* **1909**, *7*, 49-55.

[17] G. Bredig, P. S. Fiske, **1912**, *46*, 7-23.

[18] W. Langenbeck, R. Sauerbier, *Ber. dtsch. Chem. Ges. A/B* **1937**, *70*, 1540-1541.

[19] a) R. Breslow, *J. Am. Chem. Soc.* **1958**, *80*, 3719-3726.; b) S. P. Nolan, *N-Heterocyclic Carbenes in Synthesis*, Wiley, **2006**.

[20] V. Prelog, M. Wilhelm, *HCA* **1954**, *37*, 1634-1660.

[21] a) H. Pracejus, *Justus Liebigs Ann. Chem.* **1960**, *634*, 9-22.; b) H. Pracejus, H. Mätje, *J. Prakt. Chem.* **1964**, *24*, 195-205.

[22] E. H. Cordes, W. P. Jencks, *J. Am. Chem. Soc.* **1962**, *84*, 826-831.

[23] a) L. M. Litvinenko, A. I. Kirichenko, *176*, 97-100.; b) W. Steglich, G. Höfle, *Angew. Chem. Int. Ed. Engl.* **1969**, *8*, 981-981.

[24] S.-i. Yamada, G. Otani, *Tetrahedron Letters* **1969**, *10*, 4237-4240.

[25] a) U. Eder, G. Sauer, R. Wiechert, *Angew. Chem. Int. Ed. Engl.* **1971**, *10*, 496-497.; b) Z. G. Hajos, D. R. Parrish, *J. Org. Chem.* **1974**, *39*, 1615-1621.

[26] a) R. B. Woodward, B. W. Au-Yeung, P. Balaram, L. J. Browne, D. E. Ward, B. W. Au-Yeung, P. Balaram, L. J. Browne, P. J. Card, C. H. Chen, *J. Am. Chem. Soc.* **1981**, *103*, 3213-3215.; b) R. B. Woodward, E. Logusch, K. P. Nambiar, K. Sakan, D. E. Ward, B. W. Au-Yeung, P. Balaram, L. J. Browne, P. J. Card, C. H. Chen, *J. Am. Chem. Soc.* **1981**, *103*, 3210-3213.; c) R. B. Woodward, E. Logusch, K. P. Nambiar, K. Sakan, D. E. Ward, B. W. Au-Yeung, P. Balaram, L. J. Browne, P. J. Card, C. H. Chen, *J. Am. Chem. Soc.* **1981**, *103*, 3215-3217.

[27] M. E. Jung, W. D. Vaccaro, K. R. Buszek, *Tetrahedron Letters* **1989**, *30*, 1893-1896.

[28] a) A. Berkessel, H. Gröger, D. MacMillan, *Asymmetric Organocatalysis: From Biomimetic Concepts to Applications in Asymmetric Synthesis*, Auflage: 1. Auflage ed., Wiley-VCH Verlag GmbH & Co. KGaA, Weinheim, **2005**.; b) R. R. Knowles, E. N. Jacobsen, *PNAS* **2010**

[29] W. J. Rutter, *Fed. Proc.* **1964**, *23*, 1248-1257.

[30] S. Mukherjee, J. W. Yang, S. Hoffmann, B. List, *Chem. Rev.* **2007**, *107*, 5471-5569.

[31] A. Erkkilä, I. Majander, P. M. Pihko, *Chem. Rev.* **2007**, *107*, 5416-5470.

[32] C. Sparr, R. Gilmour, *Angew. Chem.* **2011**, *123*, 8541-8545.

[33] D. Seidel, *J. Am. Chem. Soc.* **2010**, *132*, 8224-8224.

[34] R. P. Wurz, *Chem. Rev.* **2007**, *107*, 5570-5595.

[35] D. Enders, O. Niemeier, A. Henseler, *Chem. Rev.* **2007**, *107*, 5606-5655.

[36] A. G. Doyle, E. N. Jacobsen, *Chem. Rev.* **2007**, *107*, 5713-5743.

[37] a) T. Akiyama, J. Itoh, K. Yokota, K. Fuchibe, *Angew. Chem. Int. Ed.* **2004**, *43*, 1566-1568.; b) M. Yamanaka, J. Itoh, K. Fuchibe, T. Akiyama, *J. Am. Chem. Soc.* **2007**, *129*, 6756-6764.

[38] T. Hashimoto, K. Maruoka, *Chem. Rev.* **2007**, *107*, 5656-5682.

[39] a) M. Frohn, Y. Shi, *Synthesis* **2000**, *2000*, 1979-2000.; b) Z.-X. Wang, Y. Tu, M. Frohn, J.-R. Zhang, Y. Shi, *J. Am. Chem. Soc.* **1997**, *119*, 11224-11235.

[40] a) E. R. Jarvo, S. J. Miller, *Tetrahedron* **2002**, *58*, 2481-2495.; b) E. A. C. Davie, S. M. Mennen, Y. Xu, S. J. Miller, *Chem. Rev.* **2007**, *107*, 5759-5812.

[41] D. W. C. MacMillan, *Nature* **2008**, *455*, 304-308.

[42] C. Grondal, M. Jeanty, D. Enders, *Nat Chem* **2010**, *2*, 167-178.

[43] a) M. Marigo, T. C. Wabnitz, D. Fielenbach, K. A. Jørgensen, *Angew. Chem. Int. Ed.* **2005**, *44*, 794-797.; b) Y. Hayashi, H. Gotoh, T. Hayashi, M. Shoji, *Angew. Chem. Int. Ed.* **2005**, *44*, 4212-4215.; c) K. L. Jensen, G. Dickmeiss, H. Jiang, Ł. Albrecht, K. A. Jørgensen, *Acc. Chem. Res.* **2012**, *45*, 248-264.

[44] a) D. Seebach, U. Grošelj, D. M. Badine, W. B. Schweizer, A. K. Beck, *HCA* **2008**, *91*, 1999-2034.; b) D. Seebach, A. K. Beck, D. M. Badine, M. Limbach, A. Eschenmoser, A. M. Treasurywala, R. Hobi, W. Prikoszovich, B. Linder, *HCA* **2007**, *90*, 425-471.

[45] E.-M. Tanzer, L. E. Zimmer, W. B. Schweizer, R. Gilmour, *Chem. Eur. J.* **2012**, *18*, 11334-11342.

[46] I. G. Molnár, E.-M. Tanzer, C. Daniliuc, R. Gilmour, *Chem. Eur. J.* **2014**, *20*, 794-800.

[47] R. Gordillo, J. Carter, K. N. Houk, *Adv. Synth. Catal.* **2004**, *346*, 1175-1185.

[48] D. Seebach, R. Gilmour, U. Grošelj, G. Deniau, C. Sparr, M.-O. Ebert, A. K. Beck, L. B. McCusker, D. Šišak, T. Uchimaru, *HCA* **2010**, *93*, 603-634.

[49] J. B. Brazier, G. Evans, T. J. K. Gibbs, S. J. Coles, M. B. Hursthouse, J. A. Platts, N. C. O. Tomkinson, *Org. Lett.* **2009**, *11*, 133-136.

[50] a) U. Grošelj, W. B. Schweizer, M.-O. Ebert, D. Seebach, *HCA* **2009**, *92*, 1-13.; b) D. Seebach, U. Grošelj, W. B. Schweizer, S. Grimme, C. Mück-Lichtenfeld, *HCA* **2010**, *93*, 1-16.

[51] C. Sparr, R. Gilmour, *Angew. Chem. Int. Ed.* **2011**, *50*, 8391-8395.
[52] J. F. Austin, D. W. C. MacMillan, *J. Am. Chem. Soc.* **2002**, *124*, 1172-1173.
[53] S. Lakhdar, J. Ammer, H. Mayr, *Angew. Chem. Int. Ed.* **2011**, *50*, 9953-9956.
[54] a) J. D. v. d. Waals, A.W. Sijthoff (Leiden), **1873**.; b) K.-T. Tang, J. P. Toennies, *Angew. Chem. Int. Ed.* **2010**, *49*, 9574-9579.
[55] *Nobel Prize in Physics 1910 - Presentation Speech*. http://www.nobelprize.org/nobel_prizes/physics/laureates/1910/press.html.
[56] C. Bissantz, B. Kuhn, M. Stahl, *J. Med. Chem.* **2010**, *53*, 5061-5084.
[57] a) H.-J. Schneider, *Angew. Chem. Int. Ed.* **2009**, *48*, 3924-3977.; b) J.-M. Lehn, *Supramolecular Chemistry*, 1 edition ed., Wiley-VCH, Weinheim ; New York, **1995**.
[58] Y. Sohtome, K. Nagasawa, *Chem. Commun.* **2012**, *48*, 7777-7789.
[59] J. N. Israelachvili, *Intermolecular and Surface Forces, Third Edition: Revised Third Edition*, 3 edition ed., Academic Press, Burlington, MA, **2011**.
[60] C. A. Hunter, K. R. Lawson, J. Perkins, C. J. Urch, *J. Chem. Soc., Perkin Trans. 2* **2001**, 651-669.
[61] a) M. L. Waters, *Current Opinion in Chemical Biology* **2002**, *6*, 736-741.; b) C. R. Martinez, B. L. Iverson, *Chem. Sci.* **2012**, *3*, 2191-2201.
[62] a) E. A. Meyer, R. K. Castellano, F. Diederich, *Angew. Chem. Int. Ed.* **2003**, *42*, 1210-1250.; b) L. M. Salonen, M. Ellermann, F. Diederich, *Angew. Chem. Int. Ed.* **2011**, *50*, 4808-4842.
[63] P. Yakovchuk, E. Protozanova, M. D. Frank-Kamenetskii, *Nucl. Acids Res.* **2006**, *34*, 564-574.
[64] S. K. Burley, G. A. Petsko, *Science* **1985**, *229*, 23-28.
[65] a) C. A. Hunter, J. K. M. Sanders, *J. Am. Chem. Soc.* **1990**, *112*, 5525-5534.; b) K. C. Janda, J. C. Hemminger, J. S. Winn, S. E. Novick, S. J. Harris, W. Klemperer, *The Journal of Chemical Physics* **1975**, *63*, 1419-1421.; c) R. Laatikainen, J. Ratilainen, R. Sebastian, H. Santa, *J. Am. Chem. Soc.* **1995**, *117*, 11006-11010.; d) G. D. Smith, R. L. Jaffe, *J. Phys. Chem.* **1996**, *100*, 9624-9630.
[66] C. R. Patrick, G. S. Prosser, *Nature* **1960**, *187*, 1021-1021.
[67] a) J. D. Dunitz, *ChemBioChem* **2004**, *5*, 614-621.; b) J. D. Dunitz, W. B. Schweizer, *Chem. Eur. J.* **2006**, *12*, 6804-6815.
[68] a) S. Tsuzuki, T. Uchimaru, M. Mikami, *J. Phys. Chem. A* **2006**, *110*, 2027-2033.; b) A. P. West, S. Mecozzi, D. A. Dougherty, *J. Phys. Org. Chem.* **1997**, *10*, 347-350.; c) J. M. Steed, T. A. Dixon, W. Klemperer, *The Journal of Chemical Physics* **1979**, *70*, 4940-4946.; d) S. Lorenzo, G. R. Lewis, I. Dance, *New J. Chem.* **2000**, *24*, 295-304.; e) O. R. Lozman, R. J. Bushby, J. G. Vinter, *J. Chem. Soc., Perkin Trans. 2* **2001**, 1446-1452.
[69] S. Kumar, A. Das, *The Journal of Chemical Physics* **2013**, *139*
[70] I. K. Mati, S. L. Cockroft, *Chem. Soc. Rev.* **2010**, *39*, 4195-4205.
[71] a) F. Hof, D. M. Scofield, W. B. Schweizer, F. Diederich, *Angew. Chem. Int. Ed.* **2004**, *43*, 5056-5059.; b) F. R. Fischer, W. B. Schweizer, F. Diederich, *Angew. Chem. Int. Ed.* **2007**, *46*, 8270-8273.; c) F. R. Fischer, W. B. Schweizer, F. Diederich, *Chem. Commun.* **2008**, 4031-4033.
[72] F. Cozzi, R. Annunziata, M. Benaglia, M. Cinquini, L. Raimondi, K. K. Baldridge, J. S. Siegel, *Org. Biomol. Chem.* **2003**, *1*, 157-162.
[73] M. Harmata, *Acc. Chem. Res.* **2004**, *37*, 862-873.
[74] a) F.-G. Klärner, B. Kahlert, *Acc. Chem. Res.* **2003**, *36*, 919-932.; b) B. Branchi, V. Balzani, P. Ceroni, M. C. Kuchenbrandt, F.-G. Klärner, D. Bläser, R. Boese, *J. Org. Chem.* **2008**, *73*, 5839-5851.
[75] S. L. Cockroft, C. A. Hunter, *Chem. Soc. Rev.* **2007**, *36*, 172-188.

[76] C. A. Hunter, C. M. R. Low, C. Rotger, J. G. Vinter, C. Zonta, *PNAS* **2002**, *99*, 4873-4876.
[77] H. Adams, S. L. Cockroft, C. Guardigli, C. A. Hunter, K. R. Lawson, J. Perkins, S. E. Spey, C. J. Urch, R. Ford, *ChemBioChem* **2004**, *5*, 657-665.
[78] Z. R. Laughrey, S. E. Kiehna, A. J. Riemen, M. L. Waters, *J. Am. Chem. Soc.* **2008**, *130*, 14625-14633.
[79] M. O. Sinnokrot, C. D. Sherrill, *J. Phys. Chem. A* **2003**, *107*, 8377-8379.
[80] a) M. O. Sinnokrot, C. D. Sherrill, *J. Am. Chem. Soc.* **2004**, *126*, 7690-7697.; b) E. C. Lee, B. H. Hong, J. Y. Lee, J. C. Kim, D. Kim, Y. Kim, P. Tarakeshwar, K. S. Kim, *J. Am. Chem. Soc.* **2005**, *127*, 4530-4537.
[81] S. E. Wheeler, K. N. Houk, *J. Chem. Theory Comput.* **2009**, *5*, 2301-2312.
[82] a) M. Salwiczek, E. K. Nyakatura, U. I. M. Gerling, S. Ye, B. Koksch, *Chem. Soc. Rev.* **2012**, *41*, 2135-2171.; b) C. J. Pace, H. Zheng, R. Mylvaganam, D. Kim, J. Gao, *Angew. Chem. Int. Ed.* **2012**, *51*, 103-107.; c) P. Martín-Gago, M. Gomez-Caminals, R. Ramón, X. Verdaguer, P. Martin-Malpartida, E. Aragón, J. Fernández-Carneado, B. Ponsati, P. López-Ruiz, M. A. Cortes, B. Colás, M. J. Macias, A. Riera, *Angew. Chem. Int. Ed.* **2012**, *51*, 1820-1825.
[83] a) S.-M. Hsu, Y.-C. Lin, J.-W. Chang, Y.-H. Liu, H.-C. Lin, *Angew. Chem. Int. Ed.* **2014**, *53*, 1921-1927.; b) S. Burattini, B. W. Greenland, D. H. Merino, W. Weng, J. Seppala, H. M. Colquhoun, W. Hayes, M. E. Mackay, I. W. Hamley, S. J. Rowan, *J. Am. Chem. Soc.* **2010**, *132*, 12051-12058.; c) A. Mangalum, B. P. Morgan, A. G. Tennyson, R. C. Smith, *Macromol. Chem. Phys.* **2014**, *215*, 351-357.
[84] G. B. Jones, *Tetrahedron* **2001**, *57*, 7999-8016.
[85] E. J. Corey, H. E. Ensley, *J. Am. Chem. Soc.* **1975**, *97*, 6908-6909.
[86] J. F. Maddaluno, N. Gresh, C. Giessner-Prettre, *J. Org. Chem.* **1994**, *59*, 793-802.
[87] B. Mezrhab, F. Dumas, J. d'Angelo, C. Riche, *J. Org. Chem.* **1994**, *59*, 500-503.
[88] J. K. Whitesell, *Chem. Rev.* **1992**, *92*, 953-964.
[89] M. Tamres, *J. Am. Chem. Soc.* **1952**, *74*, 3375-3378.
[90] Y. Umezawa, S. Tsuboyama, H. Takahashi, J. Uzawa, M. Nishio, *Tetrahedron* **1999**, *55*, 10047-10056.
[91] Y. Umezawa, S. Tsuboyama, H. Takahashi, J. Uzawa, Motohiro, *Bioorganic & Medicinal Chemistry* **1999**, *7*, 2021-2026.
[92] H. Takahashi, S. Tsuboyama, Y. Umezawa, K. Honda, M. Nishio, *Tetrahedron* **2000**, *56*, 6185-6191.
[93] M. Nishio, M. Hirota, Y. Umezawa, *The CH-Pi Interaction: Evidence, Nature, and Consequences*, 1 edition ed., Wiley-VCH, New York, **1998**.
[94] M. Nishio, *Phys. Chem. Chem. Phys.* **2011**, *13*, 13873-13900.
[95] S. Tsuzuki, A. Fujii, *Phys. Chem. Chem. Phys.* **2008**, *10*, 2584-2594.
[96] a) J. J. Novoa, F. Mota, *Chemical Physics Letters* **2000**, *318*, 345-354.; b) J. J. J. Dom, B. Michielsen, B. U. W. Maes, W. A. Herrebout, B. J. van der Veken, *Chemical Physics Letters* **2009**, *469*, 85-89.; c) O. Takahashi, Y. Kohno, K. Saito, *Chemical Physics Letters* **2003**, *378*, 509-515.; d) M. Hirota, K. Sakaibara, H. Suezawa, T. Yuzuri, E. Ankai, M. Nishio, *J. Phys. Org. Chem.* **2000**, *13*, 620-623.
[97] S. Sakaki, K. Kato, T. Miyazaki, Y. Musashi, K. Ohkubo, H. Ihara, C. Hirayama, *J. Chem. Soc., Faraday Trans.* **1993**, *89*, 659-664.
[98] S. Tsuzuki, K. Honda, T. Uchimaru, M. Mikami, K. Tanabe, *J. Am. Chem. Soc.* **2000**, *122*, 3746-3753.
[99] B. K. Mishra, S. Karthikeyan, V. Ramanathan, *J. Chem. Theory Comput.* **2012**, *8*, 1935-1942.

[100] W. R. Carroll, C. Zhao, M. D. Smith, P. J. Pellechia, K. D. Shimizu, *Org. Lett.* **2011**, *13*, 4320-4323.
[101] N. J. Zondlo, *Acc. Chem. Res.* **2013**, *46*, 1039-1049.
[102] a) R. U. Lemieux, *Acc. Chem. Res.* **1996**, *29*, 373-380.; b) F. A. Quiocho, *Annual Review of Biochemistry* **1986**, *55*, 287-315.; c) F. A. Quiocho, *Pure and Applied Chemistry* **1989**, *61*.; d) C. D. Tatko, M. L. Waters, *J. Am. Chem. Soc.* **2004**, *126*, 2028-2034.
[103] R. Carrillo, M. López-Rodríguez, V. S. Martín, T. Martín, *Angew. Chem. Int. Ed.* **2009**, *48*, 7803-7808.
[104] a) J. C. Ma, D. A. Dougherty, *Chem. Rev.* **1997**, *97*, 1303-1324.; b) S. Mecozzi, A. P. West, D. A. Dougherty, *J. Am. Chem. Soc.* **1996**, *118*, 2307-2308.
[105] a) J. Sunner, K. Nishizawa, P. Kebarle, *J. Phys. Chem.* **1981**, *85*, 1814-1820.; b) M. Meot-Ner, C. A. Deakyne, *J. Am. Chem. Soc.* **1985**, *107*, 474-479.
[106] a) X. Xiu, N. L. Puskar, J. A. P. Shanata, H. A. Lester, D. A. Dougherty, *Nature* **2009**, *458*, 534-537.; b) D. A. Dougherty, *J. Nutr.* **2007**, *137*, 1504S-1508S.; c) M. M. Torrice, K. S. Bower, H. A. Lester, D. A. Dougherty, *PNAS* **2009**, *106*, 11919-11924.; d) S. Mecozzi, A. P. West, D. A. Dougherty, *PNAS* **1996**, *93*, 10566-10571.; e) D. A. Dougherty, *Science* **1996**, *271*, 163-168.
[107] S. E. Wheeler, K. N. Houk, *J. Am. Chem. Soc.* **2009**, *131*, 3126-3127.
[108] a) H.-J. Schneider, *Angew. Chem. Int. Ed. Engl.* **1991**, *30*, 1417-1436.; b) H.-J. Schneider, *Chem. Soc. Rev.* **1994**, *23*, 227-234.
[109] a) M. Dhaenens, L. Lacombe, J.-M. Lehn, J.-P. Vigneron, *J. Chem. Soc., Chem. Commun.* **1984**, 1097-1099.; b) J.-M. Lehn, R. Méric, J.-P. Vigneron, I. Bkouche-Waksman, C. Pascard, *J. Chem. Soc., Chem. Commun.* **1991**, 62-64.
[110] S. Lin, E. N. Jacobsen, *Nat Chem* **2012**, *4*, 817-824.
[111] Y. Mori, S. Yamada, *Molecules* **2012**, *17*, 2161-2168.
[112] a) W. S. Jen, J. J. M. Wiener, D. W. C. MacMillan, *J. Am. Chem. Soc.* **2000**, *122*, 9874-9875.; b) N. A. Paras, D. W. C. MacMillan, *J. Am. Chem. Soc.* **2001**, *123*, 4370-4371.; c) N. A. Paras, D. W. C. MacMillan, *J. Am. Chem. Soc.* **2002**, *124*, 7894-7895.; d) S. G. Ouellet, J. B. Tuttle, D. W. C. MacMillan, *J. Am. Chem. Soc.* **2005**, *127*, 32-33.; e) J. B. Tuttle, S. G. Ouellet, D. W. C. MacMillan, *J. Am. Chem. Soc.* **2006**, *128*, 12662-12663.; f) A. B. Northrup, D. W. C. MacMillan, *J. Am. Chem. Soc.* **2002**, *124*, 2458-2460.; g) S. P. Brown, N. C. Goodwin, D. W. C. MacMillan, *J. Am. Chem. Soc.* **2003**, *125*, 1192-1194.; h) S. Lee, D. W. C. MacMillan, *Tetrahedron* **2006**, *62*, 11413-11424.; i) C. J. Borths, D. E. Carrera, D. W. C. MacMillan, *Tetrahedron* **2009**, *65*, 6746-6753.
[113] a) M. P. Brochu, S. P. Brown, D. W. C. MacMillan, *J. Am. Chem. Soc.* **2004**, *126*, 4108-4109.; b) T. D. Beeson, D. W. C. MacMillan, *J. Am. Chem. Soc.* **2005**, *127*, 8826-8828.; c) I. K. Mangion, A. B. Northrup, D. W. C. MacMillan, *Angew. Chem. Int. Ed.* **2004**, *43*, 6722-6724.; d) A. E. Allen, D. W. C. MacMillan, *J. Am. Chem. Soc.* **2010**, *132*, 4986-4987.
[114] a) H.-Y. Jang, J.-B. Hong, D. W. C. MacMillan, *J. Am. Chem. Soc.* **2007**, *129*, 7004-7005.; b) T. H. Graham, C. M. Jones, N. T. Jui, D. W. C. MacMillan, *J. Am. Chem. Soc.* **2008**, *130*, 16494-16495.; c) J. C. Conrad, J. Kong, B. N. Laforteza, D. W. C. MacMillan, *J. Am. Chem. Soc.* **2009**, *131*, 11640-11641.; d) D. A. Nagib, M. E. Scott, D. W. C. MacMillan, *J. Am. Chem. Soc.* **2009**, *131*, 10875-10877.; e) S. Rendler, D. W. C. MacMillan, *J. Am. Chem. Soc.* **2010**, *132*, 5027-5029.; f) N. T. Jui, J. A. O. Garber, F. G. Finelli, D. W. C. MacMillan, *J. Am. Chem. Soc.* **2012**, *134*, 11400-11403.; g) T. D. Beeson, A. Mastracchio, J.-B. Hong, K. Ashton, D. W. C. MacMillan, *Science* **2007**, *316*, 582-585.

[115] P. I. Dalko, L. Moisan, *Angew. Chem. Int. Ed.* **2001**, *40*, 3726-3748.
[116] a) G. S. Hammond, *J. Am. Chem. Soc.* **1955**, *77*, 334-338.; b) J. E. Leffler, *Science* **1953**, *117*, 340-341.
[117] S. Lakhdar, T. Tokuyasu, H. Mayr, *Angew. Chem. Int. Ed.* **2008**, *47*, 8723-8726.
[118] Z. Lili, Z. Zhongjun, L. Huiling, H. Xuri, *Tetrahedron: Asymmetry* **2013**, *24*, 474-479.
[119] a) M. Brandl, M. S. Weiss, A. Jabs, J. Sühnel, R. Hilgenfeld, *Journal of Molecular Biology* **2001**, *307*, 357-377.; b) G. B. McGaughey, M. Gagné, A. K. Rappé, *J. Biol. Chem.* **1998**, *273*, 15458-15463.
[120] F. An, S. Paul, J. Ammer, A. R. Ofial, P. Mayer, S. Lakhdar, H. Mayr, *Asian Journal of Organic Chemistry* **2014**, n/a-n/a.
[121] a) S. M. Ngola, D. A. Dougherty, *J. Org. Chem.* **1998**, *63*, 4566-4567.; b) L. Wang, N. Sun, S. Terzyan, X. Zhang, D. R. Benson, *Biochemistry* **2006**, *45*, 13750-13759.
[122] a) D. Seebach, E. Dziadulewicz, L. Behrendt, S. Cantoreggi, R. Fitzi, *Liebigs Ann. Chem.* **1989**, *1989*, 1215-1232.; b) R. Fitzi, D. Seebach, *Tetrahedron* **1988**, *44*, 5277-5292.; c) D. Seebach, R. Naef, *HCA* **1981**, *64*, 2704-2708.
[123] E. V. Anslyn, D. A. Dougherty, *Modern physical chemistry*, University Science, Sausalito, Calif., **2004**.
[124] A. M. Köster, *Nachr. Chem. Tech. Lab.* **1997**, *45*, 917-918.
[125] A. Bauzá, D. Quiñonero, P. M. Deyà, A. Frontera, *Chemical Physics Letters* **2013**, *567*, 60-65.
[126] A. D. Buckingham, *Q. Rev. Chem. Soc.* **1959**, *13*, 183-214.
[127] a) J. Hernández-Trujillo, A. Vela, *J. Phys. Chem.* **1996**, *100*, 6524-6530.; b) S. Schweizer, J. Reed, *Biophys J* **2008**, *95*, 3381-3390.; c) P. E. M. Lopes, G. Lamoureux, A. D. Mackerell, *J. Comput. Chem.* **2009**, *30*, 1821-1838.
[128] a) F. Weigend, R. Ahlrichs, *Phys. Chem. Chem. Phys.* **2005**, *7*, 3297-3305.; b) S. Grimme, J. Antony, S. Ehrlich, H. Krieg, *The Journal of Chemical Physics* **2010**, *132*.; c) S. Grimme, S. Ehrlich, L. Goerigk, *J. Comput. Chem.* **2011**, *32*, 1456-1465.; d) F. Furche, R. Ahlrichs, C. Hättig, W. Klopper, M. Sierka, F. Weigend, *Wiley Interdisciplinary Reviews: Computational Molecular Science* **2014**, *4*, 91-100.
[129] a) E. Díez, J. San-Fabián, J. Guilleme, C. Altona, L. A. Donders, *Molecular Physics* **1989**, *68*, 49-63.; b) A. Navarro-Vázquez, J. C. Cobas, F. J. Sardina, J. Casanueva, E. Díez, *J. Chem. Inf. Comput. Sci.* **2004**, *44*, 1680-1685.; c) C. Altona, in *eMagRes*, John Wiley & Sons, Ltd, **2007**.
[130] a) C. Altona, J. H. Ippel, A. J. A. W. Hoekzema, C. Erkelens, M. Groesbeek, L. A. Donders, *Magn. Reson. Chem.* **1989**, *27*, 564-576.; b) C. Altona, R. Francke, R. de Haan, J. H. Ippel, G. J. Daalmans, A. J. A. W. Hoekzema, J. van Wijk, *Magn. Reson. Chem.* **1994**, *32*, 670-678.
[131] a) H. Mayr, T. Bug, M. F. Gotta, N. Hering, B. Irrgang, B. Janker, B. Kempf, R. Loos, A. R. Ofial, G. Remennikov, H. Schimmel, *J. Am. Chem. Soc.* **2001**, *123*, 9500-9512.; b) H. Mayr, A. R. Ofial, *Angew. Chem. Int. Ed.* **2006**, *45*, 1844-1854.
[132] H. Mayr, S. Lakhdar, B. Maji, A. R. Ofial, *Beilstein Journal of Organic Chemistry* **2012**, *8*, 1458-1478.
[133] W. Yongjiang, X. Xiaoliang, P. Wen, *Synthetic Communications* **2009**, *39*, 2032-2041.
[134] K.-S. Choi, S.-G. Kim, *Tetrahedron Letters* **2010**, *51*, 5203-5206.
[135] a) L. Hojabri, A. Hartikka, F. M. Moghaddam, P. I. Arvidsson, *Adv. Synth. Catal.* **2007**, *349*, 740-748.; b) A. Hartikka, L. Hojabri, P. P. Bose, P. I. Arvidsson, *Tetrahedron: Asymmetry* **2009**, *20*, 1871-1876.
[136] C. D. M. Churchill, S. D. Wetmore, *J. Phys. Chem. B* **2009**, *113*, 16046-16058.

[137] a) F. Mühlthau, O. Schuster, T. Bach, *J. Am. Chem. Soc.* **2005**, *127*, 9348-9349.; b) F. Mühlthau, D. Stadler, A. Goeppert, G. A. Olah, G. K. S. Prakash, T. Bach, *J. Am. Chem. Soc.* **2006**, *128*, 9668-9675.
[138] S. W. Baldwin, A. Long, *Org. Lett.* **2004**, *6*, 1653-1656.
[139] a) G. Wuitschik, M. Rogers-Evans, K. Müller, H. Fischer, B. Wagner, F. Schuler, L. Polonchuk, E. M. Carreira, *Angew. Chem. Int. Ed.* **2006**, *45*, 7736-7739.; b) G. Wuitschik, M. Rogers-Evans, A. Buckl, M. Bernasconi, M. Märki, T. Godel, H. Fischer, B. Wagner, I. Parrilla, F. Schuler, J. Schneider, A. Alker, W. B. Schweizer, K. Müller, E. M. Carreira, *Angew. Chem. Int. Ed.* **2008**, *47*, 4512-4515.; c) J. A. Burkhard, G. Wuitschik, M. Rogers-Evans, K. Müller, E. M. Carreira, *Angew. Chem. Int. Ed.* **2010**, *49*, 9052-9067.; d) G. Wuitschik, E. M. Carreira, B. r. Wagner, H. Fischer, I. Parrilla, F. Schuler, M. Rogers-Evans, K. Müller, *J. Med. Chem.* **2010**, *53*, 3227-3246.
[140] T. J. Peelen, Y. Chi, S. H. Gellman, *J. Am. Chem. Soc.* **2005**, *127*, 11598-11599.
[141] T. Poloński, *Tetrahedron* **1985**, *41*, 611-616.
[142] L. Samulis, N. C. O. Tomkinson, *Tetrahedron* **2011**, *67*, 4263-4267.
[143] D. H. McDaniel, H. C. Brown, *J. Org. Chem.* **1958**, *23*, 420-427.
[144] N. C. Polfer, J. Oomens, *Phys. Chem. Chem. Phys.* **2007**, *9*, 3804-3817.
[145] V. N. Bagratashvili, V. S. Letokhov, A. A. Makarov, E. A. Ryabov, *Multiple Photon Infrared Laser Photophysics and Photochemistry*, Harwood Academic Pub, S.l., **1991**.
[146] a) N. Nibbering, M. L. E. Gross, *The Encyclopedia of Mass Spectrometry: Volume 4: Fundamentals of and Applications to Organic*, Auflage: REV. ed., Academic Pr Inc, Amsterdam ; Boston, **2004**.; b) J. R. Eyler, *Mass Spectrom. Rev.* **2009**, *28*, 448-467.
[147] N. C. Polfer, *Chem. Soc. Rev.* **2011**, *40*, 2211-2221.
[148] a) N. C. Polfer, J. Oomens, *Mass Spectrom. Rev.* **2009**, *28*, 468-494.; b) S. A. McLuckey, D. E. Goeringer, *J. Mass Spectrom.* **1997**, *32*, 461-474.
[149] D. Oepts, A. F. G. van der Meer, P. W. van Amersfoort, *Infrared Physics & Technology* **1995**, *36*, 297-308.
[150] S. Lakhdar, H. Mayr, *Chem. Commun.* **2011**, *47*, 1866-1868.
[151] a) S. H. Yoon, J. Chamot-Rooke, B. R. Perkins, A. E. Hilderbrand, J. C. Poutsma, V. H. Wysocki, *J. Am. Chem. Soc.* **2008**, *130*, 17644-17645.; b) J. Oomens, S. Young, S. Molesworth, M. van Stipdonk, *Journal of the American Society for Mass Spectrometry* **2009**, *20*, 334-339.; c) R. C. Dunbar, J. D. Steill, J. Oomens, *Phys. Chem. Chem. Phys.* **2010**, *12*, 13383-13393.
[152] L. Fiebig, J. Kuttner, G. Hilt, M. C. Schwarzer, G. Frenking, H.-G. Schmalz, M. Schäfer, *J. Org. Chem.* **2013**, *78*, 10485-10493.
[153] A. Milo, E. N. Bess, M. S. Sigman, *Nature* **2014**, *507*, 210-214.
[154] A. D. Becke, *The Journal of Chemical Physics* **1993**, *98*, 5648-5652.
[155] a) A. D. McLean, G. S. Chandler, *The Journal of Chemical Physics* **1980**, *72*, 5639-5648.; b) R. Krishnan, J. S. Binkley, R. Seeger, J. A. Pople, *The Journal of Chemical Physics* **1980**, *72*, 650-654.
[156] M. C. Holland, S. Paul, W. B. Schweizer, K. Bergander, C. Mück-Lichtenfeld, S. Lakhdar, H. Mayr, R. Gilmour, *Angew. Chem. Int. Ed.* **2013**, *52*, 7967-7971.
[157] U. Grošelj, Č. Podlipnik, J. Bezenšek, J. Svete, B. Stanovnik, D. Seebach, *HCA* **2013**, *96*, 1815-1821.
[158] a) F. N. R. Petersen, M. Ø. Jensen, C. H. Nielsen, *Biophys J* **2005**, *89*, 3985-3996.; b) A. T. Macias, A. D. MacKerell, *J. Comput. Chem.* **2005**, *26*, 1452-1463.
[159] A. L. Ringer, M. S. Figgs, M. O. Sinnokrot, C. D. Sherrill, *J Phys Chem A* **2006**, *110*, 10822-10828.

[160] a) A. Baiker, *Catalysis Today* **2005**, *100*, 159-170.; b) C. J. Baddeley, in *Heterogeneous Catalysts for Clean Technology* (Eds.: K. Wilson, A. F. Lee), Wiley-VCH Verlag GmbH & Co. KGaA, **2013**, pp. 103-124.; c) M. Heitbaum, F. Glorius, I. Escher, *Angew. Chem. Int. Ed.* **2006**, *45*, 4732-4762.
[161] H.-U. Blaser, B. Pugin, in *Chiral Reactions in Heterogeneous Catalysis* (Eds.: G. Jannes, V. Dubois), Springer US, **1995**, pp. 33-57.
[162] P. McMorn, G. J. Hutchings, *Chem. Soc. Rev.* **2004**, *33*, 108-122.
[163] a) Y. Tao, H. Kanoh, L. Abrams, K. Kaneko, *Chem. Rev.* **2006**, *106*, 896-910.; b) P. N. Liu, J. G. Deng, Y. Q. Tu, S. H. Wang, *Chem. Commun.* **2004**, 2070-2071.
[164] a) D. C. Sherrington, *Catalysis Today* **2000**, *57*, 87-104.; b) B. Clapham, T. S. Reger, K. D. Janda, *Tetrahedron* **2001**, *57*, 4637-4662.
[165] a) C. Saluzzo, T. Lamouille, D. Hérault, M. Lemaire, *Bioorganic & Medicinal Chemistry Letters* **2002**, *12*, 1841-1844.; b) A. Cornejo, J. M. Fraile, J. I. García, M. J. Gil, S. V. Luis, V. Martínez-Merino, J. A. Mayoral, *J. Org. Chem.* **2005**, *70*, 5536-5544.
[166] a) Á. Zsigmond, K. Bogár, F. Notheisz, *Journal of Catalysis* **2003**, *213*, 103-108.; b) S. B. Ogunwumi, T. Bein, *Chem. Commun.* **1997**, 901-902.
[167] a) M. Komiyama, T. Takeuchi, T. Mukawa, H. Asanuma, in *Molecular Imprinting*, Wiley-VCH Verlag GmbH & Co. KGaA, **2002**, pp. 9-19.; b) M. E. Davis, A. Katz, W. R. Ahmad, *Chem. Mater.* **1996**, *8*, 1820-1839.
[168] D. Dang, P. Wu, C. He, Z. Xie, C. Duan, *J. Am. Chem. Soc.* **2010**, *132*, 14321-14323.
[169] A. Baiker, in *Chiral Catalyst Immobilization and Recycling* (Eds.: D. E. D. Vos, I. F. J. Vankelecom, P. A. Jacobs), Wiley-VCH Verlag GmbH, **2000**, pp. 155-171.
[170] M. Studer, H.-U. Blaser, C. Exner, *Adv. Synth. Catal.* **2003**, *345*, 45-65.
[171] P. B. Wells, R. P. K. Wells, in *Chiral Catalyst Immobilization and Recycling* (Eds.: D. E. D. Vos, I. F. J. Vankelecom, P. A. Jacobs), Wiley-VCH Verlag GmbH, **2000**, pp. 123-154.
[172] A. Tai, T. Sugimura, in *Chiral Catalyst Immobilization and Recycling* (Eds.: D. E. D. Vos, I. F. J. Vankelecom, P. A. Jacobs), Wiley-VCH Verlag GmbH, **2000**, pp. 173-209.
[173] M. von Arx, M. Wahl, T. A. Jung, A. Baiker, *Phys. Chem. Chem. Phys.* **2005**, *7*, 273-277.
[174] Y. Orito, S. Imai, S. Niwa, N.-G. Hung, *Journal of Synthetic Organic Chemistry, Japan* **1979**, *37*, 173-174.
[175] a) É. Sípos, A. Tungler, I. Bitter, M. Kubinyi, *Journal of Molecular Catalysis A: Chemical* **2002**, *186*, 187-192.; b) É. Sípos, A. Tungler, I. Bitter, *Reaction Kinetics and Catalysis Letters* **2003**, *79*, 101-109.; c) É. Sípos, A. Tungler, G. Fogassy, *Journal of Molecular Catalysis A: Chemical* **2004**, *216*, 171-180.
[176] E. Tálas, F. Zsila, P. Szabó, J. L. Margitfalvi, *Journal of Molecular Catalysis A: Chemical* **2012**, *357*, 87-94.
[177] R. Fitzi, D. Seebach, *Angew. Chem.* **1986**, *98*, 363-364.
[178] J. Li, S. Luo, J.-P. Cheng, *J. Org. Chem.* **2009**, *74*, 1747-1750.
[179] D. Macmillan, K. Ahrendt, The Regents of the University of California, **2001**.
[180] S. A. Snyder, A. L. Zografos, Y. Lin, *Angew. Chem. Int. Ed.* **2007**, *46*, 8186-8191.
[181] F. Alonso, P. Riente, M. Yus, *Eur. J. Org. Chem.* **2009**, *2009*, 6034-6042.
[182] H. Zheng, K. Comeforo, J. Gao, *J. Am. Chem. Soc.* **2009**, *131*, 18-19.
[183] s. Gang, C. Shen, X. Yang, J. Tang, R. Zhang, G. Zou, East China Normal University, **2007**.
[184] Y. Zhang, L. Zhao, S. S. Lee, J. Y. Ying, *Adv. Synth. Catal.* **2006**, *348*, 2027-2032.
[185] D. Crich, X. Huang, *J. Org. Chem.* **1999**, *64*, 7218-7223.

[186] P. Lan, D. Berta, J. A. Porco, M. S. South, J. J. Parlow, *J. Org. Chem.* **2003**, *68*, 9678-9686.
[187] C. Hubert, B. Garrigues, *Can. J. Chem.* **1998**, *76*, 234-237.
[188] A. M. P. Koskinen, H. Hassilla, V. T. Myllymäki, K. Rissanen, *Tetrahedron Letters* **1995**, *36*, 5619-5622.

Curriculum Vitae

Mareike C. Holland (MSc ETH Chemistry)
Place and Date of Birth: 10.10.1987, Mainz, Germany
Nationality: German

Education and Training:

01/2011–06/2014	**Swiss Federal Institute of Technology (ETH) Zurich, Switzerland** Ph.D. studies in organic chemistry in the group of Prof. Ryan Gilmour (Sep. 2012 move of the group to the Westfälische Wilhelms-University, Münster)
10/2010–11/2010	**Swiss Federal Institute of Technology (ETH) Zurich, Switzerland** Internship in the group of Prof. Ryan Gilmour
09/2009–09/2010	**Swiss Federal Institute of Technology (ETH) Zurich, Switzerland** Master in chemistry; Final Grade: 5.34 Research projects in the groups of Prof. François Diederich and Prof. Antonio Mezzetti/ Prof. Antonio Togni
03/2010–06/2010	**University of Gothenburg (GU), Sweden** Master thesis in medicinal chemistry in the group of Prof. Kristina Luthman in collaboration with adjunct professor Dr. Roger Olsson (Director of Medicinal Chemistry at ACADIA Pharmaceuticals, Malmö) under supervision of Prof. Ryan Gilmour (ETH); Grade: 5.50
10/2006–09/2009	**Swiss Federal Institute of Technology (ETH) Zurich, Switzerland** Bachelor in chemistry; Final Grade: 5.17
09/2006	**Max Planck Institute for Immunobiology in Freiburg** Two week internship in the Metschnikoff Laboratory
08/2006	**Boehringer Ingelheim in Ingelheim** Three week work experience under supervision of Dr. Ulrich Scholz
04/2006	**Rabanus Maurus-Gymnasium Mainz, Germany** High School Graduation (Abitur); Final Grade: 1.2
08/2005	**Max Planck Institute for Molecular Physiology in Dortmund** Two week internship in the group of Prof. Herbert Waldmann
10/2004–02/2006	**Johannes Gutenberg University (JGU) Mainz, Germany** Early study program in chemistry prior to high school graduation (Frühstudium).
01/2003–12/2003	**Kavanagh College Dunedin, New-Zealand** Exchange high school year
1997–2006	**Rabanus Maurus-Gymnasium Mainz, Germany**
1993–1997	**Carl Zuckmayer primary school Nackenheim, Germany**

Teaching and other Involvement inside University:

Since 02/2013	Supervision of a Master thesis
10/2013–11/2013	Supervision of a Master research module
04/2013–08/2013	Supervision of a Master thesis

06/2013–07/2013	Supervision of a Master research module
02/2012–06/2012	Assistant to the Advanced Organic Chemistry Laboratory for chemistry students
06/2011–05/2012	Board member of the Behringer Simon Lecture committee
02/2011–06/2011	Tutor for Organic Chemistry II for chemistry students
12/2010–12/2012	Board member of the union of PhD students, postdocs and scientific staff of the Department of Chemistry and Applied Bioscience at ETH Zurich
01/2007–09/2010	Student president
09/2009–12/2009	Tutor for Inorganic Chemistry I for chemistry students
01/2009–06/2009	Tutor for Chemistry for engineering students Tutor for Organic Chemistry II for pharmacy students
12/2008–06/2009	Head of the event committee of the chemistry student association
06/2007–12/2009	Member of several committees concerning university policy
12/2007–12/2008	Editor-in-chief of the magazine for chemistry students

Social Activities outside University:

Jan. 2nd to 5th 2014	Organization of the annual workshop of the "Friends of the Chemistry-Olympiad"
Since 08/2009	Designer of the annual magazine of the "Friends of the Chemistry-Olympiad"
Since 01/2007	Member of the advisory board of the "Friends of the Chemistry-Olympiad"
01/2009–01/2013	Cash auditor of the "Friends of the Chemistry-Olympiad"
02/2005–03/2006	Responsible for internal affairs of the association of school students in Mainz
2003–2006	Tutoring of high school students

Competitions, Awards and Honours:

12/2013	Recipient of EU grant CALIPSO to study conformational diversity using free electron laser FELIX in Nijmegen
07/2013	Syngenta poster prize at the ESOC 2013
07/2013	Invited participation at the Nobel Laureate Meeting on Chemistry in Lindau
05/2013	1st place poster prize at the MSCEC 2013
2006	GDCh-Award (German chemical society) for the best chemistry student of the graduating year level at the Rabanus-Maurus Gymnasium
2004–2006	Participation in the Chemistry Olympiad (twice)
2003	First in Class Award in Chemistry at Kavanagh College, New Zealand
2001/2002	Participation in a state chemistry competition for junior high school
2001	Participation in the national history competition (Geschichtswettbewerb des Bundespräsidenten); Ranking: 3rd prize